International Doctorate Program in Molecular Oncology and Endocrinology
Doctorate School in Molecular Medicine

XXII cycle - 2006–2009
Coordinator: Prof. Giancarlo Vecchio

"Critical role of HMGA proteins in regulation of ATM expression and in cellular response to DNA damage"

Dario Palmieri

University of Naples Federico II
Dipartimento di Biologia e Patologia Cellulare e Molecolare
"L. Califano"

Administrative Location

Dipartimento di Biologia e Patologia Cellulare e Molecolare "L. Califano"
Università degli Studi di Napoli Federico II

Partner Institutions

Italian Institutions
Università degli Studi di Napoli "Federico II", Naples, Italy
Istituto di Endocrinologia ed Oncologia Sperimentale "G. Salvatore", CNR, Naples, Italy
Seconda Università di Napoli, Naples, Italy
Università degli Studi di Napoli "Parthenope", Naples, Italy
Università del Sannio, Benevento, Italy
Università di Genova, Genoa, Italy
Università di Padova, Padua, Italy
Università degli Studi "Magna Graecia", Catanzaro, Italy
Università degli Studi di Firenze, Florence, Italy
Università degli Studi di Bologna, Bologna, Italy
Università degli Studi del Molise, Campobasso, Italy
Università degli Studi di Torino, Turin, Italy
Università di Udine, Udine, Italy

Foreign Institutions
Université Libre de Bruxelles, Brussels, Belgium
Universidade Federal de Sao Paulo, Brazil
University of Turku, Turku, Finland
Université Paris Sud XI, Paris, France
University of Madras, Chennai, India
University Pavol Jozef Šafàrik, Kosice, Slovakia
Universidad Autonoma de Madrid, Centro de Investigaciones Oncologicas (CNIO), Spain
Johns Hopkins School of Medicine, Baltimore, MD, USA
Johns Hopkins Krieger School of Arts and Sciences, Baltimore, MD, USA
National Institutes of Health, Bethesda, MD, USA
Ohio State University, Columbus, OH, USA
Albert Einstein College of Medicine of Yeshiwa University, N.Y., USA

Supporting Institutions
Ministero dell'Università e della Ricerca
Associazione Leonardo di Capua, Naples, Italy
Dipartimento di Biologia e Patologia Cellulare e Molecolare "L. Califano", Università degli Studi di Napoli "Federico II", Naples, Italy
Istituto Superiore di Oncologia (ISO), Genoa, Italy
Università Italo-Francese, Torino, Naples, Italy
Università degli Studi di Udine, Udine, Italy
Agenzia Spaziale Italiana
Istituto di Endocrinologia ed Oncologia Sperimentale "G. Salvatore", CNR, Naples, Italy

Italian Faculty

Giancarlo Vecchio, MD, Co-ordinator
Salvatore Maria Aloj, MD
Francesco Saverio Ambesi Impiombato, MD
Francesco Beguinot, MD
Maria Teresa Berlingieri, MD
Angelo Raffaele Bianco, MD
Bernadette Biondi, MD
Francesca Carlomagno, MD
Gabriella Castoria, MD
Angela Celetti, MD
Mario Chiariello, MD
Lorenzo Chiariotti, MD
Vincenzo Ciminale, MD
Annamaria Cirafici, PhD
Annamaria Colao, MD
Alma Contegiacomo, MD
Sabino De Placido, MD
Gabriella De Vita, MD
Monica Fedele, PhD
Pietro Formisano, MD
Alfredo Fusco, MD
Michele Grieco, MD
Massimo Imbriaco, MD
Paolo Laccetti, PhD
Antonio Leonardi, MD
Paolo Emidio Macchia, MD
Barbara Majello, PhD
Rosa Marina Melillo, MD
Claudia Miele, PhD
Francesco Oriente, MD
Roberto Pacelli, MD
Giuseppe Palumbo, PhD
Silvio Parodi, MD
Nicola Perrotti, MD
Giuseppe Portella, MD
Giorgio Punzo, MD
Antonio Rosato, MD
Guido Rossi, MD
Giuliana SalvatoreMD,
Massimo Santoro, MD
Giampaolo Tortora, MD
Donatella Tramontano, PhD
Giancarlo Troncone, MD
Giuseppe Viglietto, MD
Roberta Visconti, MD
Mario Vitale, MD

Foreign Faculty

Université Libre de Bruxelles, Belgium
Gilbert Vassart, MD
Jacques E. Dumont, MD

Universidade Federal de Sao Paulo, Brazil
Janete Maria Cerutti, PhD
Rui Monteiro de Barros Maciel, MD PhD

University of Turku, Turku, Finland
Mikko Laukkanen, PhD

Université Paris Sud XI, Paris, France
Martin Schlumberger, MD
Jean Michel Bidart, MD

University of Madras, Chennai, India
Arasambattu K. Munirajan, PhD

University Pavol Jozef Šafàrik, Kosice, Slovakia
Eva Cellárová, PhD
Peter Fedoročko, PhD

Universidad Autonoma de Madrid - Instituto de Investigaciones Biomedicas, Spain
Juan Bernal, MD, PhD
Pilar Santisteban, PhD

Centro de Investigaciones Oncologicas, Spain
Mariano Barbacid, MD

Johns Hopkins School of Medicine, USA
Vincenzo Casolaro, MD
Pierre A. Coulombe, PhD
James G. Herman MD
Robert P. Schleimer, PhD

Johns Hopkins Krieger School of Arts and Sciences, USA
Eaton E. Lattman, MD

National Institutes of Health, Bethesda, MD, USA
Michael M. Gottesman, MD

“Critical role of HMGA proteins in regulation of ATM expression and in cellular response to DNA damage”

TABLE OF CONTENTS

LIST OF PUBLICATIONS

This dissertation is based upon the following publications:

Chiefari E, Paonessa F, Iiritano S, Le Pera I, Palmieri D, Brunetti G, Lupo A, Colantuoni V, Foti D, Gulletta E, De Sarro G, Fusco A, Brunetti A.
The cAMP-HMGA1-RBP4 system: a novel biochemical pathway for modulating glucose homeostasis.
BMC Biol. 2009;7:24.

De Martino I, Visone R, Wierinckx A, Palmieri D, Ferraro A, Cappabianca P, Chiappetta G, Forzati F, Lombardi G, Colao A, Trouillas J, Fedele M, Fusco A
HMGA proteins up-regulate CCNB2 gene in mouse and human pituitary adenomas.
Cancer Res. 2009;69(5):1844-50.

De Martino I, Visone R, Fedele M, Petrocca F, Palmieri D, Martinez Hoyos J, Forzati F, Croce CM, Fusco A.
Regulation of microRNA expression by HMGA1 proteins.
Oncogene. 2009;28(11):1432-42.

Pentimalli F, Palmieri D, Pacelli R, Garbi C, Cesari R, Martin E, Pierantoni GM, Chieffi P, Croce CM, Costanzo V, Fedele M, Fusco A.
HMGA1 protein is a novel target of the ATM kinase.
Eur J Cancer. 2008;44(17):2668-79.

Visone R, Iuliano R, Palmieri D, Server IN, Chiappetta G, De Martino I, Fedele M, Costinean S, Oberyszyn TM, Kusewitt DF, Croce CM, Fusco A.
Hmga1 null mice are less susceptible to chemically induced skin carcinogenesis.
Eur J Cancer. 2008;44(2):318-25.

De Martino I, Visone R, Palmieri D, Cappabianca P, Chieffi P, Forzati F, Barbieri A, Kruhoffer M, Lombardi G, Fusco A, Fedele M.
The Mia/Cd-rap gene expression is downregulated by the high-mobility group A proteins in mouse pituitary adenomas.
Endocr Relat Cancer. 2007;14(3):875-86.

Fedele M, De Martino I, Pivonello R, Ciarmiello A, Del Basso De Caro ML, Visone R, Palmieri D, Pierantoni GM, Arra C, Schmid HA, Hofland L, Lombardi G, Colao A, Fusco A.
SOM230, a new somatostatin analogue, is highly effective in the therapy of growth hormone/prolactin-secreting pituitary adenomas.
Clin Cancer Res. 2007;13(9):2738-44

Fedele M, Visone R, De Martino I, Troncone G, Palmieri D, Battista S, Ciarmiello A, Pallante P, Arra C, Melillo RM, Helin K, Croce CM, Fusco A.
HMGA2 induces pituitary tumorigenesis by enhancing E2F1 activity.
Cancer Cell. 2006;Jun;9(6):459-71.

ABSTRACT

HMGA proteins are a family of chromatin remodelers involved in many cellular processes including regulation of gene expression, apoptosis and cell proliferation. They have a crucial role in cell transformation and their overexpression is a constant feature of human malignant neoplasias, representing a poor prognostic index. Sequence analysis of HMGA proteins revealed the presence of a consensus site for ATM phosphorylation, which is highly conserved among different species and the different HMGA family members. Since ATM is the main cellular sensor to DNA damage, we decided to investigate the role of HMGA proteins in the ATM pathway and in the cellular response to DNA-damaging agents. In this study we demonstrate that both members of HMGA family, HMGA1 and HMGA2, interact and are phosphorylated by ATM in response to DNA damage. Interestingly, RT-PCR and Western Blot analysis on Mouse Emrbyonic Fibroblasts (MEFs) lacking *Hmga1*, *Hmga2* or both genes, revealed that, in the absence of HMGA proteins, mRNA and protein levels of ATM are strongly reduced. Moreover, p53 phosphorylation and the consequent activation of p21 transcription, induced by ATM kinase activity, were significantly affected by the absence of HMGA proteins. Consistent with these data, ChIP and luciferase assays demonstrated that HMGA proteins bind and positively regulate the promoter of the *ATM* gene. Moreover, induction of ATM kinase activity increased HMGA-mediated activation of *ATM* promoter, suggesting that, following DNA damage, ATM is able to trigger an HMGA-dependent positive feedback loop on its own promoter. Accordingly with the reduced expression of ATM, MEFs lacking both *Hmga* genes showed a significant impairment of the DNAdamage response. In fact, *Hmga1*/*Hmga2* double knock-out MEFs displayed a reduction in the DNA repair activity and in the stress-induced senescence following the induction of DNA double strand breaks (DSBs), compared to wild-type MEFs. It has been also demonstrated that inhibition of ATM determines cell sensitization to DNA damaging therapies. Thus, we investigated the role of HMGA proteins in cellular sensitivity to genotoxic drugs. On this purpose, we treated transformed thyroid cell lines with antisense oligonucleotides to abrogate the expression of HMGA proteins, and evaluated their response to DNA-damaging agents such as ionizing radiation and UV-light. As expected, down regulation of HMGA proteins reduced cellular levels of ATM. Moreover, following the exposure to DNA-damaging agents, absence of HMGA proteins determined alteration of cell-cycle checkpoints, reduced cell proliferation and promoted apoptosis. Taken together our data indicate that HMGA proteins play a crucial role in the cellular response to DNA damage, and may represent a new target to improve tumour sensitivity to conventional anti-cancer therapies.

1. INTRODUCTION

1.1 The HMG proteins

The High Mobility Group (HMG) proteins are a family of small nuclear non-histone proteins which play a critical role in several cellular processes such as gene expression, DNA replication, meiotic recombination, apoptosis, cellular senescence and DNA repair (Bustin et al. 1990, Patterson et al. 1996). In the mammalian species the high-mobility-group HMG proteins have been grouped in three distinct families (HMGB, HMGN, and HMGA), based on their distinct DNA binding domains.

The HMGB proteins (formerly HMG1/2) are characterized by the HMG-Box, a DNA-binding domain that both introduces a tight bend into DNA and binds preferentially to a variety of distorted DNA structures. The HMGB proteins seem to act primarily as architectural facilitators in the formation of nucleoprotein complexes; for example, in the assembly of complexes involved in recombination and transcription. Recent genetic and biochemical evidences suggest that these proteins can facilitate nucleosome remodeling. One mechanism by which HMGB proteins could prime the nucleosome for migration is to loosen the wrapped DNA and so enhance accessibility to chromatin-remodeling complexes and possibly also to transcription factors. By constraining a tight loop of untwisted DNA at the edge of a nucleosome, an HMGB protein could induce movements in the contacts between certain core histones that would result in an overall change in nucleosome structure (Bianchi et al. 2000, Thomas et al. 2001).

The HMGN proteins (formerly HMG14/17) decompact the nucleosomal array altering the chromatin architecture. Two HMGN bind to each nucleosome through their nucleosome-binding domain, inducing chromatin unfolding, which results in increased gene expression and replication (Bustin 2001, Crippa et al. 1993, Vestner et al. 1998).

The HMGA family (previously HMGI) comprises four members: HMGA1a, HMGA1b, HMGA1c and HMGA2. The characteristic DNA binding domains of this protein family, the so called “AT-Hooks”, are responsible for the binding of HMGA proteins to DNA sequences rich in adenine and thymine (AT-rich regions) (Geierstanger et al. 1994). Like the other HMGs, HMGA proteins do not present a transcriptional activity *per se*, but are involved in regulation of transcription by altering the architecture of chromatin and facilitating the assembly of multiprotein complexes of transcriptional factors (Thanos and Maniatis 1992).

1.2 The HMGA family

HMGA proteins are encoded by two distinct genes, *HMGA1*, which produces by alternative splicing HMGA1a, HMGA1b and HMGA1c, and *HMGA2*, coding for the homonymous protein (Fusco and Fedele 2007). As above mentioned, all HMGA proteins are characterized by three N-terminal highly positively charged domains, called AT-Hooks, necessary for the binding to AT-rich stretches of DNA. On the contrary, the C-terminus contains a high percentage of negatively charged amminoacids. The structure and sequence of HMGA proteins are very similar and highly conserved among species, but many differences can be found in the N-terminal region and between AT-Hooks (Fedele et al. 2001). Both *HMGA* genes are widely expressed during embryogenesis, whereas their expression is absent or low in adult tissues (Zhou et al. 1995, Chiappetta et al. 1996). In particular, expression of *HMGA2* has not been detected in any of the several adult mouse and human tissues tested (Rogalla et al. 1996). Low expression has been observed in CD34-positive haematopoietic stem cells (Rommel et al. 1997), in mouse preadipocytic proliferating cells (Anand and Chada 2000) and in meiotic and post-meiotic cells secondary spermatocytes and spermatids) (Chieffi et al. 2002, Di Agostino et al. 2004). Conversely, *HMGA1* is ubiquitary expressed, albeit at low levels, in adult murine and human tissues (Chiappetta et al. 1996).
Studies of mice models have revealed a crucial role of HMGA proteins in adipogenesis (Zhou et al. 1995, Chiappetta et al. 1996, Battista et al. 1999), somatic growth (Battista et al. 1999), cardiac cell growth control (Fedele et al. 2006) and glucose homeostasis (Foti et al. 2005, Chiefari et al. 2009). Consistent with this, HMGA mutations have been detected in human diseases such as lipomas (Sreekantaiah et al. 1991, Schoenmakers et al. 1995, Ashar et al. 1995), gigantism (Ligon et al. 2005), dwarfism (Buysse et al. 2009), and diabetes (Foti et al. 2005). Moreover, HMGA2 has also been suggested recently by three genome-wide SNP studies to influence human height variation (Weedon et al. 2007, Weedon et al. 2008, Sanna et al. 2008).

1.3 Regulation of gene expression by HMGA proteins

HMGA proteins play a key role in assembling and modulating macromolecular complexes that are involved in various biological processes. In doing so, HMGA proteins directly bind to the DNA, modifying its conformation and consequently facilitating the binding of a group of transcriptional factors (TF). They interact with both DNA and TFs to generate a multiprotein stereospecific complex bound to DNA. HMGA proteins have been shown to participate in this way in the regulation of many gene, the best studied being the human interferon

(IFN)- β gene. Indeed, the activation of IFN-β expression is due to a multifactor complex that assembles in the nucleosome-free enhancer region of the gene, which includes the factors nuclear factor κB (NF-κB), the interferon regulatory factor (IRF), the activating transcriptional factor 2 (ATF2)/JUN and the HMGA1a protein (Thanos and Maniatis 1992, Thanos et al. 1993).
The direct interaction of HMGA proteins with TFs can take place even in absence of DNA. In this case they modify the conformation of TFs, thus enhancing their affinity to DNA. The enhancement of transcriptional activity of the TF serum-response factor by HMGA1a is an example of this mechanism (Chin et al. 1998).
Finally, the HMGA proteins have the ability to alter chromatin structure. . Indeed, they have been shown to be important elements, associated with matrix- and scaffold-associated regions (MARs/SARs), i. e. specific segments of genomic AT rich DNA that have a high affinity for the nuclear matrix. These sequences anchor chromatin to the nuclear scaffold and organize topologically independent DNA domains, which have functional roles both in DNA replication and transcription (Galande 2002). The binding of HMGA proteins to these regions de-represses transcription by displacement of histone H1 by DNA (Zhao et al. 1993).

1.4 HMGA proteins and cancer

In contrast to normal tissues, high levels of HMGA1 and HMGA2 are a common feature of human benign and malignant tumours.
Benign tumors of mesenchymal origin (lipomas, leiomyomas, fibroadenomas, aggressive myxomas, pulmonary hamartomas and endometrial polyps) often contain chromosomal rearrangements involving the gene *HMGA2*. These rearrangements result in the formation of new hybrid genes that code for chimeric proteins in which the AT-hooks of HMGA2 are fused to ectopic peptidic sequences (Hess 1998), with loss of the C-terminus and of the 3'UTR of the gene. Given the great variability of the partners, but also by the fact that in some cases there is no effect attributable to the partner sequence, it is probably the truncation of *HMGA2* and loss of its 3′ UTR rather than the formation of a new chimeric gene that is crucial (Kazmierczak et al. 1995, Kools and Van de Ven 1996). Rerrangements and overexpression of the *HMGA2* gene have also been described in non-mesenchymal benign human tumours, such as pituitary adenomas (Finelli et al. 2002, Pierantoni et al. 2005). Consistently, transgenic mice overexpressing *Hmga1* or *Hmga2* develop pituitary adenomas, demostrating the causal role of HMGA proteins in the transformation of pituitary gland (Fedele et al. 2002, Fedele et al 2005).
Overexpression of HMGA proteins is a constant feature of several human malignant neoplasias, including thyroid, prostate, uterus, breast, colorectum, ovary and pancreas carcinomas (Fedele et al. 2001). Moreover, it has been demonstrated

that high levels of HMGA represent a poor prognostic index as their overexpression often correlates with the presence of metastasis and with a reduced survival (Fusco and Fedele 2007).
Regarding the mechanisms underlying the induction of the HMGA genes in malignant transformation, it is reasonable to assume that it probably occurs through oncofetal transcriptional mechanisms, which have not yet been well characterized (Fusco and Fedele 2007).
Surprisingly, both heterozygous and homozygous *Hmga1*-null mice develop age-dependent splenomegaly associated with lymphoid cell expansions, resembling various human B-cell lymphomas (Fedele et al. 2006), suggesting an unexpected role for HMGA proteins as tumor suppressors. The observation that HMGA proteins accumulate on chromatin in senescent fibroblasts and are essential structural components of senescence-associated heterochromatic foci (SAHFs) (Narita et al. 2006) could be a possible explanation for this unexpected role for HMGA proteins as tumor suppressor. In fact, HMGA proteins might cooperate with the p16INK4a tumour suppressor to promote SAHF formation and proliferative arrest, and stabilize senescence by contributing to the repression of proliferation-associated genes.

1.5 Mechanisms of transformation by HMGA

In last years, several studies have demonstrated the causal role of HMGA proteins in the process of cell trasformation. A direct evidence of the oncogenic role was the demonstration that transfection of HMGA1 or HMGA2 transforms rat1a fibroblasts and human lymphoblastoid cell lines (Wood et al. 2000). Moreover, infection of normal thyroid cells (FRTL-5) with transforming retroviruses such as KiMSV induces overexpression of HMGA proteins. Prevention of HMGA proteins expression using antisense oligonucleotides prevented the acquisition of the transformed phenotype (growth in soft agar and tumor induction in athymyc mice) following viral infection, confirming that expression of HMGA proteins has a causal role in cellular transformation (Berlingieri et al. 1995)
Several mechanisms have been proposed to account for the transforming ability of the HMGA proteins. Because of their main function as regulators of gene transcription, most of these mechanisms are based on the ability of HMGA proteins to down- or up-regulate the expression of genes that have crucial roles in control of cell proliferation and invasion. Our group has recently demonstrated that HMGA2 induces E2F1 activity by displacing Histone Deacetylase 1 (HDAC1) from the pRB/E2F1 complex, thus resulting in enhanced acetylation of both E2F1 and DNA-associated histones, promoting E2F1 dependent gene expression (Fedele et al. 2006b). Another mechanism by which the HMGA proteins might have a role

in cancer progression is through their interaction with p53. It has been found that HMGA1 binds p53 and interferes with the p53-mediated transcription of BCL2-associated X (BAX) and cyclin-dependent kinase inhibitor 1A ($p21^{cip1}$) genes, as well as cooperates with p53 to activate transcription of the p53 inhibitor MDM2. HMGA1 can also interfere with the apoptotic function of p53 by another mechanism that increases the interaction with the proapoptotic p53 activator homeodomain-interacting protein kinase 2 (HIPK2) (Pierantoni et al. 2006). It has also been demonstrated that HMGA proteins induce cyclin A expression, AP1 complex activity, and enhance the expression of inflammatory proteins (Fusco and Fedele 2007). Finally, recent studies demonstrated that HMGA proteins can regulate expression of genes having a crucial role in carcinogenesis, by modulating miRNAs transcription (Fusco and Fedele 2007).

1.6 HMGA proteins and DNA repair

Several evidences propose an important role for the HMGA proteins in DNA repair. HMGA1 can compete with p53 and human MutS homologue proteins (MSH2–MSH6) for Holliday junction binding, exerting a negative influence on the DNA mismatch repair response (Subramanian and Griffith 2002). HMGA proteins also regulate the transcription of genes that are involved in DNA repair. Indeed, using transcriptional microarrays, Reeves and Adair (2005) described a number of genes involved in DNA repair that were negatively regulated in MCF7 human breast-cancer cells by HMGA1 overexpression, suggesting that HMGA proteins can influence DNA repair by negatively regulating the transcriptional activity of genes involved in various aspects of DNA-damage-recognition and removal. Consistently, Borrmann et al. (2003) reported that HMGA2 binds the promoter of the nucleotide excision-repair gene *ERCC1* and negatively modulates its activity. Moreover, it has been shown that HMGA1 can downregulate *BRCA1* expression, which is involved in homologous recombination, by binding directly to its promoter region, and that there is an inverse correlation between HMGA1 and BRCA1 expression in human breast carcinomas (Baldassarre et al. 2003). Consistent with the role of BRCA1 in double-strand break (DSB) repair, it has been shown that HMGA proteins enhance genotoxic stress induced by different DNA-damaging agents causing DSBs, such as cisplatin, bleomycin, doxorubicin and X-ray irradiation (Baldassarre et al. 2005, Boo et al. 2005). Finally, HMGA proteins can indirectly inhibit DNA repair through cyclin-A induction, and it has been recently reported that the cyclin A1–cyclin-dependent kinase 2 complex also regulates DSB repair (Muller-Tidow et al. 2004).
Recently, a novel unexpected role in DNA repair for HMGA2 has been identified. Summer and colleagues demonstrated that HMGA2 is incorporated into the cellular Base Excision Repair machinery, operating as an enzyme in the cleavage

of abasic nucleotides. In addition, HMGA2 expression protects cancer cells from the DNA damage induced citotoxicity during chemotherapy (Summer et al. 2009). These observations suggest that the role of HMGA proteins in DNA repair still remains controversial, and that new studies will be needed to further analyze the effect of HMGA1 and HMGA2 in the DNA damage response and in the processes of resistance to anti-neoplastic drugs.

1.7 The DNA damage response and the cancer connection

Although its relatively inert chemical nature, DNA is constantly under attack by a large number of agents, and it has been estimated that many thousands of DNA lesions occur every day in each cell of the human body (Jackson 2009).
Cellular DNA can be damaged in several different ways: nucleotide bases can be covalently altered, the DNA phosphodiester backbone can be broken on one strand (single strand breaks, SSBs) or on both strand (double strand break, DSBs) or chemical interstrand cross-links can be produced (Kastan and Bartek 2004). A large proportion of DNA lesions are a physiological consequence of hydrolytic reactions induced by reactive oxygen species produced by the normal cellular metabolism (Jackson 2009). Moreover, many environmental agents such as ionizing radiation (IR), ultraviolet (UV) light and chemical mutagens contribute to the DNA damage production (Jackson 2009). DNA lesions can cause inhibition of genome replication and transcription, and if they are not repaired or are repaired incorrectly, they can produce mutations or large-scale genome aberrations that may lead to cell malfunction or cell death (Mills et al. 2003, Caldecott 2008, Lobrich and Jeggo 2007). Because a broad range of DNA lesion can occur, evolution has provided a variety of different repair mechanisms to deal with both metabolic and external sources of DNA damaging agents (Jackson 2009). These mechanisms, fortunately, are able to accurately and efficiently repair the vast majority of the DNA damages (Jackson 2009).
Free oxygen radicals, generated by normal metabolic processes or following the exposure to a source of IR, can alter the backbone of DNA helix breaking the phosphodiester bonds between two nucleotides, determining SSBs.
When two or more of these breaks are present close to each other, but on opposite DNA strands, a DSB occurs. DNA DSBs are generally considered the most cytotoxic lesions produced by IR and radiomimetic drugs, and are also generated when the DNA replication machinery encounters DNA lesions such as SSBs or pyrimidine dimers, which can determine a stall of replication forks. Moreover, Topoisomerase II-inhibitors exert their cytotoxic activity inducing DSBs. Although many variations on the precise mechanisms of DSBs repair exist, two largely distinct and complementary repair pathways have been identified: Non-

Homologous End Joining (NHEJ) and Homologous Recombination (HR) (Jackson 2009, Haber 2000, Karran 2000).
Repair of DNA DSBs is intrinsically more difficult than other types of DNA damage, and inefficiently repaired DSBs may cause mutations, loss or amplification of chromosomal material and, if it inactivates essential genes, can affect cell survival (Khanna and Jackson 2001, Rich 2000, Wyman and Kanaar 2006). Moreover, defects in the DSBs repair machinery can lead to exchange of chromosomal arms, sometimes in a reciprocal fashion (Khanna and Jackson 2001). These chromosomal aberrations represent a common feature of human neoplasias. In fact, if a deleted region contains a tumour suppressor gene, or if an amplified region contains an oncogene, the chromosomal rearrangement may induce cellular transformation (Khanna and Jackson 2001). Sometimes the exchange of chromosomal arms leads to the formation of a fusion gene encoding for a chimerical protein which acquires an oncogenic potential, or places a proto-oncogene under the transcriptional control of a strong promoter, determining its over-expression. Accordingly, epidemiologic studies, animal models and the observation that many human cancer susceptibility syndromes arise from mutations in genes involved in DNA damage responses have widely demonstrated that damage to cellular DNA has a causal role in cancer (Kastan and Bartek 2004).
However, this notion is not the only interesting link between DNA repair and cancer. Induction of DNA damage is also the main therapeutic approach currently used by the majority of therapies used to treat malignancies, such as radiation therapy and chemotherapeutic agents (Kastan and Bartek 2004). Moreover the DNA damage-induced apoptosis is the main determinant of side effects of common therapies, which are usually associated to bone marrow suppression, GI toxicities, and hair loss (Kastan and Bartek 2004). Thus, DNA damage is the cause of the disease, is used to treat the disease and is responsible for the toxicity of anti-cancer therapies.

1.8 Cellular response to DNA Double Strand Breaks

The way that cells react to DSBs is to trigger a complex and co-ordinated set of events that is often termed the DNA damage response (DDR) (Zhou and Elledge 2000, Rouse and Jackson 2002). The DDR involves a number of proteins that sense the damage (DNA damage sensors) and activate downstream DNA damage transducers, which amplify the signal triggered by the sensors, and activate the effectors of DDR (Khanna and Jackson 2001).
Initiation of the activities of the PI(3)K (phosphatidyl-inositol-3-OH kinase)-like kinases (PIKKs) ATM (ataxia teleangiectasia mutated) and ATR (ATM- and Rad-3 related) and are the first step characterized to date in the activation of signal transduction pathways after DNA damage (Kastan and Bartek 2004). In particular,

the ATM kinase seems to be primarily activated following DNA damage whereas the ATR kinase is critical for cellular responses to the arrest of DNA-replication forks (Shiloh and Kastan 2001, Abraham 2001). However, although ATM and ATR have long been assumed to respond to non-overlapping damage signals (DNA DSBs in the case of ATM, and UV-induced base damage and stalled replication forks in the case of ATR) recent data suggest that ATM can activate ATR after DSBs in the S and G2 phases (Cuadrado et al. 2006), demonstrating the presence of a link between ATM and ATR pathways.

Another member of the PIKKs family, DNA-PKcs (catalytic subunit of DNA dependent protein kinase) is also involved in the DNA damage response, but its role is more directly correlated to the process of DNA repair, rather than to the activation of cell cycle checkpoints or apoptosis (Cann and Hicks 2007).

DSBs are recognized rapidly within cells, but the mechanism of DSB recognizing remains controversial (Cann and Hicks 2007). One model of DSB recognition hypothesizes that DSB-induced changes in chromatin structure are enough to activate ATM, the pinnacle kinase in the DSB signalling cascade (Bakkenist and Kastan, 2003). In this model, ATM would be the DNA damage sensor and the transducer of the DNA damage-triggered signalling, at the same time. Recent data indicate that ATM, in conjunction with the MRN (Mre11/Rad50/Nbs1) complex, can also activate ATR after DSBs in the S and G2 phases (Cuadrado et al. 2006, Jazayeri et al. 2006). Following the activation of MRN by ATM, the nuclease activity of Mre11 processes the DSB to produce ssDNA that is coated by RPA (replication protein A), which in turn leads to the recruitment of ATR, through the intermediary protein ATRIP. Hence, this first model indicates ATM and ATR as "proximal checkpoint kinases" (Shiloh 2003). In the other model of DSB recognition, the MRN complex first detects the DSB by binding to the broken ends. Once bound, the MRN complex recruits and promotes the activation of ATM (Lee and Paull 2005). Indeed, the C-terminus of Nbs1 contains an ATM interaction motif, which is required for the retention of ATM to sites of DNA damage, and activation of checkpoint pathways (Falck et al. 2005). Regardless of which protein physically recognizes the DSB, there appears to be a mutual promotion of activity between the MRN complex and ATM. In fact, ATM phosphorylates Nbs1 (Gatei et al. 2000) and the MRN complex enhances ATM kinase activity (Lee and Paull, 2005). Following their activation, ATM and ATR directly phosphorylate a number of substrates that play a direct role in the cellular response to DNA damage. Moreover, this signalling is also amplified by the ATM/ATR dependent activation of other kinases such as CHK1 and CHK2 (Zhang et al. 2004, Bartek and Lukas 2003) also known as transducer or effector kinases. The activation of CHK1 and CHK2 spread the alert signal and orchestrate the global cellular response to DNA damage. Indeed, DSB-induced activation of DNAdamage sensor initiates signal transduction pathways activating cell cycle checkpoints, DNA repair, apoptosis or senescence (Khanna and Jackson 2001).

Cell cycle checkpoints following DSBs

One of the key aspects of these DNA-damage-signalling events is the induction of checkpoint mechanisms that slow down or stop cell-cycle progression while the damage persists, preventing the replication of DNA or segregation of damaged chromosomes during mitosis (Jackson 2009).

Genotoxic stress can transiently delay cell-cycle progression in G1, S or G2 trough a checkpoint network response controlled by the ATM/ATR-CHK2/CHK1 pathway (Kastan and Bartek 2004), or even impose a prolonged a durable cell cycle arrest in either G1 or G2 phases. Given the critical significance of error-free DNA replication and chromosome segregation for the maintenance of genomic integrity and the prevention of cancer, it is not surprising that these most vulnerable stages of the cell-division cycle are protected by a wider spectrum of checkpoint-effector mechanisms (Kastan and Bartek 2004).

The dominant checkpoint response to DNA damage in mammalian cells traversing through G1 is the ATM(ATR)/CHK2(CHK1)-p53/MDM2-p21 pathway, which is capable of inducing sustained and sometimes even permanent G1 arrest (Kastan, and Lim 2000, Bartek and Lukas 2003, Wahl and Carr 2001). Although the expression of ATM and CHK2 is relatively constant during the cell cycle, the concentrations of ATR and CHK1 are low in the early-to-mid G1, and their activities become important only closer to the G1/S transition. ATM/ATR directly phosphorylate the p53 transcription factor within its amino-terminal transactivation domain, particularly on serine 15. In addition, the ubiquitin ligase MDM2, that normally binds p53 and ensures rapid p53 turnover, is targeted after DNA damage by ATM/ATR (Maya et al. 2001), as well as by CHK2/CHK1 (Kastan and Bartek 2004). These modifications of p53 and MDM2 contribute to the stabilization and accumulation of the p53 protein, as well as to its increased activity as a transcription factor. The key transcriptional target of p53 is the p21CIP1/WAF1 inhibitor of cyclin-dependent kinases (Kastan and Lim 2000, Wahl and Carr 2001), which silences the G1/S-promoting cyclin E/Cdk2 kinase and thereby causes a G1 arrest. This leads not only to the inability to initiate DNA synthesis, but it also preserves the RB/E2F pathway in its active, growth-suppressing mode, thereby causing a sustained G1 blockade (Kastan and Bartek 2004). Thus, the G1 checkpoint response targets two critical tumour suppressor pathways, governed by p53 and pRB. These are arguably the two mechanisms that are most commonly deregulated in human cancer (Kastan and Lim 2000).

Progression into the S phase and transition from G2 into M are regulated by the serine-threonine cdk2 and cdk1 (cdc2), respectively. Activation of cdk2 and cdk1 (cdc2) requires the association of their positive subunits, cyclin A and cyclin B, respectively, and the phosphorylation of Thr161 by cdk-activating kinase. These cdk-cyclin complexes are also negatively regulated by phosphorylation at Thr14

and Tyr15, which are catalyzed by inhibitory protein kinases, including Wee1, Myt1 and Mik1 (Nigg 2001).
During S phase progression and at G2/M phase transition, dephosphorylation of Thr14 and Tyr15 by the cdc25 protein phosphatase cdc25A, -B, and -C, triggers cdk2-cyclinA (intra-S phase) and cdk1 (cdc2)-cyclinB (at G2/M transition) activation. During the DNA damage response, activation of ATM/ATR and the downstream checkpoint kinases CHK1/CHK2 leads to the phosphorylation of cdc25 phosphatases, which creates binding sites for 14-3-3 proteins and sequestration of the phosphatases away from cdk2-cyclinA and cdk1 (cdc2)-cyclinB (Borgne and Meijer 1996; Peng et al. 1997, Zeng et al. 1998, Sanchez et al. 1997, Matsuoka et al. 1998).
The G2 checkpoint (also known as the G2/M checkpoint) prevents cells from initiating mitosis when they experience DNA damage during G2, or when they progress into G2 with some unrepaired damage inflicted during previous S or G1 phases (Xu et al. 2002, Nyberg et al. 2002). The accumulation of cells in G2 may also reflect a contribution of the so-called DNA replication checkpoint (often referred to as the S/M checkpoint) that may sense some of the persistent DNA lesions from the previous S phase as being inappropriately or not fully replicated DNA. The critical target of the G2 checkpoint is the mitosis-promoting activity of the cyclin B/CDK1 kinase, whose activation after various stresses is inhibited by ATM/ATR, CHK1/CHK2 and/or p38-kinase- mediated subcellular sequestration, degradation and/or inhibition of the CDC25 family of phosphatases that normally activate CDK1 at the G2/M boundary (Donzelli and Draetta 2003, Nyberg et al. 2002, Katsuhiro et al. in press, Mailand et al. 2002, Bulavin et al. 2001). In addition, other upstream regulators of CDC25C and/or cyclin B/CDK1, such as the Polo-like kinases PLK3 and PLK1 seem to be targeted by DNA-damage-induced mechanisms (Nyberg et al. 2002).

Mechanisms of DNA repair following DSBs
Following DNA damage, the main target of the cell is the repair of toxic genome lesions. Within minutes following exposure to ionizing radiation (IR), activated ATM phosphorylates H2AX in the C-terminal tail at Ser139 over a region of megabases surrounding a DSB (Burma et al. 2001). In a parallel manner, ATR phosphorylates H2AX after replicational stress (Ward and Chen 2001). Many DNA damage response proteins are then quickly recruited to the sites of DSBs, and this recruitment can be visualized almost immediately following laser beam-induced DSBs (Celeste et al. 2003). These proteins, then, build up to form ionizing radiation-induced foci (IRIF), which are the conventional manifestation of DNA damage-induced relocalization. The time frame for IRIF formation is protein dependent: H2AX (Rogaku et al. 1998) 53BP1 (p53 Binding Protein 1)(Anderson et al. 2001) and MDC1 (mediator of mammalian DNA damage-checkpoint 1) (Stewart et al. 2003) IRIF formation occur within minutes following IR exposure,

and are thought to represent sites of DNA damage. Other factors, such as Rad51, MRN complex, ATM, BRCA1 and Rad52 do not form IRIF until over 3 hours after IR exposure (Celeste et al. 2002, Haaf et al. 1995). While the exact function of thee IRIF remains to be determined, H2AX has been shown to be required for the retention of BRCA1, 53BP1 and the MRN complex to these foci (Celeste et al. 2002). H2AX is not required for the initial recruitment of these proteins, suggesting a role in the later development and maintenance of IRIF, but not in the recruitment of proteins to sites of DNA damage (Celeste et al. 2002). Probably, histone modifications such as phosphorylation of H2AX during the first phases of DNA damage repair have a crucial role in chromatin reorganization, necessary to improve the accessibility of DNA repair factors to the damaged DNA (Jackson 2009).

Following IR exposure, ATM also directly phosphorylates 53BP1 (Anderson et al. 2001), MDC1 (Goldberg et al. 2003) BRCA1 (Xu et al. 2001) and c-Abl (Baskaran et al. 1997). C-Abl can regulate the function of Rad51 in both positive (Chen et al. 1999) and negative (Yuan et al. 1998) manners, indicating that ATM can also indirectly regulate Rad51 through its activation of c-Abl. ATM also indirectly activates BRCA1 via CHK2 (Zhang et al. 2004). The BRCA-Carboxy-terminal domain (BRCT)-containing proteins Nbs1, MDC1, 53BP1 and BRCA1 are all thought to function as mediators, helping to bring together various repair and checkpoint proteins (Li and Zou 2005) MDC1, for example, has been shown to be critical for recognizing phosphorylated H2AX and helps to amplify the DSB signal through interaction with ATM for a more effective response (Lou et al. 2006). MDC1 also interacts with the recombinase Rad51 (Zhang et al. 2005) and functions in checkpoint control (Lou et al 2003). BRCA2 can interact with both Rad51 and BRCA2 (Yoshida and Miki 2004), is required for some ATM-dependent phosphorylation events (Foray et al. 2003), and has a role in checkpoint control (Xu et al. 2001). Nbs1 directly functions sensing damage and activating ATM through the MRN complex (Lee and Paull 2005). The MRN complex is also involved in repair because of the nuclease activity of Mre11 (Van den Bosch et al. 2003). Moreover, Nbs1 also functions in the intra-S-phase checkpoint (Lim et al. 2000) and helps ATM-dependent phosphorylation events required for the G1/S checkpoint (Girard et al. 2002). Finally, 53BP1 also appears to promote ATM activation following DSBs (Mochan et al. 2003) and functions in activating the G2/M checkpoint (Fernandez-Capetillo et al. 2002).

Once the DSB response have been initiated, the breaks are repaired by two main pathways: non -omologous end-joining (NHEJ) or homologous recombination (HR) (Karagiannis and El-Osta 2004).

NHEJ is the predominant pathway in mammalian cells and is used almost exclusively during G1 and early S phases (Karagiannis and El-Osta 2004). In this pathway, the regulatory subunits of DNA-PK, Ku70 and Ku80, first bind the broken ends of the DNA, thereby recruiting the catalytic subunit of DNA-PK

(DNA-PKcs). After DNA ends processing, potentially by the MRN complex or Artemis, the Ligase IV/XRCC4 complex ligates the strands together (Jackson 2001). However, ligation of processed DNA ends usually incur in deletions or additions of nucleotides, and the repaired DNA shows a different sequence respect to the original DNA. Therefore, this process is considered an error-prone pathway (Jackson 2001, Karagiannis and El-Osta 2004).
Homologous recombination preferentially uses sister chromatid as a template for this repair mechanism, and appears to be only used in late S and G2 phases (Hiom 1999). The first step in HR is the production of 3' single-stranded tails of DNA via a 5'-to-3' strand resection on each side of the break site (Karagiannis and El-Osta, 2004), by the MRN complex. Single stranded DNA is then coated with RPA (Iftode et al. 1999), and the recombinase enzyme Rad51 is loaded onto these tails. BRCA2 seems to play a critical role in this loading process, as well as in the sub-cellular localization and regulation of Rad51 (Pellegrini and Venkitaraman 2004). The Rad51-loaded filament invades the homologous site of the intact sister chromatid to produce a D-Loop structure (Karagiannis and El-Osta 2004). Using the undamaged chromatid as a template, DNA polymerases synthesize new DNA to span the break site, beginning form the 3' tails. Following this DNA synthesis, endonucleases cleave and resolve the Holliday Junctions, eventually generating two separate, intact chromatids (Karagiannis and El-Osta, 2004). Other proteins are involved in this repair mechanism, including the other Rad51-like proteins (Rad51B, Rad51C, Rad51D, XRCC2 and XRCC3) and Rad54 (Karagiannis and El Osta 2004). Rad54 is a member of the SWI2-SNF2 protein family, and its role is to unwind DNA, remodelling chromatin during repair to modulate the accessibility of DNA to DNA repair factors (Tan et al. 1999).

Apoptosis following DSBs
Depending on the severity of the DNA damage or the cell type involved, cells may undergo apoptosis instead of attempting to repair the damage (Sionov and Haupt 1999). For example, lymphocytes are particularly sensitive to apoptosis, partly because IR exposure induces Bax expression, differently form fibroblast cell lines (Sionov and Haupt, 1999). Mouse embryonic stem cells also respond to IR exposure by undergoing apoptosis (Hong and Stambrook 2004).
Following DSBs , apoptosis is initiated through an ATM directed pathway. ATM, as previously described, activates p53 directly and indirectly, via Chk2 (Bree et al. 2004). Again, ATM also inactivates MDM2, the main negative regulator of p53 (Khostravi et al. 1999). Transcription of pro-apoptotic genes is the main mechanism of p53-induced apoptosis. p53, in fact, is able to upregulate transcription of NOXA, PUMA and Bid (Schuler and Green 2005), which belongs to the BH3-only protein family, inhibitors of anti-apoptotic factors such as BCL-2 and BCL-XL (Bree et al. 2004). As mentioned above, p53 also upregulates the expression of Bax, a BH123 protein that forms channels in mitochondrial

membrane, which results in the release of Cytochrome *C* and Smac/Diablo, and determines the loss of mitochondrial membrane potential. Release of Cytochrome *C* activates the Apaf-1-Caspase 9 apoptotic pathway, and inhibition of IAPs (Inhibitor of Apoptosis Proteins) by Smac/DIABLO impairs caspase inhibition (Borner 2003). Recently it has been demonstrated that p53 modulates apoptosis also in a transcription independent manner. Following IR exposure, p53 is translocated to mitochondria, where it inhibits Bcl-2 and Bcl-XL, and activates Bak, another BH123 protein (Bree et al. 2004).

The dual functions of ATM and p53 in promoting cell cylce arrest and apoptosis lead to some seemingly contradictory phenotypes. In fact, ATM defective cells are generally carachterized by radiation hypersensitivity (Barlow et al. 1996), while thymocytes from *ATM-/-* mice are actually resistant to radiation-induced apoptosis (Xu and Baltimore 1996). This duality of function also exists in other systems defective of DNA damage response proteins, including p53 (Bernstein et al. 2002) and DNA-PKcs (Bernstein et al. 2002). These observations suggest that there are as yet unidentified proteins involved in the regulation of the cross-talk between the mutually exclusive pathways of maintenance of life and initiation of death. In fact, while much is known about individual pathways within the cellular DSB response, there is still much we need to learn about how these pathways are integrated to provide a concerted response to DNA double strand breaks (Cann and Hicks 2007).

Cellular senescence following DSBs

Recent investigations in the field of cellular senescence have revealed the importance of DNA damage responses and cell-cycle checkpoints to initiate cell-cycle arrest associated with cellular senescence. Replicative (or the "Hayflick limit") and premature senescence share a common signal, now recognized as DNA strand breaks. In replicative senescence, telomere erosion and shortening yield DNA double-strand breaks at chromosome ends that initiate DNA damage responses (Herbig et al. 2004, d'Adda di Fagagna et al. 2003). In premature senescence, oncogenic activation leads to elevated intracellular levels of reactive species, augmented numbers of active replicons, alterations in DNA replication fork progression, and the appearance of DNA single- and double-strand breaks that initiate DNA damage responses (Takahashi et al. 2006; Di Micco *et al*., 2006; Bartkova *et al*., 2006; Hemann and Narita, 2007). Similarly, DNA-damaging chemotherapeutic and radiotherapeutic agents provoke DNA-replication fork stalling and/or DNA single- and double-strand breaks with activation of the DNA damage response network (Holliday and Tarrant 1972, Kung et al. 1990, Di Leonardo et al. 1994, Waldman et al. 1996, Robles and Adami 1998). Indeed, in models of cellular senescence, ATM/ATR mediate the activation of cell-cycle checkpoints associated with cellular senescence, mainly via p53, CHK1 and

CHK2, with the participation of p21, p16 and Rb (Schmitt et al. 2007). It has been suggested previously that after genotoxic drug treatment, cell-cycle arrest and senescence development are dependent on the p53/p21 pathway in HCT116 colon cancer cells (Han et al. 2002). Similar observations concerning the importance of the p53/p21 pathway have been reported with other chemotherapeutic agents or irradiation (Di Leonardo et al. 1994, Waldman et al. 1996, Bunz et al. 1998, Linke et al. 1997). Likewise, studies with bleomycin, actinomycin D and cyclophosphamide have revealed that cells respond to these agents by engaging a p53/p16-dependent long-term senescence program (Robles and Adami 1998, Schmitt et al. 2002). However, others have reported senescence phenotypes (observed by flow cytometry after DNA staining as broader G1 or G2/M peaks, and with the appearance of a senescence-associated β-galactosidase activity) in p53-mutated cell lines derived from various types of human solid tumors, including cervical, larynx and colon carcinoma, glioma, osteosarcoma (Chang et al. 1999a) and lymphoma cell lines (Schmitt et al. 2007).

The DNA damage responses induced in the early phase of cellular senescence initiation explain how cells will activate cell-cycle checkpoints and undergo cell-cycle arrest at specific phases of the cell cycle. However, after DNA damage, cell-cycle arrests do not always lead to cellular senescence. Indeed, cell-cycle arrests often afford cells the opportunity to repair DNA damage before progressing to the next phase of the cycle. In turn, inappropriate progression of damaged cells through the cell cycle is often associated with mitotic catastrophe, apoptosis and cell death. Thus, the stabilization of cell-cycle arrests to irreversible senescence involves other yet unknown critical events. Recently, epigenetic changes, including histone H3 lysine K9 trimethylation (H3K9) associated with gene silencing, have been suggested as critical mechanisms associated with the stabilization of cell-cycle arrest to cellular senescence, as senescent cells show focal histone H3K9 trimethylation. These foci are now referred to as senescence-associated heterochromatin foci (SAHFs) (Schmitt et al. 2007, Strunnikova et al. 2005, Guney and Sedivy 2006, Zhang et al. 2007). Early evidences indicated that H3K9 trimethylation controls DNA methylation in several model organisms (Tamaru and Selker 2001, Tamaru et al. 2003, Jackson et al. 2002). Methylation of CpG islands in promoters and locus control regions is strongly associated with H3K9 trimethylation and gene silencing. Indeed, others have indicated that some gene promoters are hypomethylated, whereas others undergo hypermethylation during cellular senescence, suggesting that differential DNA methylation patterns at specific gene promoters and locus control regions may stabilize the senescence phenotype (Tollefsbol and Andrews 1993).

1.9 ATM, guardian of the genome

Ataxia-telangiectasia (A-T) is an autosomal recessive disorder that is characterized by early-onset progressive cerebellar ataxia, oculocutaneous telangiectasia, susceptibility to bronchopulmonary disease, and lymphoid tumours (Meulmeester et al. 2005). Various other abnormalities are also associated with this disorder, including the absence or the rudimentary appearance of a thymus, immunodeficiency, progressive apraxia of eye movements, insulin-resistant diabetes, clinical and cellular radiosensitivity, cell-cycle checkpoint defects and chromosomal instability (Taniguchi et al. 2002). The gene that is defective in A-T, A-T Mutated (*ATM*), was localized to chromosome 11q22–23 (Houldsworth et al. 1980) and cloned by positional cloning (Falck et al. 2001). ATM is a Ser/Thr protein kinase and is a member of the phospho- inositide 3-kinase (PI3K)-related protein kinase (PIKK) family, which also includes ATM and Rad3-related protein (ATR), the catalytic subunit of DNA-dependent protein kinase (DNA-PKcs) and SMG1, a protein kinase that is involved in the DNA damage response but is also required for nonsense-mediated decay of mRNA that contains premature terminator codons (Lavin and Kozlov 2007). The kinase domain is located close to the C-terminus in all of these proteins except SMG1, in which the kinase domain is more central. This domain has protein kinase activity, and p53 was the first substrate of ATM to be identified *in vitro* and *in vivo* (Peng et al. 1997, Xu et al. 2001, Aprelikova et al. 2001). This was not surprising, because the stabilization and activation of p53 was defective in A-T cells, and these cells were also characterized by a defective G1–S checkpoint, in which p53 has a central role (Yarden et al. 2002, Gatei et al. 2000).

ATM has also a number of other domains, including a FAT domain (which is common to ATM, mammalian target of rapamycin (mTOR) and transformation/transcription domain- associated protein (TRRAP)) (Kozlov et al. 2006) and an extreme C-terminal FATC domain that is found in combination with FAT domain in this subfamily of proteins. Other domains include an N-terminal substrate-binding domain, a leucine-zipper domain, a proline-rich region that enables it to bind to ABL kinase (Suzuki et al. 2004) and a peroxisomal targeting signal sequence (PTSI).

ATM is present in the nucleus as an inactive dimer (or higher order oligomer) that, following DNA damages or structural changes of chromatin, undergoes activation through autophosphorylation and monomerization (Bakkenist and Kastan 2003). Once activated, ATM phosphorylates its substrates on residues of serine or threonine followed by a glutamine residue (the so called S/TQ domain) (Lavin and Kozlov 2003). As above described, ATM associates with the Nbs1-Mre11-Rad50 (NMR) complex during activation process, and this complex subsequently acts as an adaptor for the phosphorylaton of many downstream pathways. The activation of ATM leads to the rapid phosphorylation of a multitude of proteins that are

involved in DNA repair, cell-cycle checkpoint activation and transcription (Kurose et al. 1981, Tanaka et al. 2007). A series of large-scale proteomic studies have identified extensive phosphoprotein networks that are responsive to DNA damage (Stark et al. 2006, Bakkenist and Kastan 2003, Di Tullio et al. 2002). In these studies, as many as 900 induced phosphorylations on ATM and ATR consensus sites of over 700 proteins have been identified. These proteins were found arranged in interconnecting modules that are involved in DNA repair, DNA replication and cell-cycle control (Stark et al. 2006). It is probably unlikely that all of these phosphorylations are direct substrates for ATM, and might be dependent on other PIKKs.

Following its activation, ATM signals to cell-cycle checkpoints to slow the passage of cells through the cycle and facilitate DNA repair (Taniguchi et al. 2002). ATM also responds to physiological breaks in DNA during the development and differentiation of B and T cells (Sapkota et al. 2002). It has been shown that ATM is also activated during the resolution of DNA DSBs that are generated by V(D)J recombination (Viniegra et al. 2005).

Although ATM is predominantly a nuclear protein that responds to DNA DSBs, there is also evidence for a cytoplasmic form, which has been found to be associated with both peroxisomes and endosomes (Banin et al. 1998, Saito et al. 2002). These findings suggest a more general signalling role for ATM that does not involve direct DNA damage. A series of abnormalities in ATM-deficient cells provide indirect evidence for an extranuclear role for ATM (Khosravi et al. 1999). These abnormalities include reduced internalization of phytohaemagglutinin (PHA), defective calcium mobilization, depolarization in response to extracellular potassium, greater growth factor demand and defective signalling through the epidermal growth factor (EGF) receptor. More direct evidence demonstrates the ability of insulin to activate ATM, as shown by the phosphorylation of 4EBP1 and the subsequent dissociation of eukaryotic translation-initiation factor (eIF)4E from 4EBP1, thereby making it available for initiation of mRNA translation (Maya et al. 2001). Pertinent to these results is the observation that some A-T patients develop insulin-resistant diabetes (Pereg et al. 2005, Chen et al. 2005).

Rapid recruitment of DNA damage recognition and repair proteins to distinct foci is observed in response to agents that damage DNA or cause the arrest or collapse of DNA-replication forks (Cortezet al 2004, Yoo et al. 2004). Although this recruitment is rapid, the order in which these proteins localize to sites of DNA damage is gradually being resolved. DNA DSBs lead to the accumulation of the MRN complex, whose retention on chromatin is dependent on the mediator of DNA damage checkpoint protein-1 (MDC1) adaptor protein. ATM also arrives early at the damaged site, initially associating with DNA regions that flank the break, before associating with the MRN complex at the break site through the C-terminus of NBS1 (Buscemi et al. 2006, Oakley et al. 2001). Interaction of MDC1 with ATM through its PHA domain regulates the accumulation of ATM at

damaged sites. MDC1 also mediates the interaction between ATM and the phosphorylated form of H2AX, which presumably contributes to the long-range phosphorylation of H2AX and the maintenance of the response (Yoo et al. 2004). The order of assembly of DNA-damage-response proteins at DNA DSBs, and the structural requirements for their interaction, has been facilitated by the use of microlasers and charged particle tracks to generate DSBs (Di Tullio et al. 2002, Huang et al. 2006). ATM-dependent phosphorylation of the histone variant H2AX to produce γH2AX seems to be the initial signal for subsequent accumulation of DNA-damage-response proteins (Ichijima et al. 2005, McManus et al. 2005).
It seems likely that ATM is at least partially activated adjacent to DNA DSBs (Buscemi et al. 2006), probably owing to the initial relaxation of chromatin structure by the break. The activation of ATM by chloroquine, histone deacetylase inhibitors or hypotonic buffer supports this hypothesis (Rao et al. 2005). However, ATM that is activated by these factors does not localize to nuclear foci and fails to phosphorylate H2AX, but it is capable of phosphorylating p53, which suggests that ATM needs to be localized to the break for complete activation. During its activation, ATM undergoes autophosphorylation on at least three sites (Ser367, Ser1893, Ser1981), and one of them (Ser1981) seems to be instrumental in the monomerization and activation of ATM (Rao et al. 2005, Chen et al. 2005). Activation of ATM by okadaic acid suggests that also phosphatase activity is important in maintaining ATM in a basal state (Dornan et al. 2006). Moreover, agents that alter chromatin structure activate ATM and cause phosphorylation of p53, but fail to induce phosphorylation of SMC1, NBS1 and other substrates (Foray et al. 2002, Rao et al. 2005).
It is indeed evident that ATM plays a central role in responding to DNA DSBs by directly phosphorylating or mediating the phosphorylation and activation of multiple substrates in signalling to the DNA repair machinery and the cell cycle checkpoints.

1.10 Role of ATM and DDR in cellular resistance to genotoxic therapies

As previously mentioned, it is clear that the field of DDR research is of huge relevance to cancer therapy. In fact, aside from surgery, DNA-damaging agents, in the form of radiotherapy and various chemotherapies, are numerically by far the most effective and broadly used treatments for cancer. Secondly, the effectiveness of such treatments and the side effects caused by them reflect the inability of cancer cells and normal cells respectively to repair therapy-induced DNA lesions. Conversely, when such treatments fail and cancer recurs, this is generally due to a fraction of the cancer cells having repaired the therapy-induced DNA lesions (Khanna and Jackson 2001, Kastan and Bartek 2004). To compensate for the loss

of specific DNA repair pathways, different or faulty DNA repair pathways may be induced to enable tumor cells to survive. The activation of other repair pathways has been suggested to be responsible for the limited response of tumors to radio- and chemotherapy. If the DNA repair pathways essential for the survival of cancer cells can be identified and disrupted, this will allow chemotherapy to be much more efficient. Thus, it can be argued that targeting both checkpoint and repair pathways in combination may selectively kill tumor cells over healthy cells (Bolderson et al. 2009). Moreover, it has been suggested that genetically unstable cells such as tumor cells are "addicted" from a single faulty DNA repair mechanism to improve their survival following DNA damages, while normal cells use several DNA repair mechanisms to correctly activate the DDR (Jackson 2009). Based on these observations, several groups have identified a number of chemical compounds that target the DSBs repair machinery, enhancing the effects of genotoxic chemo- and radiotherapy.

The first suggestion that ATM may be an attractive target for chemotherapy was that cells from patients with the genomic instability disorder ataxia telangiectasia, resulting from a mutation in the ATM gene, were exquisitely sensitive to radiation (Savitsky et al. 1995). In addition, caffeine (a known inhibitor of ATM) could increase cellular sensitivity to radiation and chemotherapeutic drugs (Sarkaria et al. 1999, Sabisz et al. 2008), although its lack of specificity and potency makes it unsuitable as a clinical agent. LY294002 is another ATM inhibitor, which broadly inhibits the kinase activity of PIKKs. Like caffeine, the widespread use of LY294002 has been restricted by its lack of specificity. However, it has been used as a research tool for the design of more specific PIKK inhibitors. A highly specific small molecule ATP competitive inhibitor of ATM named KU-55933 was identified via screening of a drug library based on LY294002 (Hickson et al. 2004). This compound can efficiently sensitize tumor cells to radiation and DSB-inducing chemotherapeutic agents, such as camptothecin and etoposide, and there are suggestions that this compound may be used as a potential clinical treatment. There is also an indication that inhibitors of the ATM-mediated pathway may also sensitize cells deficient in other DNA repair pathways to cancer treatments. Validation of this idea was initially borne out when a high-throughput iRNA screen identified ATM as a target that disrupted the growth of cells deficient in the Fanconi anemia (FA) pathway (Kennedy et al. 2007).

As for A-T cells, cells lacking DNA-PK are hypersensitive to IR and to DNA-crosslinking agents, and are defective in DSB repair, whereas increased DNA-PK activity confers radioresistance and chemoresistance on tumor cells (Collis et al. 2005, Shinohara et al. 2005); these reports lead to the conclusion that inhibition of DNA-PK could prevent efficient DNA repair, and thus could lead to accumulation of cytotoxic DNA lesions. Several selective DNA-PK inhibitors have also been developed recently: NU7026, NU7441, vanillin, IC87102, IC87361, and Su11752 (Shinohara et al. 2005, Durant et al. 2003, Ismail et al. 2004, Willmore et al.

2004). These agents impede DSB repair and sensitize tumor cells to IR and/or DNA-damaging agents such as idarubicin, daunorubicin, etoposide, doxorubicin and cisplatin to different extents and with varying degrees of specificity. In addition, there are also reports that some DNA-damaging agents can inhibit DNA-PK activity themselves, e.g. inhibiting topoisomerase II at the same time as disrupting the NHEJ pathway, providing an explanation for their greater effectiveness in cancer treatment (Lu et al. 2005).

In addition to directly inhibiting ATM, ATR and DNA-PK pharmacologically, the levels of expression could also be regulated by using small interfering RNAs (siRNAs). For example, transfection of cells with specific siRNAs that target messenger RNAs, the expression level of ATM, ATR, or DNA-PKcs was reduced by 90%, and the resulting radiosensitivity was significantly higher than with use of wortmannin or LY294002 (Collis et al. 2003)

Indeed, these data suggest that identification of new drugs or pharmacological approaches to inhibit the activity of ATM and/or to affect the DDR could reduce chemo-resistance and radio-resistance of cancer cells, main obstacles in the treatment and management of malignant cancers.

2. AIM OF THE STUDY

Despite compelling evidences and results have suggested a critical role of HMGA proteins in DNA repair, the mechanisms by which they act in this fundamental cell process are still controversial and poorly understood. By sequence analysis we found a conserved SQ motif in both HMGA1 and HMGA2, the consensus recognized and phosphorylated by ATM. Therefore we investigated whether ATM interacts and phosphorylates HMGA proteins. Our results, reported here, prompted us to further investigate the role of HMGA proteins in the ATM pathway. Given the widely described ability of HMGA proteins to modulate gene expression, we analyzed the ability of both HMGA1 and HMGA2 to bind and regulate *ATM* promoter. Subsequently, we investigated the role of this novel identified ATM/HMGA pathway in the cellular response to different stresses affecting DNA stability. Finally, since it has been recently demonstrated that inhibition of ATM kinase activity reduces cancer cells resistance to DNA damaging agents, we explored the possibility that abrogation of HMGA protein expression could be used to enhance tumor sensitivity to genotoxic treatments.

3. MATERIALS AND METHODS

3.1 Chemicals and treatments

For γ-irradiation experiments, cells were irradiated by 6 MV X-ray of a linear accelerator with doses ranging from 0 to10 Gy. For UV-irradiation experiments, cells were treated using a Stratalinker 1800 (Stratagene) with doses ranging from 0 to 20 J/m^2. For ATM inhibition experiments, cells were treated with KU-55933 (10 μM) for 1 h.

3.2 Immunoprecipitations and Western Blots

Cell extracts were prepared and co-immunoprecipitations were performed as previously described (Pentimalli et al. 2008) in the presence or absence of 100 ng/μl ethidium bromide. Anti- FLAG M2 (Sigma) or anti-HA Clone 12CA5 (Roche) monoclonal antibodies were used for co-immunoprecipitation experiments along with protein A/G-sepharose (Amersham Biosciences). Anti-P-ATM-substrate (phospho-Ser/Thr antibody) (Cell Signalling Technology) was used to evaluate the phosphorylation of HMGA proteins by ATM *in vivo*. Proteins were resolved by 3–8% NuPAGE (Invitrogen) or by 15% SDS–PAGE and transferred to high or low molecular weight nitrocellulose, respectively. Western blots were performed using the above-mentioned anti-FLAG and anti-HA antibodies, or anti-ATM polyclonal antibody (Novus Biologicals) anti-HMGA1 and anti-HMGA2 polyclonal antibodies (raised against the amino-terminal region of the proteins), anti-ATM S181p (Rockland), anti-p53 DO-1 and anti-p-p53 (Ser15) (Santa Cruz). Anti-vinculin (7F9) (Santa Cruz) was used as loading control. All the antibodies were diluted (1:200/500) in 5% non-fat dry milk (Biorad).

3.3 Cell cultures, Transfections and Plasmids

HEK-293T, MCF-7, SAOS-2, HeLa and FRO cells were cultured in DMEM supplemented by 10% foetal bovine serum (FBS), 2 mM L-glutamine, 100 U/ml penicillin and 0.1 mg/ml streptomycin (GIBCO-BRL). PC-Cl3 cells were grown in Ham's F-12 medium, Coon's modification (Sigma) supplemented with 5% foetal calf serum (FCS) (ICN Flow), and six growth factors (10 nM TSH, 10 nM hydrocortisone; 100 nM insulin; 5 μg/ml transferrin; 5 nM somatostatin; 20 μg/ml glycyl-hystidyl-lysine) (6H). MEFs were established from 14.5 dpc embryos following the standard procedures, and cultured in DMEM supplemented

by 10% FBS, 2 mM L-glutamine, 100 U/ml penicillin, 0.1 mg/ml streptomycin and 1% non-essential aminoacids (GIBCO-BRL). FRTL-5, FRTL-5-Ki and FRTL-5-asHMGI-Ki cells (provided by Dr. M.T. Berlingieri) were cultured as described by Berlingieri et al. (1995). NIH-3T3 cells were grown in DMEM supplemented with 10% FCS, 100 U/ml penicillin and 0.1 mg/ml streptomycin (GIBCO-BRL). MEFs were transfected using Neon Electroporation System (Invitrogen) according to manufacturer's instructions. All the other transfections were performed by Lipofectamine 2000, as suggested by the manufacturer. HMGA1 and HMGA2 cDNA were cloned into pCEFL-HA in frame with the HA epitope, as described elsewhere (Pierantoni et al. 2001, Fedele et al. 2006). The pFLAG-ATM previously described (Canman et al. 1998) were kindly provided by Dr M.B. Kastan. The pLucATM reporter plasmid was a kind gift of Dr D. Ginsberg.

3.4 Luciferase and Clonogenic assays

For the Luciferase assay, cells were seeded into each well of six well plate and transiently transfected with 1 μg of pLucATM and with 500 ng of pCEFLHa-HMGA1 and pCEFLHa-HMGA2 (except for PC-Cl3 cells, transfected with 50 ng of the same plasmids), together with 0.5 μg of Renilla and various amounts of the pCEFLHa plasmid to keep constant the total DNA concentration. Luciferase and Renilla activity were assessed with the dual light luciferase system (Promega). The Luciferase activity was normalized for the Renilla activity. All the experiments were performed three times in triplicate, and the mean ± S.D. was reported.
For the clonogenic assay, FRTL-5, FRTL-5-Ki, FRTL-5-asHMGI-Ki, FRO and FRO-asHMGI cells were seeded at a density of 10^3 cells per 35-mm dish. Two days after, cells were treated with different doses of UV-light or IR, as described in the results. After 10 or 15 days, cells were stained with 500 mg/ml of crystal violet in 20% methanol, and the resulting colonies were counted. The mean of colony counts normalized for untreated control was reported.

3.5 Senescence assays

Early-passage MEFs, FRTL-5, FRTL-5-Ki and FRTL-5-asHMGI-Ki cells were treated as described in the results, and Senescence-Associated-β-galactosidase activity was assessed. Cells were washed in PBS, fixed for 7 min (room temperature) in 2% formaldehyde/0,2% glutaraldehyde, washed and incubated at 37ºC (without CO_2) over-night with fresh Senescence-Associated-β-galactosidase staining. Cells were analyzed with light microscopy to determine the

percentage of senescent cells. At least 20 fields for each experimental point were analyzed. Reported values are the mean ± S.D. of three independent experiments.

3.6 Cell-cycle analysis

Cells were plated in 6-well plates at a density of 10^6 cells per well, incubated for 24 h and then exposed to 20 J/m^2 of UV. Where indicated, cells were also treated with 0,2 μg/ml of Nocodazole, following the UV-treatment. Cells were harvested at different timepoints, as indicated in the results, then fixed with ice-cold 70% ethanol, treated with RNase-I (Invitrogen) and stained with 10 μg/ml of Propidium Iodide to label DNA. Cells were sorted on a FACS-Calibur flow cytometer (Becton Dickinson), and the results were analysed with ModFit software, 3.2 version (Verity Software House). Experiments were performed in triplicate and representative cell-cycle profiles were reported.

3.7 Apoptosis Assays

FRO and FRO-asHMGI were plated in 6-well plates at a density of 10^6 cells per well, incubated for 24 h and untreated or exposed to 20 J/m^2 of UV. Cells were then harvested after 24 h, fixed with ice-cold 70% ethanol, stained with 10 μg/ml of Propidium Iodide to label DNA and FITC-Annexin V antibody (BD Biosciences), following manufacturer's instructions. Annexin V-PI positive cells were analyzed using FACS-Calibur flow cytometer (Becton Dickinson). Experiments were performed in triplicate and representative annexin V-PI profiles were reported. Apoptosis was also quantified by measuring caspase 3 and 7 activation, using Caspase-Glo 3/7 assay (Promega) on a Bio-Tek Synergy HT multi detection microlpate reader. The assay was performed three times in triplicate, and the mean ± S.D. was reported.

3.8 RNA extractions and semiquantiative (sq)RT-PCR

Total RNAs were extracted from cell culture using TRI REAGENT (Molecular Research Center, Inc.) solution, according to the manufacturer's instructions. The integrity of the RNA was assessed by denaturing agarose gel electrophoresis (virtual presence of sharp 28S and 18S bands) and spectrophotometry. RNAs were treated with Dnase-I (Invitrogen) and reverse-transcribed using random exanucleotides as primers and MuLV reverse transcriptase (Perkin Elmer). For semiquantitative PCR, reactions were optimized

for the number of cycles to ensure product intensity within the linear phase of amplification. The PCR products were separated on a 2% agarose gel, stained with ethidium bromide and scanned using a Typhoon 9200 scanner. Primers used were:
mmuATM-F: 5'-ATTGGGATGCTGTTTTCAGG-3'
mmuATM-R: 5'-TAGCCTGGGTGCTCTTTTGT-3'
mmup21-F: 5'-TCCACAGCGATATCCAGACA-3'
mmup21-R: 5'-GGCACACTTTGCTCCTGTG-3'
mmuActin-F: 5'-TCAGAAGGACTCCTATGTGG-3'
mmuActin-R: 5'-CGCAGCTCATTGTAGAAGGT-3'

3.9 Chromatin Immunoprecipitation (ChIP) assays

ChIP assays were carried out with an acetyl-Histone H3 immunoprecipitation assay kit (Upstate Biotechnology) according to manufacturer's instructions, as described by De Martino et al. 2009. Chromatin was immunoprecipitated from NIH-3T3 and 293T cells transfected with pCEFLHa-HMGA1, pCEFLHa-HMGA2 or the empty vector using 2 μg of anti-HA antibody (Santa Cruz) or normal rabbit IgG as negative control. Input and immunoprecipitated DNA were analyzed by PCR to detect the presence of human or murine *ATM* promoter. PCR reactions were performer with AmpliTaq gold DNA polymerase (Applied Biosystems). Primers used to amplify the sequence of promoters were:
mmuATMprF: 5'-ATTGGGATGCTGTTTTCAGG-3'
mmuATMprR: 5'-TAGCCTGGGTGCTCTTTTGT-3'
hsaATMprF: 5'-AACACAGCGACAGCTCCTG-3'
hsaATMprR: 5'-AGTGACGACAGTTCCGAAGG-3'

3.10 Comet Assays

MEFs irradiated or not with 4 Gy of IR were allowed to repair the DNA for 0 and 3 h in complete medium and then processed for the COMET assay (Trevigen). The assay was performed following manufacturer's instructions. Briefly, MEFs were plated at a density of 1 x 10^5 cells/ml the day before the assay. Cells were exposed or not to 4 Gy of IR, allowed to repair for 3 h and then harvested in 1 ml of PBS 1X. 50 μl of cells were suspended in 500 μl of low melting point agarose and pipetted onto a CometSlide™. Slides were incubated at 4°C for 20 min in the dark, immersed in prechilled lysis solution for 45 min and then in alkaline solution for 60 min in the dark. After two washes in TBE 1X, slides were transferred in a horizontal electrophoresis apparatus, covered with

TBE 1X buffer and run for 30 min at 1 V/cm. Slides were then incubated in ethanol for 5 min, air dried, and stained with SYBR™ Green and analysed with epifluorescence microscopy. Cell images were analysed using COMET Score™ (TriTek Corp.). Comet tail moment was used as the measure of DNA damage. In each experiment, 100 comets were measured per experimental point and the mean tail moment values ± S.D. were evaluated.

4. RESULTS AND DISCUSSION

4.1 HMGA proteins interact and are phosphorylated by ATM

Similarly to other PIKKs, ATM phosphrylates its substrates on serine or threonine residues, generally followed by glutamine (the so-called SQ/TQ or S/TQ motif). Since HMGA proteins are extensively post-translationally modified and phosphorylation has been frequently reported (Edberg et al. 2005, Sgarra et al. 2004, Zou and Wang 2005), we decided to investigate whether ATM can interact with and phosphorylate HMGA1 and HMGA2. Sequence analysis revealed that both HMGA proteins contain in their COOH terminal region a consensus site for ATM phosphorylation (serine 88/glutamine 89 for HMGA1, serine 102/glutamine 103 for HMGA2), which is highly conserved among different species and the different HMGA family members (Figure 1a). To determine whether ATM interacts *in vivo* with HMGA1, we transiently transfected 293T cells with expression vectors containing the full-length cDNAs for *ATM*, fused to the FLAG tag, and *HMGA1* fused to the HA epitope. Total cell lysates were immunoprecipitated using an anti-HA antibody and analyzed by western blot using either anti-ATM or anti-FLAG antibodies. As shown in Figure 1b, FLAG-ATM was specifically co-immunoprecipitated with HA-HMGA1. Moreover, HA-HMGA1 was able to interact and co-immunoprecipitate also with the endogenous ATM protein. Similar experiments were obtained transfecting 293T cells with FLAG-ATM and HA-HMGA2 contructs. In fact, following immunoprecipitation using anti-FLAG antibody, HA-HMGA2 was revealed by western blotting using anti-HA antibody only in cells expressing FLAG-ATM (Figure 1c). Like HA-HMGA1, also HA-HMGA2 interacted with endogenous ATM, as shown in Figure 1d. Since ATM and HMGA proteins are chromatin-associated proteins, co-immunoprecipitations in Figure 1b and 1c were performed also in the presence of ethidium bromide, to exclude that their co-immunoprecipitations may be dependent on contaminating DNA.

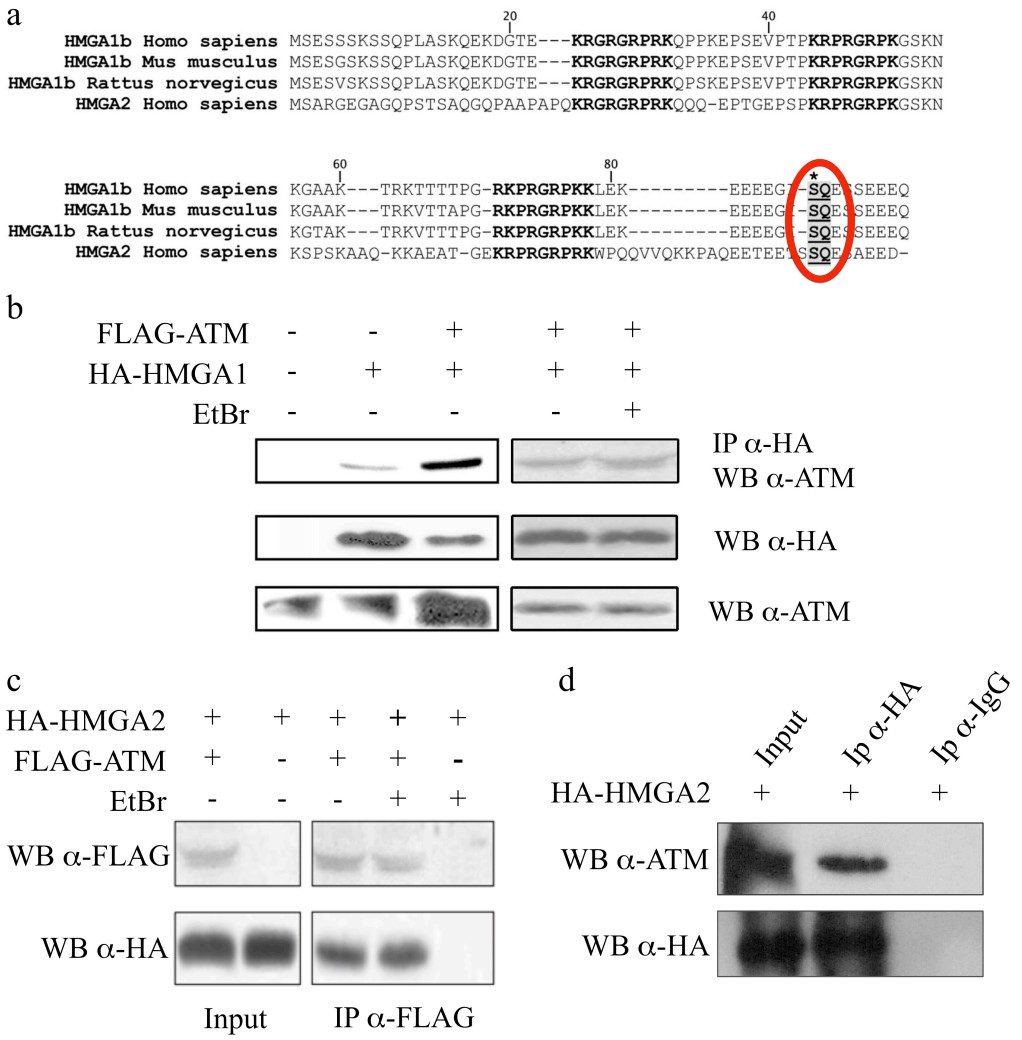

Figure 1. HMGA proteins interact with ATM. (a) Aminoacid sequence alignment of HMGA1 and HMGA2 from the indicated species (AT-hooks are shown in bold, ATM consensus site is circled in red). (b-d) 293T cells were transfected as indicated, and total cell lysates were immunoprecipitated using anti-HA or anti-FLAG antibodies. Western blots were performed using the antibodies indicated on the side. Ethidium bromide (EtBr) was added during immunoprecipitations to exclude that co-immunoprecipitation could be dependent from contaminating DNA. Normal rabbit IgG (d) were used as a negative control for the co-immunoprecitipation of HA-HMGA2 and endogenous ATM.

To assess *in vivo* that HMGA1 and HMGA2 are phosphorylated by ATM, 293T cells were transfected with HA-HMGA1 or HA-HMGA2 expression vectors and treated with 10 Gy of IR. To assess the specificity of the phosphorylation, cells

were also treated with 10 μM KU-55933, a specific inhibitor of ATM kinase, for 1 h before the exposure to IR. Cells were collected 30 min after the IR treatment and total cell lysates were immunoprecipitated using an antibody that recognizes serine and threonine residues phosphorylated by ATM (Anti-P-Sub-ATM). Analysis of the immunoprecipitates from HA-HMGA1-transfected cells by western blot using an anti-HA antibody revealed a band corresponding to the HA-HMGA1 only in cells exposed to IR. . This co-immunoprecipitation was prevented by using KU-55933 to inhibite ATM kinase activity (Figure 2a). Conversely, HA-HMGA2 was immunoprecipitated by the Anti-P-Sub-ATM also in cells not treated with IR. However, IR treatment significantly increased the amount of immunoprecipitated HA-HMGA2, and ATM inhibition by KU-55933 prevented this increase (Figure 2b).

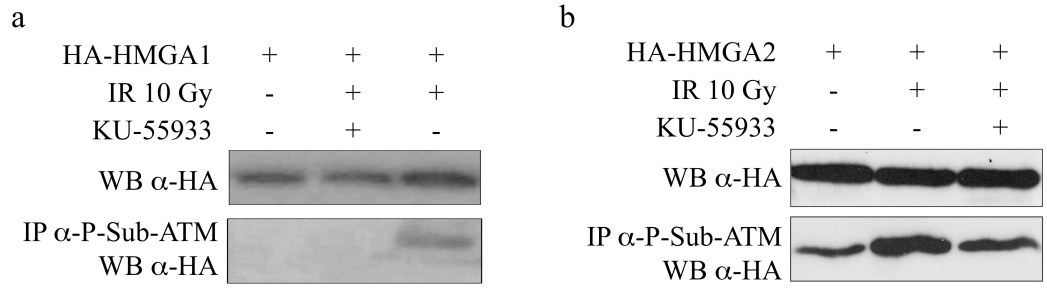

Figure 2. HMGA proteins are phosphorylated *in vivo* by ATM. 293T cells transfected with vectors expressing either HA-HMGA1 (a) or HA-HMGA2 (b) were treated or not with a 10 Gy dose of IR to induce activation of endogenous ATM. Total cell extracts were immunoprecipitated with an antibody able to recognize serine and threonine residues phosphorylated by activated ATM (Anti-P-Sub-ATM). Immunoprecipitates were analysed by SDS–PAGE followed by Western blot with anti-HA antibody. 293T cells were also pre-treated for 1 h with 10 μM KU-55933 as a control of the phosphorylation specificity.

These data indicate that both HMGA1 and HMGA2 are novel interactors and substrates of ATM, following exposure to DNA damaging agents, such as IR. Moreover, they show that HMGA2 is also phosphorylated by other kinases in unperturbed cells, but its state of phosphorylation is significantly increased by the induction of ATM kinase activity.

4.2 Lack of *Hmga1* and *Hmga2* affects ATM expression

As mentioned above, HMGA proteins positively or negatively regulate the transcriptional activity of several genes (Fusco and Fedele 2007, Fedele et al. 2001). In particular, our previous studies have demonstrated that HMGA proteins

enhance E2F1 transcriptional activity by displacing HDAC1 from the pRB/E2F1 complex (Fedele et al. 2006 Since it has been shown that the *ATM* gene is a target for positive regulation by E2F1 (Berkovich and Ginsberg, 2003), we thought to evaluate a possible physiological role of HMGA proteins in the regulation of *ATM* expression. To this aim we analyzed the expression levels of ATM mRNA and protein in Mouse Embryonic Fibroblasts (MEFs) lacking one or both *Hmga* genes (De Martino et al., manuscript in preparation). As reported in Figure 3, western blot and semi-quantitative RT-PCR analysis showed that the expression levels of ATM are strongly influenced by the presence of HMGA proteins. In fact, ATM mRNA and protein levels were strongly reduced in MEFs carrying only one disrupted *Hmga* gene (*Hmga1-/-* or *Hmga2-/-* MEFs) were strongly reduced, compared to wild-type controls, and almost absent in double knock-out MEFs (*Hmga1-/-/Hmga2-/-* or *Hmga1/2* DKO MEFs). These results, indicative of a positive regulation of ATM expression by HMGA proteins, are consistent with the above-mentioned role of HMGA in the positive regulation of E2F1 transcriptional activity. Moreover, reduced levels of active ATM, assessed using an antibody directed against its phopshorylated serine 1981 (ATMser1981), were also reduced in *Hmga1/2* DKO MEFs compared to wild-type controls. These observations suggested that HMGA proteins have a positive role in the control of both *ATM* expression and activation, leading us to further investigate a possible impairment of ATM-downstream pathways in *Hmga1/2* DKO MEFs.

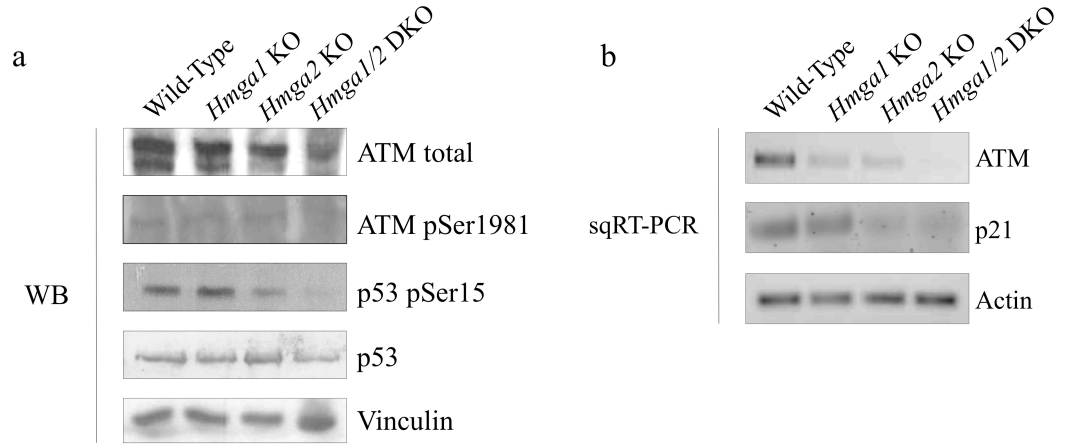

Figure 3. Reduced expression and activation of ATM in *Hmga1/2* DKO MEFs. (a) Total cell extracts from wild-type, *Hmga1* SKO, *Hmga2* SKO and *Hmga1/2* DKO MEFs were analyzed by SDS-PAGE and western blot using the indicated antibodies. Vinculin was analyzed as a loading control. (b) Semi-quantitative (sq) RT-PCR, using mRNA from cells as in (a), was used to assess *ATM* and *p21* gene expression levels. *Actin* gene expression was evaluated as well to normalize RNA levels.

Previous studies on Atm-/- MEFs have indicated a significant involvement of p53 and p21 in cellular defects in the absence of ATM protein (Xu et al. 1996, Xu et al. 1998). In fact it has been demonstrated that, following DNA damage, ATM phosphorylates p53 and enhances its transcriptional activity on several target promoter, such as p21 (Lavin and Kozlov 2007). Therefore, we first analyzed the levels of p53 phosphorylation on serine 15 (p53ser15), the p53 residue that is the target of ATM kinase activity (lavin1). According to the reduced expression of ATM in *Hmga1/2* DKO MEFs, we found that the absence of HMGA proteins reduced the phosphorylation of p53 on this residue (Figure 3a). Then, p21 expression was analyzed. As Figure 3b shows, the absence of both *Hmga* genes almost abolished the levels of p21 mRNA. However, MEFs lacking only the *Hmga1* gene showed only a slight reduction of p21 mRNA, while *Hmga2* knock-out MEFs expressed p21 mRNA levels comparable to *Hmga1/2* DKO MEFs. These data suggest that HMGA proteins, and in particular HMGA2, exert a positive effect on p21 expression, dependent, at least in part, by the ATM/p53 pathway.

4.3 HMGA proteins bind and activate *ATM* promoter

To investigate whether HMGA proteins bind ATM promoter *in vivo*, we performed ChIP experiments using both murine NIH-3T3 (Figure 4a) and human 293T (Figure 4b) cells transiently transfected with either HA-HMGA1 or HA-HMGA2 expression vectors. Transfection with the empty vector pCEFL-HA was also carried out as a negative control. Chromatin was immunoprecipitated using anti-HA or normal rabbit IgG antibody. As shown in Figures 3a and 3b, the ATM promoter was amplified only from the DNA recovered with anti-HA antibody in both NIH-3T3 and 293T cells transfected with HA-HMGA1 or HA-HMGA2, but not in cells transfected with the empty vector. No amplification was obtained in the samples immunoprecipitated using normal rabbit IgG.

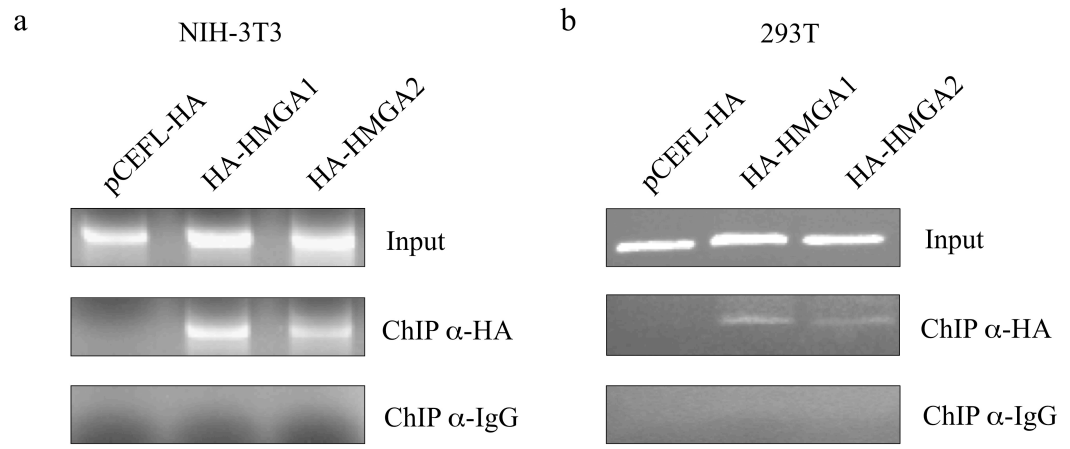

Figure 4 HMGA proteins bind the *ATM* promoter *in vivo.* Lysates from murine NIH-3T3 (a) and human cells, transfected with plasmids expressing HA-HMGA1, HA-HMGA2 and empty vector, as indicated in the above the panels, were subjected to ChIP using specific polyclonal antibody, as indicated on the right. Immunoprecipitates from each sample were analyzed by PCR using specfic primers for mouse and human ATM promoter.

To confirm the positive effect of HMGA proteins on the *ATM* promoter, we performed luciferase assays transfecting a construct expressing the luciferase reporter gene under the transcriptional control of the human *ATM* promoter (pLuc-ATM, region -512 to +9) (Berkovich and Ginsberg, 2003) along with either HMGA1 or HMGA2 expression vectors. As previously described, ATM promoter activity is dependent on the cellular context (Gueven et al. 2003), as well as HMGA proteins transcriptional activity (Martinez-Hoyos et al. 2004), therefore we performed luciferase assays in different cell types, including HeLa, SAOS-2, NIH-3T3, MCF-7 and PC-Cl3 cells. As shown in Figures 5a-e, transfection of HMGA1 had a positive effect on ATM promoter transcriptional activity in SAOS-2 and MCF-7 cells. Otherwise, HMGA2 activates ATM promoter in NIH-3T3 and HeLa cells. Finally, both HMGA1 and HMGA2 up-regulate *ATM* promoter in PC-Cl3 cells. To further confirm our observations, we transfected the pLuc-ATM reporter plasmid in wild-type, *Hmga1* KO, *Hmga2* KO and *Hmga1/2* DKO MEFs. Figure 5f shows that transcriptional activity of ATM promoter is strongly dependent on the presence of HMGA proteins. In fact, absence of HMGA1, HMGA2 or both HMGA proteins significantly reduced ATM promoter activity, accordingly with the results obtained from semi-quantitative RT-PCR and western blot experiments (Figure 2).

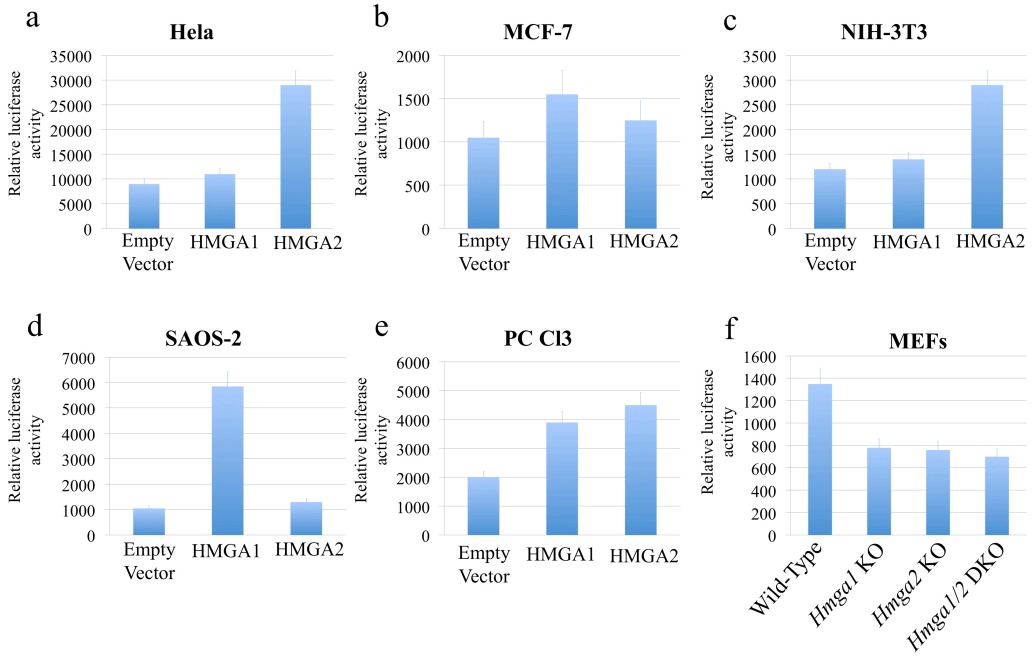

Figure 5. Regulation of *ATM* promoter by *HMGA* proteins. (a-e) HeLa (a), MCF-7 (b), NIH-3T3 (c), SAOS-2 (d) and PC-Cl3 (e) cells were transfected with expression vectors for either HMGA1 or HMGA2, along with luciferase reporter vector pLuc-ATM. Luciferase activity was assessed 48 h after the transfection. (f) Wild-type, *Hmga1* KO, *Hmga2* KO and *Hmga1/2* DKO MEFs were transfected with pLuc-ATM and luciferase activity was assessed after 48 h. The data reported are the mean ± S.D. of three independent experiments performed in triplicate.

4.4 Phosphorylation of HMGA proteins by ATM enhances their transcriprional activity on *ATM* promoter

ATM activation by DNA damaging agents determines the direct and indirect phosphorylation of a number of substrates, which results in the modulation of their function in order to trigger an effective cellular response to the DNA damage (Lavin and Kozlov 2007). Therefore, we hypothesized that ATM-dependent phosphorylation of HMGA1 and HMGA2 could have a role in the modulation of their function following the exposure to DNA damaging agents. To evaluate this potential effect of ATM kinase activity on HMGA proteins, we performed luciferase assays co-transfecting the expression vectors encoding HMGA1 (Figure 6a) or HMGA2 (Figure 6b) along with the reporter construct pLuc-ATM, and assessed HMGA protein activity on ATM promoter following the exposure to IR. The transfections were performed in PC-Cl3 normal thyroid cells, which express very low levels of endogenous HMGA1 and HMGA2 with low

amounts of the HMGA expression vectors (50 ng), to prevent any toxic effect following the overexpression of these proteins. After 24 h from the transfection, PC-Cl3 cells were treated or not with 3 Gy of IR, in order to activate ATM kinase activity. As a specificity control of ATM kinase activation, cells were also pre-incubated with KU-55933 for 1 h. As shown in Figures 6a and 6b, in the absence of HMGA proteins, both IR and KU-55933 did not affect the transcriptional activity of *ATM* promoter. Otherwise, in cells transfected with either HMGA1 or HMGA2, IR slightly but significantly ($p<0,05$) enhanced HMGA-dependent up-regulation of this promoter.
Conversely, the treatment with KU-55933 prevented the IR-dependent increase of HMGA activity on ATM promoter, indicating that this effect is dependent on ATM kinase activity.

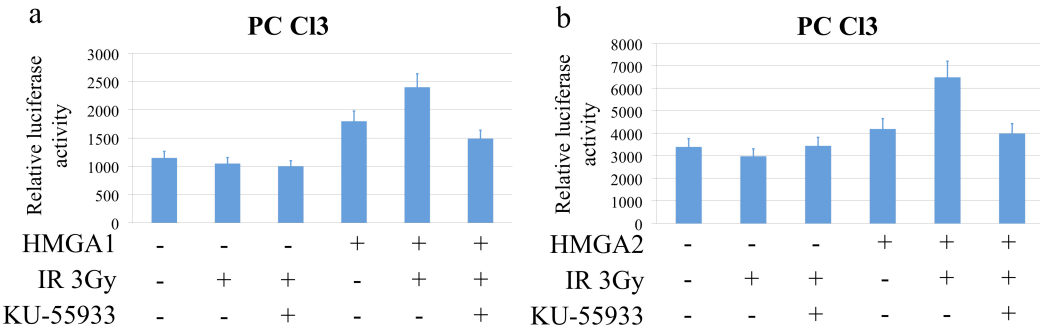

Figure 6 DNA damage activates HMGA-mediated *ATM* expression. PC-Cl3 cells were transfected with expression vectors encoding for HMGA1 (a) or HMGA2 (b), along with the luciferase reporter vector pLuc-ATM. 24 h after transfection, cells were treated or not treated with 10 μM KU-55933 for 1 h and then treated with 3 Gy of IR. 24 h after IR exposure, luciferase activity was assessed. Data reported are the mean ± SD of three independent experiments performed in triplicate.

These data clearly indicate that HMGA proteins play a crucial role in the regulation of expression of ATM. Moreover our observations indicate the existence of a positive feedback loop on *ATM* promoter dependent by HMGA proteins. Following ATM activation in response to DNA damage, HMGA proteins increase their transcriptional activity and sustain the expression of ATM.

4.5 MEFs lacking *Hmga* genes display an altered DNA damage response

The data discussed above led us to investigate the biological effect of the HMGA-mediated regulation of *ATM* gene expression. To this aim, we analyzed the DNA damage response of MEFs lacking one or both *Hmga* genes, by

performing a single-cell gel electrophoresis (Comet) assay on these cells, following IR exposure. Wild-type, *Hmga1 -/-*, *Hmga2 -/-* and *Hmga1/2* DKO MEFs were either treated or not with 4 Gy of IR to induce DNA DSBs and activate ATM-mediated DDR. Cells were harvested before or immediately after the treatment, or were allowed to repair DNA damage for 3 h. Then, we analyzed the ability of their DNA to migrate far from the cell under the influence of an electric field. Only undamaged DNA retains round shape, while damaged DNA migrates away from the nucleus depending on the molecular weight of DNA fragments, acquiring the characteristic comet shape. After the staining of DNA with Sybr Green, cells were analyzed by fluorescence microscopy and images were acquired and analyzed by the COMET SCORE^{TM} freeware (Figure 7a). To quantify the amount of damaged DNA, we evaluated the "tail moment" (a parameter that keeps in count the comet length, the tail length, and the percentage of DNA contained in the head and in the tail of the comet) of comets. *Hmga1 -/-*, *Hmga2 -/-* and *Hmga1/2* DKO MEFs displayed similar levels of DNA damage before and immediately after the treatment with IR compared to wild-type MEFs (Figure 7b). However, after 3h, wild-type MEFs almost completely recovered the damage, while *Hmga1/2* DKO still showed significant levels of damaged DNA. In contrast, *Hmga1 -/-* and *Hmga2 -/-* MEFs did not significantly differ from wild-type controls. These observations suggest that absence of both HMGA proteins determines a significant impairment of the DNA-damage repair machinery, probably because of the reduced cellular levels of ATM. However, the presence of only one of the two *HMGA* genes is sufficient to sustain enough levels of ATM that, in turn, promotes DNA damage repair.

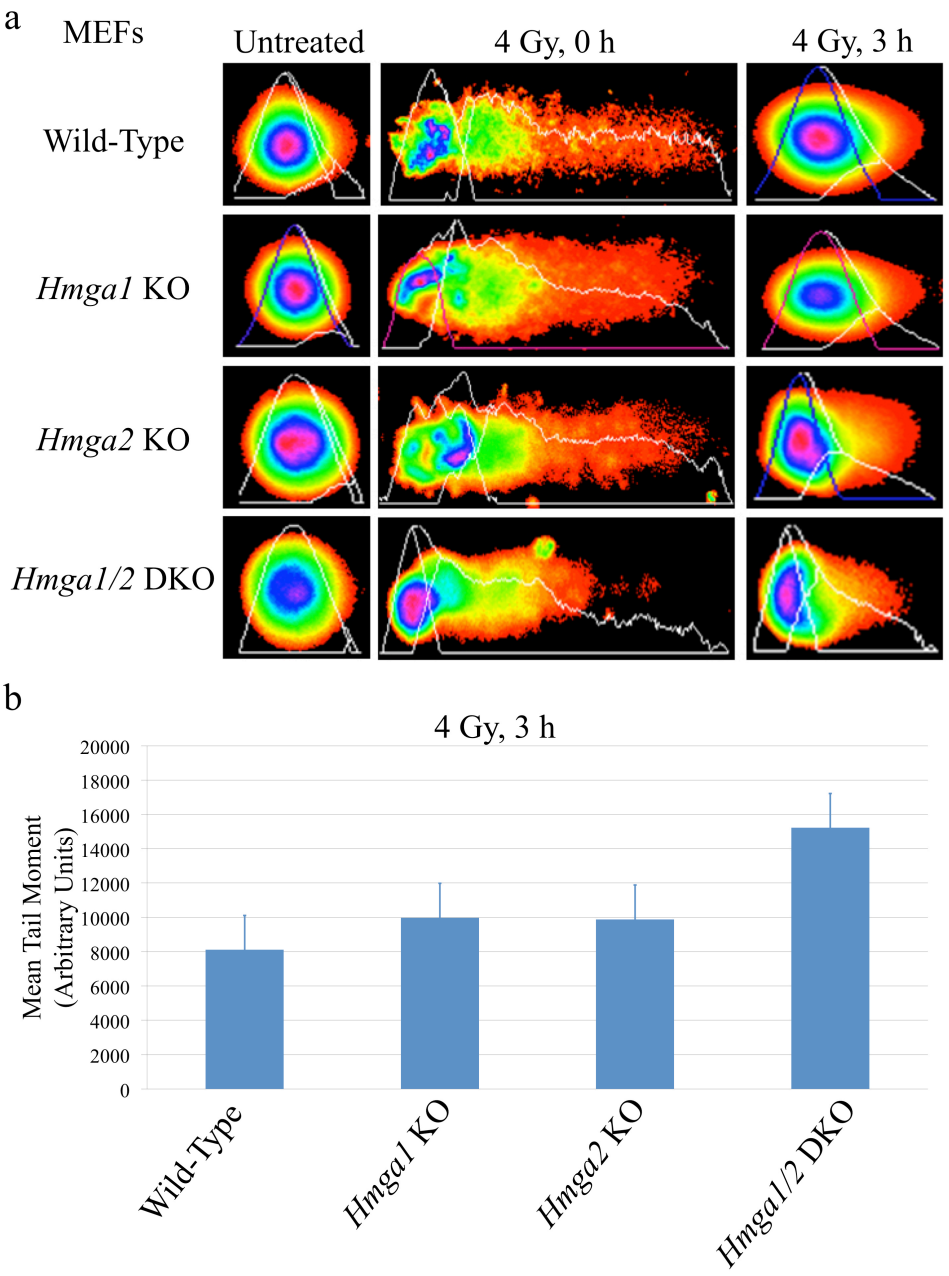

Figure 7. Impaired DNA damage repair in MEFs lacking HMGA1 and HMGA2. (a) Wild type, Hmga1-null, Hmga2-null and Hmga1/Hmga2-null MEFs, exposed or not to 4 Gy of IR, were allowed to repair for 0 h and 3 h and processed for COMET assay. Cells were stained with SYBR Green, visualized by fluorescence microscopy and then analyzed by COMET Score. A representative comet is shown.(b) DNA damage was quantified analyzing comet tail moment using COMET Score. The bars represent the mean tail moment values ± S.D. of three independent experiments (100 comets were measured per experimental point in each experiment).

4.6 Impaired expression of HMGA proteins prevents stress-induced senescence

As previously described, ATM also plays a key role in cellular senescence, and several recent reports has demonstrated that stress- and oncogene-induced senescence has a key role in the process of transformation and in the acquisition of resistance to genotoxic therapies (d'Adda di Fagagna 2008, Crescenzi et al. 2008, Viale et al. 2009). Moreover, our previous data indicated that *Hmga1/2* DKO MEFs undergo replicative senescence more rapidly than wild-type MEFs (De Martino et al. manuscript in preparation). Therefore, we decided to investigate whether absence of HMGA proteins can affect stress-induced senescence in early-passage MEFs. Wild-type, *Hmga1 -/-*, *Hmga2 -/-* and *Hmga1/2* DKO MEFs were treated with sub-lethal doses of IR (1-2Gy) and senescence-associated β-galactosidase (SA β-gal), a marker of cellular senescence, was assessed 72 h after the treatment. As shown in Figure 8a, untreated MEFs, regardless of the genotype, showed similar levels of SA β-gal positive cells. Conversely, following IR exposure, we observed a significant increase in SA β-gal positive cells only in wild-type and *Hmga2 -/-* MEFs, while *Hmga1 -/-* and *Hmga1/2* DKO MEFs were almost refractory to the stress-induced senescence. Figure 8b shows a quantification of SA β-gal positive cells for wild-type, *Hmga1 -/-*, *Hmga2 -/-* and *Hmga1/2* DKO MEFs, untreated or following IR exposure. This result suggests that absence of both HMGA1 and HMGA2 prevents stress-induced senescence, probably because of their low levels of ATM. Moreover, HMGA1 seems to be more involved than HMGA2 in this process, because only *Hmga1 -/-*, and not *Hmga2 -/-* cells, were resistant to stress-induced senescence. Therefore, other ATM-independent pathways, involved in IR-induced senescence, are likely to be affected by the absence of HMGA1.

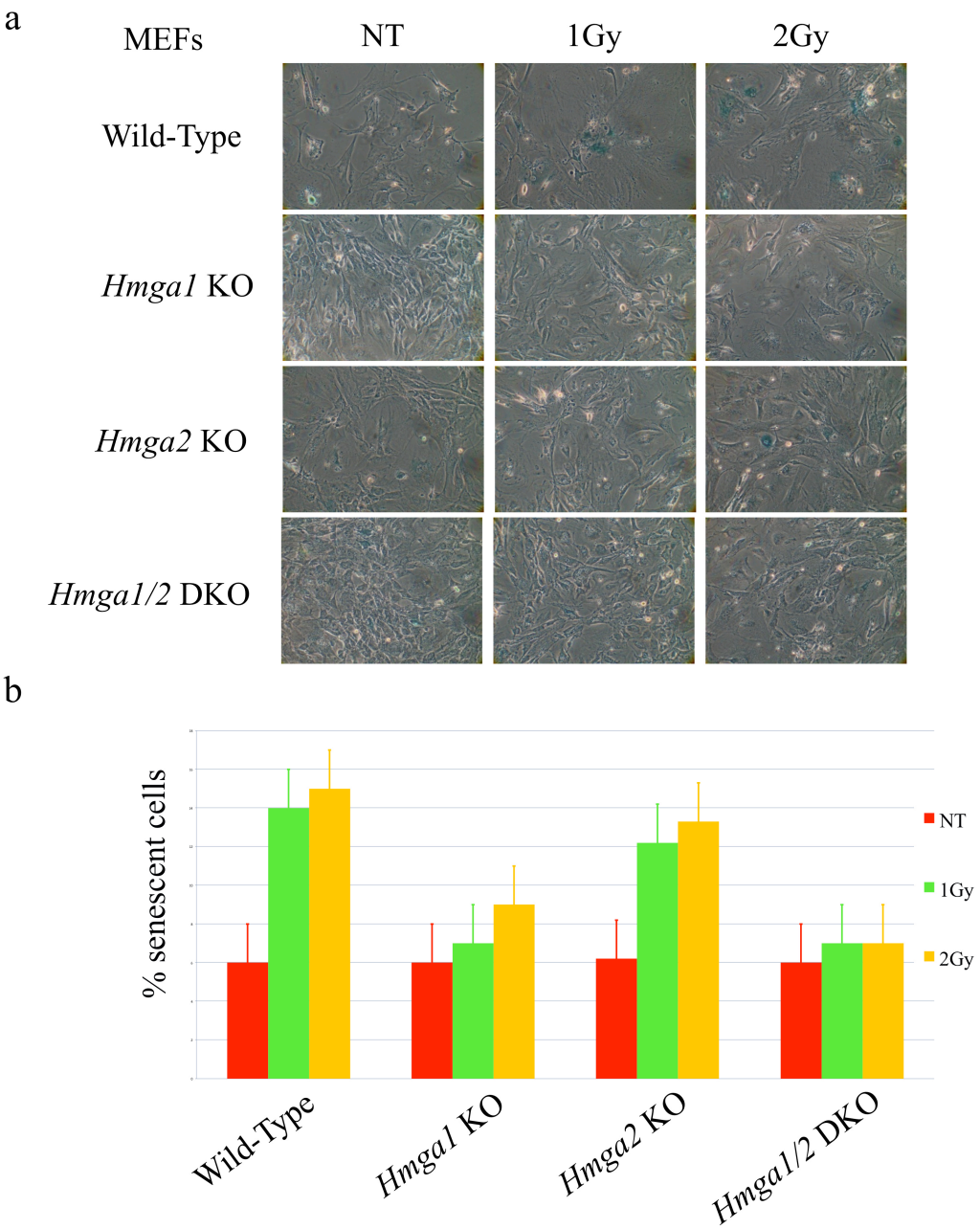

Figure 8. Absence of HMGA proteins impairs DNA damage induced senescence. (a) Early-passage wild type, Hmga1-null, Hmga2-null and Hmga1/Hmga2-null MEFs were treated or not with different doses (1-2 Gy) of IR. 96 h after IR exposure, Senescence-Associated β-galtactosidase (SA-β-gal)-staining was performed and light microscope cell images acquired. A representative image of each experimental point is reported. (b) Quantification of SA-β-gal positive cells. Values are the mean ± S.D. of three independent experiments. At least 20 different fields were analyzed for each experimental point.

4.7 Impaired expression of HMGA proteins prevents oncogene-induced DDR

Activation of oncogenes such as H-RAS, BRAF, E2F1 and MYC drives an initial hyperproliferation phase, but this burst is quickly followed by cell cycle slowing down and establishment of ATM-dependent DDR, that results in oncogene-induced senescence (OIS). OIS is a tumor suppressor mechanism that impedes the proliferation of a cell overexpressing an aggressive oncogene (d'Adda di Fagagna 2008). Then, adaptive mechanisms, such as inactivation of tumor suppressor genes, allow the restart of DNA replication and cell proliferation (d'Adda di Fagagna 2008). However the mechanisms of senescence allow transformed cells to slow down their cell cycle in order to prevent accumulation of high levels of DNA damage and exhaustion of cancer stem cells (Viale et al. 2009).

To assess the role of HMGA protein in OIS, we used a cell system originally developed in our laboratories consisting in a rat thyroid epithelial cell line (FRTL-5), stably expressing or not an HMGA1-antisense construct that impairs both HMGA1 and HMGA2 expressions (FRTL-5-asHMGI) (Berlingieri et al. 1995), and infected with the murine transforming retrovirus KiMSV carrying the oncogene Ki-Ras. As previously demonstrated (Berlingieri et al. 1995), following the infection with KiMSV, the cells (FRTL-5-Ki cells) acquired a fully transformed phenotype and overexpressed HMGA proteins. Conversely, prevention of HMGA expression (FRTL-5-asHMGI-Ki cells) impaired the acquisition of the fully transformed phenotype. Here we show, by western blot analysis of FRTL-5-Ki and FRTL-5-asHMGI-Ki cells, that absence of HMGA proteins determined a reduction in ATM cellular levels (Figure 9a). We then analyzed the amount of SA β-gal positive cells and found that, as shown in Figures 9b and 9c, prevention of HMGA1 and HMGA2 expression strongly reduced the senescence induced by the infection with KiMSV, confirming the role of HMGA proteins in OIS. Next, we investigated whether prevention of HMGA proteins expression increases cell sensitivity to genotoxic treatments such as IR exposure. To this aim we performed a clonogenic assay in FRTL-5-Ki and FRTL-5-asHMGI-Ki cells after treatement with increasing amounts of IR (1-3 Gy). As shown in Figure 9d, the number of colonies formed by FRTL-5-asHMGI-Ki following IR exposure, normalized for the number of colonies obtained from untreated cells, was significantly reduced compared to FRTL-5-Ki cells.

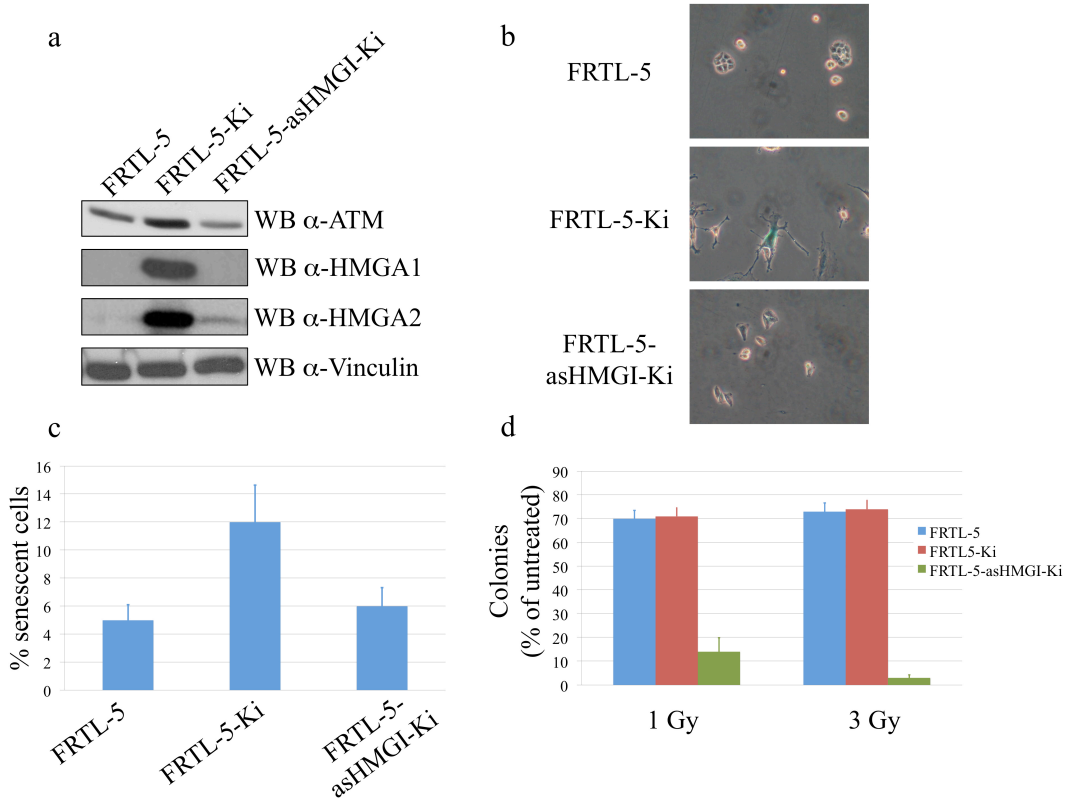

Figure 9. Inhibition of HMGA protein expression prevents ATM-dependent OIS and enhances radiosensitivity of transformed cells. (a) Total cell extracts from FRTL-5, FRTL-5-Ki and FRTL-5-asHMGI-Ki cells were analyzed by western blot using the indicated antibodies. (b) Senescence-Associated β-galtactosidase (SA-β-gal)-staining performed on FRTL-5, FRTL-5-Ki and FRTL-5-asHMGI-Ki cells. A representative image of each experimental point is reported. (c) Quantification of SA-β-gal positive cells. Values are the mean ± S.D. of three independent experiments. At least 20 different fields were analyzed for each experimental point. (d) Clonogenic assay following IR exposure on FRTL-5, FRTL-5-Ki and FRTL-5-asHMGI-Ki cells. Cells were cultured for 2 weeks after an exposure to 1 or 3 Gy of IR. Colonies were stained using Crystal Violet staining. The results were normalized with respect to the untreated cells. Values are the mean ± S.D. of three independent experiments.

One possible explanation of these observations is that HMGA1 and HMGA2, enhancing ATM expression, increase cellular DDR levels. Increased DDR slows down cell cycle following oncogene overexpression or DNA-damaging-agents treatment, allowing transformed cells to have the time to repair (not necessarily in correct manner) DNA damage and thus survive. Conversely, inhibition of HMGA proteins expression impairs the ATM-dependent DDR, thus enhancing sensitivity of cancer cells to DNA-damaging agents.

4.8 Down-regulation of HMGA1 protein enhances cancer cell sensitivity to DNA damage

Overexpression of HMGA1 is a common feature of human solid and haematological malignancies. The data here reported clearly indicate a critical role for HMGA proteins in the positive regulation of *ATM* expression and, consequently, in DDR. Over the last few years, an increasing body of evidence has accumulated to suggest that inhibition of ATM kinase activity can enhance cellular sensitivity to DNA-damaging agents (Jackson 2009). Our results suggested that inhibition of HMGA proteins affect ATM expression, resulting in the reduction of the ATM-mediated DDR and improvement of cell sensitity to DNA-damaging agents. Therefore, we further investigated whether inhibition of HMGA protein expression could represent a valid alternative to other chemical inhibitors of ATM kinase activity in human tumor cells. We used FRO anaplastic human thyroid cancer cells, which express high levels of HMGA1, and generated a FRO cell clone, stably expressing the previously mentioned anti-HMGI antisense construct (FRO-asHMGI). Western blot analysis (Figure 10a) confirmed the abrogation of both HMGA1 expression and, consistent with our previous data, ATM protein levels.

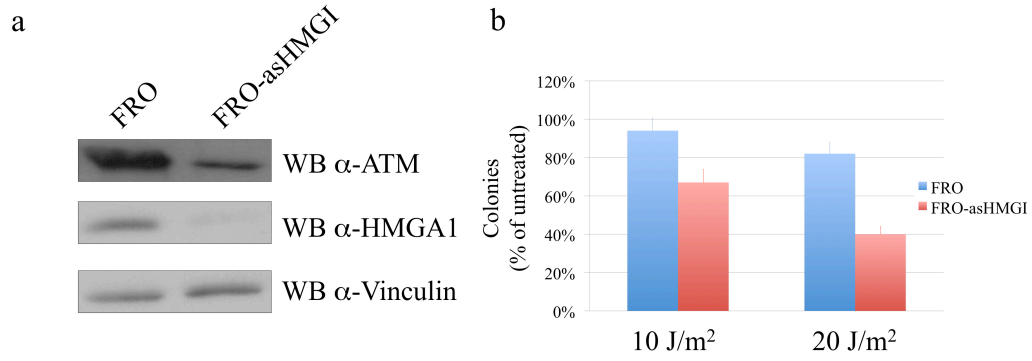

Figure 10. Downregulation of HMGA1 proteins sensitizes cancer cells to DNAdamage. (a) Western blot analysis of total cell extracts from FRO and FRO-asHMGI, using the indicated antibodies. (b) Clonogenic assay following UV exposure on FRO and FRO-asHMGI cells. Cells were not treated or treated with 10 or 20 J/m^2 and cultured for 10 days. Colonies were stained using Crystal Violet staining. The results showed are normalized with respect to the untreated cells. Values are the mean ± S.D. of three independent experiments.

Then, we performed a clonogenic assay on FRO and FRO-asHMGI following the exposure to different amount (10-20 J/m^2) of UV light, a DNA-damage that activates both ATR and ATM, inducing G1/S and intra-S phase checkpoints. In agreement with the reduction of ATM in FRO-asHMGI, these cells formed a

strongly reduced number of colonies, normalized for the colonies obtained from untreated cells, respect to wild-type FRO (Figure 10b). This result indicates that down-regulation of HMGA proteins affects cell proliferation and/or apoptosis following DNAdamage.

Next, we analyzed cell cycle following the UV exposure, in order to evaluate the ATM-dependent slowing down in response to DNA damage. At 0, 8, 16 ad 24 h after exposure to 20 J/m^2 of UV-light, asynchronously growing FRO and FRO-asHMGI cells were harvested, fixed and stained with propidium iodide, to be assayd by flow cytometry. As shown in Figure 11a, FRO cells, expressing high levels of ATM, arrested cell cycle progression in G1 and S phase 16 h after UV treatment, consistent with the triggering of cell cycle checkpoints by ATM kinase. Conversely, FRO-asHMGI failed to arrest cell cycle in G1 and accumulated in G2/M phase, where other ATM-independent checkpoint could be active. This result is consistent with other previous data (Rainey et al. 2008) showing the G1/S arrest failure following chemical inhibition of ATM. To focus our attention on G1/S and intra-S checkpoints, immediately after exposure of FRO and FRO-asHMGI to 20 J/m^2 of UV-light, cells were treated with 0.2 μg/ml of nocodazole. This treatment prevents cells from exiting G2/M phase and entering G1, allowing us to analyze the cell cycle progression and the G1- and S-phases checkpoints without the bias of cells that, having accomplished their cycle, start a new cell division. Moreover, wild-type FRO were also treated with 10 μM of KU-55933 to assess the effect of ATM inhibition. Cells were harvested 8 h after the nocodazole treatment, and analyzed by flow cytometry. Figure 11b shows that wild-type FRO, both treated and not treated with KU-55933, and FRO-asHMGI had a similar cell cycle distribution. Conversely, following nocodazole treatment, FRO-asHMGI cells accumulated in G2/M faster than FRO cells, suggesting that block of HMGA expression may have led the G1/S checkpoint to be constitutively less active then parental cells. Following the UV treatment, cell cycle progression from G1 to G2 was significantly slower in FRO cells than in both FRO cells treated with KU-55933 and FRO-asHMGI cells. These results indicate that impairment of HMGA1 expression in thyroid cancer cells prevent ATM induced G1/S checkpoint. It is reasonable to hypothesize that HMGA1, sustaining the expression levels of ATM, promotes the activation of G1/S checkpoint, which is necessary for cancer cells to slow down their cell cycle progression in order to repair DNA and prevent DNA-damaging agents-induced apoptosis.

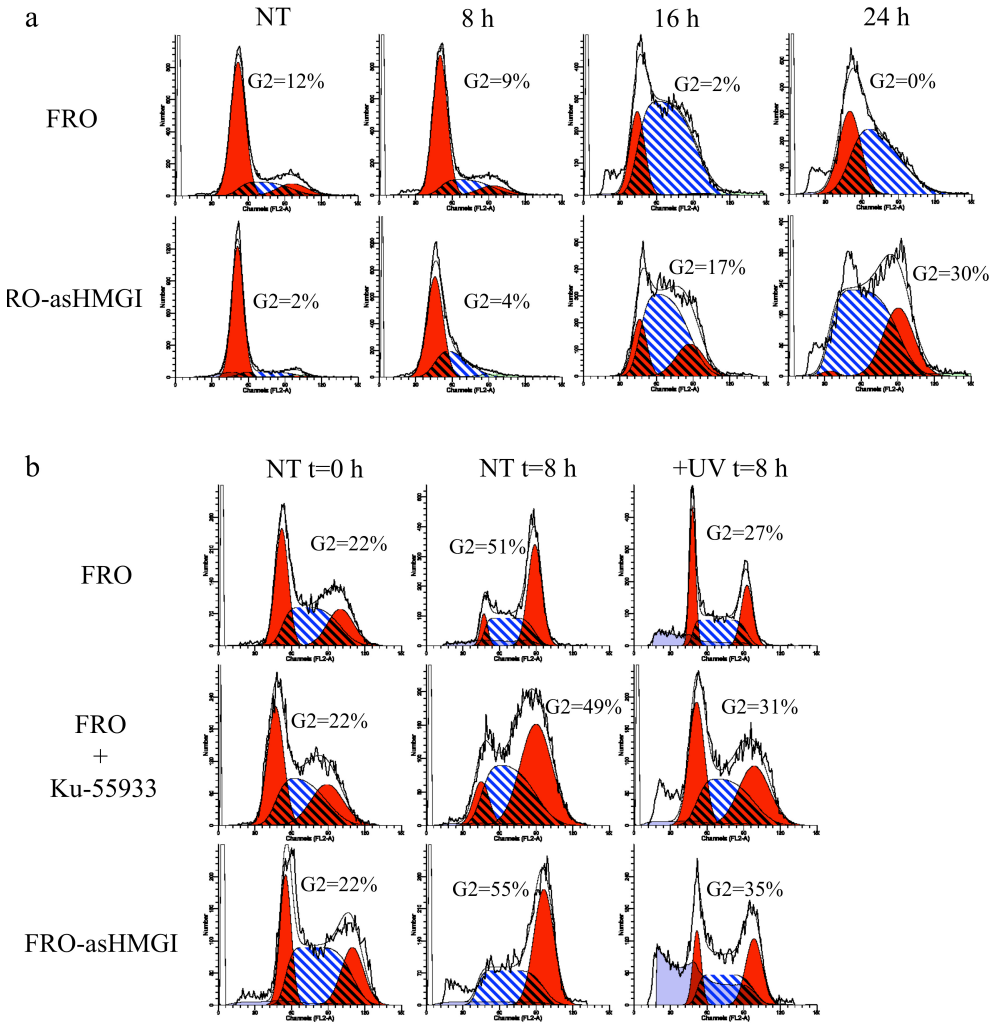

Figure 11. Inhibition of HMGA1 affects G1/S cell cycle checkpoints in response to DNA damage. (a) Cell cycle analysis of FRO and FRO-asHMGI cells. Cells were not treated (NT) or treated with 20 J/m^2, harvested 8, 16 and 24 h after the treatment, fixed and analyzed by flow cytometry. The data obtained were analyzed using ModFit software. Cells in G1 and in G2 phase of cell cycle are reported in red, cells in S phase are indicated with white and blu bars. (b) Flow cytometric analysis of FRO and FRO-asHMGI, treated or not as in (a), with the supplement of 0.2 ug/ml nocodazole, to impair cell cycle progression and induce accumulation in G2 phase, and KU-55933 in FRO cells, to inhibit ATM kinase activity. Cells were harvested immmediately or after 8 h and analyzed as in (a). Data reported are representative of three independent experiments.

To verify this hypothesis, we analyzed apoptotic markers such as caspases 3/7 activation and annexin-V staining in FRO and FRO-asHMGI cells, following UV treatment (Figure 12).

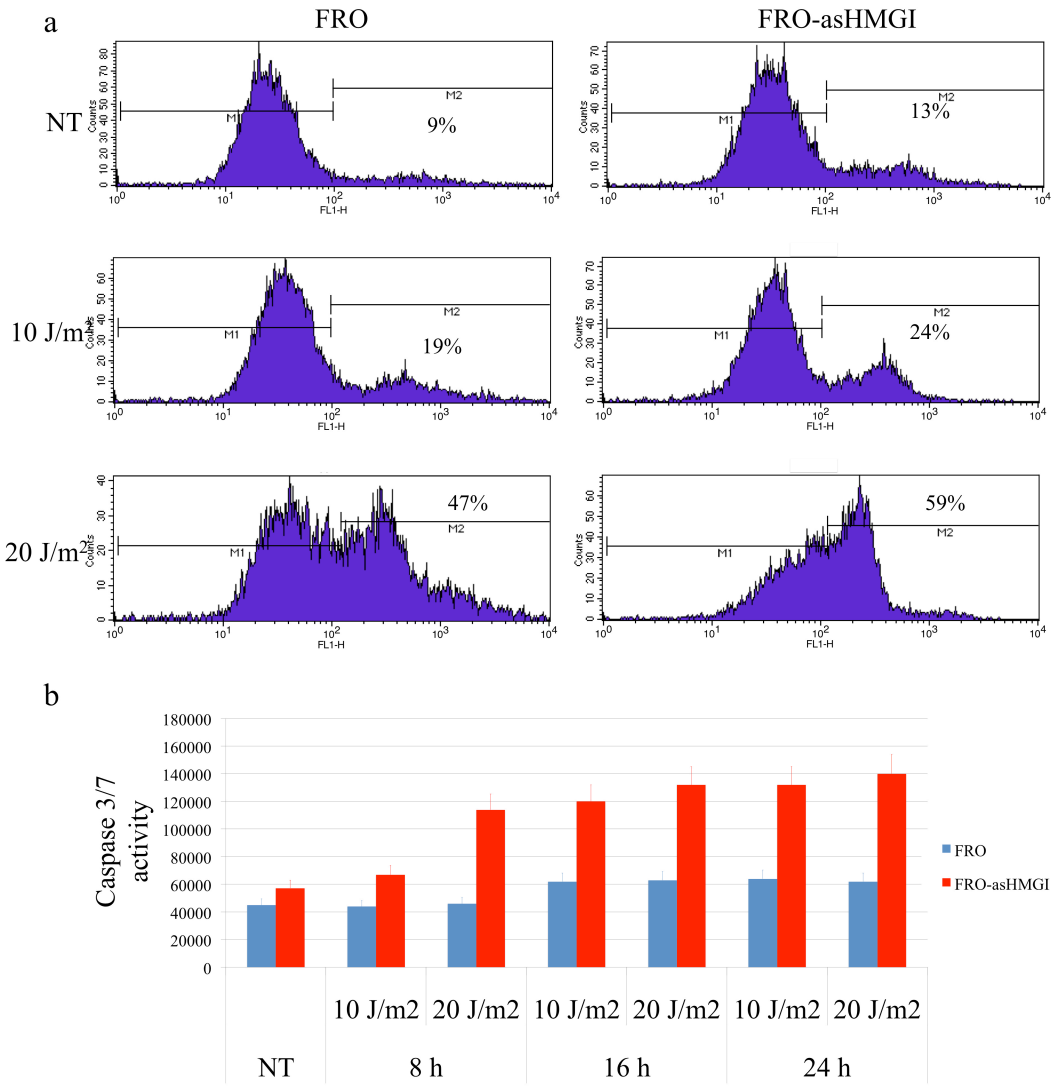

Figure 12. HMGA1 inhibition enhances DNA-damage-dependent apoptosis. (a) FRO and FRO-asHMGI cells were treated or not with 10 and 20 J/m2 of UV, harvested 24 h after the exposure and stained with anti-annexin V antibody. Flow citometry analysis was performed to quantify the amount of apoptotic-annexin V positive cells. The results reported are representative of three independent experiments. (b) Colorimetric Caspase 3/7 activity assay, performed on cells treated as in (a) and harvested at different time points (8, 16 and 24 h). Values are the mean ± S.D. of three independent experiments performed in triplicate.

Parental FRO and FRO-asHMGI cells were treated with different amount (10-20 J/m^2) of UV light, harvested after 24 h, stained with anti-annexin-V fluorescent antibody and analyzed by flow cytometry. As shown in Figure 12a, Annexin V staining confirmed that inhibition of HMGA1 increases cancer cell predisposition to apoptosis. Indeed, FRO-asHMGI cells displayed a higher percentage of

apoptotic cells already in untreated cells, compared to wild-type FRO. However, following UV exposure, both FRO and FRO-asHMGI cells underwent apoptosis, but a significant higher percentage of annexin-V positive cells was found in FRO-asHMGI then parental cells (Figure 12a). To further confirm this observation, we evaluated caspase 3 and 7 activities in both cell lines following UV exposure, using a colorimetric assay. Consistent with the results obtained with annexin-V staining, FRO-asHMGI cells displayed an increased basal activation of caspases 3 and 7 compared to parental cells. However, 8 h after UV-treatment, we observed a significant activation of caspases 3 and 7, which increased until 24 h after the exposure, only in FRO-asHMGI cells. Conversely, FRO cells showed a slower and less intense activation of apoptotic pathways, which became significant only 16 h after the exposure to UV light (Figure 12b). Therefore, these data clearly indicate that HMGA1 inhibition effectively enhances DNA-damage-dependent apoptosis.

In conclusion, our results demonstrate that abrogation of HMGA1 expression in anaplastic thyroid cancer cells reduces ATM levels and enhances cell sensitivity to DNA damage, by preventing the activation of cell cycle checkpoints necessary to activate an efficient DDR. The final effect is reduction of proliferation and increase of apoptotic pathways in HMGA1-overexpressing cancer cells, following DNA-damaging agents exposure, suggesting that HMGA1 may be a valid target to improve the efficacy of conventional genotoxic therapies.

5. CONCLUSIONS

HMGA overexpression is a common feature of human benign and malignant neoplasias. Despite their well-defined role in processes such as proliferation, apoptosis and cellular trasformation, HMGA proteins involvement in DNA repair and cancer resistance to genotoxic therapies still remains controversial. Previous studies mostly analyzed HMGA role in cell lines engineered to overexpress HMGA proteins (Fusco and Fedele 2007). Here we first report the identification of a novel role of HMGA proteins in DNA repair in cellular systems that normally express one or both HMGA proteins. In particular we identified, in MEFs derived from wild-type, *Hmga1* knock-out, *Hmga2* knock-out and *Hmga1/2* double knock out mice, a positive and partially redundant role for HMGA1 and HMGA2 in the cellular response to DNAdamage. In fact, in the absence of HMGA1 and HMGA2, DNA repair and stress-induced senescence is significantly impaired, indicating a physiologic positive role for HMGA proteins in DNA damage response. Moreover, absence of HMGA proteins in this cellular system significantly reduces the expression of ATM, the master regulator of DNArepair machinery. Luciferase and ChIP experiments demonstrated that HMGA proteins have a direct positive role in the regulation of *ATM* promoter. Moreover, we show that HMGA proteins, in response to DNA-damaging agents such as IR, are phosphorylated by ATM, and this phosphorylation event increases their activity on *ATM* promoter. These observations indicate that HMGA1 and HMGA2 are positively involved in DNAdamage response through their physiologic and DNAdamage-dependent role in the regulation of *ATM* expression. Our results have also interesting implications in the field of new potential therapeutic approaches to improve cellular sensitivity to anti-cancer drugs. In fact, it has been previously demonstrated that chemical inhibition of ATM enhances cell sensitivity to genotoxic drugs. Here we show that inhibition of HMGA1 in anaplastic thyroid cancer cells (FRO) led to down-regulation of ATM expression and, consequently, reduced cell proliferation and increased cell sensitivity following exposure to DNA-damaging agents, such as UV rays. Conversely, HMGA1-expressing cells, in response to DNA-damaging agents exposure, slowed down their cell cycle in order to improve DNA repair and reduce the treatment-induced toxic effects. These data are consistent with the finding that HMGA proteins expression in human tumors is usually considered a poor prognostic marker, often correlated with a reduced survival and response to common therapies (Fusco and Fedele, 2007).

Therefore, our previous and present results indicate that HMGA proteins could represent a novel target for cancer therapy. In fact, inhibition of HMGA1 and HMGA2 can affect cancer cell proliferation and apoptosis, inhibiting their effect

on p53 and E2F1 pathways. Moreover, as suggested here, HMGA proteins sustain ATM levels in cancer cells, improving cellular response to DNA damage and preventing the accumulation of fatal DNAlesions. The striking difference between the use of chemical inhibitors of ATM and HMGA-targeting drugs to enhance cell sensitivity to genotoxic drugs is that, while ATM is expressed in all cells, HMGA proteins are expressed at high levels only in cancer cells. Thus, HMGA1 and HMGA2 may represent new, cancer cell specific, targets for the treatment of human neoplasias.

6. ACKNOWLEDGEMENTS

I want to thank Prof. Giancarlo Vecchio, coordinator of the Molecular Oncology and Endocrinology Doctorate program, for the opportunity that he gave me to work at the Department of Cellular and Molecular Biology and Pathology "L. Califano" of the University of Napoli "Federico II"

I thank Prof. Fusco, my mentor since I was a confused undergraduate student. Now I am no longer a student, even if I am still "a little" confused! But, at least, I am sure that this is the job I want to do for the rest of my life!

I thank Dr. Monica Fedele, my guide during these years in Prof. Fusco's Lab. Her help, criticisms, suggestions and advices made me what I am now, and will be the base of whatever I will become.

I also thank Prof. Carlo Croce for the hospitality and the great time spent in his laboratory at the Ohio State University.

I want to thank all my colleagues at the Fusco's lab, Adele, Floriana, Francesco, Mara and all the others at the II floor of the "Proboscide", for all the laughs and the kind moments together, and for the "tolerance" they demonstrated to me during my MANY days to forget!

I thank all the colleagues and fantastic friends I met at the Ohio State University, because they gave me all that I needed for a perfect work- and life-time. In particular, I want to thank Eugenio, Federica, Francesca and Giulia (above all for life-lessons learned together, such as "If you want to see a concert and you are going to take a bag, don't forget your shovel!"), Rosa and Angelo, and finally Mario, Jessica, Taccioli and Claudia ("I have no words to thank you enough, you have really been the soundtrack of these last months!")

My special thank is for the colleagues and friends that faced this work with me shoulder-to-shoulder.
I thank Teresa and the "new-entry" of our team Ida, for their technical and scientific support and also for their friendship, because explaining them what I know helped me to learn it better: "I hope that my words and all the work together will be helpful for your future professional life".
I thank Ivana, my first bench-mate when I was a student, and I wish her a wonderful life: "I will miss you so much, and I'll never forget you!!!!"

And I thank Daniela, above all because in the last year she has been the best friend that I could ever ask, always close to me in good and in bad times, inside and outside the lab: “Thank you for making me feel with shoulders covered, specially when we started to work side by side. And please, forgive me for all the time you wasted with my references…I’m so sorry, and I’ll never thank you enough!!!”

I also thank my far and near friends of ever, Andrea, Bianca, Giulio, Laura and Peppe, because their presence, even if in the silence, sometimes, has been my safe harbour. Good friends are like stars: you don’t always see them, but you know they are there!

I am grateful to my family, my mom, my dad, my brother and my sister, because, even if they don’t remember it, they are the foundations of my life.

Finally, I want to express my special thank to Roby: “Thank you for these wonderful years, specially for all the love that we gave each other. And, in spite of everything, I hope you had the time of your life, as me”.

7. REFERENCES

Abraham, R. T. Cell cycle checkpoint signaling through the ATM and ATR kinases. Genes Dev 2001;15, 2177–2196.

Anand, A. & Chada K. In vivo modulation of Hmgic reduces obesity. Nature Genet 2000; 24, 377–380.

Anderson L, Henderson C, Adachi Y. Phosphorylation and rapid relocalization of 53BP1 to nuclear foci upon DNA damage Mol Cell Biol 2001;21(5):1719-29

Aprelikova O, Pace AJ, Fang B, Koller BH, Liu ET. BRCA1 is a selective coactivator of 14-3-3 sigma gene transcription in mouse embryonic stem cells. J Biol Chem 2001; 276:25647-50.

Ashar H.R., Fejzo M.S., Tkachenko A., Zhou X., Fletcher J.A., Weremowicz S., Morton C.C., Chada K. Disruption of the architectural factor HMGI-C: DNA-binding AT hook motifs fused in lipomas to distinct transcriptional regulatory domains, Cell 1995;82:57-65.

Bakkenist CJ, Kastan MB. DNA damage activates ATM through intermolecular autophosphorylation and dimer dissociation. Nature 2003; 421:499-506.

Baldassarre G, Battista S, Belletti B, Thakur S, Pentimalli F,Trapasso F, Fedele M, Pierantoni G, Croce CM, Fusco A. Negative regulation of BRCA1 gene expression by HMGA1 proteins accounts for the reduced BRCA1 protein levels in sporadic breast carcinoma. Mol Cell Biol 2003;7:2225–38.

Baldassarre G, Belletti B, Battista S, Nicoloso MS, Pentimalli F, Fedele M, Croce CM, Fusco A. HMGA1 protein expression sensitizes cells to cisplatin-induced cell death. Oncogene 2005;24: 6809–6819.

Banin S, Moyal L, Shieh S, Taya Y, Anderson CW, Chessa L, Smorodinsky NI, Prives C, Reiss Y, Shiloh Y, Ziv Y. Enhanced phosphorylation of p53 by ATM in response to DNA damage. Science 1998; 281:1674-77.

Barlow C, Hirotsune S, Paylor R, Liyanage M, Eckhaus M, Collins F, Shiloh Y, Crawley JN, Ried T, Tagle D, Wynshaw-Boris A. Atm-deficient mice: a paradigm of ataxia telangiectasia. Cell 1996;12;86(1):159-71.

Bartek, J. & Lukas, J. Chk1 and Chk2 kinases in checkpoint control and cancer. Cancer Cell 2003;3,421–429.

Bartkova, J., Rezaei, N., Liontos, M., Karakaidos, P., Kletsas, D., Issaeva, N., Vassiliou, L.V., Kolettas, E., Niforou, K., Zoumpourlis, V.C. Oncogene-induced senescence is part of the tumorigenesis barrier imposed by DNA damage checkpoints. Nature 2006;444(7119):633-637.

Baskaran R, Wood LD, Whitaker LL, Canman CE, Morgan SE, Xu Y, Barlow C, Baltimore D, Wynshaw-Boris A, Kastan MB, Wang JY. Ataxia telangiectasia mutant protein activates c-Abl tyrosine kinase in response to ionizing radiation. Nature 1997:29;387(6632):516-9.

Battista S., Fidanza V., Fedele M., Klein-Szanto A.J., Outwater E., Brunner H., Santoro M., The expression of a truncated HMGI-C gene induces gigantism associated with lipomatosis. Cancer Res 1999;59:4793-4797.

Berkovich E, Ginsberg D. ATM is a target for positive regulation by E2F-1. Oncogene 2003;16;22(2):161-7.

Berlingieri MT, Manfioletti G, Santoro M, Bandiera A, Visconti R, Giancotti V, Fusco A. Inhibition of hmgi-c protein synthesis suppresses retrovirally induced neoplastic transformation of rat thyroid cells. MCB 1995;15(3):1545–1553.

Bernstein C, Bernstein H, Payne CM, Garewal H. DNA repair/pro-apoptotic dual-role proteins in five major DNA repair pathways: fail-safe protection against carcinogenesis. Mutat Res 2002;511(2):145-78.

Bianchi ME and Agresti A. HMG proteins: dynamic players in gene regulation and differentiation. Curr Opin Genet Dev 2005;15:496–506.

Bolderson E., Derek J. Richard, Bin-Bing S. Zhou, and Kum Kum Khanna. Recent Advances in Cancer Therapy Targeting Proteins Involved in DNA Double-Strand Break Repair. Clin Cancer Res 2009;15(20) 15, 2009

Boo LM, Lin HH, Chung V, Zhou B, Louie SG, O'Reilly MA, Yen Y, Ann DK. High mobility group A2 potentiates genotoxic stress in part through the modulation of basal and DNA damage-dependent phosphatidylinositol 3-kinaserelated protein kinase activation. Cancer Res 2005;65(15):6622-30.

Borgne, A., Meijer, L. Sequential dephosphorylation of p34cdc2 on Thr-14 and Tyr-15 at the prophase/metaphase transition. J Biol Chem 1996;(44):27847-27854.

Borner C. The Bcl-2 protein family: sensors and checkpoints for life-or-death decisions. Mol Immunol 2003;39(11):615-47.

Borrmann, L. Schwanbeck R, Heyduk T, Seebeck B, Rogalla P, Bullerdiek J, Wisniewski JR.. High mobility group A2 protein and its derivatives bind a specific region of thepromoter of DNA repair gene ERCC1 and modulate its activity. Nucleic Acids Res 2003;31, 6841–6851.

Bree RT, Neary C, Samali A, Lowndes NF. The switch from survival responses to apoptosis after chromosomal breaks. DNA Repair (Amst).;3(8-9):989-95.

Bulavin, D. V., Higashimoto Y, Popoff IJ, Gaarde WA, Basrur V, Potapova O, Appella E, Fornace AJ Jr. Initiation of a G2/M checkpoint after ultraviolet radiation requires p38 kinase. Nature 2001; 411, 102–107

Bunz, F., Dutriaux, A., Lengauer, C., Waldman, T., Zhou, S., Brown, J.P., Sedivy, J.M., Kinzler, K.W., Vogelstein, B. Requirement for p53 and p21 to sustain G2 arrest after DNA damage. Science 1998;282(5393):1497-1501.

Burma S, Chen BP, Murphy M, Kurimasa A, Chen DJ. ATM phosphorylates histone H2AX in response to DNA double-strand breaks. J Biol Chem 2001;9;276(45):42462-7.

Buscemi G, Carlessi L, Zannini L, Lisanti S, Fontanella E, Canevari S, Delia D. DNA damage-induced cell cycle regulation and function of novel chk2 phosphoresidues. Mol Cell Biol 2006; 26:7832-45.

Bustin M, Lehn DA, Landsman D. Structural features of the HMG chromosomal proteins and their genes. Biochim Biophys Acta 1990;1049(3):231-43.

Bustin M. Chromatin unfolding and activation by HMGN(*) chromosomal proteins. Trends Biochem Sci 2001;26:431–437.

Buysse K., Reardon W., Mehta L., Costa T., Fagerstrom C., Kingsbury D.J., Anadiotis G., McGillivray B.C., Hellemans J., de Leeuw N., de Vries B.B., Speleman F., Menten, G. B. Mortier, The 12q14 microdeletion syndrome: additional patients and further evidence that HMGA2 is an important genetic determinant for human height. Eur J Med Genet 2009;52:101-107.

Caldecott, K.W. Single-strand break repair and genetic disease. Nat Rev Genet 2008;9:619–631.

Cann KL, Hicks GG. Regulation of the cellular DNA double-strand break response. Biochem Cell Biol 2007;85(6):663-74.

Capetillo O. ATM regulates ATR chromatin loading in response to DNA double-strand breaks. J Exp Med 2006;20;203(2):297-303.

Celeste A, Fernandez-Capetillo O, Kruhlak MJ, Pilch DR, Staudt DW, Lee A, Bonner RF, Bonner WM, Nussenzweig A. Histone H2AX phosphorylation is dispensable for the initial recognition of DNA breaks. Nat Cell Biol 2003;5(7):675-9.

Celeste A, Petersen S, Romanienko PJ, Fernandez-Capetillo O, Chen HT, Sedelnikova OA, Reina-San-Martin B, Coppola V, Meffre E, Difilippantonio MJ, Redon C, Pilch DR, Olaru A, Eckhaus M, Camerini-Otero RD, Tessarollo L, Livak F, Manova K, Bonner WM, Nussenzweig MC, Nussenzweig A. Genomic instability in mice lacking histone H2AX. Science 2002;3;296(5569):922-7.

Chang, B.D., Broude, E.V., Dokmanovic, M., Zhu, H., Ruth, A., Xuan, Y., Kandel, E.S., Lausch, E., Christov, K., Roninson, I.B. A senescence-like phenotype distinguishes tumor cells that undergo terminal proliferation arrest after exposure to anticancer agents. Cancer Res 1999;59:3761-3767.

Chen G, Yuan SS, Liu W, Xu Y, Trujillo K, Song B, Cong F, Goff SP, Wu Y, Arlinghaus R, Baltimore D, Gasser PJ, Park MS, Sung P, Lee EY. Radiation-induced assembly of Rad51 and Rad52 recombination complex requires ATM and c-Abl. J Biol Chem 1999;30;274(18):12748-5

Chen L, Gilkes DM, Pan Y, Lane WS, Chen J. ATM and Chk2-dependent phosphorylation of MDMX contribute to p53 activation after DNA damage. EMBO J 2005; 24:3411-22.

Chen L, Morio T, Minegishi Y, Nakada S, Nagasawa M, Komatsu K, Chessa L, Villa A, Lecis D, Delia D, Mizutani S. Ataxia-telangiectasia-mutated dependent phosphorylation of Artemis in response to DNA damage. Cancer Sci 2005; 96:134-41.

Chiappetta G, Avantaggiato V, Visconti R, Fedele M, Battista S, Trapasso F, Merciai BM, Fidanza V, Giancotti V, Santoro M, Simeone A, Fusco A. High level expression of the HMGI (Y) gene during embryonic development. Oncogene 1996;13(11):2439-46.

Chiefari E., Paonessa F., Iiritano S., Le Pera I., Palmieri D., Brunetti G., Lupo A., Colantuoni V., Foti D., Gulletta E., De Sarro G., Fusco A., Brunetti A. The cAMP-HMGA1-RBP4 system: a novel biochemical pathway for modulating glucose homeostasis. BMC Biol 2009;7;24-37.

Chieffi P, Battista S, Barchi M, Di Agostino S, Pierantoni GM, Fedele M, Chiariotti L, Tramontano D, Fusco A. HMGA1 and HMGA2 protein expression in mouse spermatogenesis. Oncogene 2002; 21(22):3644-50.

Chin MT, Pellacani A, Wang H, Lin SS, Jain MK, Perrella MA, and Lee ME. Enhancement of serum-response factor-dependent transcription and DNA binding by the architectural transcription factor HMG-I(Y). J Biol Chem 1998;273, 9755-60.

Collis SJ, DeWeese TL, Jeggo PA, Parker AR. The life and death of DNA-PK. Oncogene 2005;24:949–61.

Collis SJ, Swartz MJ, Nelson WG, DeWeese TL. Enhanced radiation and chemotherapy-mediated cell killing of human cancer cells by small inhibitory RNA silencing of DNA repair factors. Cancer Res 2003;63:1550–4.

Cortez D, Glick G, Elledge SJ. Minichromosome maintenance proteins are direct targets of the ATM and ATR checkpoint kinases. Proc Natl Acad Sci USA 2004;101:10078-83.

Crescenzi E., Palumbo G., de Boer J., Brady J.M. Ataxia Telangiectasia Mutated and p21CIP1 modulate cell survival of drug-induced senescent tumor cells: implications for chemotherapy. Clin Cancer Res 2008;14(6):1877-87.

Crippa MP, Trieschmann L, Alfonso PJ, Wolffe AP and Bustin M. Deposition of chromosomal protein HMG-17 during replication affects the nucleosomal ladder and transcriptional potential of nascent chromatin. EMBO J 1993;12:3855–3864.

Cuadrado M, Martinez-Pastor B, Murga M, Toledo LI, Gutierrez-Martinez P, Lopez E, Fernandez Capetillo O. ATM regulates ATR chromatin loading in response to DNA double-strand breaks. J Exp Med 2006;20;203(2):297-303.

d'Adda di Fagagna F. Living on a break: cellular senescence as a DNA-damage response. Nat Rev Can 2008;8(7):512-22.

d'Adda di Fagagna, F., Reaper, P.M., Clay-Farrace, L., Fiegler, H., Carr, P., von Zglinicki, T., Saretzki, G., Carter, N.P. Jackson, S.P., 2003. A DNA damage checkpoint response in telomere-initiated senescence. Nature 2003; 13;426(6963):194-8

Di Agostino S, Fedele M, Chieffi P, Fusco A, Rossi P, Geremia R, Sette C. Phosphorylation of high-mobility group protein A2 by Nek2 kinase during the first meiotic division in mouse spermatocytes. Mol Biol Cell 2004;15:1224-1232.

Di Leonardo, A., Linke, S.P., Clarkin, K., Wahl, G.M. DNA damage triggers a prolonged p53-dependent G1 arrest and long-term induction of Cip1 in normal human fibroblasts. Genes Dev 1994;8:2540-2551.

Di Micco, R., Fumagalli, M., Cicalese, A., Piccinin, S., Gasparini, P., Luise, C., Schurra, C., Garre, M., Nuciforo, P.G., Bensimon, A. Oncogene-induced senescence is a DNA damage response triggered by DNA hyper-replication. Nature 2006;444(7119):638-642.

DiTullio Jr RA, Mochan TA, Venere M, Bartkova J, Sehested M, Bartek J, Halazonetis TD. 53BP1 functions in an ATM-dependent checkpoint pathway that is constitutively activated in human cancer. Nat Cell Biol 2002; 4:998-1002.

Donzelli, M. & Draetta, G. F. Regulating mammalian checkpoints through Cdc25 inactivation. EMBO Rep 2003;671–677.

Dornan D, Shimizu H, Mah A, Dudhela T, Eby M, O'rourke K, Seshagiri S, Dixit VM. ATM engages autodegradation of the E3 ubiquitin ligase COP1 after DNA damage. Science 2006; 313:1122-26.

Durant S, Karran P. Vanillins – a novel family of DNA-PK inhibitors. Nucl Acids Res 2003;31:5501–12.

Edberg DD, Bruce JE, Siems WF, Reeves R. In vivo posttranslational modifications of the high mobility group A1a proteins in breast cancer cells of differing metastatic potential. Biochemistry 2004;43:11500–15.

Falck J, Coates J, Jackson SP. Conserved modes of recruitment of ATM, ATR and DNA-PKcs to sites of DNA damage. Nature 2005;31;434(7033):605-11.

Falck J, Mailand N, Syljuasen RG, Bartek J, Lukas J. The ATM-Chk2-Cdc25A checkpoint pathway guards against radioresistant DNA synthesis. Nature 2001; 410:842-47.

Fedele M, Battista S, Kenyon L, Baldassarre G, Fidanza V, Klein-Szanto AJ,Parlow AF, Visone R, Pierantoni GM, Outwater E, Santoro M, Croce CM, Fusco A. Overexpression of the HMGA2 gene in transgenic mice leads to the onset of pituitary adenomas. Oncogene 2002;21:3190-3198

Fedele M, Battista S, Manfioletti G, Croce CM, Giancotti V, Fusco A. Role of the high mobility group A proteins in human lipomas. Carcinogenesis 2001; Vol.22. no.10 pp.1583-1591.

Fedele M, Pentimalli F, Baldassarre G, Battista S, Klein-Szanto AJ, Kenyon L, Visone R, De Martino I, Ciarmiello A, Arra C, Viglietto G, Croce CM, Fusco A.Transgenic mice overexpressing the wild-type form of the HMGA1 gene develop mixed growth hormone/prolactin cell pituitary adenomas and natural killer cell lymphomas. Oncogene 2005;24:3427–3435.

Fedele M, Visone R, De Martino I, Troncone G, Palmieri D, Battista S, Ciarmiello A, Pallante P, Arra C, Melillo RM, Helin K, Croce CM, Fusco A. HMGA2 induces pituitary tumorigenesis by enhancing E2F1 activity. Cancer Cell 2006b;9:459-471.

Fedele M., Fidanza V., Battista S., Pentimalli F., Klein-Szanto A.J., Visone R., De Martino I., Curcio A., Morisco C., Del Vecchio L., Baldassarre G., Arra C., Viglietto G., Indolfi C., Croce C.M., Fusco A. Haploinsufficiency of the Hmga1 gene causes cardiac hypertrophy and myelo-lymphoproliferative disorders in mice, Cancer Res 2006;66:2536-2543.

Fernandez-Capetillo O, Chen HT, Celeste A, Ward I, Romanienko PJ, Morales JC, Naka K, Xia Z, Camerini-Otero RD, Motoyama N, Carpenter PB, Bonner WM, Chen J, Nussenzweig A. DNA damage-induced G2-M checkpoint activation by histone H2AX and 53BP1. Nat Cell Biol 2002;4(12):993-7.

Finelli P, Pierantoni GM, Giardino D, Losa M, Rodeschini O, Fedele M, Valtorta E, Mortini P, Croce CM, Larizza L, Fusco A. The High Mobility Group A2 gene is amplified and overexpressed in human prolactinomas. Cancer Res 2002;62:2398-2405.

Foray N, Marot D, Gabriel A, Randrianarison V, Carr AM, Perricaudet M, Ashworth A, Jeggo P. A subset of ATM- and ATR-dependent phosphorylation

events requires the BRCA1 protein. EMBO J.2003 2;22(11):2860-71.

Foray N, Marot D, Randrianarison V, Venezia ND, Picard D, Perricaudet M, Favaudon V, Jeggo P. Constitutive association of BRCA1 and c-Abl and its ATM-dependent disruption after irradiation. Mol Cell Biol 2002; 22:4020-32.

Foti D., Chiefari E., Fedele M., Iuliano R., Brunetti L., Paonessa F., Manfioletti G., Barbetti F., Brunetti A., Croce C.M., Fusco A., Brunetti A. Lack of the architectural factor HMGA1 causes insulin resistance and diabetes in humans and mic. Nat Med 2005;11;765-773.

Fusco A and Fedele M. Roles of HMGA proteins in cancer. Nat Rev Cancer 2007;7(12):899-910.

Galande, S. Chromatin (dis)organization and cancer: BUR-binding proteins as biomarkers for cancer. Curr Cancer Drug Targets 2002;2, 157–190.

Gatei M, Scott SP, Filippovitch I, Soronika N, Lavin MF, Weber B, Khanna KK. Role for ATM in DNA damage-induced phosphorylation of BRCA1. Cancer Res 2000;60:3299-3304.

Gatei M, Young D, Cerosaletti KM, Desai-Mehta A, Spring K, Kozlov S, Lavin MF, Gatti RA, Concannon P, Khanna K. ATM-dependent phosphorylation of nibrin in response to radiation exposure. Nat Genet 2000;25(1):115-9.

Geierstanger BH, Volkman BF, Kremer W, Wemmer DE. Short peptide fragments derived from HMG-I/Y proteins bind specifically to the minor groove of DNA. Biochemistry 1994;33(17):5347-55.

Girard PM, Riballo E, Begg AC, Waugh A, Jeggo PA. Nbs1 promotes ATM dependent phosphorylation events including those required for G1/S arrest. Oncogene 2002;21(27):4191-9.

Goldberg M, Stucki M, Falck J, D'Amours D, Rahman D, Pappin D, Bartek J, Jackson SP. MDC1 is required for the intra-S-phase DNA damage checkpoint. Nature 2003;Feb 27;421(6926):952-6.

Gueven N, Fukao T, Luff J, Paterson C, Kay G, Kondo N, Lavin MF. Regulation of the Atm promoter in vivo. Genes Chromosomes Cancer 2006;Jan;45(1):61-71.

Guney, I., Sedivy, J.M. Cellular senescence, epigenetic switches and c-Myc. Cell Cycle 2006; 5:2319-2323.

Haaf T, Golub EI, Reddy G, Radding CM, Ward DC. Nuclear foci of mammalian Rad51 recombination protein in somatic cells after DNA damage and its localization in synaptonemal complexes. Proc Natl Acad Sci U S A 1995;14;92(6):2298-302.

Haber, J.E. Partners and pathways repairing a double-strand break. Trends Genet 2000;16;259–264.

Han, Z., Wei, W., Dunaway, S., Darnowski, J.W., Calabresi, P.,Sedivy, J., Hendrickson, E.A., Balan, K.V., Pantazis, P.,Wyche, J.H. Role of p21 in apoptosis and senescence of human colon cancer cells treated with camptothecin. J Biol Chem 2002. 277(19):17154-17160

Hemann, M.T., Narita, M. Oncogenes and senescence: breaking down in the fast line. Genes Dev 2007;21(1):1-5

Herbig, U., Jobling, W. A., Chen, B. P., Chen, D. J. & Sedivy, J. M. Telomere shortening triggers senescence of human cells through a pathway involving ATM, p53, and p21(CIP1), but not p16(INK4a). Mol Cell 2004;14,501–513.

Hess JL. Chromosomal translocations in benign tumors: the HMGI proteins. Am J Clin Pathol 1998;109(3):251–261.

Hickson I, Zhao Y, Richardson CJ, et al. Identification and characterization of a novel and specific inhibitor of the ataxia-telangiectasia mutated kinase ATM. Cancer Res 2004;64:9152–9.

Hiom K. Dna repair: Rad52 - the means to an end. Curr Biol 1999;17;9(12):R446-8.

Holliday, R., Tarrant, G.M. Altered enzymes in ageing human fibroblasts. Nature 1972;238(5358):26-30.

Hong Y, Stambrook PJ. Restoration of an absent G1 arrest and protection from apoptosis in embryonic stem cells after ionizing radiation. Proc Natl Acad Sci USA 2004;5;101(40):14443-8.

Houldsworth J, Lavin MF. Effect of ionizing radiation on DNA synthesis in ataxia telangiectasia cells. Nucleic Acids Res 1980; 8:3709-20.

Huang X, Kurose A, Tanaka T, Traganos F, Dai W, Darzynkiewicz Z. Sequential

phosphorylation of Ser-10 on histone H3 and ser-139 on histone H2AX and ATM activation during premature chromosome condensation: Relationship to cell-cycle phase and apoptosis. Cytometry 2006;A; 69:222-29.

Ichijima Y, Sakasai R, Okita N, Asahina K, Mizutani S, Teraoka H. Phosphorylation of histone H2AX at M phase in human cells without DNA damage response. Biochem Biophys Res Commun 2005; 336:807-12.

Iftode C, Daniely Y, Borowiec JA. Replication protein A (RPA): the eukaryotic SSB. Crit Rev Biochem Mol Biol 1999;34(3):141-80.

Ismail IH, Martensson S, Moshinsky D, Rice A, Tang C, Howlett A, et al. SU11752 inhibits the DNA-dependent protein kinase and DNA double-strand break repair resulting in ionizing radiation sensitization. Oncogene 2004;23:873–82.

Jackson SP. Detecting, signalling and repairing DNA double-strand breaks. Biochem Soc Trans 2001;29(Pt 6):655-61.

Jackson SP. The DNA-damage response: new molecular insights and new approaches to cancer therapy. Biochem Soc Trans 2009;37(Pt 3):483-94.

Jackson, J.P., Lindroth, A.M., Cao, X., Jacobsen, S.E. Control of CpNpG DNA methylation by the KRYPTONITE histone H3 methyltransferase. Nature 2002;416(6880):556-560.

Jazayeri A, Falck J, Lukas C, Bartek J, Smith GC, Lukas J, Jackson SP. ATM- and cell cycle-dependent regulation of ATR in response to DNA double-strand breaks. Nat Cell Biol 2006;8(1):37-45.

Karagiannis TC, El-Osta A. Double-strand breaks: signaling pathways and repair mechanisms. Cell Mol Life Sci 2004;61(17):2137-47.

Karran, P. DNA double strand break repair in mammalian cells. Curr Opin Genet Dev 2000;10;144–150.

Kastan MB, Bartek J. Cell-cycle checkpoints and cancer. Nature 2004;18;432(7015):316-23.

Kastan, M. B. & Lim, D.-S. The many substrates and functions of ATM. Mol Cell Biol 2000;1;179–186.

Kazmierczak, B. Wanschura S, Rosigkeit J, Meyer-Bolte K, Uschinsky K, Haupt R, Schoenmakers EF, Bartnitzke S, Van de Ven WJ, Bullerdiek J.Molecular characterization of 12q14–15 rearrangements in three pulmonary chondroid hamartomas. Cancer Res 1995;55, 2497–2499.

Kennedy RD, Chen CC, Stuckert P, et al. Fanconi anemia pathway-deficient tumor cells are hypersensitive to inhibition of ataxia telangiectasia mutated. J Clin Invest 2007;117:1440–9.

Khanna KK, Jackson SP. DNA double-strand breaks: signaling, repair and the cancer connection. Nat Genet 2001 Mar;27(3):247-54.

Khosravi R, Maya R, Gottlieb T, Oren M, Shiloh Y, Shkedy D. Rapid ATM-dependent phosphorylation of MDM2 precedes p53 accumulation in response to DNA damage. Proc Natl Acad Sci U S A 1999;21;96(26):14973-7.

Khosravi R, Maya R, Gottlieb T, Oren M, Shiloh Y, Shkedy D. Rapid ATM-dependent phosphorylation of MDM2 precedes p53 accumulation in response to DNA damage. Proc Natl Acad Sci USA 1999;96:14973-77.

Kools, P. F. & Van de Ven, W. J. Amplification of a rearranged form of the high-mobility group protein gene HMGI-C in OsA-CI osteosarcoma cells. Cancer Genet Cytogenet 1996;91, 1–7.

Kozlov SV, Graham ME, Peng C, Chen P, Robinson PJ, Lavin MF. Involvement of novel autophosphorylation sites in ATM activation. EMBO J 2006; 25:3504-14.

Kung, A.L., Zetterberg, A., Sherwood, S.W., Schimke, R.T. Cytotoxic effects of cell cycle phase specific agents: result of cell cycle perturbation. Cancer Res 1990;15;50(22):7307-17.

Kurose A, Tanaka T, Huang X, Traganos F, Dai W, Darzynkiewicz Z. Effects of hydroxyurea and aphidicolin on phosphorylation of ataxia telangiectasia mutated on Ser 1981 and histone H2AX on Ser 139 in relation to cell cycle phase and induction of apoptosis. Cytometry A 2006;69:212-21.

Lavin M. F., Kozlov S. ATM Activation and DNA Damage Response. Cell Cycle 2007;6:8, 931-942.

Lee JH, Paull TT. ATM activation by DNA double-strand breaks through the Mre11-Rad50-Nbs1 complex. Science 2005;22;308(5721):551-4.

Li L, Zou L. Sensing, signaling, and responding to DNA damage: organization of

the checkpoint pathways in mammalian cells. J Cell Biochem 2005;1;94(2):298-306.

Ligon A.H., Moore S.D., Parisi M.A., Mealiffe M.E., Harris D.J., Ferguson H.L., Quade B.J., Morton C.C. Constitutional rearrangement of the architectural factor HMGA2: a novel human phenotype including overgrowth and lipomas. Am J Hum Genet 2005;76;340-348.

Linke, S.P., Clarkin, K.C., Wahl, G.M. p53 mediates permanent arrest over multiple cell cycles in response to gamma-irradiation. Cancer Res 1997;57:1171-1179.

Lobrich, M. and Jeggo, P.A. The impact of a negligent G2/M checkpoint on genomic instability and cancer induction. Nat Rev Cancer 2007;7;861–869.

Lou Z, Minter-Dykhouse K, Wu X, Chen J. MDC1 is coupled to activated CHK2 in mammalian DNA damage response pathways. Nature 2003; 27;421(6926):957-61.

Lu HR, Zhu H, Huang M, Chen Y, Cai YJ, Miao ZH, et al. Reactive oxygen species elicit apoptosis by concurrently disrupting topoisomerase II and DNAdependent protein kinase. Mol Pharmacol 2005;68:983–94

Mailand, N. Podtelejnikov AV, Groth A, Mann M, Bartek J, Lukas J. Dani. Regulation of G(2)/M events by Cdc25A through phosphorylation-dependent modulation of its stability. EMBO J 2002;21;5911–5920.

Martinez Hoyos J, Fedele M, Battista S, Pentimalli F, Kruhoffer M, Arra C, Orntoft TF, Croce CM, Fusco A. HAND-1 gene expression is negatively regulated by the High Mobility Group A1 proteins and is drastically reduced in human thyroid carcinomas. Oncogene 2009;8(6):876-85

Matsuoka, S., Huang, M., Elledge, S.J. Linkage of ATM to cell cycle regulation by the Chk2 protein kinase. Science 1998;282(5395):1893-1897.

Maya R, Balass M, Kim ST, Shkedy D, Leal JF, Shifman O, Moas M, Buschmann T, Ronai Z, Shiloh Y, Kastan MB, Katzir E, Oren M. ATM-dependent phosphorylation of Mdm2 on serine 395: Role in p53 activation by DNA damage. Genes Dev 2001;15:1067-77.

McManus KJ, Hendzel MJ. ATM-dependent DNA damage-independent mitotic

phosphorylation of H2AX in normally growing mammalian cells. Mol Biol Cell 2005;16:5013-25.

Meulmeester E, Pereg Y, Williams BR, Lukas J, Bartek J. ATM-mediated phosphrylations inhibit Mdmx/Mdm2 stabilization by HAUSP in favor of p53 activation. Cell Cycle 2005;4:1166-70.

Mills, K.D., Ferguson, D.O. and Alt, F.W. The role of DNA breaks in genomic instability and tumorigenesis. Immunol Rev 2003;194, 77–95.

Mochan TA, Venere M, DiTullio RA Jr, Halazonetis TD. 53BP1 and NFBD1/MDC1-Nbs1 function in parallel interacting pathways activating ataxia-telangiectasia mutated (ATM) in response to DNA damage. Cancer Res 2003;15;63(24):8586-91.

Muller-Tidow C, Ji P, Diederichs S, Potratz J, Baumer N, Kohler G, Cauvet T, Choudary C, van der Meer T, Chan WY, Nieduszynski C, Colledge WH, Carrington M, Koeffler HP, Restle A, Wiesmuller L, Sobczak-Thepot J, Berdel WE, Serve H. The cyclin A1-CDK2 complex regulates DNA double-strand break repair. Mol Cell Biol 2004;24(20):8917-8928.

Narita M, Krizhanovsky V, Nunez S, Chicas A, Hearn SA, Myers MP, Lowe SW. A novel role for high-mobility group a proteins in cellular senescence and heterochromatin formation. Cell 2006;126:503–514.

Nigg, E.A., Mitotic kinases as regulators of cell division and its checkpoints. Nat Rev Mol Cell Biol 2001;2(1):21-32.

Nyberg, K. A., Michelson, R. J., Putnam, C. W. & Weinert, T. A. Toward maintaining the genome: DNA damage and replication checkpoints. Annu Rev Genet 2002;36;617–656.

Oakley GG, Loberg LI, Yao J, Risinger MA, Yunker RL, Zernik-Kobak M, Khanna KK, Lavin MF, Carty MP, Dixon K. UV-induced hyperphosphorylation of replication protein a depends on DNA replication and expression of ATM protein. Mol Biol Cell 2001;12:1199-1213.

Patterson D, Woffle AP. Developmental roles for chromatin and chromosomal structure. Dev Biol 1996; 173: 2-13.

Peng CY, Graves PR, Thoma RS, Wu Z, Shaw AS, Piwnica-Worms H. Mitotic and G2 checkpoint control: Regulation of 14-3-3 protein binding by phosphorylation of Cdc25C on serine-216. Science 1997; 277:1501-5.

Pereg Y, Shkedy D, de Graaf P, Meulmeester E, Edelson-Averbukh M, Salek M, Biton S, Teunisse AF, Lehmann WD, Jochemsen AG, Shiloh Y. Phosphorylation of Hdmx mediates its Hdm2-and ATM-dependent degradation in response to DNA damage. Proc Natl Acad Sci USA 2005; 102:5056-61.

Pierantoni GM, Finelli P, Valtorta E, Giardino D, Rodeschini O, Esposito F, Losa M, Fusco A, Larizza L. High-mobility group A2 gene expression is frequently induced in non-functioning pituitary adenomas (NFPAs), even in the absence of chromosome 12 polysomy. Endocrine Related Cancer 2005;12:867-874.

Pierantoni GM, Rinaldo C, Esposito F, Mottolese M, Soddu S, Fusco A. High mobility group A1 (HMGA1) proteins interact with p53 and inhibit its apoptotic activity, Cell Death Differ 2006;13:1554–1563.

Rainey MD, Charlton ME, Stanton RV, Kastan MB. Transient inhibition of ATM kinase is sufficient to enhance cellular sensitivity to ionizing radiation. Cancer Res 2008;68(18):7466-74.

Rao VA, Fan AM, Meng L, Doe CF, North PS, Hickson ID, Pommier Y. Phosphorylation of BLM, dissociation from topoisomerase IIIalpha, and colocalization with gamma-H2AX after topoisomerase I-induced replication damage. Mol Cell Biol 2005;25:8925-37.

Rich, T., Allen, R.L & Wyllie, A.H. Defying death after DNA damage. Nature 2000;407;777–783.

Robles, S.J., Adami, G.R. Agents that cause DNA double strand breaks lead to p16INK4a enrichment and the premature senescence of normal fibroblasts. Oncogene 1998;16(9):1113-1123.

Rogakou EP, Pilch DR, Orr AH, Ivanova VS, Bonner WM. DNA double-stranded breaks induce histone H2AX phosphorylation on serine 139. J Biol Chem 1998; 6;273(10):5858-68.

Rogalla P, Drechsler K, Frey G, Hennig Y, Helmke B, Bonk U, Bullerdiek J. HMGI-C expression patterns in human tissues. Implications for the genesis of frequent mesenchymal tumors. Am J Pathol 1996; 149(3):775-9.

Rommel B, Rogalla P, Jox A, Kalle CV, Kazmierczak B, Wolf J, Bullerdiek J.HMGI-C, a member of the high mobility group family of proteins, is expressed in hematopoietic stem cells and in leukemic cells. Leuk Lymphoma 1997;26, 603–607.

Rouse, J. and Jackson, S.P. Interfaces between the detection,signaling, and repair of DNA damage. Science 2002;297;547–551.

Sabisz M, Skladanowski A. Modulation of cellular response to anticancer treatment by caffeine: inhibition of cell cycle checkpoints, DNA repair and more. Curr Pharm Biotechnol 2008; 9:325–36.

Saito S, Goodarzi AA, Higashimoto Y, Noda Y, Lees-Miller SP, Appella E, Anderson CW. ATM mediates phosphorylation at multiple p53 sites, including Ser(46), in response to ionizing radiation. J Biol Chem 2002; 277:12491-94.

Sanchez, Y., Wong, C., Thoma, R.S., Richman, R., Wu, Z., Piwnica-Worms, H., Elledge, S.J.,. Conservation of the Chk1 checkpoint pathway in mammals: linkage of DNA damage to Cdk regulation through Cdc25. Science 1997;277(5331):1497-1501.

Sanna S., A.U. Jackson, R. Nagaraja, C.J. Willer, W.M. Chen, L.L. Bonnycastle, H. Shen, N. Timpson, G. Lettre, G. Usala, P.S. Chines, H.M. Stringham, L.J. Scott, M. Dei, S. Lai, G. Albai, L. Crisponi, S. Naitza, K.F. Doheny, E.W. Pugh, Y. Ben-Shlomo, S. Ebrahim, D.A. Lawlor, R.N. Bergman, R.M. Watanabe, M. Uda, J. Tuomilehto, J. Coresh, J.N. Hirschhorn, A.R. Shuldiner, D. Schlessinger, F.S. Collins, G. Davey Smith, E. Boerwinkle, A. Cao, M. Boehnke, G.R. Abecasis, K.L. Mohlke, Common variants in the GDF5-UQCC region are associated with variation in human height, Nat Genet 2008;40;198-203.

Sapkota GP, Deak M, Kieloch A, Morrice N, Goodarzi AA, Smythe C, Shiloh Y, Lees-Miller SP, Alessi DR. Ionizing radiation induces ataxia telangiectasia mutated kinase (ATM)-mediated phosphorylation of LKB1/STK11 at Thr-366. Biochem J 2002; 368:507-16.

Sarkaria JN, Busby EC, Tibbetts RS, et al. Inhibitionof ATM and ATR kinase activities by the radiosensitizing agent, caffeine. Cancer Res 1999;59:4375–82.

Savitsky K, Bar-Shira A, Gilad S, et al. A single ataxia telangiectasia gene with a product similar to PI-3 kinase. Science 1995;268:1749–53.

Schmitt, C.A., Fridman, J.S., Yang, M., Lee, S., Baranov, E.,Hoffman, R.M.,

Lowe, S.W. A senescence program controlled by p53 and p16(INK4a) contributes to the outcome of cancer therapy. Cell 2002;109(3):335-346.

Schoenmakers E.F., Wanschura S., Mols R., Bullerdiek J., Van den Berghe H., Van de Ven W. J. Recurrent rearrangements in the high mobility group protein gene, HMGI-C, in benign mesenchymal tumours. Nat Genet 1995;10;436-444.

Schuler M, Green DR. Transcription, apoptosis and p53: catch-22. Trends Genet. 2005;21(3):182-7.

Sgarra R, Rustighi A, Tessari MA, et al. Nuclear phosphoproteins HMGA and their relationship with chromatin structure and cancer. FEBS Lett 2004;574:1–8.

Shiloh, Y. & Kastan, M. B. ATM: genome stability, neuronal development, and cancer cross paths. Adv Cancer Res 2001;83;209–254.

Shiloh, Y. ATM and related protein kinases: safeguarding genome integrity. Nature Rev Cancer 2003;3;155–168.

Shinohara ET, Geng L, Tan J, Chen H, Shir Y, Edwards E, et al. DNA-dependent protein kinase is a molecular target for the development of noncytotoxic radiation-sensitizing drugs. Cancer Res 2005;65:4987–92.

Sionov RV, Haupt Y. The cellular response to p53: the decision between life and death.Oncogene 1999;18(45):6145-57.

Sreekantaiah C., Leong S.P., Karakousis C.P., McGee D.L., Rappaport W.D., Villar H.V., Neal D., Fleming S., Wankel A., Herrington P.N., Carmona R., Sandberg A.A.Cytogenetic profile of 109 lipomas. Cancer Res 1991;51;422-433.

Stark GR, Taylor WR. Control of the G2/M transition. Mol Biotechnol 2006; 32:227-48.

Stewart GS, Wang B, Bignell CR, Taylor AM, Elledge SJ. MDC1 is a mediator of the mammalian DNA damage checkpoint. Nature 2003;27;421(6926):961-6.

Strunnikova, M., Schagdarsurengin, U., Kehlen, A., Garbe, J.C., Stampfer, M.R., Dammann, R. Chromatin inactivation precedes de novo DNA methylation during the progressive epigenetic silencing of the RASSF1A promoter. Mol Cell Biol 2005;25(10):3923-3933.

Subramanian, D. & Griffith, J. D. Interactions between p53, hMSH2-hMSH6 and HMGI(Y) on Holliday junctions and bulged bases. Nucleic Acids Res 2002;30,2427–2434.

Summer H, Li O, Bao Q, Zhan L, Peter S, Sathiyanathan P, Henderson D, Klonisch T, Goodman SD, Dröge P. HMGA2 exhibits dRP/AP site cleavage activity and protects cancer cells from DNA-damage-induced cytotoxicity during chemotherapy. Nucleic Acids Res 2009;37(13):4371-84.

Suzuki A, Kusakai G, Kishimoto A, Shimojo Y, Ogura T, Lavin MF, Esumi H. IGF-1 phosphorylates AMPK-alpha subunit in ATM-dependent and LKB1-independent manner. Biochem Biophys Res Commu 2004; 324:986-92.

Takahashi, A., Ohtani, N., Yamakoshi, K., Iida, S., Tahara, H., Nakayama, K., Nakayama, K.I., Ide, T., Saya, H., Hara, E. Mitogenic signalling and the p16INK4a-Rb pathway cooperate to enforce irreversible cellular senescence. Nat Cell Biol 2006;8(11):1291-1297.

Tamaru, H., Selker, E.U. A histone H3 methyltransferase controls DNA methylation in Neurospora crassa. Nature 2001;414(6861):277-283.

Tamaru, H., Zhang, X., McMillen, D., Singh, P.B., Nakayama, J., Grewal, S.I., Allis, C.D., Cheng, X., Selker, E.U. Trimethylated lysine 9 of histone H3 is a mark for DNA methylation in Neurospora crassa. Nat Genet 2003;34(1):75-79.

Tan TL, Essers J, Citterio E, Swagemakers SM, de Wit J, Benson FE, Hoeijmakers JH, Kanaar R. Mouse Rad54 affects DNA conformation and DNA-damage-induced Rad51 foci formation. Curr Biol 1999;25;9(6):325-8.

Tanaka T, Halicka D, Huang X, Traganos F, Darzynkiewicz Z. Constitutive histone H2AX phosphorylation and ATM activation, the reporters of DNA damage by endogenous oxidants. Cell Cycle 2007;5;1940-45.

Taniguchi T, Garcia-Higuera I, Xu B, Andreassen PR, Gregory RC, Kim ST, Lane WS, Kastan MB, D'Andrea AD. Convergence of the Fanconi anemia and ataxia telangiectasia signaling pathways. Cell 2002; 109:459-72.

Thanos D, Maniatis T. The high mobility group protein HMG I(Y) is required for NF-kappa B-dependent virus induction of the human IFN-beta gene. Cell 1992; 71(5):777-89.

Thanos, D., Du, W. & Maniatis, T. The high mobility group protein HMG I(Y) is an essential structural component of a virus-inducible enhancer complex. Cold Spring Harb Symp Quant Biol 1993;58, 73–81

Thomas, JO. and Travers AA. HMG1 and 2 and related "architectural" DNAbinding proteins. Trends Biochem Sci 2001;26:167-174.

Tollefsbol, T.O., Andrews, L.G. Mechanisms for methylation-mediated gene silencing and aging. Med Hypotheses 1993.41(1):83-92.

Van den Bosch M, Bree RT, Lowndes NF.The MRN complex: coordinating and mediating the response to broken chromosomes. EMBO Rep 2003;4(9):844-9.

Vestner B, Bustin M, Gruss C. Stimulation of replication efficiency of a chromatin template by chromosomal protein HMG-17. J Biol Chem 1998;273:9409–9414.

Viale A, De Franco F, Orleth A, Cambiaghi V, Giuliani V, Bossi D, Ronchini C, Ronzoni S, Muradore I, Monestiroli S, Gobbi A, Alcalay M, Minucci S, Pelicci PG. Cell-cycle restriction limits DNA damage and maintains self-renewal of leukaemia stem cells. Nature 2009;1;457(7225):51-6.

Viniegra JG, Martinez N, Modirassari P, Losa JH, Parada Cobo C, Lobo VJ, Luquero CI, Alvarez-Vallina L, Ramon Y, Cajal S, Rojas JM, Sanchez-Prieto R. Full activation of PKB/Akt in response to insulin or ionizing radiation is mediated through ATM. J Biol Chem 2005; 280:4029-36.

Wahl, G. M. & Carr, A. M. The evolution of diverse biological responses to DNA damage: insights from yeast and p53. Nature Cell Biol 2001;3; E277–E286

Waldman, T., Lengauer, C., Kinzler, K.W., Vogelstein, B. Uncoupling of S phase and mitosis induced by anticancer agents in cells lacking p21. Nature 1996;381(6584):713-716.

Ward IM, Chen J. Histone H2AX is phosphorylated in an ATR-dependent manner in response to replicational stress. J Biol Chem 2001;21;276(51):47759-62.

Wechsler T, Chen BP, Harper R, Morotomi-Yano K, Huang BC, Meek K, Cleaver JE, Chen DJ, Wabl M. DNA-PKcs function regulated specifically by protein phosphatase 5. Proc Natl Acad Sci USA 2004; 101:1247-52.

Weedon M.N., G. Lettre, R.M. Freathy, C.M. Lindgren, B.F. Voight, J.R. Perry, K.S. Elliott, R. Hackett, C. Guiducci, B. Shields, E. Zeggini, H. Lango, V. Lyssenko, N.J. Timpson, N.P. Burtt, N.W. Rayner, R. Saxena, K. Ardlie, J.H. Tobias, A.R. Ness, S.M. Ring, C.N. Palmer, A.D. Morris, L. Peltonen, V. Salomaa, Diabetes Genetics Initiative, Wellcome Trust Case Control Consortium, G. Davey Smith, L.C. Groop, A.T. Hattersley, M.I. McCarthy, J.N. Hirschhorn, T.M. Frayling, A common variant of HMGA2 is associated with adult and childhood height in the general population. Nat Genet 2007;39;245-1250.

Weedon M.N., H. Lango, C.M. Lindgren, C. Wallace, D.M. Evans, M. Mangino, R.M. Freathy, J.R. Perry, S. Stevens, A.S. Hall, N.J. Samani, B. Shields, I. Prokopenko, M. Farrall, A. Dominiczak, Diabetes Genetics Initiative, Wellcome Trust Case Control Consortium, T. Johnson, S. Bergmann, J.S. Beckmann, P. Vollenweider, D.M. Waterworth, V. Mooser, C.N. Palmer, A.D. Morris, W.H. Ouwehand, Cambridge GEM Consortium, J.H. Zhao, S. Li, R.J. Loos, I. Barroso, P. Deloukas, M.S. Sandhu, E. Wheeler, N. Soranzo, M. Inouye, N.J. Wareham, M. Caulfield, P.B. Munroe, A.T. Hattersley, M.I. McCarthy, T.M. Frayling, 19 Genome-wide association analysis identifies 20 loci that influence adult height. Nat Genet 2008;40;575-583.

Willmore E, de Caux S, Sunter NJ, Tilby MJ, Jackson GH, Austin CA, et al. A novel DNA-dependent protein kinase inhibitor, NU7026, potentiates the cytotoxicity of topoisomerase II poisons used in the treatment of leukemia. Blood 2004;103:4659–65.

Wood, L. J., Maher, J. F., Bunton, T. E. & Resar, L. M. The oncogenic properties of the HMG-I gene family. Cancer Res 2000;4256–4261.

Wyman, C. and Kanaar, R. DNA double-strand break repair: all's well that ends well. Annu Rev Genet 2006;40;363–383.

Xu B, Kim ST, Kastan MB. Involvement of Brca1 in S-phase and G2 -phase checkpoints after ionizing radiation. Mol Cell Biol 2001; 21:3445-50.

Xu Y, Baltimore D. Dual roles of ATM in the cellular response to radiation and in cell growth control. Genes Dev 1996;1;10(19):2401-10.

Xu Y, Yang EM, Brugarolas J, Jacks T, Baltimore D. Involvement of p53 and p21 in cellular defects and tumorigenesis in Atm-/- mice. Mol Cell Biol 1998;18(7):4385-90.

Xu, B., Kim, S.-T., Lim, D.-S. & Kastan, M. B. Two molecularly distinct G(2)/M checkpoints are induced by ionizing irradiation. Mol Cell Biol 2002;22;1049–1059.

Yarden RI, Pardo-Reoyo S, Sgagias M, Cowan KH, Brody LC. BRCA1 regulates the G2/M checkpoint by activating Chk1 kinase upon DNA damage. Nat Genet 2002; 30:285-89.

Yoo HY, Shevchenko A, Shevchenko A, Dunphy WG. Mcm2 is a direct substrate of ATM and ATR during DNA damage and DNA replication checkpoint responses. J Biol Chem 2004; 279:53353-64.

Yoshida K, Miki Y. Role of BRCA1 and BRCA2 as regulators of DNA repair, transcription, and cell cycle in response to DNA damage. Cancer Sci. 2004;95(11):866-71.

Yuan ZM, Huang Y, Ishiko T, Nakada S, Utsugisawa T, Kharbanda S, Wang R, Sung P, Shinohara A, Weichselbaum R, Kufe D. Regulation of Rad51 function by c-Abl in response to DNA damage. J Biol Chem 1998;13;273(7):3799-802.

Zeng, Y., Forbes, K.C., Wu, Z., Moreno, S., Piwnica-Worms,H., Enoch, T. Replication checkpoint requiresmphosphorylation of the phosphatase Cdc25 by Cds1 or Chk1. Nature 1998; 395(6701):507-510.

Zhang J, Willers H, Feng Z, Ghosh JC, Kim S, Weaver DT, Chung JH, Powell SN, Xia F. Chk2 phosphorylation of BRCA1 regulates DNA double-strand break repair. Mol Cell Biol 2004;24(2):708-18.

Zhang, R., Chen, W., Adams, P.D. Molecular dissection of formation of senescent associated heterochromatin foci. Mol Cell Biol 2007. 27(6):2343-2358.

Zhao, K., Käs, E., Gonzalez, E. & Laemmli, U. K. SARdependent mobilization of histone H1 by HMG-I/Y in vitro: HMG-I/Y is enriched in H1-depleted chromatin. EMBO J 1993;12, 3237–3247 .

Zhou, B.-B.S. and Elledge, S.J. The DNA damage response: putting checkpoints in perspective. Nature 2000; 408;433–439.

Zhou, X., Benson, K. F., Ashar, H. R. & Chada K. Mutation responsible for the mouse pygmy phenotype in the developmentally regulated factor HMGI-C. Nature 1995; 376, 771–774.

Zou Y, Wang Y. Tandem mass spectrometry for the examination of the posttranslational modifications of highmobility group A1 proteins: symmetric and asymmetric dimethylation of Arg25 in HMGA1a protein. Biochemistry 2005;44:6293–301.

HMGA2 induces pituitary tumorigenesis by enhancing E2F1 activity

Monica Fedele,[1,8] Rosa Visone,[1,2,8] Ivana De Martino,[1] Giancarlo Troncone,[3] Dario Palmieri,[1] Sabrina Battista,[1] Andrea Ciarmiello,[4] Pierlorenzo Pallante,[1] Claudio Arra,[4] Rosa Marina Melillo,[1] Kristian Helin,[5,6] Carlo Maria Croce,[2] and Alfredo Fusco[1,7,*]

[1] Istituto di Endocrinologia ed Oncologia Sperimentale del CNR and Dipartimento di Biologia e Patologia Cellulare e Molecolare, Università di Napoli ''Federico II'', 80131 Naples, Italy
[2] Division of Human Cancer Genetics, Comprehensive Cancer Center, The Ohio State University, Columbus, Ohio 43210
[3] Dipartimento di Anatomia Patologica, Università di Napoli ''Federico II'', 80131 Naples, Italy
[4] Istituto dei Tumori di Napoli Fondazione ''G. Pascale'', via Semmola, 80131 Naples, Italy
[5] Biotech Research & Innovation Centre, Fruebjergvej 3, 2100 Copenhagen, Denmark
[6] European Institute of Oncology, Department of Experimental Oncology, 20141 Milan, Italy
[7] NOGEC (Naples Oncogenomic Center) – CEINGE, Biotecnologie Avanzate, Naples, Italy
[8] These authors contributed equally to this work.
*Correspondence: afusco@napoli.com

Summary

***HMGA2* gene amplification and overexpression in human prolactinomas and the development of pituitary adenomas in *HMGA2* transgenic mice showed that HMGA2 plays a crucial role in pituitary tumorigenesis. We have explored the pRB/E2F1 pathway to investigate the mechanism by which HMGA2 acts. Here we show that HMGA2 interacts with pRB and induces E2F1 activity in mouse pituitary adenomas by displacing HDAC1 from the pRB/E2F1 complex—a process that results in E2F1 acetylation. We found that loss of E2F1 function (obtained by mating *HMGA2* and *E2F1*$^{-/-}$ mice) suppressed pituitary tumorigenesis in *HMGA2* mice. Thus, HMGA2-mediated E2F1 activation is a crucial event in the onset of these tumors in transgenic mice and probably also in human prolactinomas.**

Introduction

High mobility group A (HMGA) proteins are nonhistone nuclear compounds known as architectural transcriptional factors because they mediate the assembly of multiprotein complexes involved in gene transcription. In fact, by interacting with the minor groove of many AT-rich promoters and enhancers, HMGA proteins do not per se exert transcriptional activity, but organize chromatin into the structure required by the transcription machinery to allow gene transcription. There are four HMGA proteins: HMGA1a, HMGA1b, HMGA1c, and HMGA2. The first three are encoded by the gene *HMGA1*, whereas HMGA2 is encoded by *HMGA2. HMGA2* is almost ubiquitously expressed at high levels during embryogenesis, whereas in adult tissues it occurs only in CD34-positive hematopoietic stem cells, uterine myoblasts, testicular cells, and proliferating preadipocytes. Its function is critical for growth and adipocytic cell differentiation. In fact, its impairment results in pygmy mice with greatly reduced fat tissue, whereas its activation by truncation leads to giant mice affected by lipomatosis. *HMGA2* overexpression was first demonstrated in rat thyroid transformed cells and experimental thyroid tumors. Subsequent studies showed that *HMGA2* expression is required for thyroid cell neoplastic transformation and that HMGA2 expression is correlated with human malignant tumors. HMGA2 rearrangements are frequent in benign tumors of mesenchymal origin (reviewed by Fedele et al., 2001). We previously found that the *HMGA2* gene is amplified and overexpressed in most human prolactinomas characterized by chromosome 12 trisomy and tetrasomy (Finelli et al., 2002) and that transgenic mice expressing high levels of the *HMGA2* transgene in all tissues develop pituitary adenomas secreting prolactin and growth hormone, thereby confirming that *HMGA2* plays a critical role in human pituitary adenomas (Fedele et al., 2002).

The aim of our study was to investigate the mechanisms by which HMGA2 leads to the onset of pituitary adenomas in *HMGA2* transgenic mice and probably also in humans.

There are striking phenotypic similarities between the pRB and HMGA2 animal models. In fact, transgenic mice

SIGNIFICANCE

The molecular pathway leading to pituitary tumorigenesis is one of the challenges of endocrine oncology. Here, we describe a mechanism by which HMGA2 induces pituitary adenomas in mice. This mechanism entails an HMGA2-dependent process that relieves pRB-mediated repression of E2F1. It is likely that the same mechanism is involved in most of the human prolactinomas in which the *HMGA2* gene is amplified and overexpressed. Elucidation of the mechanism by which HMGA2 induces pituitary adenomas opens up the possibility of intervening in this mechanism to prevent or halt the onset of these tumors.

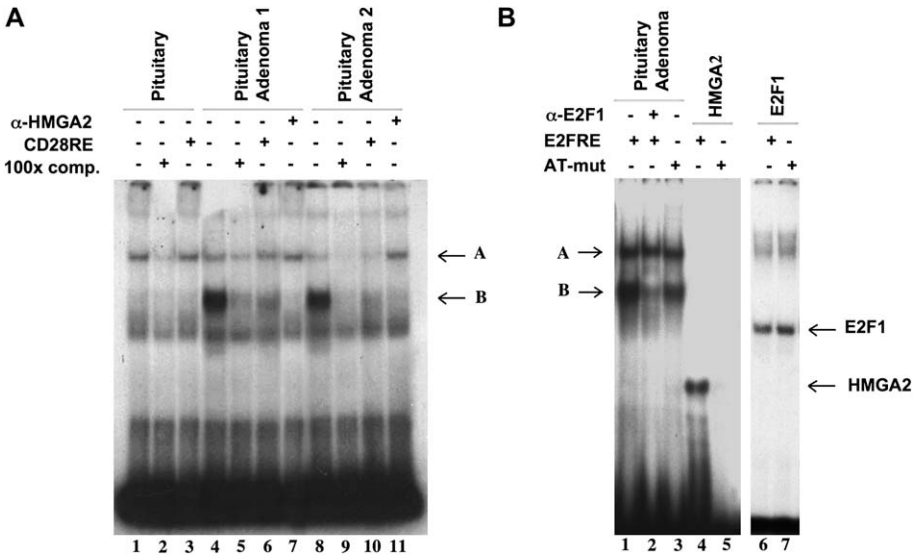

Figure 1. HMGA2 increases E2F1 DNA binding activity in pituitary adenomas

A: EMSA with extracts from a pool of pituitary glands (lanes 1–3) and two pituitary adenomas (lanes 4–11) of *HMGA2* transgenic mice using an E2F-responsive element sequence (E2FRE) as a probe. Samples were incubated with E2FRE (lanes 1, 4, and 8) or were preincubated with 100× CD28 responsive element (CD28RE), which is a specific competitor for HMGA2 binding (lanes 3, 6, and 10), with 100× E2FRE unlabeled probe (lanes 2–5 and 9), and with specific polyclonal anti-HMGA2 antibody (lanes 7 and 11), before the addition of the probe. Arrows indicate specifc complexes DNA/proteins.

B: EMSA of pituitary extracts of adenomas from *HMGA2* transgenic mice with E2FRE (lanes 1 and 2) or E2FRE mutated in the region rich in AT bases (AT-mut; lane 3). The samples in lanes 1 and 2 were incubated without (lane 1) or with anti-E2F1 antibody (lane 2), before the addition of the probe. His-HMGA2 (lanes 4–5) or GST-E2F1 (lanes 6–7) recombinant proteins were incubated with E2FRE or AT-mut, as indicated above.

overexpressing pRB show a dwarf phenotype because of defective cell proliferation (Bignon et al., 1993) as do *HMGA2* null mice. Conversely, $Rb^{+/-}$ mice are larger than their littermates (Jacks et al., 1992), as are transgenic mice carrying an activated *HMGA2* gene (Battista et al., 1999). Moreover, mice carrying a germline mutation of one *Rb* allele are highly predisposed to develop pituitary tumors (Jacks et al., 1992), and this occurs also in mice with impaired functioning of p27 or p18, both of which converge on pRB (Franklin et al., 1998).

The finding that loss of E2F1 reduced pituitary tumorigenesis in *Rb* knockout mice suggests that loss of pRB induces the onset of pituitary tumors by activating E2F1 (Yamasaki et al., 1998). We therefore investigated the role of the pRB pathway in the onset of pituitary adenomas in transgenic mice overexpressing HMGA2.

pRB and the related proteins p130 and p107 control cell cycle progression through their interactions with the E2F family of transcription factors. E2F1 is known to activate transcription of a number of genes required for the S phase of the cell cycle. Transcriptional repression of E2F1 target genes entails recruitment of pRB by E2F1 to the gene promoters. This recruitment masks the activation domain of E2F1 and prevents its interaction with the general transcriptional machinery. Before cells enter S phase, pRB is phosphorylated at multiple sites by cyclin-dependent kinases. This phosphorylation leads to pRB inactivation, release of E2F1, and transcriptional activation of its target genes (reviewed by Seville et al., 2005). Moreover, pRB recruits class I histone deacetylase proteins that repress transcription by removing acetyl groups from the histones. Removal of the acetyl groups facilitates the condensation of nucleosomes into chromatin, which in turn blocks access to transcription factors and leads to gene repression (Magnaghi-Jaulin et al., 1998).

Here we report that HMGA2 binds to pRB and prevents it from repressing the E2F1-responsive promoters mainly by displacing HDAC1 from pRB. This results in enhanced acetylation of both E2F1 and associated histones, which could account for the enhanced E2F1 activity observed in HMGA2-induced pituitary adenomas and associated with the HMGA2 overexpression. To verify the crucial role of enhanced E2F activity in the onset of pituitary adenomas, we mated transgenic mice overexpressing HMGA2 with *E2F1* knockout mice (Field et al., 1996). The adenomatous phenotype was almost totally rescued in the double mutant mice, which demonstrates that HMGA2-mediated E2F1 activation is a prerequisite for pituitary tumorigenesis.

Results

E2F1 DNA binding activity is increased in pituitary adenomas of *HMGA2* transgenic mice

To investigate whether the pRB/E2F1 pathway is involved in pituitary tumorigenesis in *HMGA2* transgenic mice, we analyzed E2F DNA binding activity in HMGA2 pituitary adenomas and normal pituitary glands from control mice by electrophoretic mobility shift assay (EMSA) using an E2F-responsive element (E2FRE) as probe. As shown in Figure 1A, E2F1 DNA binding activity was dramatically higher in HMGA2 pituitary adenomas than in pituitary glands from control mice. A specific complex containing E2F (complex A) was present in normal pituitary gland (lane 1). Another, faster-migrating complex (complex B) was associated with pituitary adenomas from HMGA2 mice (lanes 4 and 8). Competition analyses with specific anti-E2F1 antibodies showed that this band corresponds to the free E2F1-DNA complex (Figure 1B, lane 2). Band specificity was assessed by adding a 100× molar excess of unlabeled probe (Figure 1A, lanes 2, 5, and 9). Preincubation with an oligonucleotide (CD28RE) that specifically binds to HMGA2 (Baldassarre et al., 2001) prevented the formation of this complex (Figure 1A, lanes 6 and 10). Moreover, an antibody against HMGA2 significantly reduced the band corresponding to complex B (Figure 1A, lanes 7 and 11). These data show that HMGA2 plays a crucial role in the formation of complex B.

HMGA2 binds to the E2F1 responsive element and enhances the binding of E2F1 to DNA

HMGA proteins allow the assembly of multiprotein complexes by directly binding to the DNA in AT-rich sequences. We used an E2F consensus oligonucleotide (E2FRE) that has an AT stretch compatible with HMGA binding in an EMSA assay with

a recombinant HMGA2 protein. As shown in lane 4 of Figure 1B, HMGA2 was able to bind to the E2F-responsive oligonucleotide, but not to the same oligonucleotide mutated in the AT-stretch flanking the E2F-consensus sequence (AT-mut). Interestingly, the binding of free E2F1 to DNA in pituitary adenomas from HMGA2 transgenic mice was considerably decreased on the AT-mut probe (Figure 1B, lane 3). Because the binding of the recombinant E2F1 to its consensus DNA was not impaired by the AT mutation (Figure 1B, lanes 6 and 7), we suggest that the binding of HMGA2 to its consensus sequence, flanking the E2F binding site, is crucial for efficient E2F1/DNA binding.

HMGA2 interacts with the pRB protein

Since free E2F1/DNA binding depends essentially on E2F1 release from pRB, HMGA2 may interfere with the pRB pathway. To investigate whether HMGA2 interacts with pRB, we coimmunoprecipitated protein lysates from two HMGA2 pituitary adenomas and from a pool of pituitary glands from control mice. Immunoprecipitation of the protein lysates with anti-pRB antibodies resulted in the coimmunoprecipitation of HMGA2 from pituitary adenomas (Figure 2A, left panels). Western blot analysis showed that pRB was equally expressed in pituitary glands and adenomas, whereas the HMGA2 protein was expressed only in HMGA2 pituitary adenomas.

We next verified the HMGA2/pRB interaction in a heterologous cell system. HEK293 cells were transiently cotransfected with hemagglutinin (HA)-tagged-HMGA2 and pRB expression vectors. Protein lysates were immunoprecipitated with anti-pRB or anti-HA antibodies and immunoblotted with anti-HA or anti-pRB, respectively (Figure 2A, right panels). Coexpression of pRB and HMGA2 resulted in coimmunoprecipitation of the two proteins. Conversely, there was no coimmunoprecipitation when HEK293 cells were transfected with HA-HMGA2 or pRB expression vectors alone. Indeed, consistent with the endogenous expression of pRB in HEK293 cells, longer exposure times resulted in a faint band in HA-HMGA2 transfected cells (data not shown).

The HMGA2/pRB interaction is direct and involves either the pocket region or the N terminus of pRB

To determine whether HMGA2 interacts directly with pRB, we carried out Far-Western analyses in which we probed HMGA2 on pRB immunoprecipitates from cell lysates overexpressing wild-type and different mutant forms of the pRB protein (Figures 2B and 2C). Interestingly, HMGA2 was found to bind to the pRB mutant expressing only the pocket region (lane 5) as efficiently as to the wild-type pRB (lane 1). It did not bind to the naturally occurring mutant pRBΔ21 that carries a deletion of exon 21 and encodes a portion of the pocket region (lane 4). pRB mutants 661 and 13S, which carry a point mutation in the pRB pocket region and amino acid substitutions and insertions in the C-terminal region, respectively (lanes 2 and 3), did not affect binding between pRB and HMGA2.

These results are supported by in vitro binding experiments in which GST-pRB fusion proteins containing various pRB domains (Figure 2B) were incubated with a lysate from cells overexpressing HMGA2 (Figure 2D). pRB(379-928), which contains the entire wild-type pocket region of pRB plus the C-terminal region, was able to bind efficiently to HMGA2 (lane 1). In contrast, pRB(379-928)Δ21, which lacks the region corresponding to exon 21, only weakly associated with HMGA2 (lane 3). pRB(768-928) and pRB(834-928), which carry the C-terminal region plus a small region of the pocket and the C-terminal region only, respectively, did not bind to HMGA2 at all (lanes 5 and 6). Finally, pRB(1-379) and pRB(379-792), carrying the N-terminal region and the pocket region, respectively, were able to bind efficiently to HMGA2 (lanes 2 and 4). These results indicate that HMGA2 binds to pRB in two regions: the N terminus and the pocket region between amino acids 703 and 737.

The second AT-hook of HMGA2 is required for interaction with pRB

We next investigated the regions of HMGA2 that are required to form a complex with pRB. HMGA2 contains three AT-hook domains that are involved in both DNA and protein-protein interactions, and an acidic C-terminal tail preceded by a spacer region (Figure 2E). We used cell lysates expressing HA-HMGA2 mutants carrying serial deletions at the N and C terminus regions (Figure 2E) in a pull-down assay with a recombinant GST-pRB protein (Figure 2F, lanes 1–6). The only mutant that lost the capacity to bind to pRB was A2(1-44), which contains the N terminus, the first AT-hook, and the region preceding the second AT-hook. Because all the other mutants, including A2(1-56), which encodes the same protein portion as mutant A2(1-44) plus the second AT-hook, were able to bind to pRB as efficiently as the wild-type HMGA2, we suggest that the second AT-hook domain of HMGA2 is principally involved in binding to pRB. To map more precisely the HMGA2 region involved in forming a complex with pRB, we generated an HMGA2 mutant lacking only the second AT-hook [A2(Δ^{45-56})] (Figure 2E) and used it in a pull-down assay with the GST-pRB protein (Figure 2F, lane 7). The A2(Δ^{45-56}) mutant was less able than wild-type HMGA2 to bind to pRB. This confirms that the region of HMGA2 coding for the second AT-hook is principally involved in binding pRB and suggests, however, that other regions of the HMGA2 protein might also be involved in this binding.

HMGA2 overexpression counteracts pRB-mediated inhibition of E2F activity and cell proliferation

To define better the role of the pRB/HMGA2 interaction in the regulation of E2F1 transcriptional activity, we examined the activity of two E2F1-responsive promoter genes, i.e., CDC25A and CDC6, fused to a luciferase reporter gene, in the HEK293 cells transiently transfected with plasmids expressing the pRB and HMGA2 proteins. As shown in Figure 3A, pRB repressed CDC6 and CDC25A promoter activity (3-fold decrease), whereas HMGA2 increased these activities (up to 3-fold) in a dose-dependent manner. When pRB was cotransfected with increasing levels of HMGA2, pRB repression of CDC25A and CDC6 promoter activity was significantly antagonized. In particular, 5 μg of transfected HMGA2 vector abolished repression, and 10 μg of HMGA2 caused a switch from repression to activation (2.5-fold increase). Similar experiments were carried out in pRB null Saos-2 cells by transfecting pRB, HMGA2, and mutants A2(1-44) or A2(Δ^{45-56}), as indicated in Figure 3B. In the absence of pRB, HMGA2 does not affect E2F target gene activation, and neither of the mutants antagonized the pRB-mediated inhibition of the promoter-response activity, which suggests that HMGA2 binding to pRB is required for this effect.

The results of a colony-forming assay of Saos-2 cells demonstrate that HMGA2 antagonizes the pRB-mediated inhibition of cell proliferation (Figure 3C). The expression of transfected

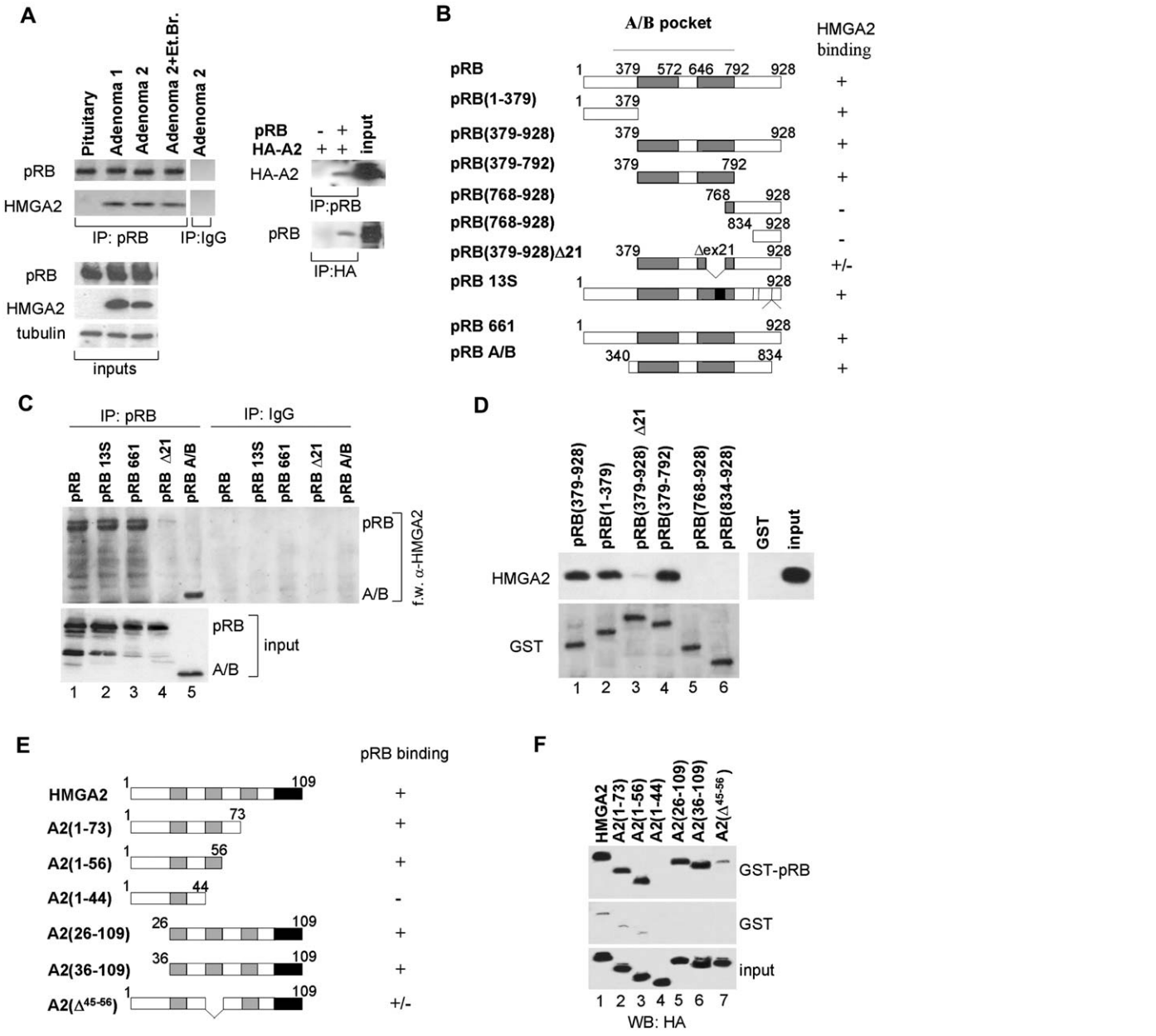

Figure 2. HMGA2 interacts with pRB

A: Left panels. Lysates from a pool of pituitary glands of control mice and from the pituitary adenomas shown in Figure 1 were subjected to Western blot analysis with either anti-pRB or anti-HMGA2 antibodies to verify protein expression. The expression of γ-tubulin served to verify equal loading of proteins. The same lysates were immunoprecipitated with anti-pRB antibody, resolved by SDS-PAGE, and analyzed by Western blot with anti-HMGA2 antibody. Immunoprecipitation in the presence of EtBr and with IgG were also performed as control of the specificity of the interaction. Right panels. Whole-cell lysates from HEK293 cells untransfected or transfected with the indicated expression plasmids were immunoprecipitated with anti-pRB (upper panel) or anti-HA (lower panel) antibodies, run on an SDS-PAGE gel, and transferred to nitrocellulose. The blot was probed with anti-HA or anti-pRB antibodies, respectively.

B: Schematic representation of GST-pRB fusion proteins and pRB expressing plasmids used for the analysis.

C: Whole-cell lysates from HEK293 cells transfected with plasmids expressing pRB proteins, as described in (**B**) were immunoprecipitated with either anti-pRB polyclonal antibody or preimmune serum. After being washed, samples were run on an SDS-PAGE gel and transferred to nitrocellulose. The blot was probed with His-HMGA2 in a Far-Western assay as described in Experimental Procedures (upper panel). The membrane was stripped and probed with an anti-pRB antibody (lower panel).

D: Whole-cell lysate from HEK293 cells transfected with a plasmid expressing HA-HMGA2 (5 μg) was subjected to GST pull-down analysis using the GST or GST-pRB fusion proteins reported in (**B**). Binding reaction products were washed, and proteins were separated by SDS-PAGE. The membrane was probed with both anti-HA and GST antibodies.

E: Schematic representation of plasmids expressing wild-type and mutant HA-HMGA2 proteins used for the analysis.

F: Whole-cell lysates from HEK293 cells transfected with the plasmids reported in (**E**) were subjected to GST pull-down analysis using GST-pRB protein beads (upper panel) or GST protein beads (medium panel) as control. Aliquots of the same lysates were probed with anti-HA antibody to evaluate the comparable expression of the transfected plasmids (lower panel).

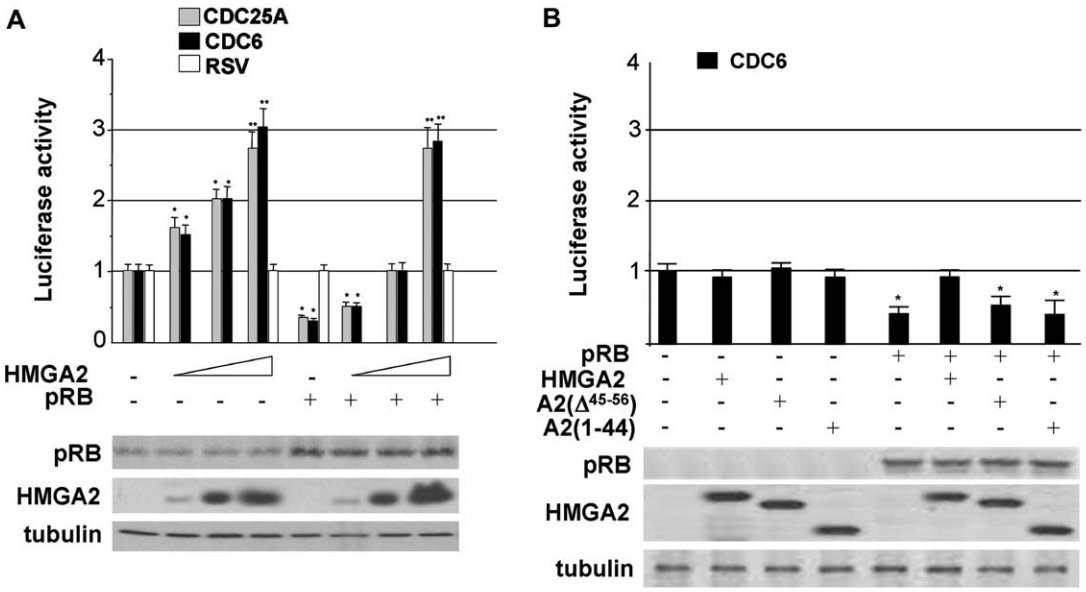

C **Colony-forming assay**

Transfected plasmids	No. of clones
Empty vector	201 ± 12.0
HMGA2	187 ± 9.0
pRB	52 ± 3.2
pRB + HMGA2	212 ± 19.3
pRB + A2(1-44)	49 ± 2.5
pRB + A2(Δ^{45-56})	56 ± 5.0

D **Focus assay**

Transfected plasmids	Transforming efficiency (f.f.u./pmol)
Empty vector	0
RasV12	$3x10^4$
HMGA2	$2x10^2$
A2(1-44)	0
A2(Δ^{45-56})	0

Figure 3. HMGA2 counteracts the pRB-mediated inhibition of E2F activity and cell proliferation

A: Luciferase activities of extracts from HEK293 cells cotransfected with CDC25A-luc or CDC6-luc reporter plasmids and increasing amounts of HMGA2 with or without a pRB expression vector. The RSV-luc plasmid served as a negative control. Relative activities were calculated by dividing normalized activities with the activity of cells transfected with the reporter plasmid alone. Aliquots of the same lysates were resolved by SDS-PAGE, transferred to Immobilion-P, and immunoblotted with the indicate antibodies (lower panels).

B: Saos-2 cells were transiently transfected with plasmids expressing HA-HMGA2 wild-type and mutated proteins and subjected to luciferase assay on the CDC6-luc reporter promoter. Relative activities were calculated as reported in (**A**). Aliquots of the same lysates were resolved by SDS-PAGE and immunoblotted with the indicate antibodies (lower panels).

C: Saos-2 cells were transiently transfected with the expression plasmids indicated on the left and selected for 14 days in the appropriate antibiotic. Cell clones were counted following staining with crystal violet.

D: *Focus* assay on Rat-2 cells transfected with the plasmids indicated on the left. The transforming efficiency was expressed as foci-forming units (f.f.u.)/pmol of transfected DNA. All the data reported are the mean ± SE of three independent experiments. *$p < 0.05$; **$p < 0.01$.

pRB greatly reduced the colony-forming ability. Cell growth inhibition was significantly reduced in the presence of a coexpressed HMGA2 construct and was not affected by either the A2(1-44) or A2(Δ^{45-56}) mutant. Conversely, HMGA2 alone had no significant effects on colony-forming ability. These results suggest that HMGA2, by interacting with pRB, inhibits the pRB negative regulation of E2F1 activity, thereby blocking its growth-suppressing potential.

The binding of HMGA2 to pRB is crucial for its transforming activity

It has been previously reported that HMGA2 induces neoplastic transformation of cultured rat fibroblasts (Wood et al., 2000), demonstrating its oncogenic potential. In order to verify whether the binding between HMGA2 and pRB, with the resulting pRB inactivation, might be responsible for the oncogenic properties of HMGA2, we evaluated the *focus*-forming ability of HMGA2 and pRB binding mutants of HMGA2. To do this, we transfected Rat-2 cells with either HMGA2 or each of the HMGA2 mutants unable to efficiently bind to pRB. As shown in Figure 3D, the wild-type HMGA2 was able to induce *foci*, whereas no *foci* were observed in transfected cells with both the HMGA2 mutants. High transforming efficiency was obtained by transfecting the activated Ha-Ras gene (Ras 12V) that we used as a positive control of the assay. These results suggest that the binding between HMGA2 and pRB is necessary for the HMGA2 oncogenicity and that the mechanism by which HMGA2 is involved in pituitary tumorigenesis may be generally involved in HMGA2-mediated cell transformation.

HMGA2 displaces HDAC1 from the pRB/E2F complex

Many cellular and viral proteins have been shown to bind pRB within the pocket region of pRB (Hu et al., 1990). Consequent to this process, E2F1 is released from the binding to pRB and becomes active. Because HMGA2 binds to pRB in this same pocket region, we tested the hypothesis that the HMGA2/pRB

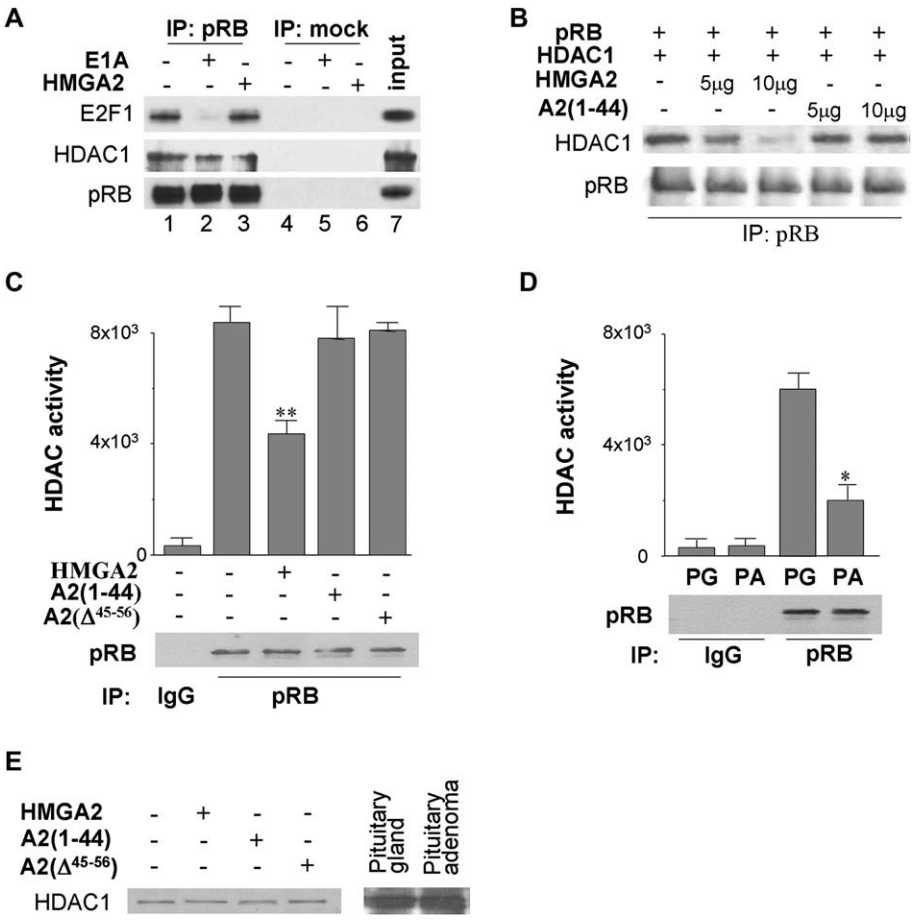

Figure 4. HMGA2 competes with HDAC1 but not with E2F1 for pRb binding

A: HEK293 cell lysates coexpressing both E2F1 and pRB transiently transfected plasmids were subjected to immunoprecipitation with anti-pRB antibody after incubation with either HMGA2 or E1A recombinant proteins, as indicated above, and then blotted against either E2F1 or HDAC1, as indicated on the left. pRB Western blot served as a control of the equal loading of the immunoprecipitated pRB protein.

B: Labeled HDAC1 and recombinant pRB were coimmunoprecipitated with or without 5 or 10 μg of either recombinant HMGA2 or A2(1-44) proteins. The samples were then blotted and probed with either HDAC1 or pRB antibody, as indicated on the left.

C: Lysates from Saos-2 cells, transiently transfected with the plasmids indicated on the left or with the empty vector, were incubated with a recombinant pRB protein and immunoprecipitated with anti-pRB antibodies. The resulted immunoprecipitates were in part subjected to histone deacetylase assay as described under Experimental Procedures and in part run on a SDS-PAGE for evaluation of the equal amount of pRB immunoprecitated in each sample.

D: Lysates from a pool of pituitary glands of wild-type mice and one pituitary adenoma of *HMGA2* transgenic mice were assayed as in (**C**). The results reported in (**C**) and (**D**) are the mean ± SE of three independent experiments. *$p < 0.05$; **$p < 0.01$.

E: Cell inputs from the experiments shown in (**C**) and (**D**) were assayed by Western blot for the expression of the HDAC1 protein.

interaction interferes with the binding between pRB and E2F1, thereby inducing E2F1 activation. To this aim, we performed coimmunoprecipitation experiments with HEK293 cells transiently cotransfected with pRB and E2F1 expression plasmids in the presence of E1A or HMGA2 recombinant proteins (Figure 4A). As previously reported (Putzer et al., 1997), E1A prevented the binding between pRB and E2F1 (lane 2), whereas HMGA2 did not (lane 3). Thus, HMGA2 does not activate E2F1 by competing with it for binding to pRB.

Another mechanism by which the pRB/E2F complex represses transcription entails recruitment of a histone deacetylase, the HDAC1 protein, to the E2F binding sites by pRB (Magnaghi-Jaulin et al., 1998). Histone acetyl transferases and histone deacetylases acetylate and deacetylate, respectively, core histone tails that protrude from the nucleosome. Histone acetylation is thought to weaken the interaction between histone N-terminal tails and DNA, thus opening up the chromatin and increasing accessibility for activating transcription factors. Therefore, the binding of the viral transforming proteins to the pRB-pocket region results in the loss of E2F and HDAC1 binding.

We thus asked whether the HMGA2/pRB interaction could displace HDAC1 from the pRB/E2F complex, and so account for E2F1 activation. To this aim, we used the same immunoprecipitates described above to also analyze the binding of HDAC1 to pRB. As shown in Figure 4A, both E1A (lane 2) and HMGA2 (lane 3) reduced the binding of pRB to HDAC1. This shows that, similarly to the E1A/pRB interaction, the HMGA2/pRB complex can affect HDAC1 recruitment.

To verify this result, we used a cell-free system in which pRB and HDAC1 recombinant proteins were incubated with or without increasing amounts of a recombinant HMGA2 protein. As shown in Figure 4B, HDAC1 was partially or completely displaced by the binding to pRB in the presence of 5 μg and 10 μg of HMGA2, respectively. This result demonstrates that HMGA2 directly interferes with the binding between HDAC1 and pRB. Moreover, to correlate the effect of HMGA2 on HDAC1 displacement from pRB with the HMGA2/pRB interaction, we also performed the experiment by using the A2(1-44) mutant, unable to bind pRB. As shown in the same Figure 4B, the binding between HDAC1 and pRB was not affected at all by the HMGA2 mutant, suggesting that the interaction between HMGA2 and pRB plays a crucial role in the displacement of HDAC1 from pRB.

Because recruitment of HDAC1 by pRB to gene promoters decreases their level of histone acetylation (Magnaghi-Jaulin et al., 1998), we evaluated whether HMGA2 overexpression was associated with decreased HDAC activity associated with the pRB complexes. To this aim, lysates from Saos-2 cells, transiently transfected with either HMGA2 or each of the two mutants A2(1-44) and A2(Δ^{45-56}), were incubated with a recombinant pRB protein and then immunoprecipitated with antibodies against pRB. These immunoprecipitates were incubated with a ^{3}H-acetylated histone H4 peptide, and the released ^{3}H-acetate was measured (Figure 4C). The same assay was carried out with mouse tissue lysates from wild-type pituitaries and *HMGA2* transgenic pituitary adenomas (Figure 4D). Consistent with the HMGA2-induced displacement of HDAC1 from the

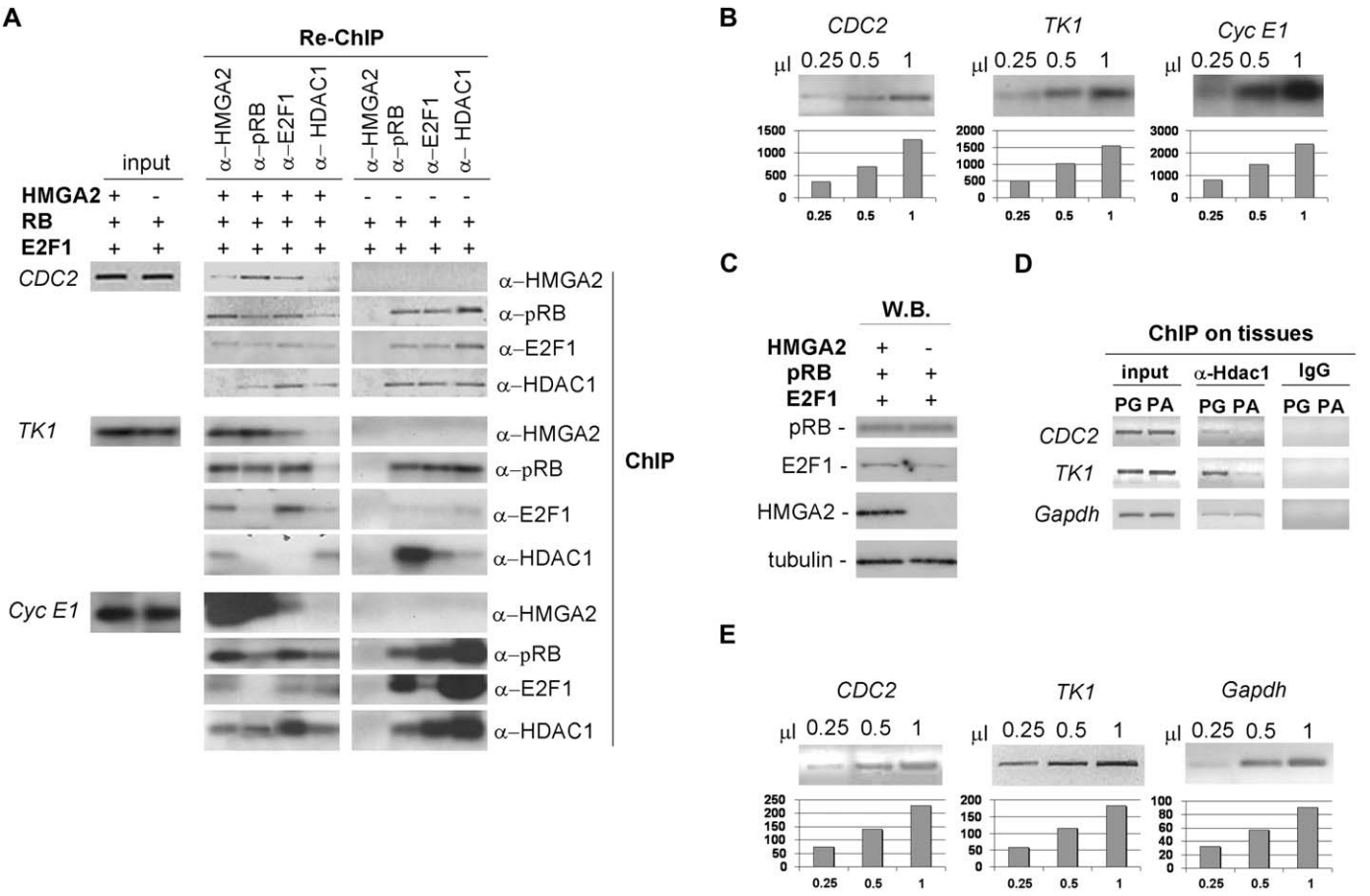

Figure 5. HMGA2 displaces HDAC1 from E2F1 target promoters

A: Lysates from cells transfected with plasmids expressing pRB, E2F1, and HMGA2 or pRb, E2F1, and empty vector, as indicated above the panel, were subjected to ChIP using specific polyclonal antibody, as indicated on the right. Before reversal of formaldehyde cross-linking, each precipitate was washed, resuspended, and subjected to re-ChIP using specific antibody as indicated on the top. Immunoprecipitates from each sample were analyzed by PCR, and a sample representing linear amplification (0.25–1 μl) of the total input chromatin (Input) was included in the PCRs as a control.

B: Increasing amounts of input samples as described in (**A**) were used as template in PCR amplifications performed using primers specific for the different promoters including E2F binding sites: *CDC2*, *TK1*, and *cyclin E1*.

C: Lysates from cells transiently transfected as described in (**A**) and indicated above the panel were subjected to Western blot analysis with anti-pRB, anti-Ha (for HMGA2), or anti-E2F1 antibodies to verify protein expression. Tubulin expression served as a control of equal protein loading.

D: Tissue extracts from a pool of normal pituitary glands (PG) and a representative HMGA2-induced pituitary adenoma (PA) were assayed by ChIP using a specific polyclonal antibody anti-HDAC1. Immunoprecipitates from each sample were analyzed by PCR, and a sample representing linear amplification (0.25–1 μl) of the Input was included in the PCRs as a control. Another control included precipitation performed without specific IgG.

E: Increasing amounts of input samples as described in (**D**) were used as template in PCR amplifications carried out with primers specific for the different promoters: *CDC2*, *TK1*, and *Gapdh*.

pRB active repressor complex, HDAC activity was significantly lower in cells and pituitary adenomas overexpressing HMGA2 than in mock-transfected cells and normal pituitary, respectively. To exclude that this effect could be due to a downregulation of HDAC1 expression following HMGA2 overexpression, we also monitored HDAC1 expression in the inputs of the experiments shown in Figures 4C and 4D. As shown in Figure 4E, no differences in HDAC1 expression were observed between HMGA2-transfected and parental cells or between pituitary adenoma and normal gland.

HMGA2 binds to E2F target promoters in vivo and interferes with the association of the single subcomplexes

We next evaluated whether HMGA2 is part of the complexes, including pRB, E2F1, and HDAC1 that form at the E2F binding sites of the E2F-responsive promoters in vivo, and whether it can displace HDAC1. In a combination of chromatin immunoprecipitation (ChIP) and Re-ChIP analyses, HEK293 cells were transfected with pRB and E2F1 or pRB and E2F1 plus HMGA2 (Figure 5C), and crosslinked genomic DNA was immunoprecipitated in two rounds with two specific antibodies directed against protein components of the complex (Figure 5A). Re-ChIPed DNA was analyzed by PCR using promoter-specific primers that encompass the E2F binding sites, under conditions of linear amplification (Figure 5B). Figure 5A shows that HMGA2 can associate in vivo with three E2F-responsive promoters, i.e., those driving *CDC2*, *TK1*, and *cyclin E1* gene transcription, and is a component of a promoter-bound multimeric complex containing E2F1, pRB, and HDAC1. A comparison of the subcomplexes with and without HMGA2 revealed three mechanisms whereby HMGA2 can activate E2F1 in vivo. First, in agreement

with our in vitro results, HDAC1/pRB binding was decreased in the presence of HMGA2 on all the promoters analyzed, especially the TK1 promoter. Second, pRB/E2F binding is decreased in the presence of HMGA2 on the cyclin E1 promoter, suggesting that HMGA2 can displace pRB from E2F1, at least on this promoter. Finally, E2F1 binding on the TK1 promoter was significantly increased in the presence of HMGA2, suggesting that, at least on this promoter, HMGA2 can directly enhance the binding of free E2F1 to the DNA target. This effect was also observed in the EMSA with an E2F consensus oligonucleotide (Figure 1). Quantitative data of this experiment, evaluated by densitometric analyses, are shown in the Figure S1 in the Supplemental Data available online.

To improve the significance of the HMGA2-mediated displacement of HDAC1 from the E2F-responsive promoters, we performed ChIP analyses on tissue extracts from normal and neoplastic pituitary tissues from wild-type and transgenic mice, respectively, using specific anti-HDAC1 antibodies. The DNA that was immunoprecipitated was analyzed by PCR using promoter-specific primers that encompass the E2F binding sites under conditions of linear amplification (Figure 5E). As shown in Figure 5D, differently from what occurs in normal pituitary glands from control mice, the binding of HDAC1 to the protein complex bound to the E2F-responsive promoters is much more reduced compared to normal tissue.

Overexpression of HMGA2 promotes acetylation of histones and E2F1 protein on E2F target promoters in vivo

We have shown that HMGA2 can displace HDAC1 from pRB at the E2F binding sites—a process that could account for the decreased HDAC activity associated with HMGA2 overexpression. HDAC can also affect proteins that can be acetylated. An example of this is E2F1, whose acetylation augments DNA binding and stabilizes the protein (Martinez-Balbas et al., 2000).

To analyze the acetylation status of histones and E2F1 on E2F1 target promoters in vivo, we transfected Saos-2 cells with pRB or pRB and HMGA2 (Figure 6A) and subjected the lysates to a ChIP assay using specific anti-acetylated histone H3 antibodies (Figure 6B). Immunoprecipitated DNA was analyzed by PCR using promoter-specific primers that encompass the E2F binding sites under conditions of linear amplification (Figure 6C). Control vector-transfected cells had high levels of acetylated histone H3 in association with the E2F binding sites of the analyzed promoters (Figure 6B). Overexpression of pRB decreased the association of the acetylated histone H3 with the same promoters, but not with the glyceraldehyde-3-phosphate dehydrogenase (Gapdh) unrelated promoter. In contrast, coexpression of pRB and HMGA2 abolished the effects of pRB. In order to investigate E2F1 acetylation on the same promoters and correlate it with the HMGA2/pRB interaction, we transfected HEK293 cells with either HMGA2 or A2(1-44) and subjected the lysates to a ChIP assay with a specific anti-acetylated E2F1 antibody. As shown in Figure 6D, E2F1 acetylation was enhanced by the HMGA2 overexpression, whereas it did not change in cells transfected with the A2(1-44) mutant. This result, consistent with our previous data demonstrating the role of the HMGA2/pRB interaction in displacing HDAC1 from the E2F-responsive promoters, was also confirmed by an additional experiment in which total lysates from cells transfected as in Figure 6D were immunoprecipitated with the anti-acetylated E2F1 antibody and then blotted for E2F1 (Figure 6F).

Finally, to evaluate whether these results correspond to real regulation of the expression of these genes in vivo, we carried out a semiquantitative reverse transcriptase-PCR. The expression levels of *CDC2* and *TK1* mRNA were measured in Saos-2 cells upon overexpression of pRB or pRB and HMGA2. In agreement with the results reported above, these genes were specifically downregulated upon pRB expression, but not upon coexpression of pRB and HMGA2 (Figure 6G).

Loss of E2F1 suppresses the development of pituitary tumors in HMGA2 transgenic mice

The afore-reported data demonstrate that HMGA2 induces E2F1 activity in pituitary adenomas by enhancing E2F1 acetylation and the binding of free E2F to the target promoter. This suggests that E2F1 activity is a critical event in pituitary tumorigenesis of HMGA2 mice.

To address this hypothesis, we crossed *HMGA2* transgenic mice ($HMGA2^{TG}$) with $E2f1^{-/-}$ mice to generate double mutants. We obtained $HMGA2^{TG};E2f1^{+/-}$ and $HMGA2^{TG};E2f1^{-/-}$ in a mixed 129/Sv × C57BL/6 genetic background. We monitored the female double mutants for the development of pituitary tumors, using $HMGA2^{TG};E2f1^{+/+}$ female mice as controls. All control animals (9/9) and nearly all $HMGA2^{TG};E2f1^{+/-}$ (13/14) double mutants developed grossly detectable pituitary tumors by the age of 15 months (see arrow in Figure 7A). In contrast, only 4 of the 16 (25%) $HMGA2^{TG};E2f1^{-/-}$ mice developed pituitary tumors (Figures 7A and 7B) at the same age. The loss of E2F1 function significantly affected the penetrance of pituitary tumors in $HMGA2^{TG}$ mice ($p = 0.0121$; log rank test). In addition, the tumors in the $HMGA2^{TG};E2f1^{+/+}$ mice featured multiple neoplastic nodules constituted by cords and solid nests of monomorphous polygonal tumor that had a high mitotic activity and intense PCNA labeling (Figures 7Cd and 7Ce); the nodules enlarged, distorted or completely replaced the anterior pituitary lobe. In contrast, the pituitary adenomas in the $HMGA2^{TG};E2f1^{-/-}$ animals were neither grossly enlarged nor distorted, and the anterior lobe showed a normal acinar pattern, except for a small nodule containing a few blood-filled spaces and rare mitotic figures and PCNA labeling (Figures 7Cj and 7Ck). The Gordon-Sweet silver method was used for the histological diagnosis of these nodules (Figure 7Cl) and showed focal disruption of the reticulin fiber network, which is pathognomic for the adenomatous transformation of pituitary cells (Figures 7Cc and 7Cf). These results provide strong evidence that E2F1 activation is required for the development of pituitary adenomas in HMGA2 transgenic mice.

In order to further investigate the molecular mechanisms involved in the pituitary alterations of the few cases of $HMGA2^{TG};E2F1^{-/-}$ mice that develop small adenomas, we analyzed the status of pRB/HMGA2 complexes and E2F "free" activation in these E2F1 null tumors. As shown in Figure 7D, HMGA2 and pRB still retain their capacity to interact with each other. However, the E2F "free" DNA binding activity does not show any significant increase in these tumors compared to control wild-type pituitary glands (Figure 7E, lane 3). Conversely, a strong increase in E2F free DNA binding was always observed in pituitaries from $HMGA2^{TG};E2f1^{+/+}$ mice even before the appearance of the pituitary tumor (Figure 7E, lane 2). Thus, even though HMGA2 is still able to bind pRB in absence of E2F1, there are

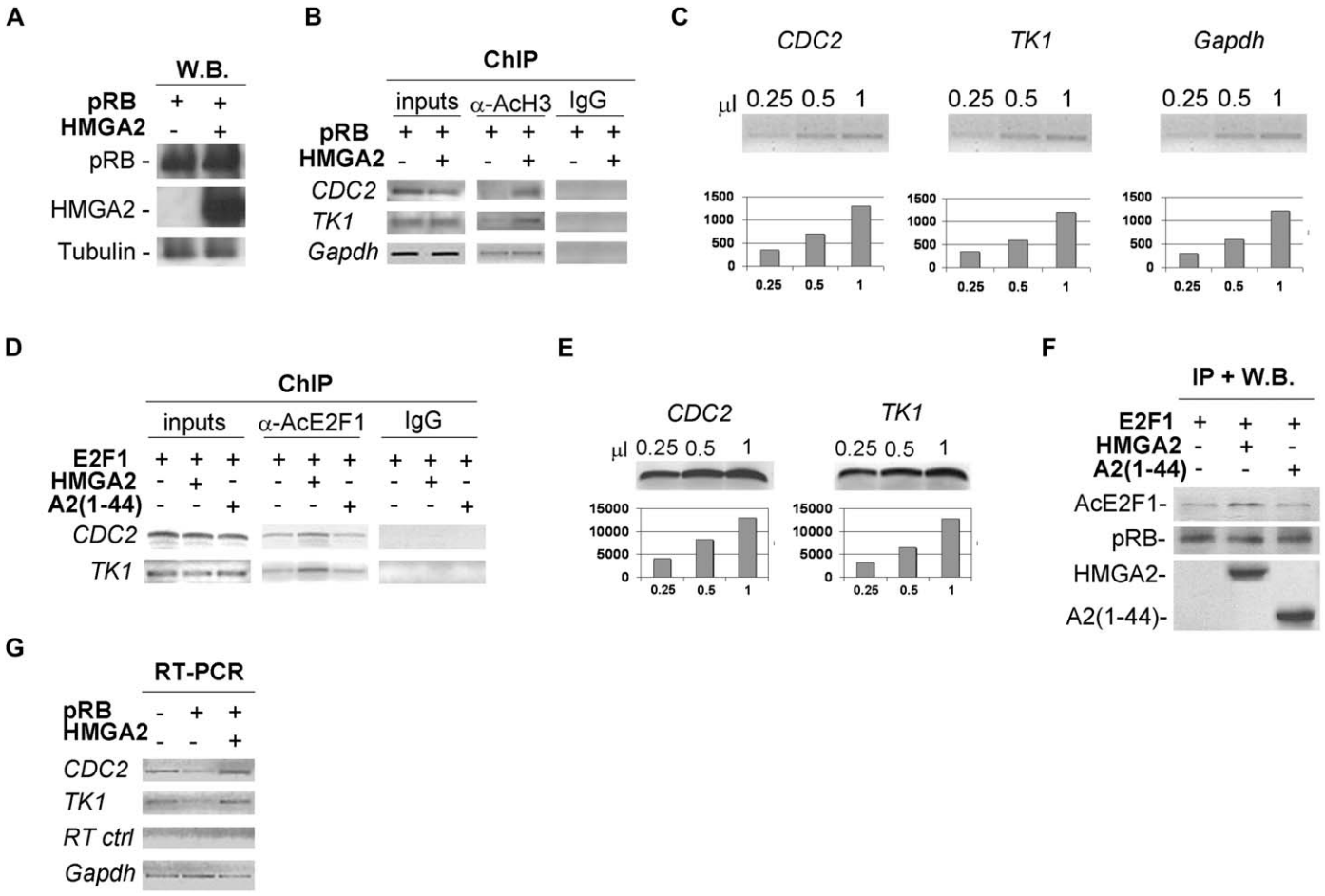

Figure 6. HMGA2 overexpression increases acetylation of both histones and E2F1 protein on E2F target promoters

A: Western blot analysis showing the protein expression of pRB and HMGA2 in Saos-2 cells transiently transfected with the relative expression plasmids, as indicated on the top. Tubulin expression served as a control of equal protein loading.

B and C: Lysates from Saos-2 cells transfected as described in (**A**) were subjected to ChIP using specific polyclonal antibodies anti-acetylated histone H3 (**B**). Immunoprecipitates were analyzed by PCR, and a sample representing linear amplification (0.25–1 μl) of the Input was included in the PCRs as a control. Another control included precipitation performed without specific IgG. Increasing amounts of input samples (**C**) were used as template to verify the linear range of amplification.

D: HEK293 cells transfected with E2F1, HMGA2, A2(1-44), or the backbone vector alone were assayed by ChIP using a specific polyclonal antibody anti-acetylated E2F1 under the same conditions as described in (**B**).

E: Increasing amount of input samples from the experiment described in (**D**) were used as template to verify the linear range of amplification.

F: HEK293 cells transfected as described in (**D**) were immunoprecipitated with anti-acetylated E2F1 antibody and assayed by Western blot for E2F1 (upper panel). The inputs were assayed by Western blot for the expression of endogenous pRB and transfected HMGA2 and A2(1-44) proteins (middle and lower panels).

G: RNA from Saos-2 cells transiently transfected as described in (**A**) was analyzed by RT-PCR for the expression of *CDC2*, *TK1*, and *Gapdh*. The RT control lanes represent RT-PCR without reverse transcription.

no alternative E2F proteins whose DNA binding activity is enhanced following this interaction, suggesting that other E2F-independent mechanisms may be responsible for the pituitary alterations in the minority of these mice.

Discussion

Tumors of the pituitary gland can be found in 20% of the population, and at least one-third of these cause health complications. In fact, although not classified as malignant, most pituitary adenomas grow rapidly and can invade downward into the paranasal sinuses, laterally into the cavernous sinuses, and upward into the parenchyma of the brain. Little is known about the molecular events responsible for pituitary transformation (reviewed by Asa and Ezzat, 2002). A large body of evidence implicates HMGA2 in pituitary tumorigenesis (Fedele et al., 2002; Finelli et al., 2002). In an attempt to identify the mechanism by which HMGA2 acts, we explored the pRB pathway. We selected this strategy because of experimental data indicating that the *HMGA2* gene interferes with this pathway (Bignon et al., 1993; Fedele et al., 2002; Jacks et al., 1992). Moreover, the finding that mice with heterozygous *RB* mutations develop pituitary tumors (Jacks et al., 1992) suggests that impairment of the pRB/E2F pathway is involved in pituitary tumorigenesis. Thus far, *RB* mutations have not been identified in human pituitary adenomas (Cryns et al., 1993). However, methylation of the *RB* gene-promoter region at a CpG island in human pituitary tumor cells resulted in loss of protein expression (Simpson et al., 2000),

A

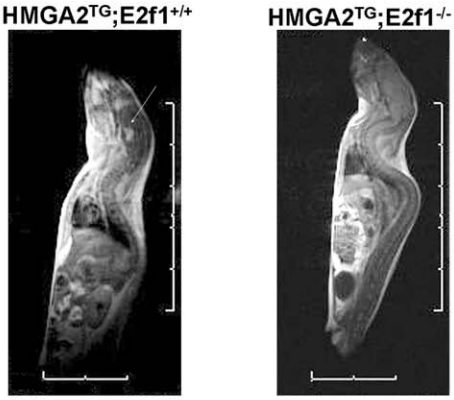

B

	HMGA2^{TG};E2f1 $^{+/+}$	HMGA2^{TG};E2f1 $^{+/-}$	HMGA2^{TG};E2f1 $^{-/-}$
Normal	0/9	0/14	8/16
Hyperplasia	0/9	1/14	4/16
Adenoma	9/9	13/14	4/16

C

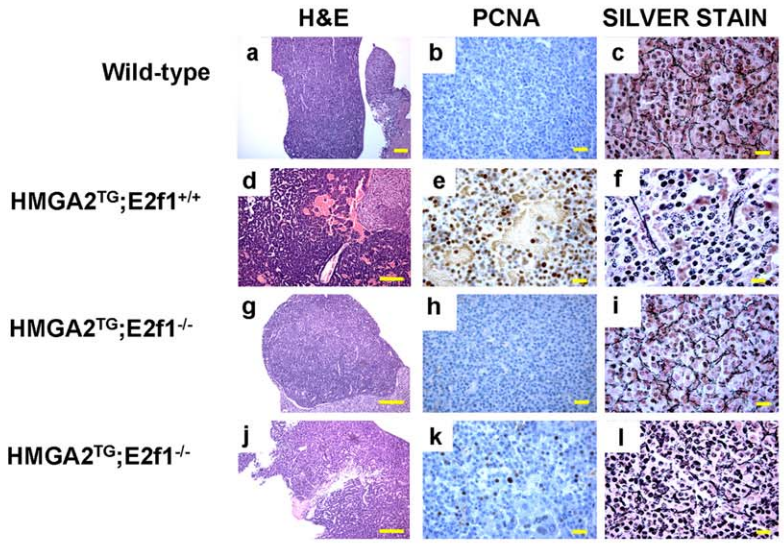

D

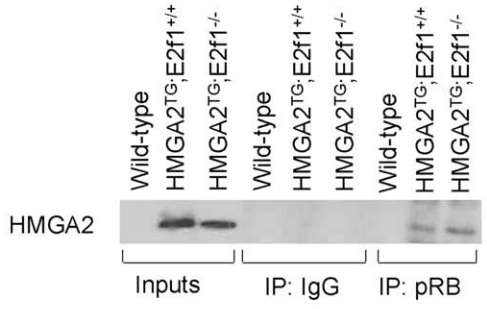

E

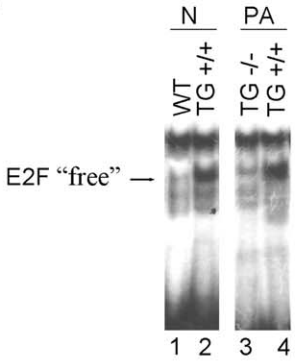

Figure 7. The absence of E2F1 suppresses pituitary tumorigenesis in *HMGA2* transgenic mice

A: MRI analysis of a representative 12-month-old transgenic mouse homozygous for the knockout mutation of *E2F1* (right: *HMGA2^{TG};E2f1$^{-/-}$*), compared with a sex-age matched control transgenic mouse (left: *HMGA2^{TG}; E2f1$^{+/+}$*). The arrow indicates the pituitary tumor that is absent in the *E2f1$^{-/-}$* mouse.

B: *HMGA2* transgenic mice and *E2f1$^{-/-}$* mice were crossed to generate *HMGA2^{TG};E2f1$^{+/+}$*, *HMGA2^{TG};E2f1$^{+/-}$*, and *HMGA2^{TG};E2f1$^{-/-}$* mice. The total number of pituitary tumors developed by each genotype is shown.

C: Histological analysis (hematoxylin and eosin staining) of the anterior pituitary from a wild-type animal showing a normal architecture (Ca), absence of PCNA labeling (Cb), and a normal acinar pattern and reticulin network (Gordon-Sweet silver stain) (Cc). *HMGA2^{TG};E2f1$^{+/+}$* mice had a very large tumor that enlarged and completely replaced the anterior lobe (Cd); most neoplastic cells showed PCNA labeling (Ce), and the reticulin network was lost (Cf). *HMGA2^{TG};E2f1$^{-/-}$* mice showing either a morphology (Cg), PCNA labeling (Ch), and reticulin network (Ci) similar to wild-type mice, or neoplastic nodules

which confirms that pRB is important in human pituitary tumorigenesis.

By repressing E2F1 activity, the pRB protein prevents cells from progressing beyond the G1 phase of the cell cycle. Phosphorylation of pRB by cyclin-cdk complexes or expression of viral transforming proteins relieves this repression and allows cells to progress toward S phase (reviewed by Seville et al., 2005). Interaction of pRB with histone deacetylase HDAC1 is involved in pRB repression of E2F1 activity, and this interaction is disrupted by both phosphorylation and viral transforming proteins (Magnaghi-Jaulin et al., 1998).

Here we demonstrate that HMGA2 induces the development of pituitary adenomas by enhancing E2F1 activity. In fact, E2F1 activity was drastically increased in all pituitary tumors analyzed. Moreover, the absence of E2F1, obtained by mating *HMGA2* transgenic with *E2f1* knockout mice, greatly inhibited the formation of pituitary tumors. In fact, most *HMGA2^{TG};E2f1$^{-/-}$* mice did not develop tumors, and only a few had small, slow growing adenomas. The reduced severity of pituitary lesions in *HMGA2^{TG};E2f1$^{-/-}$* animals suggests that loss of *E2F1* may delay the onset or progression of these tumors. It is noteworthy that the loss of one wild-type *E2F1* allele did not alter the frequency of pituitary tumors in *HMGA2^{TG}* mice.

The mechanism by which the HMGA2 protein affects the pRB/E2F pathway and enhances E2F1 activity is quite unique. In fact, although HMGA2 binds to the pRB pocket, it does not compete with the E2F protein in pRB binding, unlike proteins encoded by the adenovirus *E1A* gene. Conversely, our data show that HMGA2 activates E2F by interfering with HDAC1 recruitment by pRB on various E2F-responsive promoters (Figure 8). Displacement of HDAC1 would result in acetylation of both E2F1 and DNA-associated histones, thereby promoting E2F1 activation.

It would be worthwhile to investigate whether HMGA2 is able to displace also the other HDAC members (as suggested by our preliminary experiments) and any other protein associated to the pRB/E2F complex.

HDAC1 displacement from pRB is not the only way by which HMGA2 activates E2F1. HMGA2 also acts directly on the E2F-responsive DNA elements, and at least on the *TK1* promoter causes enhanced E2F1 DNA binding (Figure 5A). Although we do not demonstrate in vitro that HMGA2/pRB binding caused displacement of E2F1 from pRB, we show that HMGA2, at least on the *cyclin E1* promoter, displaced pRB from the E2F1-DNA complex (Figure 5A). On the basis of our results it is reasonable to suppose that displacement of pRB from E2F1 does not occur simply through competition between E2F1 and HMGA2 for the A/B pocket of pRB, but through a more indirect mechanism due to the enhanced E2F1 acetylation dependent upon the HMGA2 overexpression. In fact, it has been proposed (Martinez-Balbas et al., 2000) that acetylation stimulates the functions of the non-RB bound "free" form of E2F1, including DNA binding and its protein stability.

In conclusion, HMGA2 induces pituitary adenomas by enhancing E2F1 activity through displacement of HDAC1 from pRB and consequent induction of E2F1 acetylation. It is likely that the same mechanism may be involved in most human prolactinomas in which the *HMGA2* gene is amplified and overexpressed. Should this be the case, one may envisage a therapeutic strategy aimed at disrupting this mechanism.

Experimental procedures

Electrophoretic mobility shift assay

Protein/DNA binding was determined by electrophoretic mobility shift assay (EMSA), as previously described (Battista et al., 2005). The E2F1 oligonucleotide (Santa Cruz, CA; sc-2507) was mutated as follows (mutated bases in bold) in the AT-mut oligonucleotide: 5′-A**C**TT**GG**GTTTCGCGC CCTTTCTCAA-3′. The antibodies used were anti-HMGA2 (polyclonal Ab raised against a synthetic peptide located in the NH2-terminal region) and anti-E2F1 (sc-193, Santa-Cruz). The DNA-protein complexes were resolved on 6% (w/v) nondenaturing acrylamide gels and visualized by exposure to autoradiographic films. Binding reactions with the purified proteins were carried out as previously described (Baldassarre et al., 2001).

Protein extraction, immunoblot analysis, and immunoprecipitation

Tissues were rapidly dissected, frozen on dry ice, and stored at −80°C. Protein extraction, Western blot, and immunoprecipitation were carried out as previously described (Pierantoni et al., 2001). The antibodies used were anti-HMGA2 (polyclonal antibody raised against a synthetic peptide located in the NH2-terminal region), anti-pRB (C-15, Santa Cruz, CA), anti-HA (F-7; Santa Cruz), anti-GST (B-14, Santa Cruz), anti-E2F1 (C-20, Santa Cruz), and anti-HDAC1 (06-720, Upstate Biotechnology Inc., Lake Placid, NY).

Plasmids and recombinant proteins

HA-tagged HMGA2 expression plasmids containing the entire and various separate portions of the HMGA2 coding sequence were obtained by PCR amplification and subcloned into the pCEFL-HA expression vector. The expression vectors for pRB and all pRB mutants (each subcloned into the CMV-neo-Bam vector) were kindly donated by G. Condorelli. CDC25A-luc and CDC6-luc plasmids were already described (Hateboer et al., 1998; Vigo et al., 1999). pRB(379-928), pRB(1-379), pRB(379-928)Δ21, pRB(379-792), pRB(768-928), pRB(834-928), and E2F1 were expressed as GST fusion proteins, whereas HMGA2 and E1A-12S were expressed as His fusion proteins. pGEX2T plasmids carrying the different deletion mutants of pRB were kindly provided by S. Soddu. The pCMVHAE2F1 and pGST20TE2F-1 vectors are described elsewhere (Helin et al., 1993; Helin and Harlow, 1994). The GST and His fusion proteins were expressed in *Escherichia coli* strain BL21 (DE3) (Stratagene) and purified using glutathione sepharose or nickel beads as previously described (Baldassarre et al., 2001; Pierantoni et al., 2001). The pRB full-length recombinant protein was from Abcam (ab 1111).

Pull-down and Far-Western experiments

Pull-down analysis was carried out as previously described (Pierantoni et al., 2001). For Far-Western analysis, 50 μg of cell lysates expressing pRB and different pRB mutants were separated by SDS PAGE and transferred to a nitrocellulose membrane. The membrane was air-dried, and the proteins were denaturated for 10 min in 6 M guanidine hydrochloride in HBB buffer (10 mM HEPES, pH 7.5, 60 mM KCl, 1 mM EDTA, and 1 mM DTT). The proteins were renaturated sequentially in 3, 1.5, 0.75, 0.38, and 0.19 M GuHCl in the same buffer (10 min each step). The membrane was extensively rinsed with HBB and blocked with HBB supplemented with 5% nonfat milk and 0.5% NP40 for 1 hr at 4°C and for 30 min in HBB with 1% milk. The His-HMGA2 protein was incubated with the membrane in PIB buffer (10 mM HEPES, pH 7.5, 13 mM NaCl, 50 mM KCl, 1% milk, and 0.5% NP40, 1 mM DTT) for 4 hr at 4°C. The unbound material was removed with extensive

that differed from those in *HMGA2^{TG};E2f1$^{+/+}$* mice in that they were smaller (Cj), had less intense PCNA labeling (Ck), and only partial loss of the reticulin network (Cl). Scale bars (in yellow): 100 μm H&E, 75 μm PCNA staining, 25 μm Gordon-Sweet silver stain.

D: Coimmunoprecipitation of HMGA2 and pRB in tissue extracts from pituitary glands and tumors from mice as indicated on the top.

E: EMSA analysis of wild-type (WT), *HMGA2^{TG};E2f1$^{+/+}$* (TG +/+), and *HMGA2^{TG};E2f1$^{-/-}$* (TG −/−) pituitary samples, either normal (N) or adenomatous (PA), using a consensus E2F as probe.

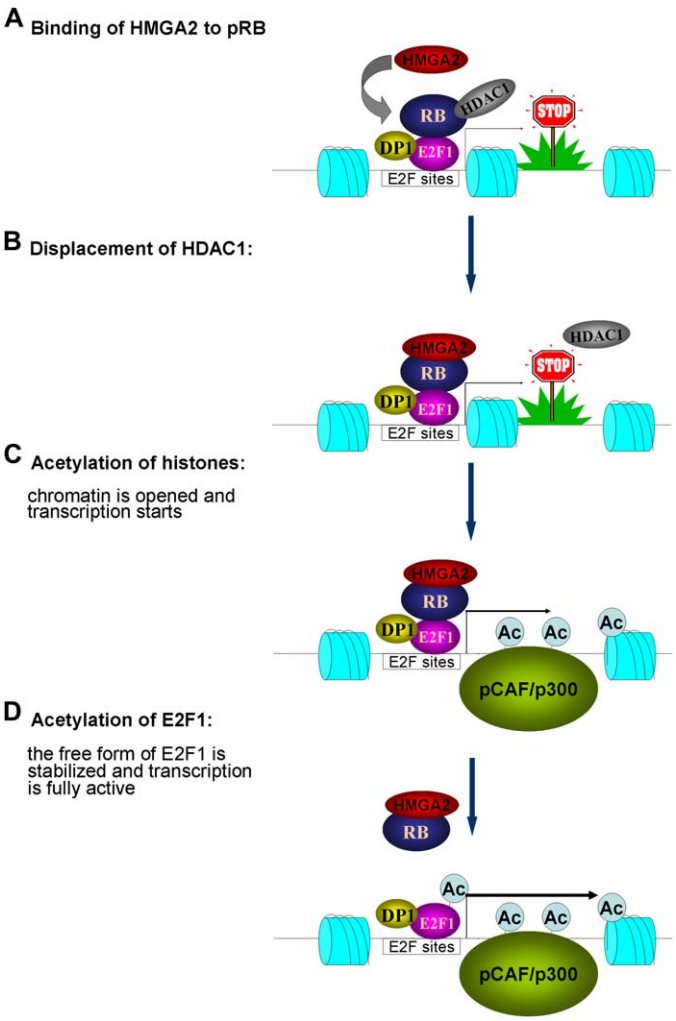

Figure 8. Model of E2F1 activation by HMGA2

Following HMGA2 overexpression, transcription through E2F1 sites switches from repression to activation throughout four steps.

A: HMGA2 binds to pRB, which is complexed with E2F1 and HDAC1 to form the active repression.

B: The interaction between HMGA2 and pRB displaces HDAC1.

C: In the absence of HDAC1, the histone acetylase enzymes are recruited and, by acetylating histones, relieve transcriptional repression.

D: Histone acetylases also acetylate E2F1 causing the stabilization of its ''free'' active form.

washes for 30 min in the same buffer. Binding was detected with Western blot analysis and anti-His antibody (Santa Cruz).

Cell lines and transfections

The HEK293, Rat-2, and Saos-2 cell lines were grown in Dulbecco's modified Eagle medium (DMEM) (Gibco-BRL) supplemented with 10% fetal-calf serum (Gibco-BRL). HEK293 cells were transfected by calcium phosphate precipitation by standard procedures. Rat-2 and Saos-2 cells were transfected by lipofectamine-plus reagent (Invitrogen) according to the manufacturer's instructions. For the luciferase activity assay, cells were transfected with 0.2 μg of CDC25A-luc or CDC6-luc reporter plasmids with or without 0.2 μg of pRB expression vector and increasing amounts (1 μg, 5 μg, and 10 μg) of HA-HMGA2 expression vector or 1 μg of HA-A2(1-44) or HA-A2(Δ^{45-56}) plasmid. One microgram of pCMVβgal plasmid was cotransfected to verify equal transfection efficiency in the cell lines tested. Cells were harvested 36 hr after transfection, and luciferase and β-galactosidase activities were measured with a luminometer (Lumat LB9507, Berthold) with the Dual light kit (Tropix). The data represent the average of three independent experiments, performed in duplicate, with standard errors. Colony and Focus assays were carried out as previously described (Pierantoni et al., 2001; Fedele et al., 1998).

Competition experiments

Whole-cell lysates from HEK293 cells transiently cotransfected with HA-E2F1 and pCMV-pRB were incubated for 1 hr with His-HMGA2 or His-E1A recombinant proteins and subjected to immunoprecipitation with anti-pRB antibody (C-15, Santa Cruz, CA), resolved by SDS-PAGE on a 12% gel, and analyzed by Western blot with anti-E2F1 (C-20, Santa-Cruz), anti-HDAC1 (06-720, Upstate Biotechnology), or anti-pRB antibodies (C-15, Santa Cruz). In another experiment, labeled HDAC1 and a recombinant GST protein were subjected to immunoprecipitation with or without 5 or 10 μg of recombinant His-HMGA2 or His-A2(1-44). The samples were resolved by 12% SDS-PAGE gel and probed with anti-pRB antybody (C-15, Santa Cruz).

Deacetylase assay

Deacetylase assays were carried out with a histone deacetylase assay kit (Upstate Biotechnology) according to the manufacturer's instructions. All experiments were carried out three times, and samples were assayed in duplicate.

Chromatin immunoprecipitation and reprecipitation

Chromatin immunoprecipitation (ChIP) was carried out with an acetyl-histone H3 immunoprecipitation assay kit (Upstate Biotechnology) according to the manufacturer's instruction. For ChIp experiments with the polyclonal antibody anti-HDAC1 (Upstate Biotechnology), anti-E2F1 (C-20 Santa Cruz), anti-pRB (C-15 Santa Cruz), and anti-HMGA2 (polyclonal antibody raised against a synthetic peptide located in the NH2-terminal region), conditions were as previously reported (Shang et al., 2000). For Re-ChIP experiments, complexes were eluted by incubation for 30 min at 37°C in 250 μl of Re-ChIP elution buffer (2 mM DTT, 1% Triton X-100, 2 mM EDTA, 150 mM NaCl, 20 mM Tris-HCl, pH 8.1) and then diluted 4-fold in Re-ChIP dilution buffer (1% Triton X-100, 2 mM EDTA, 150 mM NaCl, 20 mM Tris-HCl, pH 8.1) and subject again to the ChIP procedure. Crosslinking was reversed by incubating samples overnight at 65°C with 20 μl of 5 M NaCl. Samples were then incubated in proteinase K solution (10 mM EDTA, 40 mM Tris-HCl, pH 6.5, 40 μg/ml of Proteinase K) for 1 hr at 45°C. DNA was purified with phenol/chloroform/isoamyl alcohol and precipitated by adding 2 volumes of ethanol and tRNA. PCR reactions were carried out by standard procedures, for a number of cycles optimized to ensure product intensity within the linear phase of amplification. The PCR products were separated on a 2% agarose gel, stained with ethidium bromide, and either scanned using a Typhoon 9200 scanner or blotted and hybridized with specific probes. Primer sequences are available as Supplemental Data.

Reverse transcriptase-PCR

Total RNA was isolated using TRI-reagent solution (Sigma) according to the manufacturer's protocol and treated with DNase (Invitrogen). Reverse transcription was performed by standard procedures. Primer sequences are available as Supplemental Data.

Generation and genotyping of mutant mice

E2f1-deficient animals of mixed 129/SvxC57BL/6 genetic background (Jackson Laboratory) were mated to *HMGA2* transgenic (*HMGA2*^{TG}) animals (Fedele et al., 2002) to generate *HMGA2*^{TG};*E2f1*$^{+/-}$ mice. Subsequent intermating of *HMGA2*^{TG};*E2f1*$^{+/-}$ males and females produced *HMGA2*^{TG};*E2f1*$^{-/-}$ mice. Animals were genotyped from tail DNA using Southern blot and PCR as previously described (Fedele et al., 2002) and according to the Jackson protocol. Mice were maintained under specific pathogen-free conditions in our Laboratory Animal Facility (Istituto dei Tumori di Napoli, Naples, Italy), and all studies were conducted in accordance with Italian regulations for experimentations on animals.

Histological analyses

Paraffin-embedded sections 4–5 μm thick were stained with hematoxylin and eosin and with the Gordon-Sweet silver method for the reticulin matrix. Immunohistochemical staining to identify proliferating cells was carried out

with the PCNA antibody (Novocastra) and the streptavidin-biotin peroxidase technique (DAKO Corp., CA).

Magnetic resonance

Magnetic resonance imaging was carried out at the Istituto dei Tumori di Napoli G. Pascale with a 1.5-T magnet system using local receiver coils and an 8 cm field of view. Sagittal slices 3 mm thick were obtained with T1 weighting (TR/TE = 400/11 ms).

Supplemental Data

The Supplemental data for this article can be found online at http://www.cancercell.org/cgi/content/full/9/6/459/DC1/.

Acknowledgments

This work was supported by grants from the Associazione Italiana Ricerca sul Cancro (AIRC) to A.F. and Regione Campania to M.F. We are grateful to Jean Ann Gilder (Scientific Communication) for editing the text. A.F. thanks Professor G. Della Porta for his continuous support.

Received: September 28, 2005
Revised: February 23, 2006
Accepted: April 18, 2006
Published: June 12, 2006

References

Asa, S.L., and Ezzat, S. (2002). The pathogenesis of pituitary tumours. Nat. Rev. Cancer *2*, 836–849.

Baldassarre, G., Fedele, M., Battista, S., Vecchione, A., Klein-Szanto, A.J., Santoro, M., Waldmann, T.A., Azimi, N., Croce, C.M., and Fusco, A. (2001). Onset of natural killer cell lymphomas in transgenic mice carrying a truncated HMGI-C gene by the chronic stimulation of the IL-2 and IL-15 pathway. Proc. Natl. Acad. Sci. USA *98*, 7970–7975.

Battista, S., Fidanza, V., Fedele, M., Klein-Szanto, A.J., Outwater, E., Brunner, H., Santoro, M., Croce, C.M., and Fusco, A. (1999). The expression of a truncated HMGI-C gene induces gigantism associated with lipomatosis. Cancer Res. *59*, 4793–4797.

Battista, S., Fedele, M., Martinez-Hoyos, J., Pentimalli, F., Pierantoni, G.M., Visone, R., De Martino, I., Croce, C.M., and Fusco, A. (2005). High-mobility-group A1 (HMGA1) proteins down-regulate the expression of the recombination activating gene 2 (RAG2). Biochem. J. *389*, 91–97.

Bignon, Y.J., Chen, Y., Chang, C.Y., Riley, D.J., Windle, J.J., Mellon, P.L., and Lee, W.H. (1993). Expression of a retinoblastoma transgene results in dwarf mice. Genes Dev. *7*, 1654–1662.

Cryns, V.L., Alexander, J.M., Kilbanski, A., and Arnold, A. (1993). The retinoblastoma gene in human pituitary tumors. J. Clin. Endocrinol. Metab. *77*, 644–646.

Fedele, M., Berlingieri, M.T., Scala, S., Chiariotti, L., Viglietto, G., Rippel, V., Bullerdiek, J., Santoro, M., and Fusco, A. (1998). Truncated and chimeric HMGI-C genes induce neoplastic transformation of NIH3T3 murine fibroblasts. Oncogene *17*, 413–418.

Fedele, M., Battista, S., Manfioletti, G., Croce, C.M., Giancotti, V., and Fusco, A. (2001). Role of the high mobility group A proteins in human lipomas. Carcinogenesis *22*, 1583–1591.

Fedele, M., Battista, S., Kenyon, L., Baldassarre, G., Fidanza, V., Klein-Szanto, A.J., Parlow, A.F., Visone, R., Pierantoni, G.M., Outwater, E., et al. (2002). Overexpression of the HMGA2 gene in transgenic mice leads to the onset of pituitary adenomas. Oncogene *21*, 3190–3198.

Field, S.J., Tsai, F.Y., Kuo, F., Zubiaga, A.M., Kaelin, W.G., Jr., Livingston, D.M., Orkin, S.H., and Greenberg, M.E. (1996). E2F-1 functions in mice to promote apoptosis and suppress proliferation. Cell *85*, 549–561.

Finelli, P., Pierantoni, G.M., Giardino, D., Losa, M., Rodeschini, O., Fedele, M., Valtorta, E., Mortini, P., Croce, C.M., Larizza, L., et al. (2002). The High Mobility Group A2 gene is amplified and overexpressed in human prolactinomas. Cancer Res. *62*, 2398–2405.

Franklin, D.S., Godfrey, V.L., Lee, H., Kovalev, G.I., Schoonhoven, R., Chen-Kiang, S., Su, L., and Xiong, Y. (1998). CDK inhibitors p18(INK4c) and p27(Kip1) mediate two separate pathways to collaboratively suppress pituitary tumorigenesis. Genes Dev. *12*, 2899–2911.

Hateboer, G., Wobst, A., Petersen, B.O., Le Cam, L., Vigo, E., Sardet, C., and Helin, K. (1998). Cell cycle-regulated expression of mammalian *CDC6* is dependent on E2F. Mol. Cell. Biol. *18*, 6679–6697.

Helin, K., and Harlow, E. (1994). Heterodimerization of the transcription factors E2F-1 and DP-1 is required for efficient binding to the adenovirus E4 (ORF6/7) protein. J. Virol. *68*, 5027–5035.

Helin, K., Wu, C.-L., Fattaey, A.R., Lees, J.A., Dynlacht, B.D., Ngwu, C., and Harlow, E. (1993). Heterodimerization of the transcription factors E2F-1 and DP-1 leads to cooperative transactivation. Genes Dev. *7*, 1850–1861.

Hu, Q.J., Dyson, N., and Harlow, E. (1990). The regions of the retinoblastoma protein needed for binding to adenovirus E1A or SV40 large T antigen are common sites for mutations. EMBO J. *9*, 1147–1155.

Jacks, T., Fazeli, A., Schmitt, E.M., Bronson, R.T., Goodell, M.A., and Weinberg, R.A. (1992). Effects of an PRB mutation in the mouse. Nature *359*, 295–300.

Magnaghi-Jaulin, L., Groisman, R., Naguibneva, I., Robin, P., Lorain, S., Le Villain, J.P., Troalen, F., Trouche, D., and Harel-Bellan, A. (1998). Retinoblastoma protein represses transcription by recruiting a histone deacetylase. Nature *391*, 601–605.

Martinez-Balbas, M.A., Bauer, U.M., Nielsen, S.J., Brehm, A., and Kouzarides, T. (2000). Regulation of E2F1 activity by acetylation. EMBO J. *19*, 662–671.

Pierantoni, G.M., Fedele, M., Pentimalli, F., Benvenuto, G., Pero, R., Viglietto, G., Santoro, M., Chiariotti, L., and Fusco, A. (2001). High mobility group I (Y) proteins bind HIPK2, a serine-threonine kinase protein which inhibits cell growth. Oncogene *20*, 6132–6141.

Putzer, B.M., Rumpf, H., Rega, S., Brockmann, D., and Esche, H. (1997). E1A 12S and 13S of the transformation-defective adenovirus type 12 strain CS-1 inactivate proteins of the PRB family, permitting transactivation of the E2F-dependent promoter. J. Virol. *71*, 9538–9548.

Seville, L.L., Shah, N., Westwell, A.D., and Chan, W.C. (2005). Modulation of pRB/E2F functions in the regulation of cell cycle and in cancer. Curr. Cancer Drug Targets *5*, 159–170.

Shang, Y., Hu, X., DiRenzo, J., Lazar, M.A., and Brown, M. (2000). Cofactor dynamics and sufficiency in estrogen receptor-regulated transcription. Cell *103*, 843–852.

Simpson, D.J., Hibberts, N.A., Mc Nicol, A.M., Clayton, R.N., and Farrell, W.E. (2000). Loss of pPRB expression in pituitary adenomas is associated with metylation of the PRB1 CpG island. Cancer Res. *60*, 1211–1216.

Vigo, E., Müller, H., Prosperini, E., Hateboer, G., Cartwright, P., Moroni, M.C., and Helin, K. (1999). CDC25A phosphatase is a target of E2F and is required for efficient E2F-1 induced S phase. Mol. Cell. Biol. *19*, 6379–6395.

Wood, L.J., Maher, J.F., Bunton, T.E., and Resar, L.M.S. (2000). The oncogenic properties of the HMG-I gene family. Cancer Res. *60*, 4256–4261.

Yamasaki, L., Bronson, R., Williams, B.O., Dyson, N.J., Harlow, E., and Jacks, T. (1998). Loss of E2F-1 reduces tumorigenesis and extends the lifespan of Rb1(+/−) mice. Nat. Genet. *18*, 360–364.

SOM230, A New Somatostatin Analogue, Is Highly Effective in the Therapy of Growth Hormone/Prolactin-Secreting Pituitary Adenomas

Monica Fedele,[1] Ivana De Martino,[1] Rosario Pivonello,[2] Andrea Ciarmiello,[4] M. Laura Del Basso De Caro,[3] Rosa Visone,[1] Dario Palmieri,[1] Giovanna M. Pierantoni,[1] Claudio Arra,[4] Herbert A. Schmid,[6] Leo Hofland,[7] Gaetano Lombardi,[2] Annamaria Colao,[2] and Alfredo Fusco[1,5]

Abstract

Purpose: We have previously shown that transgenic mice ubiquitously overexpressing the *HMGA2* gene develop growth hormone/prolactin-secreting pituitary adenomas. This animal model has been used to evaluate the therapeutic efficacy of SOM230, a somatostatin analogue with high affinity for the somatostatin receptor subtypes 1, 2, 3, and 5, on the growth of the pituitary adenomas.

Experimental Design: Four groups of 3- and 9-month-old HMGA2 transgenic mice were treated for 3 months with a continuous s.c. injection of two different dosages of SOM230 (5 or 50 μg/kg/h), one dose of octreotide, corresponding to that used in human therapy, and a placebo, respectively. The development of the tumor before and after therapy was monitored by magnetic resonance imaging of the pituitary region and evaluation of the serum prolactin levels.

Results: The highest dose of SOM230 induced a drastic regression of the tumor, whereas octreotide was not able to induce any significant tumor regression, although tumor progression was significantly slowed down. No significant differences were observed between the animals treated with the lowest dose of SOM230 and those receiving placebo.

Conclusions: These results clearly support the efficacy of the SOM230 treatment in human pituitary adenomas secreting prolactin based on the dramatic tumor shrinkage and fall in prolactin levels. This beneficial effect could be of crucial clinical usefulness in patients bearing tumors resistant to dopaminergic drugs.

Pituitary tumors account for ~15% of intracranial tumors. Although they are usually benign adenomas, they are associated with significant morbidity due to local compressive effects on brain structures and cranial nerves, leading to headaches and visual disturbances. Morbidity can also result from tumor-derived hormonal hypersecretion or following treatment that inadvertently damages adjacent normal pituitary hormone secretion. About two thirds of pituitary tumors express and secrete pituitary hormones. Among these, prolactinomas are the most common lesions, representing ~50% of all the clinically diagnosed pituitary adenomas. The current strategy for treating patients with functional pituitary tumors aims to normalize excess pituitary hormone secretion, targeting neuroendocrine receptors with dopamine agonists and somatostatin analogues (1). This approach has the potential to abrogate or suppress excess of hormone secretion. In addition, as pituitary cell hormone secretion and proliferation are strictly linked, treatment with dopamine and/or somatostatin agonists can also inhibit pituitary tumor growth. Thus far, the only drugs widely used to treat pituitary tumors over the past 2 decades are somatostatin analogues, such as octreotide and lanreotide, which have high affinity for somatostatin receptor (SSTR) 2. They are effective in the tumor mass shrinkage of 20% to 50% of treated patients depending on the receptor density and subtype expression (2). Different somatostatin analogues have been found to have SSTR subtype specificity and have revealed functional interactions between somatostatin receptor subtypes. In fact, *in vitro* experiments have shown that SSTR2-selective ligands do not prevent prolactin release from prolactin-secreting pituitary tumor cells, whereas a SSTR5-selective analogue suppresses prolactin secretion by ~40%, indicating divergent roles for SSTR2- and SSTR5-mediated actions in prolactinomas (3). By this point of view, the development of molecules that

Authors' Affiliations: [1]Istituto di Endocrinologia ed Oncologia Sperimentale del CNR e/o Dipartimento di Biologia e Patologia Cellulare e Molecolare, [2]Dipartimento di Endocrinologia ed Oncologia Molecolare e Clinica, and [3]Istituto di Patologia, Università di Napoli "Federico II"; [4]Istituto dei Tumori di Napoli Fondazione "G. Pascale"; [5]NOGEC (Naples Oncogenomic Center)-CEINGE Biotecnologie Avanzate & SEMM, European School of Molecular Medicine, Naples, Italy; [6]Novartis Institutes of Biomedical Research, Oncology, Basel, Switzerland; and [7]Department of Internal Medicine, Erasmus University, Rotterdam, the Netherlands

Received 10/17/06; revised 12/20/06; accepted 1/22/07.

Grant support: Associazione Italiana Ricerca sul Cancro (A. Fusco) and Novartis Pharma.

The costs of publication of this article were defrayed in part by the payment of page charges. This article must therefore be hereby marked *advertisement* in accordance with 18 U.S.C. Section 1734 solely to indicate this fact.

Requests for reprints: Alfredo Fusco, Dipartimento di Biologia e Patologia Cellulare e Molecolare, Università di Napoli "Federico II," via Pansini, 5, 80131 Naples, Italy. Phone: 39-081-3737857; Fax: 39-081-3737808; E-mail: afusco@napoli.com.

doi:10.1158/1078-0432.CCR-06-2505

bind with high-affinity different SSTR subtypes should have a superior therapeutic potential. SOM230 is a promising drug candidate that fulfills these criteria because it exhibits an almost universal binding to somatotropin release-inhibiting factor receptor subtypes (SSTR1, SSTR2, SSTR3, and SSTR5) and exerts potent inhibitory effects on the growth hormone/insulin-like growth factor-I axis in several *in vivo* animal models (4, 5). Preclinical studies on experimental models *in vivo* are needed to elucidate the real efficacy of a therapy based on SOM230 administration for functional pituitary adenomas secreting either growth hormone or prolactin or both of them. Since the last decade, several transgenic mouse models of pituitary adenomas have been generated by targeting expression of oncogenic transgenes to anterior pituitary cells using pituitary-specific promoters (6–8). Our group has recently developed a genetically engineered mouse model for pituitary tumorigenesis (9). These mice, overexpressing in all tissues the *HMGA2* gene, develop growth hormone/prolactin-secreting pituitary adenomas by 6 months of age, with an almost total penetrance in the female gender. This animal model represents an excellent model for evaluating new therapies for pituitary adenomas. Therefore, to evaluate the therapeutic efficacy of SOM230 on pituitary tumor development and hormone secretion, and to compare it with that of octreotide, four groups of 3- and 9-month-old HMGA2 transgenic female mice were treated for 3 months with SOM230 (at two different doses), octreotide, and a placebo, respectively. SOM230, at the highest dose of 50 μg/kg/h, drastically affected the tumor progression and induced a significant regression of the tumor. In contrast, the octreotide at the same dose significantly slowed down the progression of the tumor without inducing regression.

Therefore, these results indicate that administration of SOM230 may represent an elective treatment for pituitary adenomas secreting growth hormone and prolactin.

Materials and Methods

Mice and treatment. Two groups of 32 HMGA2 female transgenic mice have been treated either at 9 months or at 3 months of age as follows: 8 placebo, 8 octreotide (50 μg/kg/h), 8 SOM230 (5 μg/kg/h), and 8 SOM230 (50 μg/kg/h). The treatment was delivered by s.c. injection, for 3 months, by using Alzet osmotic pumps model 2004. A saline solution (0.9% NaCl) was used as placebo. All the mice have been housed in the Animal facility of the Istituto dei Tumori di Napoli G. Pascale.

Quantitative reverse transcription-PCR. To evaluate SOM230-responsive SSTR expression in HMGA2 transgenic mice pituitary tumors, the relative amount of sst1, sst2A, sst2B, sst3, and sst5 was calculated in four tumors removed by the mice not treated by somatostatin analogues by quantitative reverse transcription-PCR. Quantitative PCR was done as described previously (10). Briefly, polyadenylated mRNA was isolated during Dynabeads Oligo(dT)25 (Dynal AS, Oslo, Norway) from tumor tissue samples. cDNA was synthesized using the polyadenylated mRNA, which was eluted from the beads in 40 μL H_2O for 2 min at 65°C, using Oligo(dT)12-18 Primer (Applied Biosystems, Foster City, CA). One twentieth of the cDNA library was used for quantification of the SSTR subtype mRNA levels. A quantitative reverse transcription-PCR was done by Taqman Gold nuclease assay (Perkin-Elmer Corp., Foster City, CA) and the ABI PRISM 7700 Sequence Detection System (Perkin-Elmer) for real-time amplification according to the manufacturer's instructions. The assay was done using 15 μL Taqman Universal PCR Master Mix (Applied Biosystems), 300 nmol/L forward primer, 300 nmol/L reverse primer, 200 nmol/L probe, and 10 μL cDNA template in a total reaction volume of 25 μL. The detection of hypoxanthine phosphoribosyl transferase (HPRT) mRNA served as a control and was used for normalization of somatostatin subtype mRNA levels.

The specific mouse primer sequences (Biosource, Nivelles, Belgium) that were used included the following: HPRT, 5′-TGAAGAGCTACTGTAATGATCAGTCAAC-3′ (forward) and 5′-AGCAAGCTTGCAACCTTAACCA-3′ (reverse); sst1, 5′-TTGACTTGGGGATCTGAAGG-3′ (forward) and 5′-ATTAATAAGCGGCACCATCG-3′ (reverse); sst2A, 5′-TGAGTGGTACGGAGGATGGG-3′ (forward) and 5′-CTCCGTGGTCTCATTCAGCC-3′ (reverse); sst2B, 5′-CAAGGCAGACAATTCACAATCC-3′ (forward) and 5′-GTTTCTGCCGGGCAGCT-3′ (reverse); sst3, 5′-CCTCTGCAGCAACCCTGTA-3′ (forward) and 5′-CAGATGAAGGATAGGTAACAGTGG-3′ (reverse); and sst5, 5′-GCGCTCAGAACGCAAGGT-3′ (forward) and 5′-CAGCAGCCCACGAACACC-3′ (reverse).

The probe sequences that were used included the following: HPRT, 5′-FAM-TGCTTTCCCTGGTTAAGCAGTACAGCCC-TAMRA-3′; sst1, 5′-FAM-TGAAATCTCCAGGTACAGGTTTAAAGAACTGGCA-TAMRA-3′; sst2A, 5′-FAM-AGAGGAGCGACAGTAAGCAGGACAAATCC-TAMRA-3′; sst2B, 5′-FAM-ATTGCCTGGGTGTGACCTGGTGGA-TAMRA-3′; sst3, 5′-FAM-TTAGGGCTGGTTGGCTGCTGACTGATCCTCATCTCAG-TAMRA-3′; and sst5, 5′-FAM-ACTCGCATGGTGGTGGTAGTGGTGC-TAMRA-3′.

The relative amount of SSTR mRNA was determined by means of a standard curve generated in each experiment from known amounts of mouse genomic DNA. For the determination of the amount of HPRT mRNA, a standard curve was obtained by including dilutions of a pool cDNAs known to contain HPRT. The amount of SSTRs mRNA was calculated relative to the amount of HPRT and is given in arbitrary units.

Serum hormone measurements. Serum prolactin concentration was measured before and after the treatment using mouse prolactin RIAs consisting of reagents provided by Dr. A.F. Parlow (National Hormone & Peptide Program, Harbor-UCLA Medical Center, Torrance, CA).

Magnetic resonance. Magnetic resonance imaging (MRI) analyses have been done at the Istituto dei Tumori di Napoli G. Pascale on a 1.5-T magnet system using local receiver coils and an 8-cm field of view. Sagittal slices (3 mm thick) have been obtained with T1-weighting (repetition time/echo time = 400/11 ms). The images were analyzed by Acrobat Photoshop; the tumor size, expressed in pixel, has been obtained by the product of the two major diameters of the lesion as appeared in the median sagittal section.

Histologic analysis. Histologic evaluation was done on 10% neutral phosphate-buffered formaldehyde-fixed, paraffin-embedded pituitary adenomas. Paraffin sections were stained with H&E and Gordon-Sweet silver impregnation to assess reticulin fiber network, which is essential

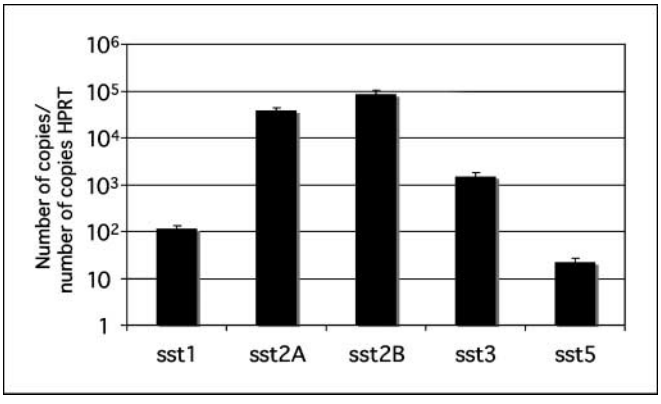

Fig. 1. SSTR expression in pituitary adenomas from HMGA2 transgenic mice. The results obtained from three independent real-time analyses of *sst1, sst2A, sst2B, sst3*, and *sst5* genes were plotted as a histogram, showing their relative copy number compared with the housekeeping *HPRT* gene.

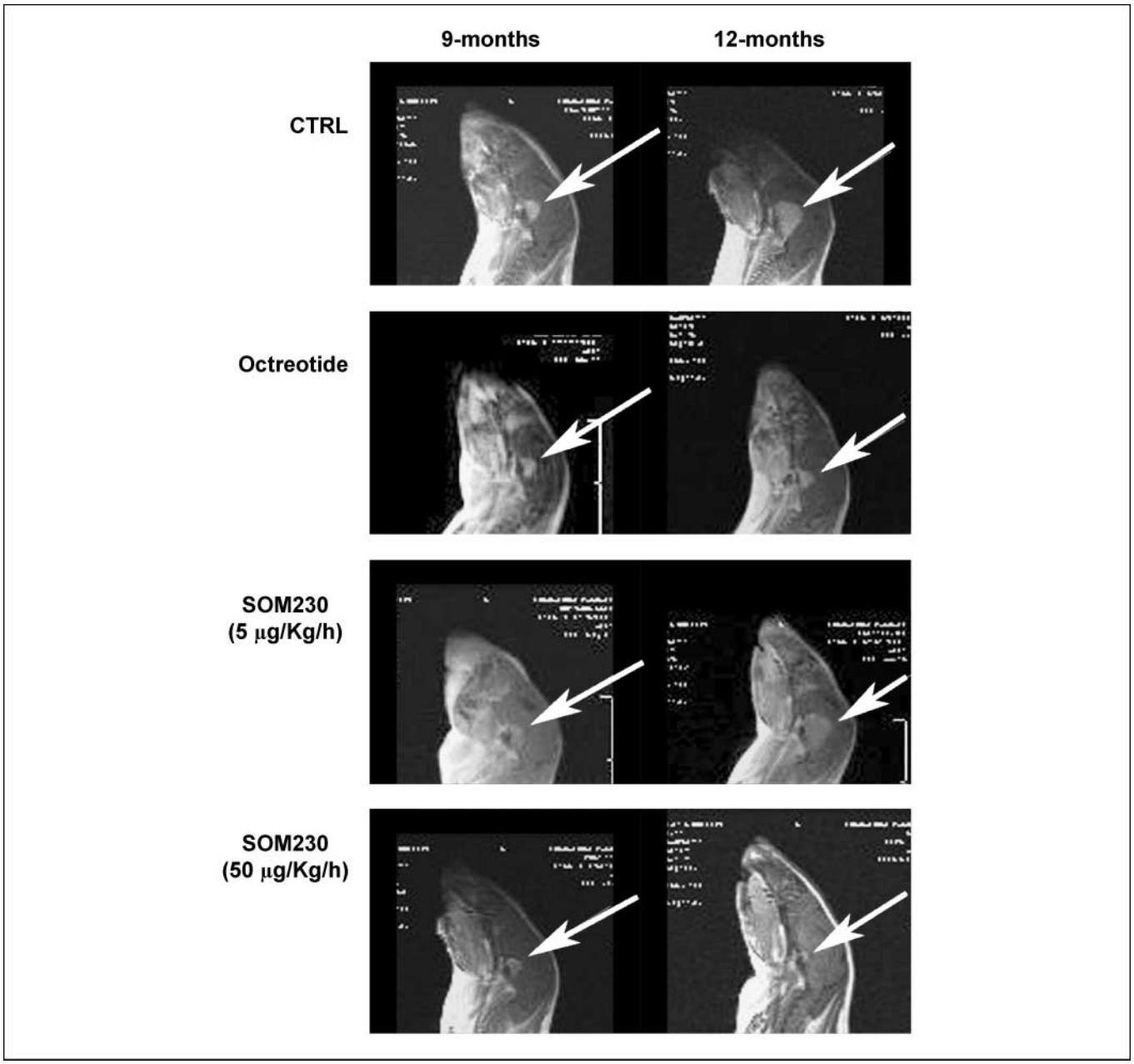

Fig. 2. MRI of HMGA2 transgenic mice before and after the treatment at 9 to 12 months of age. Representative mouse for each treated group before (*left*) and after (*right*) the treatment. Arrows, pituitary adenoma.

for distinguishing normal adenohypophysial architecture, hyperplasia, and adenoma.

Statistical analysis. For the comparison of statistical significance between two groups, Student's t test was used. A P value of <0.05 was considered statistically significant.

Results

Characterization of SSTRs in pituitary tumors from HMGA2 transgenic mice. A significant relative amount of sst1, sst2A, sst2B, sst3, and sst5 was found in the pituitary tumors removed by HMGA2 mice. The number of sst2A and sst2B is significantly higher than that of all the others, although a rather heterogeneous expression of the formers and a rather homogeneous expression of the latters were found. The expression of SSTRs is shown in Fig. 1.

Treatment of HMGA2 transgenic mice with SOM230 reduces tumor proliferation. The expression of SSTR subtypes 1, 2, 3, and 5 by the pituitary adenomas occurring in the HMGA2 transgenic mice might account for testing the SOM230 for their treatment. Female HMGA2 transgenic mice were used for preclinical studies with SOM230 because they develop growth hormone/prolactin-secreting pituitary adenomas with an almost complete penetrance. SOM230 was given to 3- and 9-month-old mice by continuous s.c. injection as indicated in Materials and Methods. In parallel, we also used octreotide and a placebo as positive and negative control of pituitary adenoma treatment, respectively.

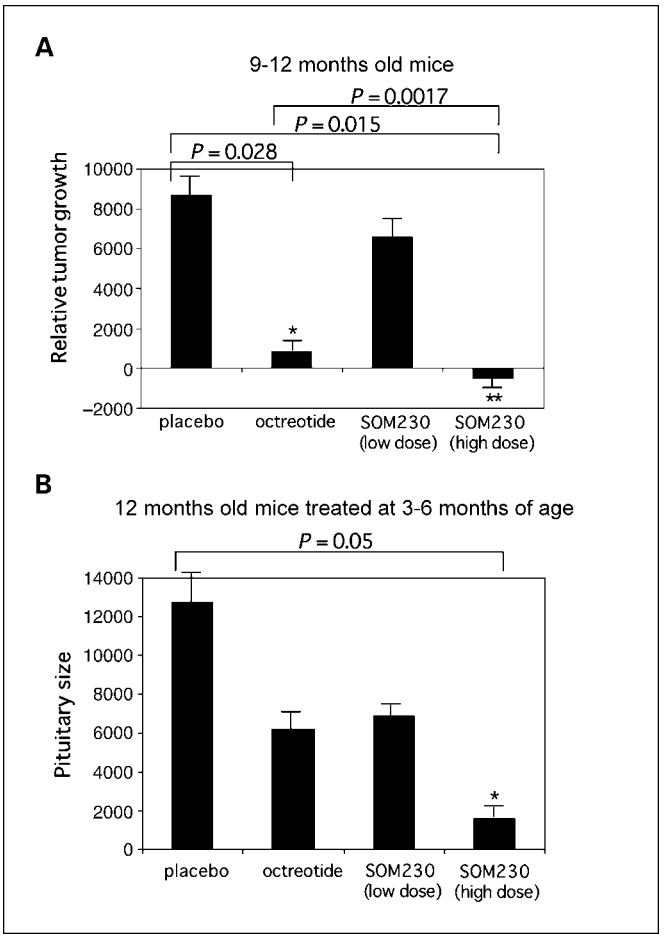

Fig. 3. Size analysis of tumors in treated mice. *A,* mice treated at 9 mo of age were analyzed by MRI before treatment and 3 mo later at the end of the treatment. Tumor size was evaluated as indicated in Materials and Methods. Columns, mean of the size difference before and after the treatment for each animal group; bars, SE. *B,* mice treated at 3 mo of age were analyzed by MRI only at 12 mo of age and 6 mo later at the end of the treatment when the tumor was easily detectable. Tumor size was evaluated as before. Columns, mean tumor size for each treated group; bars, SE. Top of the graphs, *P* value obtained by the comparison of the groups. Asterisks, values that differ statistically from the placebo group.

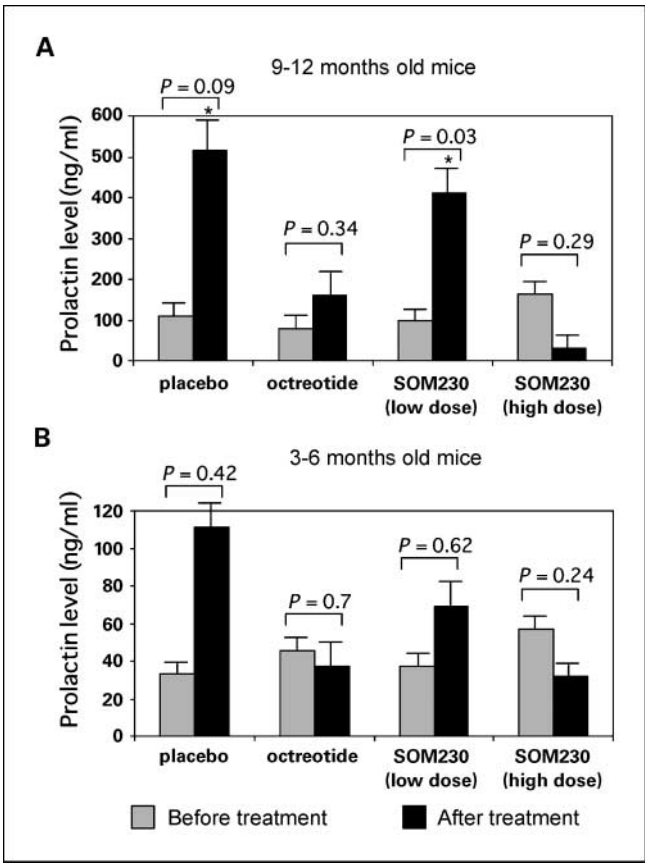

Fig. 4. Serum prolactin concentration measurement in treated mice. *A,* columns, mean prolactin levels before and after the treatment at 9 mo of age for each animal group; bars, SE. *B,* columns, mean prolactin levels before and after the treatment at 3 mo of age for each animal group; bars, SE. Top of the graphs, *P* value obtained by the comparison of the value in each group. Asterisks, values obtained after the treatment of each group, whose difference from the value of the same group before the treatment is statistically different.

In 9-month-old mice, tumor growth was monitored before and after the treatment by MRI analysis (Fig. 2). The comparison of the images clearly shows a decrease of tumor size in mice treated with high dosage of SOM230 (50 μg/kg/h). Conversely, a clear increase in tumor size was observed in mice treated with either a placebo (control) or a low dosage of SOM230 (5 μg/kg/h). Finally, no increase in tumor size was shown in mice treated with octreotide. We measured tumor size for each mouse before and after the treatment as indicated in Materials and Methods and plotted the results as shown in Fig. 3A. The comparison of groups revealed that the pituitary tumors of HMGA2 transgenic mice significantly ($P = 0.028$) slow down their growth in response to 50 μg/kg/h octreotide. Interestingly, 50 μg/kg/h SOM230 significantly ($P = 0.015$) affect the tumor progression of HMGA2 transgenic mice, even better than octreotide does, resulting in a reduction of the tumor size. In fact, the effect of SOM230 on tumor proliferation is significantly stronger ($P = 0.0017$) than that exerted by the octreotide.

In 3-month-old mice, tumor growth was monitored by MRI (data not shown) only at 12 months of age (after 6 months from the end of the treatment) to follow up the tumor growth in mice that received the treatment before the onset of the tumor. As shown in Fig. 3B, tumor size, as appeared by MRI analysis at 12 months of age, was measured for each treated mouse. The only group that showed a significant size reduction compared with placebo-treated mice ($P = 0.053$) was that treated with SOM230 at high dosage (50 μg/kg/h). Conversely, both octreotide and 5 μg/kg/h SOM230 did not significantly reduce the tumor size compared with a placebo ($P = 0.23$ and 0.35, respectively). Importantly, no side effects were observed

Table 1. Incidence of pituitary adenomas in treated mice

Treatment	Age at the time of treatment	
	3 mo, *n* (%)	9 mo, *n* (%)
Placebo	8/8 (100)	8/8 (100)
Octreotide	8/8 (100)	8/8 (100)
SOM230 (low dose)	6/8 (75)	8/8 (100)
SOM230 (high dose)	2/8 (25)	2/8 (25)

in treated mice over the period they were infused and no differences in terms of body weights were observed among the animals at the end of the treatment.

HMGA2 transgenic mice treated with SOM230 show reduced prolactin secretion. Plasma prolactin concentration in transgenic mice before and after the treatment was measured by RIA. In mice treated at 9 to 12 months of age, prolactin levels were significantly increased in both placebo-treated and SOM230-treated (low dose) mice in comparison with the respective control mice (placebo group: $P = 0.09$; SOM230 (low dose): $P = 0.03$). Conversely, octreotide-treated mice did not increase significantly their prolactin levels ($P = 0.34$) and SOM230-treated (high dose) mice showed a trend to decrease prolactin concentration following treatment, although it was not statistically relevant ($P = 0.29$; Fig. 4A). In mice at 3 to 6 months, the prolactin levels were not significantly increased even in the placebo-treated mice because of the still low tumor growth due to the early stage at this age. Nevertheless, a trend versus a slower increase or a mild decrease was observed in all the other treated groups in comparison with the respective controls (Fig. 4B).

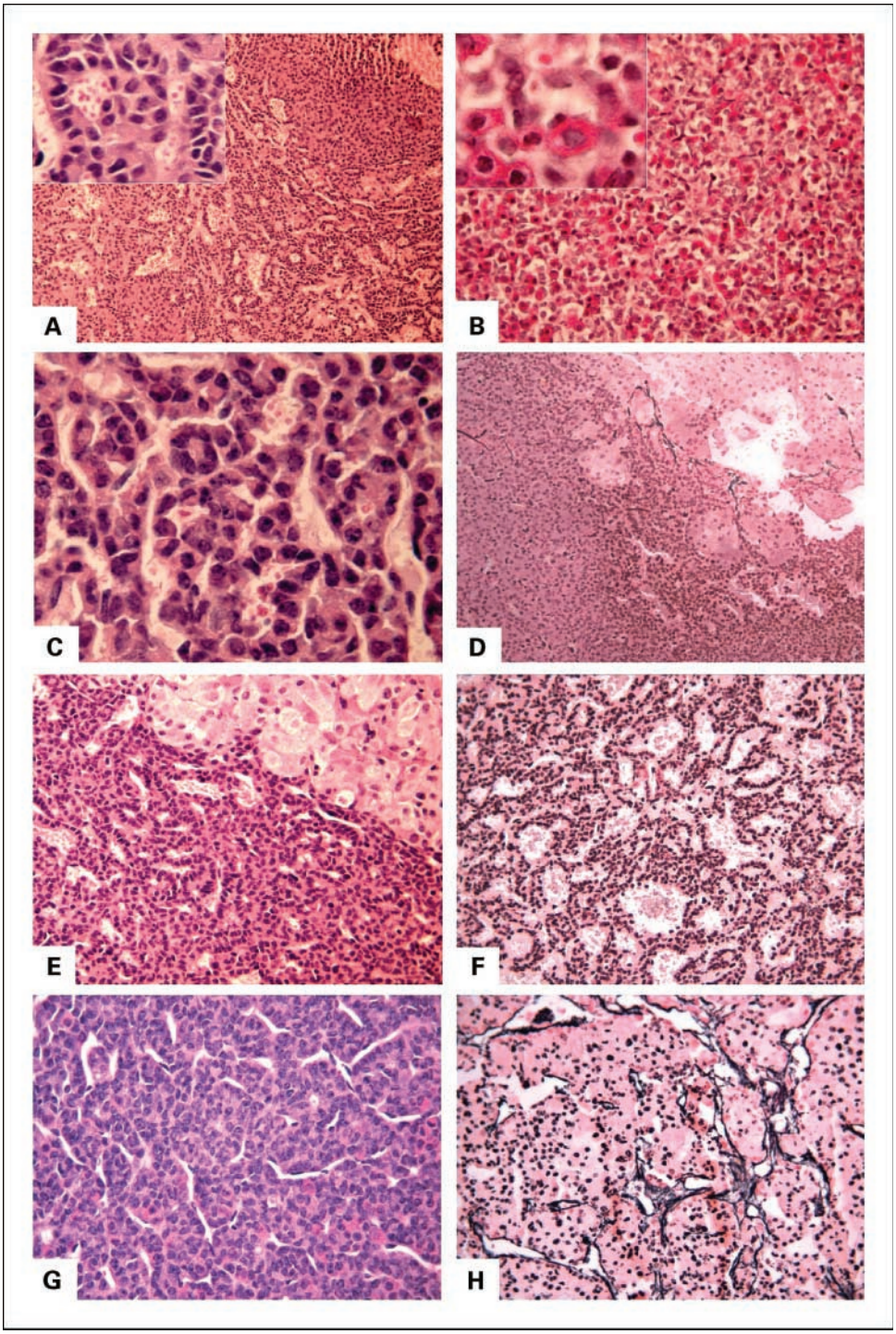

Fig. 5. Cytohistologic characterization of the pituitary tumors in treated mice. *A,* transgenic mice of the placebo group developed sharp delineated pituitary tumors with a follicular type architecture and several blood lakes. *B,* a healthy pituitary gland from a wild-type mouse is shown for comparison. *C,* mice treated with octreotide show the same phenotype as in (*A*). *D,* in most neoplastic cells from octreotide-treated mice, the reticulin network was lost. *E,* mice treated with SOM230 (low dose) show the same phenotype as in (*A*) and (*C*). *F,* in most neoplastic cells from SOM230-treated (low dose) mice, the reticulin network was lost. *G,* total rescue of the normal phenotype was observed in mice treated with SOM230 (high dose). *H,* intact reticulin network in pituitary cells from SOM230-treated (high dose) mice. *A, B, C, E,* and *G,* H&E staining. *D, F,* and *H,* Gordon-Sweet silver stain. Original magnifications, ×100 [*A* and *B* (main images) and *D-H*] and ×400 [*A* and *B* (*insets*) and *C*].

Decreased incidence of pituitary tumors in mice treated with SOM230. All the pituitary glands and tumors from treated mice were fixed in formalin and analyzed by H&E staining for the characterization of the histologic phenotype and the obtaining of the definitive diagnosis. The results of this analysis are summarized in Table 1.

In Fig. 5, some representative histologic analyses are shown. Most of mice treated with 50 μg/kg/h SOM230, both at 3 and 9 months of age, reacted to the therapy with a complete rescue of the normal phenotype (Fig. 5G). The same result was achieved by only one fourth of the mice treated with 5 μg/kg/h SOM230 at 3 months of age. All the other treated mice showed a clear tumoral phenotype with histologic characteristics similar to the placebo group (compare Fig. 5C and E with Fig. 5A), although mice treated with either octreotide, both at 3 and 9 month of age, or SOM230 (low dose), at 3 months of age, showed in most cases smaller tumors compared with control transgenic mice (data not shown). The Gordon-Sweet silver method was used for the histologic diagnosis of these nodules and showed focal disruption of the reticulin fiber network, which is pathognomic for the adenomatous transformation of pituitary cells (Fig. 5D and F).

Discussion

Our previous studies proposed a crucial role of the *HMGA2* gene overexpression in pituitary tumorigenesis. In fact, *HMGA2* was found amplified and overexpressed in human prolactinomas, and transgenic mice overexpressing the *HMGA2* gene developed pituitary adenomas secreting growth hormone and prolactin. Therefore, this animal model may represent a unique tool for testing the efficacy of new drugs for the therapy of human pituitary adenomas. Currently available treatment for human pituitary adenomas uses somatotropin release-inhibiting factor analogues, such as octreotide and lanreotide, which bind preferentially and with high affinity to sst2 (11). Therefore, a research of new drugs able to compete with the other receptors has been prosecuted. Recently, a new drug molecule, SOM230, which binds with high affinity to all human somatotropin release-inhibiting factor receptor subtypes, except for sst4, has been identified and characterized (5). It has the potential to act as a drug combination that contains both sst2- and sst5-selective somatotropin release-inhibiting factor analogue agonists and that was shown to inhibit growth hormone release more potently than single-agent treatment in pituitary adenoma cultures (3, 12). Moreover, the affinity of SOM230 to sst5 suggests potential inhibitory effects on prolactin secretion, given that it has been found that sst5-selective agents inhibit prolactin secretion from prolactinomas, whereas sst2-selective agonists were inactive (12).

A recent study by the group of Melmed compared the relative efficacy of SOM230 and octreotide on hormone secretion from primary cultures of rat pituitaries, human fetal pituitary tissues, and pituitary adenomas, finding no significant improvement by SOM230 on growth hormone and prolactin suppression compared with octreotide, although a trend toward greater efficacy of SOM230 in both growth hormone–secreting and prolactin-secreting adenomas, compared with octreotide, was suggested (13). In the current study, the relative efficacy of octreotide and SOM230 on hormone secretion and tumor growth was studied in our *in vivo* model of pituitary tumorigenesis, such as the HMGA2 transgenic mice, by a 3-month continuous s.c. infusion of the different compounds. Our results clearly show that the treatment with SOM230 at the dose of 50 μg/kg/h is extremely effective because it is able to induce a drastic regression of the tumor when the treatment was started while the tumor was already evident. When the treatment was begun at the third month after birth, no pituitary tumor being present, it gave rise to the prevention of the neoplastic phenotype. Conversely, the treatment with octreotide did not lead to the regression of the disease and could not avoid the development of the tumor in mice treated for 3 months before the onset of the tumor. However, the compound showed a certain efficacy because the growth of the tumor was less rapid in the octreotide-treated compared with mock-treated animals. Interestingly, no effect at all was achieved after the treatment with SOM230 at the dosage of 5 μg/kg/h, suggesting that the treatment with SOM230 requires a minimal dosage to get a valid effect.

The results of this study indicate the potential usefulness of SOM230 in the treatment of human prolactinomas. It is widely accepted that dopaminergic compounds, such as bromocriptine and cabergoline, are extremely effective in normalizing prolactin levels and reducing tumor mass, up to its disappearance, in 80% to 90% of patients in different series (14–17). The minority of patients with tumors resistant to dopaminergic drugs are very difficult to treat and have potentially the risk of further tumor progression with neurologic damage and even death because of the tumor (18). The results of the current study support the possible usefulness of SOM230 in patients with prolactinomas, especially in those patients who are resistant to cabergoline.

In conclusion, these results taken together propose the treatment with SOM230 as a valid tool for the therapy of human pituitary adenomas with an efficacy that it is higher in comparison with that obtained with octreotide, currently used for the treatment of human prolactinomas. However, our data also show that the dosage of SOM230 must be appropriate because a low dosage does not give any therapeutic effect.

Acknowledgments

We thank Angelo Ferraro for the real-time PCRs and Andrea Affuso for mice minipump implants.

References

1. Heaney AP, Melmed S. Molecular targets in pituitary tumours. Nat Rev Cancer 2004;4:285–95.
2. Newman CB, Melmed S, Snyder PJ, et al. Safety and efficacy of long-term octreotide therapy of acromegaly: results of a multicenter trial in 103 patients—a clinical research center study. J Clin Endocrinol Metab 1995;80:2768–75.
3. Shimon I, Yan X, Taylor JE, Weiss MH, Culler MD, Melmed S. Somatostatin receptor (SSTR) subtype-selective analogues differentially suppress *in vitro* growth hormone and prolactin in human pituitary adenomas. Novel potential therapy for functional pituitary tumors. J Clin Invest 1997;100:2386–92.
4. Bruns C, Lewis I, Briner U, Meno-Tetang G,Weckbecker G. SOM230: a novel somatostatin peptidomimetic with broad somatotropin release inhibiting factor (SRIF) receptor binding and a unique antisecretory profile. Eur J Endocrinol 2002;146:707–16.
5. Weckbecker G, Briner U, Lewis I, Bruns C. SOM230: a new somatostatin peptidomimetic with potent inhibitory effects on the growth hormone/insulin-like growth factor-I axis in rats, primates, and dogs. Endocrinology 2002;143:4123–30.
6. McAndrew J, Paterson AJ, Asa SL, McCarthy KJ,

Kudlow JE. Targeting of transforming growth factor-α expression to pituitary lactotrophs in transgenic mice results in selective lactotroph proliferation and adenomas. Endocrinology 1995;136:4479–88.

7. Helseth A, Siegal GP, Haug E, Bautch VL. Transgenic mice that develop pituitary tumors. A model for Cushing's disease. Am J Pathol 1992;140:1071–80.

8. Tascou S, Trappe R, Nayernia K, et al. TSPY-LTA transgenic mice develop endocrine tumors of the pituitary and adrenal gland. Mol Cell Endocrinol 2003;200:9–18.

9. Fedele M, Battista S, Kenyon L, et al. Overexpression of the HMGA2 gene in transgenic mice leads to the onset of pituitary adenomas. Oncogene 2002;21:3190–8.

10. Ferone D, Pivonello R, Van Hagen PM, et al. Quantitative and functional expression of somatostatin receptor subtypes in human thymocytes. Am J Physiol Endocrinol Metab 2002;283:1056–66.

11. Bruns C, Raulf F, Hoyer D, Schloos J, Lubbert H, Weckbecker G. Binding properties of somatostatin receptor subtypes. Metabolism 1996;45:17–20.

12. Shimon I, Taylor JE, Dong JZ, et al. Somatostatin receptor subtype specificity in human fetal pituitary cultures. Differential role of SSTR2 and 5 for growth hormone, thyroid-stimulating hormone, and prolactin regulation. J Clin Invest 1997;99:789–98.

13. Murray RD, Kim K, Ren SG, et al. The novel somatostatin ligand (SOM230) regulates human and rat anterior pituitary hormone secretion. J Clin Endocrinol Metab 2004;89:3027–32.

14. Bevan JS, Webster J, Burke CW, Scanlon MF. Dopamine agonists and pituitary tumour shrinkage. Endocr Rev 1992;13:220–40.

15. Colao A, Lombardi G. Growth-hormone and prolactin excess. Lancet 1998;352:1455–61.

16. Colao A, Di Sarno A, Cappabianca P, Di Somma C, Pivonello R, Lombardi G. Withdrawal of long-term cabergoline therapy for tumoral and nontumoral hyperprolactinemia. N Engl J Med 2003;349:2023–33.

17. Molitch ME, Thorner MO, Wilson C. Management of prolactinomas. J Clin Endocrinol Metab 1997;82:996–1000.

18. Di Sarno A, Landi ML, Cappabianca P, et al. Resistance to cabergoline as compared with bromocriptine in hyperprolactinemia: prevalence, clinical definition, and therapeutic strategy. J Clin Endocrinol Metab 2001;86:5256–61.

The *Mia/Cd-rap* gene expression is downregulated by the high-mobility group A proteins in mouse pituitary adenomas

Ivana De Martino[1], Rosa Visone[1], Dario Palmieri[1], Paolo Cappabianca[2], Paolo Chieffi[3], Floriana Forzati[1], Antonio Barbieri[4], Mogens Kruhoffer[5], Gaetano Lombardi[6], Alfredo Fusco[1,7] and Monica Fedele[1]

[1]Dipartimento di Biologia e Patologia Cellulare e Molecolare and Istituto di Endocrinologia ed Oncologia Sperimentale del CNR, University of Naples 'Federico II', via Pansini 5, 80131 Naples, Italy
[2]Dipartimento di Scienze Neurologiche, Divisione di Neurochirurgia, University of Naples 'Federico II', Naples, Italy
[3]Dipartimento di Medicina Sperimentale, II University of Naples, Naples, Italy
[4]Istituto dei Tumori di Napoli Fondazione 'G Pascale', Naples, Italy
[5]Department of Clinical Biochemistry, Aarhus University Hospital, Aarhus, Denmark
[6]Dipartimento di Endocrinologia ed Oncologia Molecolare e Clinica, University of Naples 'Federico II', Naples, Italy
[7]NOGEC (Naples Oncogenomic Center), CEINGE Biotecnologie Avanzate and SEMM, European School of Molecular Medicine, Naples, Italy

(Correspondence should be addressed to A Fusco; Email: afusco@napoli.com)

Abstract

The high-mobility group A (HMGA) family of proteins orchestrates the assembly of nucleoprotein structures playing important roles in gene transcription, recombination, and chromatin structure through a complex network of protein–DNA and protein–protein interactions. Recently, we have generated transgenic mice carrying wild type or truncated *HMGA2* genes under the transcriptional control of the cytomegalovirus promoter. These mice developed pituitary adenomas secreting prolactin and GH mainly due to an increased E2F1 activity, directly consequent to the HMGA2 overexpression. To identify other genes involved in the process of pituitary tumorigenesis induced by the *HMGA2* gene, in this study we have analyzed the gene expression profile of three HMGA2-pituitary adenomas in comparison with a pool of ten normal pituitary glands from control mice, using the Affymetrix MG MU11K oligonucleotide array representing ~13 000 unique genes. We have identified 82 transcripts that increased and 72 transcripts that decreased at least four-fold in all the mice pituitary adenomas analyzed compared with normal pituitary glands. Among these genes, we focused our attention on the *Mia/Cd-rap* gene, whose expression was essentially suppressed in all of the pituitary adenomas tested by the microarray. We demonstrated that the HMGA proteins directly bind to the promoter of the *Mia/Cd-rap* gene and are able to downregulate its expression. In order to understand a possible role of Mia/Cd-rap in pituitary cell growth, we performed a colony assay in GH3 and GH4 cells. Interestingly, Mia/Cd-rap expression inhibits their proliferation, suggesting a potential tumor suppressor role of Mia/Cd-rap in pituitary cells.

Endocrine-Related Cancer (2007) **14** 875–886

Introduction

The high-mobility group A (HMGA) family consists of three proteins: HMGA1a and HMGA1b that result from alternative splicing of the same gene, i.e. *HMGA1* (Johnson *et al.* 1989), and HMGA2, which is encoded by a different gene (Manfioletti *et al.* 1991). They are small nuclear proteins that bind to the minor groove of DNA through highly cationic regions called 'AT-hooks' (Reeves 2001). The HMGA proteins function as an architectural transcription factor: they do not independently regulate gene transcription, but modulate gene expression through the formation of stereospecific complexes on the promoter/enhancer regions of genes by direct interaction with other transcription factors and through substrate interactions that bend, unwind, or distort the structure of DNA (Thanos & Maniatis 1995). Both the genes have a critical role in the development, during which they are abundantly expressed. In fact,

DOI:10.1677/ERC-07-0036

Online version via http://www.endocrinology-journals.org

the generation of HMGA2-knockout mice resulted in a pygmy phenotype associated with a drastic reduction of the fat tissue (Zhou *et al.* 1995), whereas HMGA1 null mice showed cardiac hypertrophy and type 2 diabetes (Foti *et al.* 2005, Fedele *et al.* 2006*a*).

Rearrangements of the *HMGA2* gene have been frequently found in human benign tumors, mainly of mesenchymal origin, such as lipomas, lung hamartomas, and uterine leiomyomas (Ashar *et al.* 1995, Schoenmakers *et al.* 1995). Both the *HMGA* genes have a critical role in the process of carcinogenesis because they are overexpressed in most human malignant neoplasias (Melillo *et al.* 2001) and the blockage of their expression has been shown to prevent thyroid cell transformation and lead malignant cells to death (Scala *et al.* 2000, Berlingieri *et al.* 2002). Moreover, both *HMGA1* and *HMGA2* behave as classical oncogenes in focus assays on mouse and rat fibroblasts (Fedele *et al.* 1998, Wood *et al.* 2000). The generation of transgenic mice overexpressing either the *HMGA1* or the *HMGA2* gene confirmed their oncogenicity also *in vivo*. In fact, both the HMGA1 and HMGA2 transgenic mice develop growth hormone/prolactin (GH/PRL)-secreting pituitary adenomas and T/NK lymphomas (Baldassarre *et al.* 2001, Fedele *et al.* 2002, Fedele *et al.* 2005).

Consistently with the development of pituitary adenomas in HMGA2 transgenic mice, *HMGA2* gene amplification and overexpression have been shown in a large set of human prolactinomas supporting a critical role of HMGA2 in this human neoplasia (Finelli *et al.* 2002). The mechanism by which HMGA2 is involved in pituitary tumorigenesis is on the ability of the HMGA2 to interfere with the pRB/E2F1 pathway. In fact, we have recently shown that HMGA2 interacts with retinoblastoma protein (pRB) and induces an increased E2F1 activity in pituitary adenomas by displacing histone deacetylase (HDAC1) from the pRB/E2F1 complex and resulting in E2F1 acetylation (Fedele *et al.* 2006*b*). The suppression of pituitary tumorigenesis by mating $HMGA2^{TG}$ and $E2F1^{-/-}$ mice demonstrates a critical role for the HMGA2-mediated E2F1 activation in the onset of these tumors in transgenic mice, and likely in human prolactinomas.

Although the E2F1 activation might represent a major point in the generation of pituitary adenomas in transgenic mice, we cannot exclude the fact that other complementary mechanisms may be envisaged for the role of HMGA2 in pituitary tumorigenesis. In fact, also in the E2F1 minus background, the HMGA2 mice develop a certain number of pituitary neoplasias, even though with a lower frequency and a minor phenotype. Thus, the aim of the present work has been to find out other molecular changes that might contribute tothe development of the HMGA2-induced pituitary tumors. Therefore, we analyzed the expression profile of three pituitary adenomas developed by HMGA2 transgenic mice in comparison with a pool of normal pituitary glands from wild-type animals. We screened an array in which ~13 000 were represented, and we identified 82 transcripts that increased and 72 that decreased with a greater than or equal to four-fold change in pituitary adenomas versus normal ones. These results were validated by semiquantitative reverse transcription (RT)-PCR performed on pituitary tumors originating from different HMGA2 transgenic mice. Then, we focused our attention on the *Mia/Cd-rap* gene, whose expression was drastically downregulated in HMGA2-induced pituitary adenomas. Mia/Cd-rap is a small, secreted protein that is expressed normally at the onset of chondrogenesis (Dietz & Sandell 1996). Interestingly, it is secreted by malignant melanoma cells and elicits growth inhibition of melanoma cells *in vitro* (Blesch *et al.* 1994).

Here we report that the HMGA proteins are able to bind to the promoter of the *Mia/Cd-rap* gene both *in vitro* and *in vivo* indicating a direct role of HMGA proteins in the regulation of the transcription of the *Mia/Cd-rap* gene. Functional studies by luciferase assays confirmed the critical role of the HMGA proteins in the downregulation of the Mia/Cd-rap promoter. To understand the relevance of Mia/Cd-rap downregulation in pituitary adenoma cell growth, we expressed Mia/Cd-rap in GH3 and GH4 cells and performed colony assays. Consistently with a putative tumor suppressor role for Mia/Cd-rap in pituitary cells, we found that its expression causes growth inhibition.

Materials and methods

RNA extraction

Pituitary glands adenomas from wild type and HMGA2 mice (Fedele *et al.* 2002, 2006*b*) were snap-frozen in liquid nitrogen and stored at −80 °C until use. Total RNAs were extracted from tissues and cell lines using TRI REAGENT (Molecular Research Center Inc., Cincinnati, OH, USA) solution, according to manufacturer's instructions. The integrity of the RNA was assessed by denaturing agarose gel electrophoresis (virtual presence of sharp 28S and 18S bands) and spectrophotometry.

Microarray analysis

The Affymetrix standard protocol has been described extensively elsewhere (Affymetrix GeneChip). Briefly, cRNA was prepared from 8 μg total RNA, hybridized to MG MU11K Affymetrix oligonucleotide arrays (containing about 13 000 murine transcripts), scanned, and analyzed according to Affymetrix (Santa Clara, CA,

USA) protocols. Scanned image files were visually inspected for artifacts and normalized by using GENECHIP 3.3 software (Affymetrix). The individual gene expression levels for each of the three pituitary adenomas arrays were divided by the expression level in the normal pituitary tissue. Thus, the data were presented as relative to the expression in normal pituitary tissue. The fold change values, indicating the relative change in the expression levels between mutated and wild-type samples, were used to identify genes differentially expressed between these conditions.

Cluster analysis by Multiexperiment Viewer (MeV)

Microarray data have been elaborated by the MeV system to get gene expression signature of the samples analyzed. The MeV is a system of cluster analysis for genome wide expression data from DNA microarray hybridization that uses standard statistical algorithms to arrange genes according to similarity in the pattern of gene expression. In our analysis, we used a four-fold difference in expression level between normal and tumoral samples.

Semiquantitative RT-PCR

RNAs were treated with DNaseI (Invitrogen) and reverse transcribed using random exonucleotides and MuLV reverse transcriptase (Perkin–Elmer, Waltham, MA, USA). To ensure that RNA samples were not contaminated with DNA, negative controls were obtained by performing PCR on samples that were not reverse transcribed, but otherwise identically processed. For semiquantitative PCR, reactions were optimized for the number of cycles to ensure product intensity within the linear phase of amplification. The PCR products were separated on a 2% agarose gel, stained with ethidium bromide, and scanned using a Typhoon 9200 scanner. Digitized data were analyzed using Imagequant (Molecular Dynamics, Sunnyvale, CA, USA). Primers sequences and different annealing conditions are available as supplemental data (Supplemental Table 1, which can be viewed online at http://erc.endocrinology-journals.org/supplemental/).

Cell cultures and transfections

All cell lines, except for αT3-1 (kindly provided by Dr P Mellon, University of California, San Diego, CA, USA), were purchased from ATCC. They were all cultured in DMEM containing 10% fetal bovine serum (HyClone, Logan, UT, USA) and 50 μg/ml gentamicin (Life Technologies Inc.) in a humidified atmosphere of 95% air and 5% CO_2. B16F0 are murine melanoma cells; AtT20 and αT3-1 are murine pituitary adenoma cells secreting adrenocorticotrophin (ACTH) and gonadotropic hormones, respectively; RC-4B/C are rat pituitary adenoma cells secreting GH, follicle-stimulating hormone, luteinizing hormone, gonadotrophin-releasing hormone, ACTH, and thyrotrophin (TSHb); GH1, GH3, and GH4 are rat pituitary adenoma cells secreting PRL and GH.

Transfections were carried out by using Lipofectamine 2000, according to manufacturer's instructions.

Plasmids

The 5′ flanking region of the mouse *Mia/Cd-rap* gene spanning nucleic acid residues −1396 to −1 with respect to the ATG protein start codon was amplified by PCR and inserted into the promoterless luciferase plasmid pGL_3-basic (Promega) to obtain the MIA-luc pGL_3 plasmid. The human Mia/Cd-Rap expression plasmid, pCMV6-XL4/Mia, was commercially available (TC116021 – OriGene Technologies, Rockville, MD, USA). pBABE-puro had been already described (Monaco *et al.* 2001).

Luciferase and colony assays

For the Luciferase assay, a total of 2×10^5 B16F0 cells were seeded into each well of six-well plates and were transiently transfected with 1 μg MIA-luc pGL_3 and with the indicate amounts of pCEFLHa-HMGA1 (Melillo *et al.* 2001) and pCEFLHa-HMGA2 (Fedele *et al.* 2006*b*), together with 0.5 μg Renilla and various amounts of the pCEFLHa plasmid to keep the total DNA concentration constant. Transfection efficiencies were normalized by using Renilla luciferase expression assayed with the dual luciferase system (Promega). All transfection experiments were repeated at least three times.

For the colony assay, GH3 and GH4 cells were seeded at a density of 2.5×10^6 per 10 mm dish. Two days after, the cells were transfected with 10 μg pCMV6-XL4 plus 2 μg pBabe-puro, or 10 μg pCMV6-XL4/Mia plus 2 μg pBabe-puro. After about 15 days, the cells were stained with 500 mg/ml crystal violet in 20% methanol, and the resulting colonies were counted.

Protein extraction and western blot

Tissues and cell culture were lysed in buffer 1% NP40, 1 mmol/l EDTA, 50 mmol/l Tris–HCl (pH 7.5), and 150 mmol/l NaCl, supplemented with complete protease inhibitors mixture (Roche Diagnostic Corp). Total proteins were separated by SDS-PAGE and transferred to nitrocellulose membranes (Bio-Rad). Membranes were blocked with 5% nonfat milk and incubated with antibody against MIA (A-20 Santa Cruz Biotechnology, Santa Cruz, CA, USA, sc-17047). Bound antibody was detected by the appropriate secondary antibody and revealed with an enhanced chemiluminescence system (Amersham-Pharmacia Biotech).

Electrophoretic mobility shift assay (EMSA)

Protein/DNA-binding was determined by EMSA, as previously described (Battista *et al.* 1995). Briefly, 5–20 ng of recombinant protein were incubated in the presence of a ^{32}P-end-labeled double-strand oligonucleotide (specific activity, 8000–20 000 c.p.m./fmol). Spanning from base −1130 to −1100 of the mouse *Mia/Cd-rap* promoter region (5′-AAACCCTGAAA-TAAATCTTTTTTTCCCCTT-3′). The DNA–protein complexes were resolved on 6% non-denaturing acrylamide gels and visualized by exposure to autoradiographic films.

Chromatin immunoprecipitation (ChIP)

ChIP was carried out with an acetyl-histone H3 immunoprecipitation assay kit (Upstate Biotechnology, Charlottesville, VA, USA) according to manufacture's instruction. Approximately, 3×10^7 cells of the NIH3T3 cell line were grown on 75 cm^2 dishes and cross-linked by the addition of formaldehyde (to 1% final concentration) to the attached cells. Cross-linking was allowed to proceed at room temperature for 5 min and was terminated with glycine (final concentration, 0.125 mol/l). The cells were collected and lysed in buffer containing 5 mmol/l piperazine-N, N′-bis[2-ethanesulfonic acid] (PIPES); (pH 8.0), 85 mmol/l KCl, 0.5% NP40, and protease inhibitors(1 mmol/l phenylmethylsulfonyl fluoride, 10 μg/ml aprotinin, and 10 μg/ml leupeptin), on ice for 10 min. Nuclei were pelleted by centrifugation at 2300 ***g*** for 5 min at 4 °C and resuspended in buffer containing 50 mmol/l Tris–Cl (pH 8.1), 10 mmol/l EDTA, 1% SDS, the same protease inhibitors, and incubated on ice for 10 min. Chromatin was sonicated on ice to an average length of about 400 bp with a Branson sonicator model250. Samples were centrifuged at 16 000 ***g*** for 10 min at 4 °C. Chromatin was pre-cleared with protein A Sepharose (blocked previously with 1 mg/ml BSA) at 4 °C for 2 h. Pre-cleared chromatin of each sample was incubated with 2 μg antibody anti-HA (sc-7392, Santa Cruz Biotechnology) at 4 °C overnight. An aliquot of wild-type sample was incubated also with anti-IgG antibody. Next, 60 μl a 50% slurry of blocked protein A Sepharose was added and immune complexes were recovered. The supernatants were saved as 'input.' Immunoprecipitates were washed twice with 2 mmol/l EDTA, 50 mmol/l Tris–Cl (pH 8.0) buffer and four times with 100 mmol/l Tris–Cl (pH 8.0), 500 mmol/l LiCl, 1% NP40, and 1% deoxycholicacid buffer. The antibody-bound chromatin was eluted from the beads with 200 μl elution buffer (50 mmol/l $NaHCO_3$, 1% SDS). The samples were incubated at 67 °C for 5 h in thepresence of 10 μg RNase and NaCl to a final concentration of 0.3 mol/l to reverse formaldehyde cross-links. The samples were then precipitated with ethanol at −20 °C overnight. The pellets were resuspended in 10 mmol/l Tris (pH 8)−1 mM EDTA and treated with proteinase K to a final concentration of 0.5 mg/ml at 45 °C for 1 h. DNA was extracted with phenol/chloroform/isoamylalcohol, ethanol precipitated, and resuspended in water. Input DNA and immunoprecipitated DNAs were analyzed by PCR for the presence of *Mia/Cd-rap* promoter sequence. The PCR were performed with AmpliTaq gold DNA polymerase (Perkin–Elmer). The primers used to amplify the sequence of the *Mia/Cd-rap* promoter were 5′-TTGCTGGTGCA-TGCCTTA-3′ (forward) and 5′-TCTTAACCGCT-GAGCCATCT-3′(reverse). The PCR products were resolved on a 2% agarose gel, stained with ethidium bromide, and scanned using a Typhoon 9200 scanner.

Results

Gene expression profile analysis

RNAs were extracted from a pool of normal pituitary glands and from three pituitary adenomas developed in three different HMGA2 transgenic mice, and were hybridized to one MG Affymetrix MU11K-A oligonucleotide array containing about 13 000 transcripts. The number of transcripts that increased or decreased in all pituitary adenomas versus normal gland is shown in the Fig. 1. Of the 13.059 transcripts represented on the array, 1560 had a one- to three-fold, 290 had a three- to four-fold, 154 had a four- to ten-fold, and 11 had a greater than ten-fold change. We examined the 154 transcripts that had a fold change ≥4 in all HMGA2-induced pituitary adenomas versus normal pituitary gland. Among these transcripts, 82 were increased and 72 were decreased, including 108 known genes, 30 expression sequence tags and 16 unknown genes. The relative fold changes of these genes, grouped according to their biological function, are shown in Table 1.

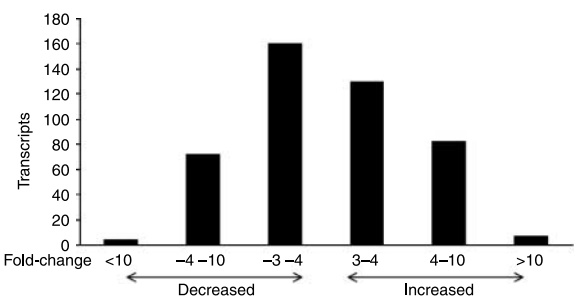

Figure 1 Gene expression profile of pituitary adenomas of HMGA2 transgenic mice. The expression profile of three HMGA2-induced pituitary adenomas was compared with that of normal pituitary gland of wild-type mice. Transcripts are grouped according to fold change.

Table 1 Genes differentially expressed with a greater than or equal to four-fold change in high-mobility group A 2 (HMGA2)-induced pituitary adenomas versus normal pituitary gland

Description	GenBank accession no.	FC Ad1	FC Ad2	FC Ad3
Immune function				
Thy-1	X03151	4.0	1.3	5
Ob/Ob haptoglobin	M96827	10.2	2.2	1.2
MRP8	M83218	107	3.7	1.3
Clon B6 myeloid second. granule prot	L37297	105.1	2.2	1.7
Interferon inducible protein 1-8U	W12941	−2.25	−2.7	−3.3
VCAM-1	X67783	32.6	3.7	4.1
Il-6 receptor	X51975	−3.7	−2.6	−4.3
Ig-κ chain (HyHEL-10)	M35667	3.2	7.5	1.9
G protein-γ 3 subunit	AA049022	−2.5	−1.5	−7.9
GM-CSF	X03019	−4.1	−4.9	−5
Myelopeptide-2	M23236	9.2	10.6	9.5
IFN-γ	AA015168	−7.5	−10.2	−13
Antigen pB7	M55561	5.5	−5.2	−5.6
Cell proliferation				
β-Enolase	W33721	−1.5	−2.2	−1.3
CAD protein	AA466758	2.1	3	5.3
dUTPase	AA110424	1.1	1.4	5.2
Galectin-3	W10936	14.3	8.2	6.3
Signal transduction				
PKC-α	M25811	2	1.8	6.6
FKBP65 binding protein	L07063	6.3	8.3	12.2
mR-PTPμ	X58287	2.7	2.8	4
GTP-binding protein Gb4	M63658	2.4	3.7	6.8
p36	D10024	−4	−4.4	−11
AEBP1	X80478	−12.6	−3.3	−36.9
AP-2	NM_011547	8.4	12.5	4.4
A-RAF	AA060840	−11.5	−11.7	−12.2
Vitronectin	m77123	21.7	10.5	6.1
STEP61	U28217	−5.4	−9.9	−18.2
Cell cycle				
CycD3	AA266783	4.4	6.1	3.5
CycB2	X66032	5.6	8	6.1
CycB	X58708	4.5	6.3	4.4
cdc2	U58633	4	11.2	3.6
GADD-45	l28177	−2.6	−5.9	−3.9
Antigens				
SSAV provirus polygene	C76668	2.1	1.6	5.1
(*Emv-3*) gag gene	U63133	−1.1	−1.4	−2
Mitochondrial proteins				
Heme oxygenase	M33203	30.5	3.2	2
Fosfadilserine decarb. Proenzime	AA162205	23.9	40.8	36
Creatine kinase	W50891	8	6.8	9.3
HMG proteins				
HMGA1	AA290110	2.3	1.2	5.6
HMG2	Z46757	10.7	4.4	23.1
Enzymes				
Argininosuccinate synthetase	M31690	−5.6	−4.5	−6
PAF-acetylhydrolase	U34277	−5.9	−6.7	−8.6
Transglutaminase Tgase	M55154	−1.1	−5.8	−5.3
Aldehyde dehydrogenase ALDH2	U07235	−1.3	−3.2	−5.3
Rib-1	X60103	−16	−16.9	−18.5
Dipeptidase	D13139	−4	−3.8	−3.9
Aldolase 3, isoform C	W53351	−11.5	−5.5	−9.4
Cytochrome P-450 Naphthalene Hydrox.	M77497	−13	−21	−12.2
11β HSDH	X83202	−5.5	−7.2	−7.9
Ubiquitin-conjugating enzyme E2	W99019	5.6	8.6	3.1

Table 1 *(continued)*

Description	GenBank accession no.	FC Ad1	FC Ad2	FC Ad3
Retinaldehyde-specific dehydrogenase	X99273	−7.2	−6.7	−6.2
Membrane-type matrix metalloproteinase 1	U54984	−1.8	−3.1	−6
CAMK2 β subunit	X63615	−22.6	−22.7	−31.1
Acetylcholinesterase	X56518	18.1	4.3	9.6
DNA topoisomerase II	d12513	6	9.1	5.1
Ribonucleotide reductase M2 subunit	m14223	4.4	7.9	5
Transcriptional factors				
ID4	X75018	1.4	1.6	1.9
ID1	M31885	−4.5	−6.6	−7.5
Zif 268	M22326	−8.3	−1.4	−14.1
SOX-2	U31967	−8.8	−7	−10.6
δ-like 1 protein	X80903	4.3	6.7	6
MLZ4 zinc protein	AA015118	6.4	4.6	9.1
SOX-11	AF009414	7.4	9.3	11.2
Hormones				
FSH-β	U12932	−9.6	−5.3	−7.9
LH-β	U25145	−14	−2	−1.2
GH	Z46663	15.3	18.7	22.1
Pituitary glycoprotein hormone	M22992	−1.7	−1.1	−10.6
Thyroid-stimulating hormone	M54943	−7.1	−7.7	−7.3
Oncogenes and oncoproteins				
PTTG	AA711028	−1.2	−5.6	−2.4
GARG-16	U43084	−3.6	−5.6	−10.4
Bcl3	W62846	9.1	8.3	6.1
IFC oncogene	U28495	11.2	11	10.3
Lipidic metabolism				
Choline Chinase	AK078101	1.3	1.9	4.4
APOBEC-1	W29206	4.2	1.6	4.6
ALBP (adipocyte lipid-binding protein)	K02109	10.8	6.1	9.6
Allergic disease and inflammation				
IgE receptor	W41745	9.2	1.2	−1.1
Extensin precursor	AA031158	34	12.2	3.8
Mouse complement component C3	k02782	9.6	5.8	4.6
Extracellular matrix and cellular-structure				
Laminin β-3	U43298	−3.8	−9.2	−14.3
Decorin	X53929	−4.6	−4.6	−5.4
Tubulin β2	AA030364	7.1	9.3	11.3
Vsm α-ACTIN	X13297	26.4	9.9	2.8
Reelin	U24703	−6.2	−12	−32.7
E-chaderin	X06115	−5.4	−6.2	−5.1
Tubulin β4	AA030364	9.9	4.3	11.3
Semaphorin H	Z80941	−12.1	−8.6	−7.6
ATP-binding cassette trasp.(ABCR)	AF000149	−9.9	−10.5	−12.3
Syntaxin 1A	D45208	−5.6	−4.9	−5.6
Folate-binding protein 1	M64782	−10.1	−14.1	−16
Growth factors				
Igf2	U71085	8.6	3.5	2.8
MIA/CD-RAP	X97965	−106.6	−126.6	−121
Peroxisome membrane protein (PMP22)	L28835	6.5	9.6	4.1
Development				
Raly	L17076	−5.4	−3	−3
Noggin	U79163	7.5	8.3	10.3
NFI-β	U57634	−4.5	−4.2	−7.5
Receptors				
Nicotinic Acetyl Choline rec. β subunit	M14537	−13.4	−15	−24.8
FGR receptor	M33760	−5.9	−3.1	−12.5
T-cell receptor β chain	M26417	−7.2	−5.6	−6.6

continued

Table 1 *(continued)*

Description	GenBank accession no.	FC Ad1	FC Ad2	FC Ad3
RIP140	W85018	−6.8	−4.9	−7.1
Serotonin 4L receptor	W85018	−4.1	−5.6	−4.9
Fc-γ receptor	m14215	31.6	7.4	6
Other functions				
ANKT	AA266783	4.4	6.1	7.5
γ-casein	D10215	1	1.1	1.1
EN7	X53247	13.4	1.4	−1.7
DMR-N9 gene	Z38011	−4.3	7.3	−4.5
Actin-2	W50919	−7	−4.4	−6.7
Dihydropyrimidinase related protein 4	ab006715	−10	−10.6	−12.1
Hoxc-5	U28071	−5.7	−6.6	−8.5
Prosurvival factors				
BDNF	X55573	4.1	5.9	4.9

FC, fold change, Ad, pituitary adenoma.

A natural basis for organizing gene expression data is to group together genes with similar patterns of expression. Using the MeV, a free Java application which is used to compare datasets from microarray expression experiments (Eisen *et al.* 1998), we clustered the gene expression profile of HMGA2-induced pituitary adenomas in comparison with the normal gland. The results, illustrated in Fig. 2, clearly show the similar pattern of expression of several genes in all pituitary adenomas with respect to the normal pituitary gland.

Validation of microarray data

To validate the results obtained by microarray analysis, we evaluated the expression of about 100 transcripts, whose expression differed of a fold change >4 or ≤ 4 in all the three pituitary adenomas compared with normal glands. To this aim, we performed semiquantitative RT-PCRs in normal glands and HMGA2-induced pituitary adenomas derived from mice different from those used for the Gene Chip microarray. For all of these genes, we confirmed the differential expression associated with the pituitary tumors. The results of some representative RT-PCR analyses are shown in Fig. 3A. Among these differentially expressed genes, there are some upregulated (e.g. Cyclin B2, ANKT and noggin) and other downregulated (e.g. Rib-1, CamK2 and Mia/Cd-rap) in pituitary tumors with respect to the normal gland. Most of the genes analyzed show the same regulation in their expression also in pituitary adenomas developed in transgenic mice overexpressing the *HMGA1* gene (Fedele *et al.* 2005). Some of these representative results are shown in the Fig. 3B.

Subsequently, we analyzed by RT-PCR the expression of these genes also in murine and rat cell lines derived by pituitary adenomas of different histotype in comparison with normal mouse or rat pituitary gland (Fig. 3C and data not shown). Some genes, such as *Mia/Cd-rap* and CamK2, as for the pituitary adenomas of HMGA mice, are downregulated in all the cell lines, whereas other genes, such as *FKBP65* or *reelin*, change their expression depending on the cellular histotype.

HMGA proteins regulate Mia/Cd-rap expression

We concentrated our attention on the *Mia/Cd-rap* gene for two main reasons: i) it was the most downregulated gene in all of the HMGA2-induced pituitary adenomas analyzed and ii) it has been already associated with tumor development, even though it is upregulated in different human neoplasias such as chondrosarcoma, melanoma, and breast cancer (Blesch *et al.* 1994, Chansky *et al.* 1998).

Mia/Cd-rap protein is downregulated in mouse pituitary adenomas

To further validate the microarray data obtained for the *Mia/Cd-rap* gene, we also analyzed the Mia/Cd-rap protein expression in tissue extracts of pituitaries and pituitary adenomas from control and transgenic mice (either HMGA1 or HMGA2) respectively. As shown in Fig. 4A, normal pituitary from control mice show high levels of Mia/Cd-rap protein expression, whereas it was completely lost in pituitary adenomas from both HMGA1 and HMGA2 transgenic mice.

HMGA proteins bind to the Mia/Cd-rap promoter

To investigate whether the HMGA proteins are directly involved in *Mia/Cd-rap* transcriptional regulation, we evaluated the HMGA-binding activity to the

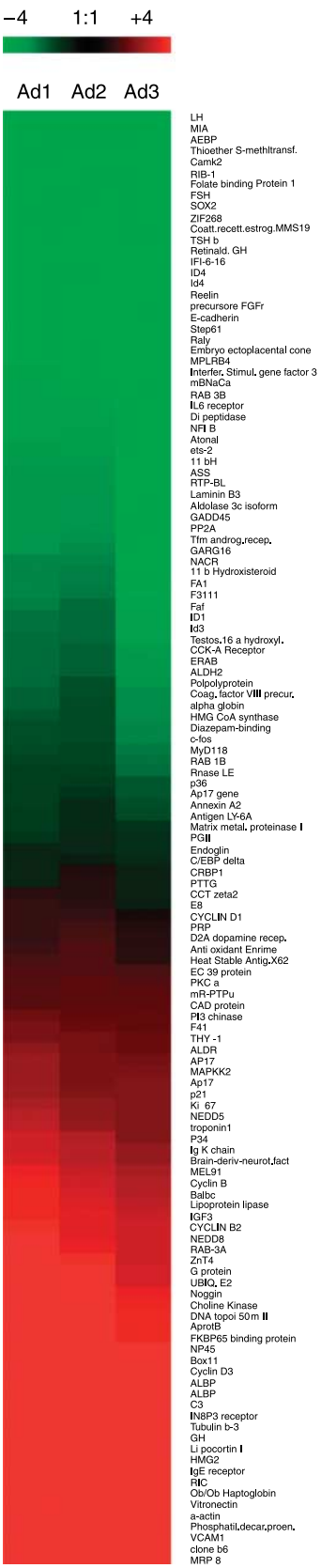

Mia/Cd-rap promoter *in vitro* using oligonucleotides spanning from base −1130 to −1100 of the mouse *Mia/Cd-rap* promoter region (Bosserhoff *et al.* 1997), including AT-rich putative HMGA-binding sites. As shown in Fig. 4B, lanes 1–2, increasing amounts (5 and 20 ng) of the recombinant HMGA2 protein were capable of binding the ^{32}P-end-labeled double-strand oligonucleotide in EMSA. The binding specificity was demonstrated by competition experiments showing loss of binding with the addition of 100-fold molar excess of the specific unlabeled oligonucleotide (lane 3). We performed the same experiment with a recombinant HMGA1 protein, and also in this case a specific binding with the Mia/Cd-rap promoter (Fig. 4B, lanes 5–7) was detected.

To verify that HMGA proteins are able to bind to Mia/Cd-rap promoter *in vivo,* we performed experiments of ChIP in the NIH3T3 cell line transiently transfected with either the HA-HMGA2 or HA-HMGA1 expression plasmids. Chromatin prepared as described under Materials and methods was immunoprecipitated with anti-HA or normal rabbit IgG antibody. The results, shown in Fig. 4C, confirmed that both HMGA2 and HMGA1 proteins bind to the promoter of *Mia/Cd-rap* gene. In fact, the *Mia/Cd-rap* promoter region was amplified from the DNA recovered with anti-HA antibody in HA-HMGA1- and HA-HMGA2- but not in mock-transfected cells. Moreover, no amplification was observed in the samples immunoprecipitated with a specific rabbit IgG.

HMGA proteins regulate the Mia/Cd-rap promoter activity

To define the functional consequences of the interaction between HMGA proteins and *Mia/Cd-rap* promoter, we co-transfected the B16F0 cell line, in which Mia/Cd-rap protein is endogenously expressed, with a construct expressing the luciferase reporter gene under the control of the mouse *Mia/Cd-rap* promoter region −1396 to +1 (mMIAprom-luc) and increasing the amounts of an *HMGA2* (or *HMGA1*) expression vector. As shown in Fig. 4D, the overexpression of HMGA2 (or HMGA1) resulted in a decreased activity of the *Mia/Cd-rap* promoter in a dose-dependent manner. Interestingly, the HMGA1 protein showed a significantly higher

Figure 2 Clustered display of gene expression in three pituitary adenomas developed in three HMGA2 transgenic mice when compared with normal pituitary gland using the MEV program. A four-fold difference in expression level between adenomas and normal samples was used. The green and red colors show downregulated and upregulated genes respectively. Each gene is represented by a single row of colored boxes; each adenoma is represented by a single column.

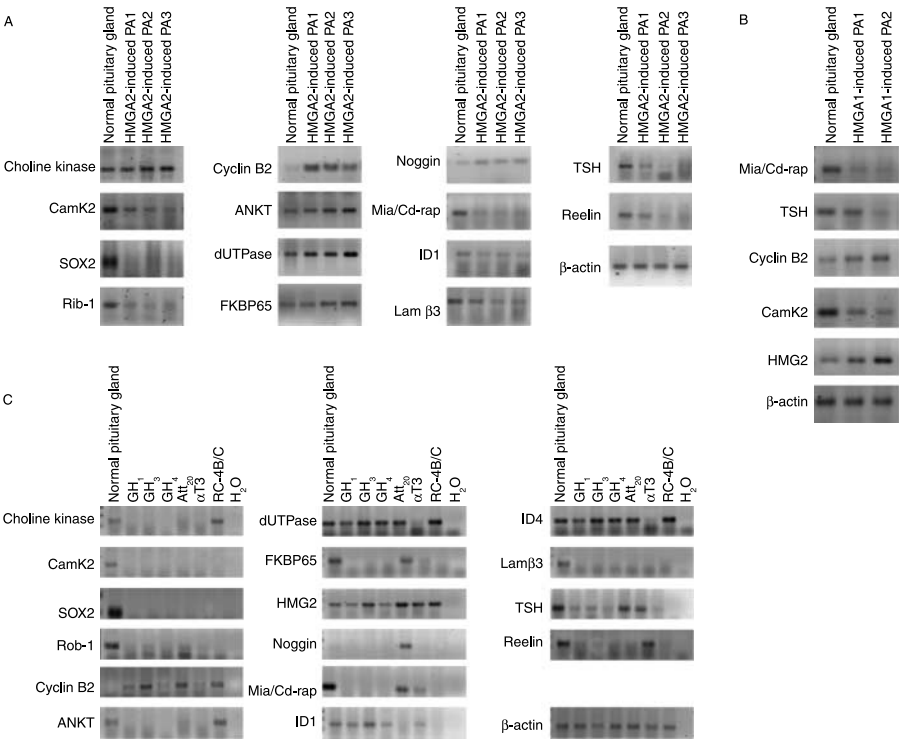

Figure 3 Validation of microarray data by semiquantitative RT-PCR. (A) Representative RT-PCRs on a panel of three HMGA2-induced pituitary adenomas and a pool of wild-type pituitary glands. (B) Representative RT-PCRs on a panel of two HMGA1-induced pituitary adenomas and a pool of wild-type pituitary glands. (C) Some of the genes regulated in HMGA-induced pituitary adenomas were assayed by semiquantitative RT-PCR on a panel of seven cell lines originating by rat and mouse pituitary adenomas of different histotype in comparison with a pool of wild-type mouse pituitary glands. Amplification of the *β-actin* gene has been evaluated as a control of the RNA amount used.

inhibitory effect on the Mia/Cd-rap promoter activity in comparison with the HMGA2 protein (80% with 1 μg HMGA1 versus 55% with 1 μg HMGA2).

Mia/Cd-rap expression inhibits growth of pituitary adenoma cells

To investigate the functional role of Mia/Cd-rap in pituitary cell growth, we performed colony assay experiments by transfecting Mia/Cd-rap in pituitary adenoma GH3 and GH4 cells. After puromycin selection, the number and growth of the colonies obtained by transfection with the Mia expression plasmid decreased dramatically compared with empty vector in both cell lines (Fig. 5). These results show that Mia/Cd-rap inhibits the cell growth of rat pituitary adenoma cells, suggesting it as a negative regulator of pituitary cell proliferation.

Discussion

Pituitary tumors constitute about 15% of intracranial neoplasms and are mostly benign with slow growth. Most pituitary neoplasms secrete hormone gene products, leading to disturbed endocrine functions. About two-thirds of pituitary tumors express and secrete pituitary hormones. Among these, prolactinomas are the most common lesions, representing about 50% of all the clinically diagnosed pituitary adenomas. The genesis of pituitary tumors remains still largely unknown, and several factors, such as gene mutations, locally produced growth factors, and hypothalamic dysregulation, play a critical role in the transformation of pituitary cells. A crucial role for the *HMGA2* gene in the process leading to the generation of human pituitary adenomas was first suggested by the phenotype of transgenic mice overexpressing a truncated or a wild-type *HMGA2* gene under the transcriptional control of the strong and ubiquitous promoter of the cytomegalovirus. Most of these mice (85% of females and 40% of males), in fact, developed pituitary adenomas secreting PRL and GH (Fedele *et al.* 2002). After these findings, we investigated the role of the *HMGA2* gene in human prolactinomas. Interestingly, cytogenetic analysis of prolactinomas revealed not only an increased dosage of the *HMGA2* gene, which resulted from multiple

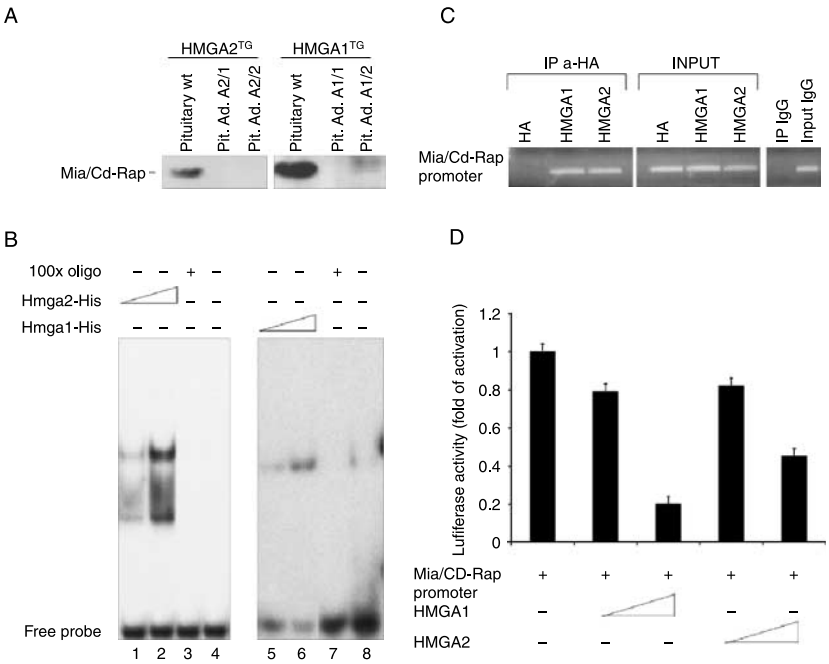

Figure 4 HMGA proteins regulate the murine *Mia/Cd-rap* promoter. (A) Mia/Cd-rap protein expression in pituitary adenomas and normal pituitary glands from HMGA (both HMGA1 and HMGA2) transgenic mice and wild-type animals respectively. (B) EMSA performed with a radiolabeled oligonucleotide spanning from base −1130 to −1100 of the mouse *Mia/Cd-rap* promoter region, and incubated with 5 ng (lanes 5) and 20 ng (lanes 6) of the recombinant HMGA1-His protein or with 5 ng (lane 1) and 20 ng (lanes 2) of the recombinant HMGA2-His protein. Where indicated, a 100-fold molar excess of unlabelled MIApr oligonucleotide was added as a specific competitor. (C) Chromatin immunoprecipitation assay performed on NIH3T3 cells transfected with pCEFLHA, pCEFLHa-HMGA1, or pCEFLHa-HMGA2. The recovered DNA was used as a template for PCR with primers that specifically amplify the murine *Mia/Cd-rap* promoter. Input indicates PCR products with chromosomal DNA without immunoprecipitation. As an immunoprecipitation control, IgG was used. (D) Luciferase activity (fold of activation) of the *Mia/Cd-rap* promoter in the B16F0 murine melanoma cell line. Where indicated 0.5 and 1 μg of either HMGA1 or HMGA2 expression vectors were cotransfected with the Mia-luc plasmid.

mechanisms, mainly simple chromosome gain (trisomy or tetrasomy of chromosome 12), but also over-representation of the *HMGA2* gene through der (12) chromosomes (Finelli *et al.* 2002). The strong correlation between the phenotype of the *HMGA2* transgenic mice and the *HMGA2* overexpression in human prolactinomas suggested that this animal model might represent a unique tool for studying the molecular mechanisms underlying the generation of pituitary adenomas induced by the *HMGA2* overexpression. In fact, these mice allowed us to demonstrate that the mechanism of the HMGA2-induced pituitary adenoma development is based on the increased E2F1 activity (Fedele *et al.* 2006*b*). Since other additional mechanisms can be envisaged on the base of a minimal residual tumoral phenotype showed by some HMGA2 transgenic mice lacking a functional *E2F1* gene (Fedele *et al.* 2006*c*), in the present study we have analyzed the gene expression profile of three HMGA2-pituitary adenomas in comparison with a pool of ten normal pituitary glands in order to identify other genes involved in the process of pituitary tumorigenesis induced by the *HMGA2* gene. The results of our analysis led to the identification of 82 transcripts that increased and 72 transcripts that decreased at least fourfold in all mice pituitary adenomas analyzed when compared with normal

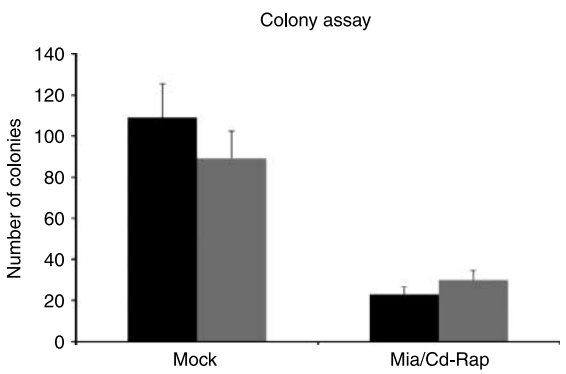

Figure 5 Effect of Mia/Cd-rap expression on pituitary adenoma cell proliferation. Colony forming assay experiment performed on GH3 (black bars) and GH4 (gray bars) cells transfected with a vector expressing Mia/Cd-rap. As a control the empty vector (mock) was used. The reported results are the mean of three experiments and error bars show S.D.

pituitary gland. It is noteworthy that among the overexpressed genes, we found *galectin-3*. This is consistent with previous reports showing a role for the galectin-3 protein in pituitary cell proliferation and tumor progression (Riss *et al.* 2003). Here we focused on the *Mia/Cd-rap* gene because its expression was essentially suppressed in all of the mouse pituitary adenomas analyzed and, even though it has been already associated with a neoplastic phenotype (Blesch *et al.* 1994, Chansky *et al.* 1998), it has been never described in pituitary tumorigenesis so far. We demonstrated, by EMSA and ChIP, that both HMGA1 and HMGA2 proteins directly bind to the promoter of this gene and downregulate its expression in transcription assays. It is noteworthy to observe that even though both the HMGA proteins are able to regulate the *Mia/Cd-rap* gene, this effect is more pronounced with HMGA2 than with HMGA1. Finally, by colony assays in GH3 and GH4 cells we were able to demonstrate that re-expression of Mia in this pituitary adenoma cell line dramatically reduces their proliferative potential, indicating a potential tumor suppressor role for this gene in pituitary tumors.

The protein Mia/Cd-rap is mainly expressed in cartilage during embryogenesis (Dietz & Sandell 1996), and is related to cellular motility, metastasis, and modulation of immune responses in melanoma cells. In fact, it has been shown that Mia/Cd-rap interacts with components of the extracellular matrix, such as laminin and fibronectin, suggesting that it may have a function in regulating detachment of melanoma and possibly other cells from the extracellular matrix, which is an important step in metastasis (Bosserhoff *et al.* 1997).

Therefore, the previous published data about the *Mia/Cd-rap* gene appear in contrast with those reported here which suggest a tumor suppressor function of this gene rather than an oncogenic function. It is reasonable to retain that, as it occurs for other proteins, such as HMGA1 (Martinez Hoyos *et al.* 2004), the Mia/Cd-rap protein function may depend on the cellular context. Interestingly, a recent study proves that HMG1, another member of the HMG family, is an important factor in MIA regulation and melanoma progression. In fact, a sequence-specific DNA motif in the highly conserved region of the Mia/Cd-rap promoter is recognized by HMG1 (Golob *et al.* 2000). Besides, recent data showed that HMG1 is upregulated in malignant melanoma cell lines compared with normal human embryonal melanocytes (NHEM) normal skin cell line and that it plays a pivotal role in Mia/Cd-rap transcriptional activation (Poser *et al.* 2003). Consistently, the promoter sequence of *Mia/Cd-rap* contains many potential regulatory domains including an AT-rich domain, which are known as DNA-binding sites for the HMGA proteins (Bosserhoff *et al.* 1997).

In conclusion, in this study we have identified *Mia/Cd-rap* as a gene directly downregulated by the HMGA proteins in HMGA-induced pituitary adenomas. Moreover, we showed that *Mia/Cd-rap* expression is inversely correlated with the proliferative potential of pituitary adenoma cells, thereby suggesting a relevant role of its downregulation in the generation of pituitary adenomas.

Acknowledgements

This work was supported by grants from the Associazione Italiana Ricerca sul Cancro (AIRC) to Alfredo Fusco and Regione Campania to Monica Fedele. We thank the Associazione Partenopea per le Ricerche Oncologiche (APRO) for its support. The authors declare that there is no conflict of interest that would prejudice the impartiality of this scientific work.

References

Ashar HR, Schoenberg Fejzo M, Tkachenko A, Zhou X, Fletcher JA, Weremowicz S, Morton CC & Chada K 1995 Disruption of the architectural factor HMCI-C: DNA-binding AT hook motifs fused in lipomas to distinct transcriptional regulatory domains. *Cell* **82** 57–65.

Baldassarre G, Fedele M, Battista S, Vecchione A, Klein-Szanto AJ, Santoro M, Waldmann TA, Azimi N, Croce CM & Fusco A 2001 Onset of natural killer cell lymphomas in transgenic mice carrying a truncated *HMGI-C* gene by the chronic stimulation of the IL-2 and IL-15 pathway. *PNAS* **98** 7970–7975.

Battista S, Martelli ML, Fedele M, Chiappetta G, Trapasso F, De Vita G, Battaglia C, Santoro M, Viglietto G, Fagin JA *et al.* 1995 A mutated *p53* gene alters thyroid cell differentiation. *Oncogene* **11** 2029–2037.

Berlingieri MT, Pierantoni GM, Giancotti V, Santoro M & Fusco A 2002 Thyroid cell transformation requires the expression of the HMGA1 proteins. *Oncogene* **21** 2971–2980.

Blesch A, Bosserhoff AK, Apfel R, Behl C, Hessdoerfer B, Schmitt A, Jachimczak P, Lottspeich F, Buettner R & Bogdahn U 1994 Cloning of a novel malignant melanoma-derived growth-regulatory protein, MIA. *Cancer Research* **54** 5695–5701.

Bosserhoff AK, Kondo S, Moser M, Dietz UH, Copeland NG, Gilbert DJ, Jenkins NA, Buettner R & Sandell LJ 1997 Mouse *CD-RAP/MIA* gene: structure, chromosomal localization, and expression in cartilage and chondrosarcoma. *Developmental Dynamics* **208** 516–525.

Chansky H, Robbins JR, Cha S, Raskind WH, Conrad EU & Sandell LJ 1998 Expression of cartilage extracellular matrix and potential regulatory genes in a new human chondrosarcoma cell line. *Journal of Orthopaedic Research* **5** 521–530.

Dietz UH & Sandell LJ 1996 Cloning of a retinoic acid-sensitive mRNA expressed in cartilage and during chondrogenesis. *Journal of Biolgical Chemistry* **271** 3311–3316.

Eisen MB, Spellman PT, Brown PO & Botstein D 1998 Cluster analysis and display of genome-wide expression patterns. *PNAS* **95** 14863–14868.

Fedele M, Berlingieri MT, Scala S, Chiariotti L, Viglietto G, Rippel V, Bullerdiek J, Santoro M & Fusco A 1998 Truncated and chimeric *HMGI-C* genes induce neoplastic transformation of NIH3T3 murine fibroblasts. *Oncogene* **17** 413–418.

Fedele M, Battista S, Kenyon L, Baldassarre G, Fidanza V, Klein-Szanto AJ, Parlow AF, Visone R, Pierantoni GM, Outwater E *et al.* 2002 Overexpression of the *HMGA2* gene in transgenic mice leads to the onset of pituitary adenomas. *Oncogene* **21** 3190–3198.

Fedele M, Pentimalli F, Baldassarre G, Battista S, Klein-Szanto AJ, Kenyon L, Visone R, De Martino I, Ciarmiello A, Arra C *et al.* 2005 Transgenic mice overexpressing the wild-type form of the *HMGA1* gene develop mixed growth hormone/prolactin cell pituitary adenomas and natural killer cell lymphomas. *Oncogene* **24** 3427–3435.

Fedele M, Fidanza V, Battista S, Pentimalli F, Klein-Szanto AJ, Visone R, De Martino I, Curcio A, Morisco C, Del Vecchio L *et al.* 2006*a* Haploinsufficiency of the *HMGA1* gene causes cardiac hypertrophy and myelo-lymphoproliferative disorders in mice. *Cancer Research* **66** 2536–2543.

Fedele M, Visone R, De Martino I, Troncone G, Palmieri D, Battista S, Ciarmiello A, Pallante P, Arra C, Melillo RM *et al.* 2006*b* HMGA2 induces pituitary tumorigenesis by enhancing E2F1 activity. *Cancer Cell* **6** 459–471.

Fedele M, Pierantoni GM, Visone R & Fusco A 2006*c* Critical role of the *HMGA2* gene in pituitary adenomas. *Cell Cycle* **5** 2045–2048.

Finelli P, Pierantoni GM, Giardino D, Losa M, Rodeschini O, Fedele M, Valtorta E, Mortini P, Croce CM, Larizza L *et al.* 2002 The high mobility group *A2* gene is amplified and overexpressed in human prolactinomas. *Cancer Research* **62** 2398–2405.

Foti D, Chiefari E, Fedele M, Iuliano R, Brunetti L, Paonessa F, Manfioletti G, Barbetti F, Brunetti A, Croce CM *et al.* 2005 Lack of the architectural factor HMGA1 causes insulin resistance and diabetes in humans and mice. *Nature Medicine* **7** 765–773.

Golob M, Buettner R & Bosserhoff AK 2000 Characterization of a transcription factor binding site, specifically activating MIA transcription in melanoma. *Journal of Investigative Dermatology* **115** 42–47.

Johnson KR, Lehn DA & Reeves R 1989 Alternative processing of mRNA's coding for human HMG I and HMG Y proteins. *Molecular Cell Biology* **9** 2114–2123.

Manfioletti G, Giancotti V, Bandiera A, Buratti E, Sautiewre P, Cary P, Crane-Robinson C, Coles B & Goodwin GH 1991 cDNA cloning of the HMGI-c phosphoprotein, a nuclear protein associated with neoplastic and undifferentiated phenotypes. *Nucleic Acids Research* **19** 6793–6797.

Martinez Hoyos J, Fedele M, Battista S, Pentimalli F, Kruhoffer M, Arra C, Orntoft TF, Croce CM & Fusco A 2004 Identification of the genes up- and down-regulated by the high mobility group A1 (HMGA1) proteins: tissue specificity of the *HMGA1*-dependent gene regulation. *Cancer Research* **64** 5728–5735.

Melillo RM, Pierantoni GM, Scala S, Battista S, Fedele M, Stella A, De Biasio MC, Chiappetta G, Fidanza V, Condorelli G *et al.* 2001 Critical role of the HMGI(Y) proteins in adipocytic cell growth and differentiation. *Molecular Cell Biology* **21** 2485–2495.

Monaco C, Visconti R, Barone MV, Pierantoni GM, Berlingieri MT, De Lorenzo C, Mineo A, Vecchio G, Fusco A & Santoro M 2001 The RFG oligomerization domain mediates kinase activation and re-localization of the RET/PTC3 oncoprotein to the plasma membrane. *Oncogene* **20** 599–608.

Poser I, Golob M, Buettner R & Bosserhoff AK 2003 Upregulation of HMG1 leads to melanoma inhibitory activity expression in malignant melanoma cells and contributes to their malignancy phenotype. *Molecular Cell Biology* **23** 2991–2998.

Reeves R 2001 Molecular biology of HMGA proteins: hubs of nuclear function. *Gene* **277** 63–81.

Riss D, Jin L, Qian X, Bayliss J, Scheithauer BW, Young WF Jr, Vidal S, Kovacs K, Raz A & Lloyd RV 2003 Differential expression of galectin-3 in pituitary tumors. *Cancer Research* **63** 2251–2255.

Scala S, Portella G, Fedele M, Chiappetta G & Fusco A 2000 Adenovirus-mediated suppression of HMGI(Y) protein synthesis as potential therapy of human malignant neoplasias. *PNAS* **97** 4256–4261.

Schoenmakers EF, Wanschura S, Mols R, Bullerdiek J, Van den Berghe H & Van de Ven WJ 1995 Recurrent rearrangements in the high mobility group protein gene, *HMGI-C*, in benign mesenchymal tumours. *Nature Genetics* **4** 436–444.

Thanos D & Maniatis T 1995 Virus induction of human *IFN ß* gene expression requires the assembly of an enhanceosome. *Cell* **83** 1091–1100.

Wood LJ, Maher JF, Bunton TE & Resar LM 2000 The oncogenic properties of the *HMG-I* gene family. *Cancer Research* **60** 4256–4261.

Zhou X, Benson KF, Ashar HR & Chada K 1995 Mutation responsible for the mouse pygmy phenotype in the developmentally regulated factors HMGI-C. *Nature* **37** 771–7747.

available at www.sciencedirect.com

ScienceDirect

journal homepage: www.ejconline.com

Hmga1 null mice are less susceptible to chemically induced skin carcinogenesis

Rosa Visone[a,b,g], *Rodolfo Iuliano*[a,b], *Dario Palmieri*[a], *Ilter Nurettin Server*[b], *Gennaro Chiappetta*[c], *Ivana De Martino*[a,b], *Monica Fedele*[d], *Stefan Costinean*[b], *Tatiana M. Oberyszyn*[e], *Donna F. Kusewitt*[f], *Carlo M. Croce*[b], *Alfredo Fusco*[a,g,*]

[a]*Dipartimento di Biologia e Patologia Cellulare e Molecolare, Università degli Studi di Napoli "Federico II", via Pansini, 5, 80131, Naples, Italy*
[b]*Division of Human Cancer Genetics, Comprehensive Cancer Center, Ohio State University, 410 West 12th Avenue, Columbus, OH 43210, USA*
[c]*Istituto Nazionale dei Tumori di Napoli, Fondazione Senatore Pascale, Naples, Italy*
[d]*Istituto di Endocrinologia ed Oncologia Sperimentale del CNR, via Pansini, 5, 80131, Naples, Italy*
[e]*Department of Pathology, The Ohio State University, Columbus, OH 43210, USA*
[f]*Department of Veterinary Biosciences, The Ohio State University, Columbus, OH, USA*
[g]*NOGEC (Naples Oncogenomic Center)-CEINGE, Biotecnologie Avanzate-Napoli, & SEMM – European School of Molecular Medicine – Naples Site, via Comunale Margherita, 482, 80145, Naples, Italy*

ARTICLE INFO

Article history:
Received 30 July 2007
Received in revised form
2 November 2007
Accepted 13 November 2007

Keywords:
HMGA1
Skin carcinogenesis
TPA
Papilloma
Carcinoma

ABSTRACT

The HMGA1 proteins have a critical role in the process of carcinogenesis. They are overexpressed in most human malignant neoplasias, and the inhibition of their expression has been shown to prevent cell transformation and results in malignant cell death. To determine whether HMGA1 proteins are also required for *in vivo* carcinogenesis, we compared the tumour susceptibility of mice wild-type or knockout for the *Hmga1*-null allele using a two-stage chemical skin carcinogenesis protocol. *Hmga1*$^{-/-}$ mice exhibited a decreased number and a delayed onset of skin papillomas in comparison with wild-type mice. Moreover, the progression of skin papillomas to carcinomas was observed in only 5% of *Hmga1*$^{-/-}$ compared to 18% of wild-type mice. These results suggest a lower susceptibility of *Hmga1*$^{-/-}$ mice to skin carcinogenesis induced by chemical agents.

1. Introduction

The HMGA family of mammalian high mobility group consists of three related members: HMGA1a, HMGA1b (encoded by the same gene and generated by alternative splicing), and HMGA2 (derived from a different gene).[1] They are small nuclear polypeptides that bind to the minor groove of DNA through highly cationic regions called 'AT-hooks'.[2] HMGA proteins function as architectural transcription factors: they do not independently regulate gene transcription, but modulate gene expression through the formation of stereospecific complexes on the promoter/enhancer regions of genes. These complexes are formed by direct interaction with other transcription factors and through DNA-protein interactions that bend, unwind or distort the structure of DNA.[3] HMGA proteins seem to play their major physiologic role during embryonic development. In fact, HMGA is abundantly expressed during embryogenesis, while their expression is negligible

* *Corresponding author:* Address: Dipartimento di Biologia e Patologia Cellulare e Molecolare, Università degli Studi di Napoli "Federico II", via Pansini, 5, 80131, Naples, Italy. Tel.: +39 81 3737857; fax: +39 81 3737808.
E-mail address: afusco@napoli.com (A. Fusco).
0959-8049/$ - see front matter © 2007 Published by Elsevier Ltd.
doi:10.1016/j.ejca.2007.11.017

in normal adult tissue.[4] The generation of *Hmga1*-ko mice, recently reported by our group,[5] has revealed the critical function of this gene in development. Cardiac hypertrophy and type 2 diabetes were observed in *Hmga1*-ko mice,[5,6] even in mice heterozygous for the gene, suggesting that a quantitatively appropriate HMGA1 expression is required for normal development. Interestingly, the severe insulin resistance of *Hmga1*-null mice resembles that shown by three diabetic patients with impaired HMGA1 function.[6]

Alterations in the structure and/or the expression of the HMGA proteins play an important role in benign and malignant tumours. In fact, *HMGA* gene rearrangements, due to chromosomal translocation, are frequently detected in human benign tumours of mesenchymal origin.[7,8] Moreover, HMGA1 overexpression was first documented in transformed thyroid cells,[9] then in experimental carcinomas,[10] and subsequently in human thyroid,[11] colorectal,[12] pancreatic duct cell,[13] uterine,[14] breast,[15] ovarian cancers,[16] and in glioblastomas.[17] Thus, HMGA1 protein overexpression appears to be a constant feature of malignant human neoplasias. The oncogenic activity of *HMGA1* gene overexpression has been demonstrated *in vitro* and *in vivo*.[18,19] Moreover, blocking HMGA1 synthesis prevents malignant transformation of rat thyroid cells by murine transforming retroviruses,[20] and an adenovirus carrying the *HMGA1* gene in antisense orientation induces apoptotic cell death of anaplastic human thyroid carcinoma cell lines but not of normal thyroid cells.[21] These findings demonstrate that HMGA proteins have a causal role in neoplastic transformation. Furthermore, the development of haematological malignancies, including B cell lymphoma and myeloid granuloerythroblastic leukaemia in *Hmga1*-knockout mice also revealed an unsuspected tumour suppressor role for this gene.[5]

To verify whether *Hmga1* gene plays a pivotal role in *in vivo* transformation, we evaluated the susceptibility of *Hmga1*-ko mice to chemically induced skin neoplasias. For this purpose, we used *Hmga1*-ko mice in a two-stage skin carcinogenesis protocol based on initiation with 7,12-dimethylbenz[*a*]anthracene (DMBA) followed by promotion with 12-O-tetradecanoylphorbol-13-acetate (TPA). Overexpression of HMGA1 in murine skin carcinomas[22] and regulation of HMGA1-specific transcription start sites by TPA[23] led us to choose this model of carcinogenesis. Moreover, this animal model of carcinogenesis allowed us to determine whether the *Hmga1* gene had a role in the early or late steps of tumour development.

In the present study we report that mice homozygous for the *Hmga1*-null allele develop fewer papillomas compared to wild-type mice, and fewer of these lesions progress to carcinomas. Moreover, we document reduced expression of c-Fos protein in the $Hmga1^{-/-}$ mice, suggesting an explanation of the decreased sensitivity of these mice to chemically induced skin carcinogenesis.

2. Materials and methods

2.1. Experimental skin carcinogenesis

Mice carrying a disrupted *Hmga1* gene were generated by homologous recombination in an ES cell line, as described;[5] the disrupted *Hmga1* gene was subsequently transferred into an inbred C57Bl/6J genetic background. Mice 6–7 weeks old were used. Each mouse was identified with an ear tag and genotyped by Southern blot analysis. The dorsal skin was shaved and treated with a single application of DMBA (7,12-dimethylbenz[*a*]anthracene; Sigma, St Louis, MO) (25 μg in 200 μl acetone), followed by twice weekly application of TPA (12-O-tetradecanoylphorbol-13-acetate; Sigma, St Louis, MO) (200 μl of 10^{-4}M in acetone). TPA treatment was stopped after 26 weeks. The number and size of skin tumours on each mouse were recorded at regular intervals. Mice were sacrificed after 32 weeks, and the neoplastic lesions were excised, and frozen or fixed for histolologic, immunohistochemical and molecular analysis. All the mice had been housed in the Animal facility of the Comprehensive Cancer Center at the Ohio State University, and their care was in accordance with institution guidelines.

2.2. Histological and immunohistochemical procedures

For light microscopy, tissues were fixed by immersion for 24 h in Bouin's solution and embedded in paraffin using standard procedures. Sections (5 μm) were stained with haematoxylin and eosin or haematoxylin and periodic acid–Schiff (PAS) reagent. Frozen sections (4–8 μm) of normal and pathological tissues were cut in a cryostat and allowed to dry for 1 h at room temperature before fixation in acetone for 10 min. The slides were air dried for 2 h at room temperature and then placed in a buffer bath (phosphate buffered saline, PBS) for 5 min before immunohistochemistry.

For immunohistochemical studies of paraffin-embedded samples, 3–4 μm paraffin sections were deparaffinised, placed in a solution of absolute methanol and 0.3% hydrogen peroxide for 30 min and washed in PBS. The slides were incubated overnight at 4 °C in a humidified chamber with antibodies diluted 1:100 in PBS. The slides were subsequently incubated with biotinylated goat anti-rabbit IgG for 20 min (Vectostain ABC kits, Vector Laboratories) and then with premixed reagent ABC (Vector) for 20 min. The immunostaining was performed by incubating the slides in diaminobenzidine (DAB-DAKO) solution containing 0.06 mM DAB and 2 mM hydrogen peroxide in 0.05% PBS (pH 7.6) for 5 min. After chromogen development, the slides were washed, dehydrated with alcohol and xylene, and mounted with coverslips using a permanent-mounting medium (Permount). Micrographs were taken on Kodak Ektachrome film with a photo Zeiss system. The antibodies used in this study were raised against the synthetic peptide SSSKQQPLASKQ specific for the HMGA1 proteins.[11] For HMGA2 immunohistochemistry, antibodies raised against the recombinant HMGA2 protein were used.[24] The specificity of the reaction was validated by the absence of staining when carcinoma samples were stained with antibodies pre-incubated with the peptide against which the antibodies were raised (data not shown). Similarly, no positivity was observed when tumour samples were stained with a pre-immune serum (data not shown).

2.3. Protein extraction and Western blot analysis

Frozen sections 10–15 μm thick from papillomas and carcinomas were resuspended in NIH lysis buffer [1% Nonidet P-40;

1 mM EDTA; 50 mM Tris-HCl (pH 8.0); 150 mM NaCl; 2 mM phenylmethylsulfonyl fluoride (PMSF); 50 mM NaF; 10 mM Na_3V_4; 20 mM NaPP; 1.5 mM aprotinin]. Tissue lysates were clarified by centrifugation at 12,000 rpm for 20 min at 4 °C. The supernatant was then used for immunoblotting. Western blotting was performed by standard procedures using the following antibodies: anti-c-Fos (Santa Cruz, sc-52-G), anti-vinculin (Santa Cruz, sc-7649), monoclonal anti-Rab11 (PharMingen/DB Biosciences) and mouse TrueBlot secondary antibody (eBiosceince, San Diego, CA). Briefly, the protein extracts were separated by 4–20% SDS-polyacrylamide gel electrophoresis (SDS-PAGE) and transferred to nitrocellulose membranes (Biorad). Membranes were blocked with 5% non-fat milk in TTBS and incubated with antibodies diluted in the same solution. Bound antibodies were detected by the appropriate horseradish peroxidase-conjugated secondary antibodies followed by enhanced chemiluminescence (Amersham).

2.4. Statistical analysis

Data are expressed as mean ± SEM. Differences were analysed by Student's *t* test. Kaplan–Meyer survival curves were used to analyse the percentage of tumour-free mice in dependence of the weeks of treatment. Differences were analysed by Log-rank test. *P* values $\leqslant 0.05$ were considered significant for both statistical assays.

3. Results

3.1. The onset of papillomas is delayed in Hmga1-null mice

To address the role of HMGA1 in cancer development, we applied a two-stage chemical skin carcinogenesis protocol to *Hmga1*-null mice. Sixteen $Hmga1^{+/+}$, 22 $Hmga1^{+/-}$ and 19 $Hmga1^{-/-}$ mice were given a single initiating treatment with DMBA and tumour promotion was stimulated by TPA application twice weekly. After 8 weeks, the number of $Hmga1^{-/-}$ mice developing skin papillomas was 26%, which was significantly lower then the number of wild-type mice (68%) ($P < 0.01$) (Fig. 1a). The $Hmga1^{+/-}$ mice showed an intermediate phenotype, with a tumour incidence of 37%. A significant difference in the number of papillomas *per* mouse in $Hmga1^{-/-}$ and $Hmga1^{+/+}$ mice at specific time points was also observed (Fig. 1b). These differences were statistically significant at the 12th and 16th week, when the average number of papillomas *per* mouse was reduced by approximately 60% in $Hmga1^{-/-}$ mice compared to $Hmga1^{+/+}$ mice [average ± SE: 1.2 ± 0.3 and 2.8 ± 0.4 ($P < 0.05$) after 12 weeks from the beginning of the treatment; 2.1 ± 0.3 and 4.1 ± 0.4 ($P < 0.001$) after 16 weeks]. The $Hmga1^{+/-}$ mice again showed an intermediate phenotype [average ± SE: 2.1 ± 0.3 at the 12th week; 2.4 ± 0.5 at the 16th week].

3.2. HMGA1 deficiency resulted in decreased malignant transformation

In the two-stage mouse skin carcinogenesis, papilloma regression is a common event; however, a small percentage of benign lesions progress to form squamous cell carcinomas (SCC). At 32 weeks after DMBA treatment, the incidence of mice bearing SCC was 18% ± 5 for wild-type mice and 5% ± 3 for $Hmga1^{-/-}$ mice with a significant *P* value of 0.0419; thus, wild-type mice developed many more carcinomas than $Hmga1^{-/-}$ mice (Fig. 2). Therefore, these data suggest that HMGA1 proteins also have a role in the malignant progression of skin tumours.

At the histological analysis, papillomas appeared as discrete exophytic masses consisting of a central connective tissue core forming papillae covered by thickened epithelium. This epithelium showed orderly differentiation and was covered by a keratinised layer of variable thickness (Fig. 3a and b). Some mice also developed, with a reduced incidence, benign epidermal tumours resembling human keratoacanthomas. These tumours consisted of large cup-shaped, keratin-filled central regions surrounded by a rim of very well differentiated squamous epithelium, which formed a distinct lip (data not shown). Conversely, SCC were composed of cords and islands of well-differentiated keratinising neoplastic epithelium that invaded the dermis and subcutis and penetrated the panniculus carnosus (Fig. 3c and d). No microscopic or macroscopic differences in appearance were observed between tumours of the same type in the different animal groups.

3.3. Expression of Hmga1 and Hmga2 in the skin papillomas and carcinomas induced in Hmga1-null mice

The expression of both HMGA1 and HMGA2 proteins is induced during cell transformation *in vitro* and *in vivo*.[24] As shown in Fig. 4, we analysed the expression of the Hmga proteins in papilloma and carcinoma samples originating from wild-type and *Hmga1*-null mice. As expected, immunohistochemical analysis of papilloma and carcinoma samples did not show any expression of the Hmga1 protein in neoplasias of the *Hmga1*-null mice (Fig. 4b and d, respectively), while its induction was observed in all of the papillomas and carcinomas from the wild-type mice (Fig. 4a and c, respectively). Hmga2 protein expression was also detected in the carcinoma samples from both $Hmga1^{+/+}$ and $Hmga1^{-/-}$ mice (Fig. 4g and h, respectively), whereas it was absent in the papillomas from the same groups (Fig. 4c and d). These findings suggest that Hmga1 induction occurs earlier than Hmga2 induction during the process of skin tumour development.

3.4. The expression of Rab11a and c-Fos is decreased in normal skin and papillomas of Hmga1-null mice

Previous studies have demonstrated that HMGA1 enhances *c-fos* transcription in eukaryotic cells.[25] Moreover, *in vivo* carcinogenesis studies showed that c-Fos plays a crucial role in the transition from benign to malignant skin tumours by regulating expression of Rab11a.[26,27] Therefore, we analysed the expression of c-Fos and Rab11a proteins first in the untreated back skin of $Hmga1^{-/-}$, $Hmga1^{+/-}$ and $Hmga1^{+/+}$ mice (Fig. 5a and data not shown). The levels of c-Fos and Rab11a proteins were significantly lower in *Hmga1*-null skin compared to that of wild-type mice (Fig. 5b), and intermediate between $Hmga1^{-/-}$ and $Hmga1^{+/+}$ in heterozygous mice (data not shown). Then, we analysed c-Fos and Rab11a expression in SCC and

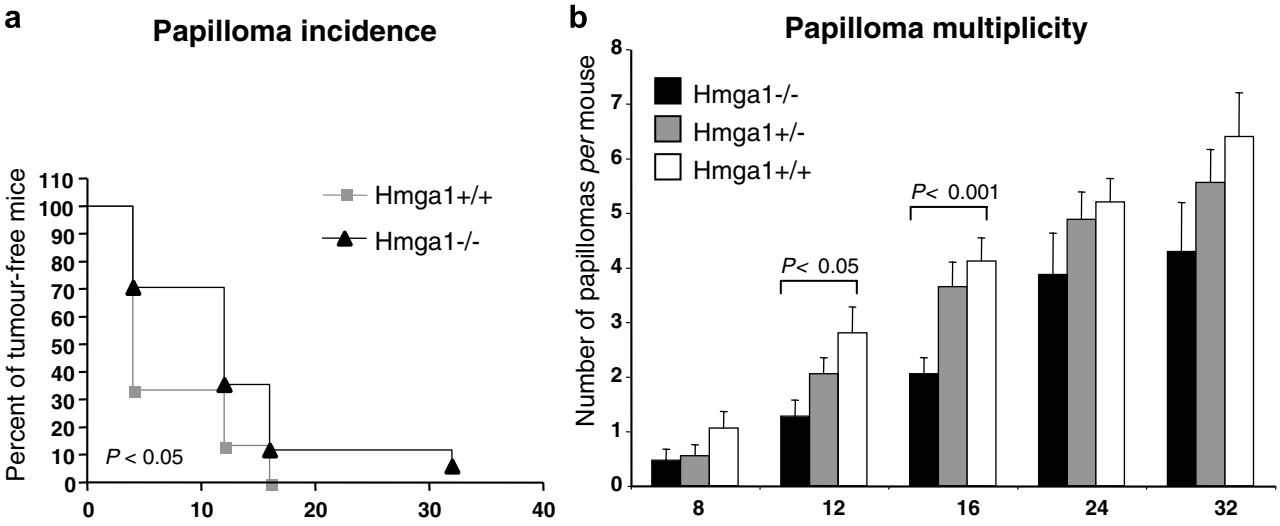

Fig. 1 – *Hmga1*$^{-/-}$ mice develop fewer skin tumours than wild-type mice. Mice of the indicated genotypes were subjected to a two-stage DMBA/TPA skin carcinogenesis protocol. (a) Papilloma incidence, i.e. percentage of mice with papillomas, was analysed using Kaplan–Meyer curves showing the tumour-free survival. A significant difference was observed between the two groups indicated ($P < 0.05$). (b) Papilloma multiplicity, i.e. the number of papillomas *per* mouse, calculated each week until the end of the treatment, is shown for each mouse group as indicated. The differences between *Hmga1*$^{-/-}$ mice and their respective wild-type controls were significant at 12 weeks ($P < 0.05$) and 16 weeks ($P < 0.001$) from the beginning of the carcinogenesis protocol.

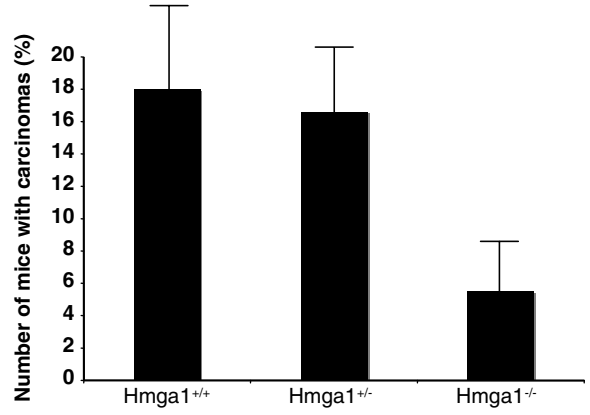

Fig. 2 – Malignant transformation of papillomas to carcinomas is less frequent in *Hmga1*-null mice than in heterozygous and wild-type mice. Percentage of carcinoma incidence *per* mouse was calculated for each mouse group at the end of the 32nd week from the beginning of the carcinogenesis protocol. The difference between *Hmga1*$^{-/-}$ mice and their respective wild-type controls were significant ($P < 0.05$).

papillomas from *Hmga1*-null, -heterozygous and wild-type mice. As shown in Fig. 5b, Western blot analysis revealed lower levels of c-Fos in both *Hmga1*$^{-/-}$ SCC and papillomas than in the corresponding tumours from wild-type mice. Intermediate levels were observed in the Hmga1$^{+/-}$ samples. Similarly, Rab11a expression levels were decreased in Hmga1$^{+/-}$ SCC and papillomas in comparison with wild-type samples, and further decreased in Hmga1$^{-/-}$ papilloma but unexpectedly increased in Hmga1$^{-/-}$ SCC compared to wild-type.

This finding suggests that the lack of Hmga1 expression in the keratinocytes of *Hmga1*$^{-/-}$ mice reduced malignant transition of papillomas to SCC by interfering with the c-Fos/Rab11a pathway. It is likely that the increase of Rab11a expression in SCC, in the absence of Hmga1 protein, must be considered an epiphenomenon associated to the neoplastic phenotype.

4. Discussion

It is widely accepted that the HMGA proteins play a crucial role in the development of malignant tumours. HMGA proteins have been found to be overexpressed in almost all of the malignant neoplasias so far analysed, and there is a correlation between HMGA expression levels and the grade of malignancy.[13,28] Moreover, a causal role in cell transformation has been demonstrated for these proteins. In fact, HMGA overexpression can transform cells *in vitro* and *in vivo*,[18,19] and blocking HMGA2 expression by antisense methodology prevents malignant transformation of rat thyroid cells by *v-mos* and *v-ras-Ki* oncogenes.[24] However, when mice carrying a disrupted *Hmga2* gene (pygmy mice) were either treated with radioactive iodine or crossed with transgenic mice carrying the E7 papilloma virus oncogene under the transcriptional control of thyroglobulin gene promoter, they developed thyroid carcinomas with the same frequency as wild-type mice, and the tumours they developed were indistinguishable from tumours in wild type mice. Therefore, these results indicated that *HMGA2* gene expression is not required for *in vivo* thyroid cell malignant transformation,[29] suggesting that HMGA1 proteins, rather than HMGA2, may be required for cell transformation. This hypothesis is also supported by the evidence

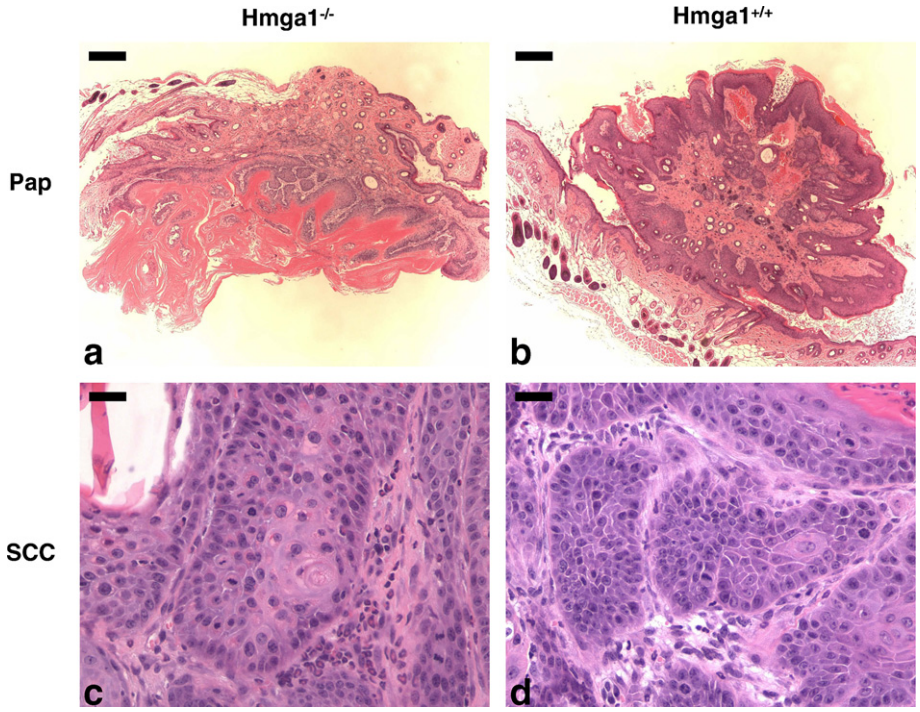

Fig. 3 – Histological examination of papillomas and carcinomas in *Hmga1*$^{-/-}$ and *Hmga1*$^{+/+}$mice. (a,b) Papillomas (bar scale = 100 μm). (c,d) Squamous cell carcinomas (bar scale = 50 μm). Pap = papillomas; SCC = squamous cell carcinomas.

that blocking HMGA1 protein synthesis using an adenovirus carrying HMGA1 antisense sequences prevents transformed thyroid cell growth;[21] in addition, rat thyroid cell transformation by the Kirsten murine sarcoma virus does not take place in the absence of the HMGA1 protein induction.[20] Alternatively, the expression of only one of the *HMGA* genes may be required to transform thyroid cells to the malignant phenotype. The absence of *HMGA1* gene induction in HMGA2 antisense virally infected thyroid cells[24] is consistent with this hypothesis.

The recent generation of *Hmga1*-knockout mice[5] offers an excellent opportunity to define the role of individual *HMGA* genes in the process of carcinogenesis *in vivo*. In the present study, mice homozygous and heterozygous for the *Hmga1*-null allele and wild-type mice were treated with DMBA and TPA in a classical two-stage skin carcinogenesis protocol. After 8 weeks of treatment *Hmga1*$^{-/-}$ mice had significantly fewer skin tumours than wild-type mice. Moreover, at the 12th and 16th weeks of chemical treatment, the total number of papillomas *per* mouse was significantly higher in wild-type than *Hmga1*$^{-/-}$ mice. Taken together, these findings indicate that HMGA1 plays a critical role in the development of chemically induced skin tumours. Furthermore, malignant progression of papillomas to carcinomas was observed in only 5% of *Hmga1*$^{-/-}$ mice compared to 18% of wild-type mice, suggesting a further role for HMGA1 in tumour malignant progression. This result is consistent with the literature data that show a frequent association of HMGA1 expression and the presence of a highly malignant phenotype.[11–17]

Although we show evidence that HMGA1 plays a critical role in development of the malignant phenotype, our results also demonstrate that malignant tumours can still arise in the absence of the HMGA1 proteins. Thus, it is likely that HMGA2, which we showed to be induced in skin carcinomas, may substitute for HMGA1. Of course, we cannot exclude that other genes, as yet unidentified, may duplicate some functions of the HMGA1 proteins.

It has been demonstrated that benign skin tumours do not progress to malignant skin tumours in mice lacking c-Fos protein and that this failure is due to Rab11a inactivation.[26] Moreover, it has been shown that HMGA1 enhances SRF-dependent activation of the *c-fos* promoter and that TPA mediates the activation of Rab11a in mouse skin in a c-Fos-dependent manner.[25,26] We analysed Rab11a and c-Fos expression in both *Hmga1*$^{-/-}$ and *Hmga1*$^{+/+}$ mice. Notably, decreased expression of Rab11a and c-Fos was found in keratinocytes and papillomas of the *Hmga1*$^{-/-}$ mice, in comparison with the wild-type mice, suggesting that the reduced expression of c-Fos in *Hmga1*-null mice might contribute to the decreased susceptibility to the development of malignant skin tumours.

The correlation among HMGA1, c-Fos and Rab11a expression suggests a mechanism by which HMGA1 could be involved in malignant progression. Nevertheless, other biological roles of the HMGA proteins, such as their reported capacity to inhibit DNA repair,[30,31] may be taken into consideration. In fact, the results shown here could also be explained by considering that HMGA1 overexpression would increase the incidence of mutations that facilitate the process of carcinogenesis.

In conclusion, the data reported here indicate that the expression of the *HMGA1* gene plays a critical role in the process of chemically induced skin cancer development.

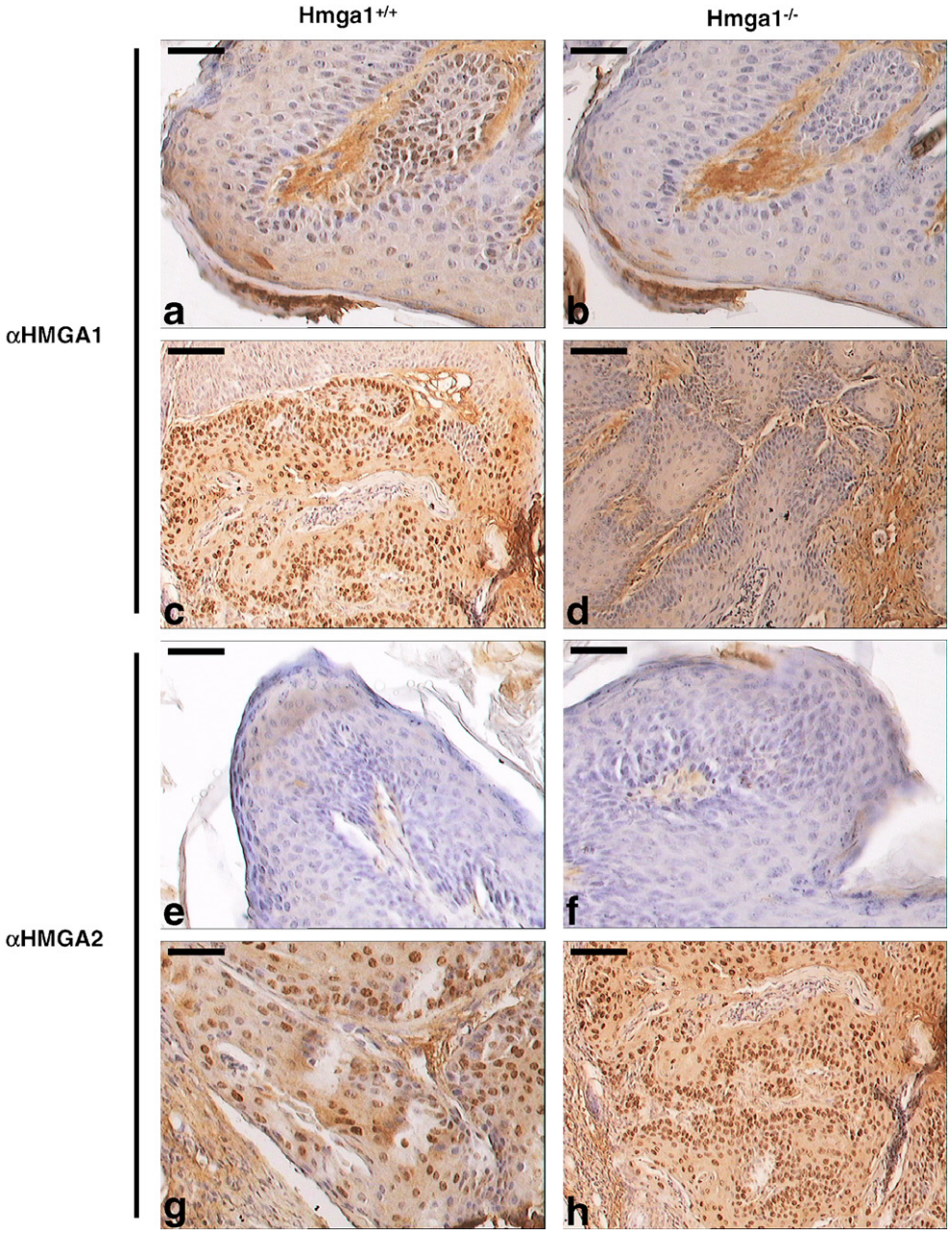

Fig. 4 – Immunohistochemical detection of Hmga1 and Hmga2 proteins in mouse skin tumours. Paraffin sections from benign and malignant mouse skin tumours arising in mice subjected to the carcinogenesis protocol were analysed by immunohistochemistry using antibodies raised against specific Hmga1 and Hmga2 peptides. (a) Immunostaining for HMGA1 of a representative skin papilloma developed by a *Hmga1*$^{+/+}$ mouse (bar scale = 50 μm). A positive nuclear staining was observed. (b) Immunostaining for HMGA1 of a representative skin papilloma developed by a *Hmga1*$^{-/-}$ mouse (bar scale = 50 μm). No immunoreactivity was observed. (c) Immunostaining for HMGA1 of a representative squamous cell carcinoma developed by a *Hmga1*$^{+/+}$ mouse (bar scale = 100 μm). A positive nuclear staining was observed. (d) Immunostaining for HMGA1 of a representative squamous cell carcinoma developed by a *Hmga1*$^{-/-}$ mouse (bar scale = 100 μm). No staining was observed. (e) Immunostaining for HMGA2 of a representative skin papilloma developed by a *Hmga1*$^{+/+}$ mouse (bar scale = 50 μm). No immunoreactivity was observed. (f) Immunostaining for HMGA2 of a representative skin papilloma developed by a *Hmga1*$^{-/-}$ mouse (bar scale = 50 μm). No immunoreactivity was observed. (g) Immunostaining for HMGA2 of a representative squamous cell carcinoma deriving from a *Hmga1*$^{+/+}$ mouse. A positive nuclear staining was observed (bar scale = 50 μm). (h) Immunostaining for HMGA2 of a representative squamous cell carcinoma deriving from a *Hmga1*$^{-/-}$ mouse. A positive nuclear staining was observed (bar scale = 100 μm).

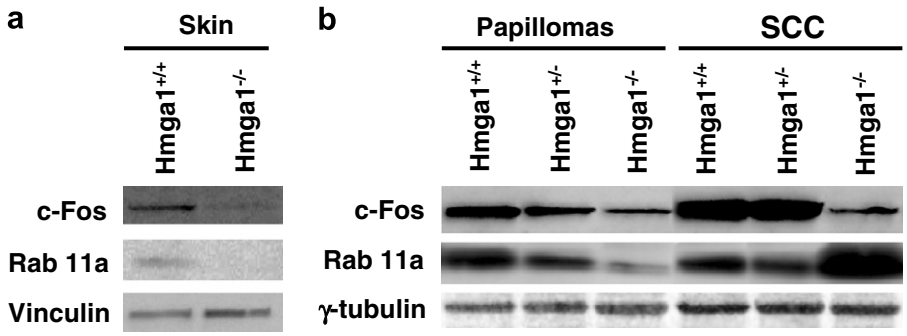

Fig. 5 – c-Fos and Rab11a expression is reduced in tumours and skin from *Hmga1*$^{-/-}$ mice. Western blot analysis showing the expression of c-Fos and Rab11a proteins in untreated skin (a) and papillomas (b) from *Hmga1*$^{-/-}$, *Hmga1*$^{+/-}$ and *Hmga1*$^{+/+}$ mice. Anti vinculin and γ-tubulin antibodies were used as control for equal protein loading, respectively.

Conflict of interest statement

None declared.

Acknowledgements

This work was supported by grants from the Associazione Italiana Ricerca sul Cancro (AIRC) to A.F. and by National Cancer Institute to C.M.C. We thank the Associazione Partenopea per le Ricerche Oncologiche (APRO) for its support.

REFERENCES

1. Fedele M, Battista S, Manfioletti G, Croce CM, Giancotti V, Fusco A. Role of the high mobility group A proteins in human lipomas. *Carcinogenesis* 2001;**22**:1583–91.
2. Reeves R. Molecular biology of HMGA proteins: hubs of nuclear function. *Gene* 2001;**277**:63–81.
3. Thanos D, Maniatis T. Virus induction of human IFN beta gene expression requires the assembly of an enhanceosome. *Cell* 1995;**83**:1091–100.
4. Chiappetta G, Avantaggiato V, Visconti R, et al. High level expression of the HMGI (Y) gene during embryonic development. *Oncogene* 1996;**13**:2439–46.
5. Fedele M, Fidanza V, Battista S, et al. Haploinsufficiency of the Hmga1 gene causes cardiac hypertrophy and myelo-lymphoproliferative disorders in mice. *Cancer Res* 2006;**66**:2536–43.
6. Foti D, Chiefari E, Fedele M, et al. Lack of the architectural factor HMGA1 causes insulin resistance and diabetes in humans and mice. *Nat Med* 2005;**11**:765–73.
7. Schoenmakers EF, Wanschura S, Mols R, Bullerdiek J, Van den Berghe H, Van de Ven WJ. Recurrent rearrangements in the high mobility group protein gene, HMGI- C, in benign mesenchymal tumors. *Nat Genet* 1995;**10**:436–44.
8. Ashar HR, Fejzo MS, Tkachenko A, et al. Disruption of the architectural factor HMGI-C: DNA-binding AT hook motifs fused in lipomas to distinct transcriptional regulatory domains. *Cell* 1995;**82**:57–65.
9. Giancotti V, Pani B, D'Andrea P, et al. Elevated levels of a specific class of nuclear phosphoproteins in cells transformed with v-ras and v-mos oncogenes and by cotransfection with c- myc and polyoma middle T genes. *Embo J* 1987;**6**:1981–7.
10. Giancotti V, Buratti E, Perissin L, et al. Analysis of the HMGI nuclear proteins in mouse neoplastic cells induced by different procedures. *Exp Cell Res* 1989;**184**:538–45.
11. Chiappetta G, Bandiera A, Berlingieri MT, et al. The expression of the high mobility group HMGI(Y) proteins correlates with the malignant phenotype of human thyroid neoplasms. *Oncogene* 1995;**10**:1307–14.
12. Fedele M, Bandiera A, Chiappetta G, et al. Human colorectal carcinomas express high levels of high mobility group HMGI(Y) proteins. *Cancer Res* 1996;**56**:1896–901.
13. Abe N, Watanabe T, Masaki T, et al. Pancreatic duct cell carcinomas express high levels of high mobility group I(Y) proteins. *Cancer Res* 2000;**60**:3117–22.
14. Bandiera A, Bonifacio D, Manfioletti G, et al. Expression of HMGI(Y) proteins in squamous intraepithelial and invasive lesions of the uterine cervix. *Cancer Res* 1998;**58**:426–31.
15. Liu WM, Guerra-Vladusic FK, Kurakata S, Lupu R, Kohwi-Shigematsu T. HMG-I(Y) recognizes base-unpairing regions of matrix attachment sequences and its increased expression is directly linked to metastatic breast cancer phenotype. *Cancer Res* 1999;**59**:5695–703.
16. Masciullo V, Baldassarre G, Pentimalli F, et al. HMGA1 protein over-expression is a frequent feature of epithelial ovarian carcinomas. *Carcinogenesis* 2003;**24**:1191–8.
17. Donato G, Martinez Hoyos J, Amorosi A, et al. High mobility group A1 expression correlates with the histological grade of human glial tumors. *Oncol Rep* 2004;**11**:1209–13.
18. Wood LJ, Maher JF, Bunton TE, Resar LM. The oncogenic properties of the HMG-I gene family. *Cancer Res* 2000;**60**:4256–61.
19. Fedele M, Pentimalli F, Baldassarre G, et al. Transgenic mice overexpressing the wild-type form of the HMGA1 gene develop mixed growth hormone/prolactin cell pituitary adenomas and natural killer cell lymphomas. *Oncogene* 2005;**24**:3427–35.
20. Berlingieri MT, Pierantoni GM, Giancotti V, Santoro M, Fusco A. Thyroid cell transformation requires the expression of the HMGA1 proteins. *Oncogene* 2002;**21**:2971–80.
21. Scala S, Portella G, Fedele M, Chiappetta G, Fusco A. Adenovirus-mediated suppression of HMGI(Y) protein synthesis as potential therapy of human malignant neoplasias. *Proc Natl Acad Sci U S A* 2000;**97**:4256–61.
22. Rajeswari MR, Singh D, Jain A, Ray R. Elevated levels of high-mobility-group chromosomal proteins, HMGA1, in murine skin carcinoma. *Cancer Lett* 2001;**1**:93–9.
23. Ogram SA, Reeves R. Differential regulation of a multiprotein gene. Selective 12-O-tetradecanoylphorbol-13 acetate

induction of a single transcription start site in the HMG-I/Y gene. *J Biol Chem* 1995;**23**:14235–42.
24. Berlingieri MT, Manfioletti G, Santoro M, et al. Inhibition of HMGI-C protein synthesis suppresses retrovirally induced neoplastic transformation of rat thyroid cells. *Mol Cell Biol* 1995;**15**:1545–53.
25. Chin MT, Pellacani A, Wang H, et al. Enhancement of serum-response factor-dependent transcription and DNA binding by the architectural transcription factor HMG-I(Y). *J Biol Chem* 1998;**273**:9755–60.
26. Gebhardt C, Breitenbach U, Richter KH, et al. c-Fos-dependent induction of the small ras-related GTPase Rab11a in skin carcinogenesis. *Am J Pathol* 2005;**167**:243–53.
27. Saez E, Rutberg SE, Mueller E, et al. c-fos is required for malignant progression of skin tumors. *Cell* 1995;**82**(5):721–32.
28. Chiappetta G, Manfioletti G, Pentimalli F, et al. High mobility group HMGI(Y) protein expression in human colorectal hyperplastic and neoplastic diseases. *Int J Cancer* 2001;**91**:147–51.
29. Scala S, Portella G, Vitagliano D, et al. HMGI-C gene expression is not required for in vivo thyroid cell transformation. *Carcinogenesis* 2001;**22**:251–6.
30. Adair JE, Kwon Y, Dement GA, Smerdon MJ, Reeves R. Inhibition of nucleotide excision repair by high mobility group protein HMGA1. *J Biol Chem* 2005;**280**: 32184–92.
31. Baldassarre G, Belletti B, Battista S, et al. HMGA1 protein expression sensitizes cells to cisplatin-induced cell death. *Oncogene* 2005;**24**:6809–19.

available at www.sciencedirect.com

ScienceDirect

journal homepage: www.ejconline.com

HMGA1 protein is a novel target of the ATM kinase

Francesca Pentimalli[a,b], *Dario Palmieri*[a], *Roberto Pacelli*[c], *Corrado Garbi*[a], *Rossano Cesari*[b,d], *Eric Martin*[b,e], *Giovanna Maria Pierantoni*[a], *Paolo Chieffi*[f], *Carlo Maria Croce*[g], *Vincenzo Costanzo*[a,h], *Monica Fedele*[a], *Alfredo Fusco*[a,i,*]

[a]*Istituto di Endocrinologia ed Oncologia Sperimentale del CNR c/o Dipartimento di Biologia e Patologia Cellulare e Molecolare, Facoltà di Medicina e Chirurgia di Napoli, Università degli Studi di Napoli 'Federico II', Via S. Pansini 5, 80131 Naples, Italy*
[b]*Kimmel Cancer Center, Thomas Jefferson University, 233 S. 10th Street, Philadelphia, PA 19107, USA*
[c]*Istituto di Biostrutture e Bioimmagini del CNR, Dipartimento di Diagnostica per Immagini e Radioterapia, Università degli Studi di Napoli 'Federico II', Via S. Pansini 5, 80131 Naples, Italy*
[d]*H. San Raffaele-Telethon Institute for Gene Therapy (HSR-TIGET), 20132 Milano, Italy*
[e]*Department of Medical Oncology, Dana Farber Cancer Institute, Department of Medicine and Genetics, Harvard Medical School, Boston, MA 02115, USA*
[f]*Dipartimento di Medicina Sperimentale, II Università di Napoli, 80138 Naples, Italy*
[g]*Division of Human Cancer Genetics, Comprehensive Cancer Center, Ohio State University, 410 West 12th Avenue, Columbus, OH 43210, USA*
[h]*Genome Stability, Clare Hall Laboratories, London Research Institute, Cancer Research UK, South Mimms, Herts, EN6 3LD, UK*
[i]*NOGEC (Naples Oncogenomic Center)-CEINGE, Biotecnologie Avanzate, via Comunale Margherita, 80131 Naples, Italy*

ARTICLE INFO

Article history:
Received 12 May 2008
Received in revised form 14 July 2008
Accepted 17 July 2008
Available online 8 September 2008

Keywords:
HMGA1
ATM
DNA damage

ABSTRACT

The high mobility group HMGA1 protein belongs to a family of architectural factors that play a role in chromosomal organisation and gene transcription regulation. HMGA1 overexpression represents a common feature of human malignant tumours and is causally associated with neoplastic transformation and metastatic progression. Recently, HMGA1 expression has been correlated with the presence of chromosomal rearrangements and suggested to promote genomic instability. Here, we report a novel interaction between HMGA1 protein and the ataxia-telangiectasia mutated (ATM) kinase, the major key player in the cellular response to DNA damage caused by several agents such as ionising radiation (IR). We identified an SQ motif on HMGA1, which is effectively phosphorylated by ATM *in vitro* and *in vivo*. Interestingly, confocal microscopy revealed that HMGA1 colocalises with the activated form of ATM (ATM S1981p). Moreover, HMGA1 ectopic expression decreases cell survival following exposure to IR as assessed by clonogenic survival in MCF-7 cells, further supporting the hypothesis that HMGA1 might act as a downstream target of the ATM pathway in response to DNA damage.

1. Introduction

The high molecular group A (HMGA) proteins are a class of nuclear, non-histone proteins involved in a wide range of cellular processes such as chromatin remodelling, gene transcription, differentiation and neoplastic transformation.[1]

The HMGA family consists of the *HMGA1* gene, which codes by alternative splicing for two major isoforms, the HMGA1a and

* *Corresponding author:* Address: Istituto di Endocrinologia ed Oncologia Sperimentale 'Gaetano Salvatore', Università degli Studi di Napoli 'Federico II', Via Pansini 5, 80131 Napoli, Italy. Tel.: +39 081 7463602/7463749; fax: +39 081 2296674.
E-mail addresses: afusco@napoli.com, alfusco@unina.it (A. Fusco).
0959-8049/$ - see front matter © 2008 Elsevier Ltd. All rights reserved.
doi:10.1016/j.ejca.2008.07.033

HMGA1b proteins, and the *HMGA2* gene. HMGA proteins contain three DNA binding domains, referred to as 'AT-hooks', that allow the binding to the minor groove of AT rich DNA sequences and a highly acidic carboxy-terminal region. HMGA proteins behave as architectural factors of gene transcription,[1] regulating, positively or negatively, the expression of a large number of genes in a way dependent on the cellular context.[2]

HMGA proteins are highly expressed during embryogenesis, whilst they are expressed only at low levels in normal adult tissues.[3] HMGA1 overexpression represents a common feature of human malignant tumours including thyroid,[4] breast,[5] ovary[6] and prostate,[7] and is causally associated with the acquisition of a transformed phenotype. In fact, HMGA1 protein suppression prevents thyroid cell transformation by the Kirsten murine sarcoma virus,[8] and an adenovirus carrying the *HMGA1* gene in the antisense orientation induces death of human thyroid carcinoma cells.[9] Moreover, HMGA1 overexpression induces the neoplastic phenotype in Rat1a cells and human CB33 lymphoid cells[10] and in the human breast epithelial MCF-7 cells.[11] Accordingly, transgenic mice overexpressing the wild-type form of the *Hmga1* gene develop pituitary adenomas and natural killer cell lymphomas.[13] Interestingly, in several human prostate cancer cell lines HMGA1 expression has been positively correlated to the extent of chromosomal rearrangements,[14] and its ectopic expression was able to enhance the presence and heterogeneity of unbalanced chromosomal rearrangements in LNCaP prostate cell line,[14] suggesting a role for HMGA1 proteins in the acquisition of genomic instability, one of the hallmarks of cancer cells. In human breast tumours HMGA1 overexpression has been correlated to the downregulation of *BRCA1*,[5] a gene involved in DNA repair following different types of DNA damage.[15] Moreover, HMGA1 overexpression was found to decrease cell survival following exposure to DNA-damaging agents of human breast cancer-derived MCF-7 cells, by inhibition of nucleotide excision repair (NER), through downregulation of XPA,[16] or by inhibition of double-strand breaks (DSBs) repair, through a mechanism involving *BRCA1* downregulation.[5] Recently, also HMGA2 expression has been shown to promote enhanced sensitivity in response to doxorubicin and other related DNA-damaging agents, likely through modulation of the signalling pathway responsible for the maintenance of genomic integrity.[17]

Genome stability is threatened by DNA-damaging agents that can either be endogenous, deriving from normal cell metabolism, or exogenous such as ionising radiation (IR). IR induces DNA double-strand breaks (DSBs) that can potentially lead to mutations, translocations, abnormal recombination and chromosome breakage or loss. Detection of damaged DNA triggers checkpoint pathways that prevent cell cycle progression and activate the DNA repair system. If the type or amount of damage overwhelm the survival response machinery, apoptosis is triggered.[18]

ATM, the gene mutated in the human disease ataxia-telangiectasia (AT),[19] is crucial for initiating signalling pathways following exposure to IR or other agents that cause DSBs. Like other syndromes that are caused by defects in the DNA-damage response, AT patients show an increased risk for cancer, chromosome fragility and radiosensitivity.[20] Once activated by DNA damage,[21] ATM phosphorylates numerous substrates to induce cell cycle arrest, to reduce chromosomal breakage and to enhance cell survival. ATM belongs to the 'PI3K-like protein kinases' (PIKKs) family of proteins, which all contain a domain with motifs typical of the phosphatidylinositol 3-kinase (PI3K).[18] ATM, similarly to other PIKKs, features a serine/threonine kinase activity. In particular, ATM targets serine or threonine residues followed by glutamine,[22] named the SQ/TQ (or S/TQ) motif, which is characteristic of DNA-damage response proteins.

Since HMGA proteins have been recently shown to play a role in the cellular response to DNA-damaging agents, we hypothesised that HMGA might function as adaptor mediators of the ATM-induced signalling pathway following IR. Our studies demonstrate the interaction between HMGA1b and ATM proteins and identify the HMGA1 protein as a novel target of the ATM kinase. Even though the physiological role of this interaction needs further studies, we provide evidence that HMGA play a role in the cellular response to DNA damage caused by IR.

2. Materials and methods

2.1. Cell cultures

Human embryonic kidney 293T cells were cultured in DMEM supplemented by 10% (v/v) foetal bovine serum (FBS), 2 mM L-glutamine, 100 U/ml penicillin and 0.1 mg/ml streptomycin (GIBCO-BRL). Human lymphoblasts GM2184 and GM1526 were obtained from Coriell Cell Repositories and cultured in RPMI supplemented by 15% (v/v) FBS, 2 mM L-glutamine, 100 U/ml penicillin and 0.1 mg/ml streptomycin (GIBCO-BRL). Wild-type and *Hmga1* –/– AB2.1 ES cells, described elsewhere,[23] were cultured on a layer of mitomycin C-inactivated fibroblasts. Before γ-irradiation fibroblasts were removed by three passages onto 0.1% (w/v) gelatin-treated plates, and the undifferentiated state was maintained by the addition of 10^3 units/ml leukaemia inhibiting factor (Chemicon). Wild-type, *Hmga1* +/– and *Hmga1* –/– mouse embryonic fibroblasts (MEFs) were established from 14.5 dpc embryos following the standard procedures. MEFs were cultured in DMEM supplemented by 10% (v/v) FBS, 2 mM L-glutamine, 100 U/ml penicillin, 0.1 mg/ml streptomycin and 1% (v/v) non-essential aminoacids (GIBCO-BRL).

For γ-irradiation experiments, cells were irradiated by 6 MV X-ray of a linear accelerator with doses ranging from 0 to 10 Gy.

2.2. Plasmid constructs and recombinant proteins

HMGA1b full-length and its deletion mutants were cloned into pCEFL-HA, in frame with the HA epitope, as described elsewhere.[24] Wild-type *HMGA1b* full-length was also cloned into pcDNA3.1/Hygro (Invitrogen) for co-immunoprecipitation experiments. The pFLAG-ATM-wild-type (wt) and kinase-dead (kd) expressing vectors previously described[25] were kindly provided by Dr. M.B. Kastan. The recombinant HMGA1b full-length and truncated (aa 1–79) proteins were generated by cloning the corresponding cDNAs in frame to the polyhistidine tag in pET21c expression vector (Novagen). Serine 88 of HMGA1b was mutated to alanine by PCR using pET-HMGA1b wild-type as template, and the resulting cDNA was cloned into pET21c vector in frame to the polyhistidine tag.

BL21/DE3 cells were transformed with each vector (pET-HMGA1b, pET-HMGA1b (1–79), pET-HMGA1b S88A), grown in Luria Broth (LB) and induced with isopropyl-β-D-thiogalactoside, then harvested and sonicated. Recombinant proteins were purified using the His-Trap purification kit (Amersham Biosciences), then dialysed and analysed by SDS–PAGE.

2.3. Transfections, immunoprecipitation and Western blots

Transient transfections into 293T cells were performed with FuGene6 (Roche) according to the manufacturers' specifications. Mammalian cell extracts were prepared and co-immunoprecipitations were performed as previously described,[23] in the presence or absence of 100 ng/μl ethidium bromide. Anti-FLAG M2 (Sigma) or anti-HA Clone 12CA5 (Roche) monoclonal antibodies were used for co-immunoprecipitation experiments along with protein A/G-sepharose (Amersham Biosciences). Anti-ATM/ATR substrate (phospho-Ser/Thr antibody) (Cell Signalling Technology) was used to evaluate the phosphorylation of HMGA proteins by ATM *in vivo*. Proteins were resolved by 3–8% (v/v) NuPAGE (Invitrogen) or by 15% (v/v) SDS–PAGE and transferred to high or low molecular weight nitrocellulose, respectively. Western blots were performed using the above-mentioned anti-FLAG and anti-HA antibodies, or anti-ATM polyclonal antibody (Novus Biologicals) and anti-HMGA1 polyclonal antibody (raised against the amino-terminal region of the protein). All the antibodies were diluted (1:200) in 5% (w/v) non-fat dry milk (Biorad).

2.4. In vitro kinase assays

For *in vitro* kinase assays, the ATM kinase was obtained by immunoprecipitation with an anti-FLAG antibody from 293T transfected cells or with an anti-ATM antibody (Novus Biologicals) from human lymphoblasts. Beads were washed twice with buffer A, twice with buffer A containing 0.5 M LiCl and twice with kinase buffer as previously described.[19] ATM kinase reactions were carried out at 30 °C for 15 min in 50 μl of kinase buffer containing 10 μCi of [γ-^{32}P]ATP and 10 μg of each substrate (for recombinant proteins) or 50 mM of cold ATP and 200 μM of each substrate (for peptides). 5 mM caffeine (Sigma) was used as a specific kinase inhibitor. Following the kinase reaction, HMGA1 peptides (produced by Neosystem) were spotted onto P81 phosphocellulose squares (Upstate) and washed extensively with 1% orthophosphoric acid. ^{32}P incorporation was measured by a β-counter scintillator (Beckman Coulter). Recombinant proteins, instead, were resolved by 15% SDS–PAGE and phosphorylation was revealed by autoradiography.

2.5. Immunofluorescence microscopy

Wild-type and *Hmga1* –/– MEFs were grown on glass coverslips, then fixed for 20 min in 4% (v/v) paraformaldehyde in PBS following mock or γ-irradiation. Cells were then permeabilised with 0.2% (v/v) Triton X-100 in PBS for 5 min at room temperature and blocked in PBS containing 1% (w/v) BSA for 20 min. Cells were incubated with primary antibodies for 1 h at room temperature in a humidified chamber, then washed with PBS and incubated for an additional hour with the secondary antibody. Primary antibodies used for immunostaining were: goat anti-HMGA1b sc-1564 (Santa Cruz), rabbit anti-HMGA1 (raised against the amino-terminal region of the protein), rabbit anti-ATM S1981p (Rockland) and mouse anti-γH2AX (Cell Signaling). As secondary antibodies we used anti-goat rhodamine-conjugated, anti-rabbit fluorescein-conjugated and anti-mouse rhodamine-conjugated (Jackson ImmunoResearch). All the antibodies were diluted (1:100) in PBS.

2.6. FACS analysis

Cells were plated in 6-well plates at a density of 2.5×10^5/well, incubated for 24 h and then exposed to a range of ionising radiations (0–10 Gy). Before harvesting at different timepoints following IR (0, 12, 24, 48 h), cells were pulsed for an hour with 10 μM BrdU (BrdU Flow kit, BD Pharmingen), then fixed and stained with a FITC-anti-BrdU antibody according to the manufacturers' instructions. 7-Amino-actinomycin D (7-AAD) fluorescent dye was used to label DNA. Cells were sorted on a FACScan flow cytometer (Becton Dickinson), and the results were analysed with FlowJo software, 4.3 version (TreeStar).

2.7. Clonogenic assay

Cell lines were plated in 6-well plates at a density of 300–800 cells/well, incubated for 24 h and then exposed to a range of doses of ionising radiations (0–10 Gy), followed by a two-week incubation. Prior to counting colonies, cells were fixed and stained with crystal violet. Populations of more than 50 cells were scored as surviving colonies. The mean of colony counts normalised for plating efficiency is reported.

3. Results

3.1. ATM and HMGA1 proteins interact in vivo

To determine whether ATM and HMGA1 interact *in vivo*, we transiently transfected 293T cells with expression vectors containing the full-length cDNAs for *ATM* and *HMGA1b* genes fused to the FLAG or HA tag, respectively. Total cell lysates were immunoprecipitated using an anti-HA antibody and analysed by immunoblotting with an anti-ATM antibody. A band corresponding to FLAG-ATM was effectively co-immunoprecipitated only in cells expressing HA-HMGA1b demonstrating that the two proteins are able to interact *in vivo* (Fig. 1a). Moreover, HA-HMGA1b is able to co-immunoprecipitate also the endogenous ATM protein, which is highly expressed in 293T cells[21] (Fig. 1a, middle lane). Since both ATM and HMGA1 are chromatin-associated proteins, we performed a co-immunoprecipitation experiment in the presence of ethidium bromide to exclude that their co-immunoprecipitation may be dependent on contaminating DNA (Fig. 1a).

The reverse co-immmunoprecipitation was carried out transfecting 293T cells with a vector containing the wild-type *HMGA1b* cDNA along with the FLAG-ATM-wt vector or a kinase-dead FLAG-ATM-kd mutant, in which the catalytic activity is impaired.[24] The analysis by immunoblot revealed that FLAG-ATM-wt is also able to co-immunoprecipitate the

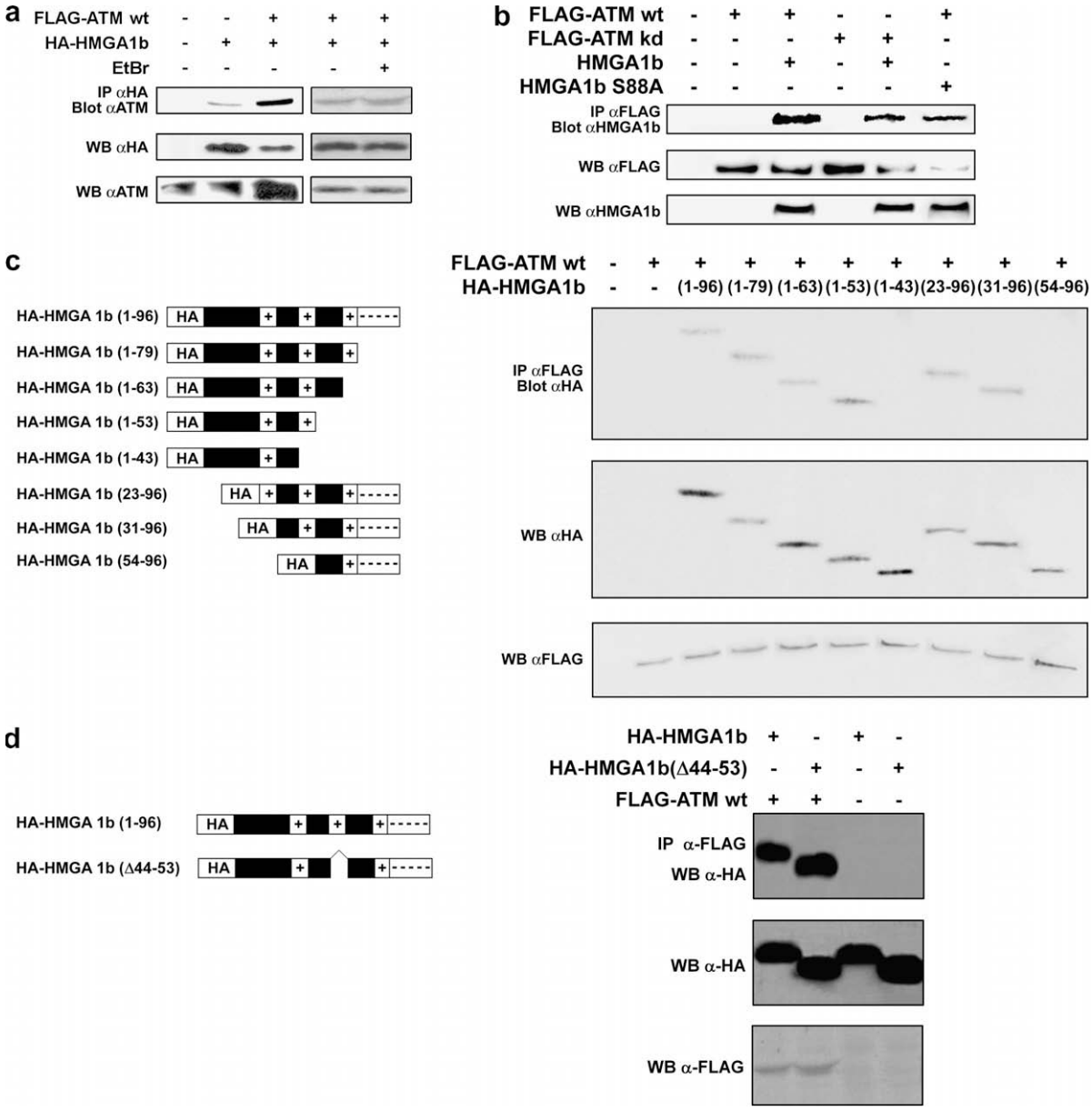

Fig. 1 – *HMGA1b and ATM protein interaction.* **(a) 293T cells were transiently transfected with a vector expressing HA-HMGA1b, alone or along with a FLAG-ATM expression vector. Total cell lysates were immunoprecipitated with anti-HA antibody and blotted with anti-ATM antibody (upper panel). To determine protein levels, Western blots were performed with anti-HA antibody (middle panel) and with anti-ATM antibody (lower panel). Immunoprecipitation in the presence of EtBr was also performed as a control of the specificity of the protein–protein interaction. (b) 293T cells were transiently transfected with vectors expressing FLAG-ATM, wild-type (wt) or kinase-dead (kd), alone or in combination with a vector expressing HMGA1b wild-type or HMGA1b S88A. Total cell lysates were immunoprecipitated with anti-FLAG antibody and blotted with anti-HMGA1b antibody (upper panel). To determine protein levels, Western blots were performed with anti-FLAG antibody (middle panel) and with anti-HMGA1b antibody (lower panel). (c) 293T cells were transiently transfected with a vector expressing FLAG-ATM wt alone or along with vectors expressing either the wild-type form of HMGA1b (1-96) or deletion mutants spanning several regions of the HMGA1b protein as shown in the diagram (AT-hooks (+) and the acidic tail (-----) are indicated). Total cell lysates were immunoprecipitated with anti-FLAG antibody and blotted with anti-HA antibody (upper panel). To determine protein levels, Western blots were performed with anti-HA antibody (middle panel) and with anti-FLAG antibody (lower panel). (d) 293T cells were transiently transfected with vectors expressing the wild-type form of HMGA1b or a deletion mutant (Δ44–53) lacking the second AT-hook, as shown in the diagram. Cells were also transfected with a vector expressing ATM wt and compared to cells not transfected. Total cell lysates were immunoprecipitated with anti-FLAG antibody and blotted with anti-HA antibody (upper panel). To determine protein levels, Western blots were performed with anti-HA antibody (middle panel) and with anti-FLAG antibody (lower panel).**

HMGA1b protein (Fig. 1b). Mutations of the ATM catalytic domain do not seem to impair the interaction since the FLAG-ATM-kd mutant retains its ability to co-immunoprecipitate HMGA1b (Fig. 1b). Likewise, mutation of the putative ATM target site on HMGA1b, serine 88 to alanine, (see below), does not affect the interaction (Fig. 1b).

3.2. *The presence of at least two AT-hook domains of HMGA1 is necessary for its interaction with ATM*

To identify the region of HMGA1 required for ATM binding, we used a series of amino- or carboxy-terminal deletion mutants of the HMGA1 proteins, fused to the HA tag (Fig. 1c). 293T cells were transiently transfected with each HMGA1 mutant along with a FLAG-ATM-wt expression vector. Total cell lysates were then immunoprecipitated with an anti-FLAG antibody and analysed by immunoblotting using an anti-HA antibody. Neither the progressive carboxy-terminal (1–79, 1–63, 1–53) nor the amino-terminal (23–96, 31–96) deletion mutants of HMGA1 showed reduced ability to co-immunoprecipitate ATM, compared with the full-length protein (1–96) (Fig. 1c). Conversely, no interaction was observed between ATM and the HMGA1 mutants 1–43 and 54–98, both containing just one AT-hook domain and both lacking the second AT-hook (Fig. 1c). To evaluate whether the second AT-hook domain of HMGA1 is required for the interaction, we generated a HMGA1 mutant lacking the second AT-hook domain (Δ44–53) and tested its ability to interact with FLAG-ATM. As shown in Fig. 1d, this HMGA1 mutant retains the ability to interact with ATM, indicating that the presence of at least two AT-hook domains, rather than just the second AT-hook, is required for HMGA1–ATM interaction.

3.3. *HMGA1 is phosphorylated by ATM in vitro and in vivo*

Since HMGA proteins are extensively post-translationally modified and phosphorylation has been frequently reported,[26–28] we decided to investigate whether HMGA1 is targeted by ATM kinase activity. By sequence analysis we found that HMGA1 contains in its COOH terminal region a consensus site for ATM phosphorylation, an SQ motif (serine 88/glutamine 89), which is highly conserved amongst different species and the different HMGA family members (Fig. 2a).

We then tested a 20 amino acid peptide, corresponding to the HMGA1 acidic tail (aa 77–96), which contains serine 88, as a substrate for ATM kinase activity. The endogenous wild-type ATM kinase was immunoprecipitated from the total protein extract of the human lymphoblastoid cell line GM2184. Before harvesting, cells were treated with a 10 Gy dose of IR to increase ATM kinase activation as previously described.[21] As shown in Fig. 2b, ATM was able to phosphorylate *in vitro* the C-terminal peptide of HMGA1. The phosphorylation was highly specific as it was strongly inhibited by 5 mM caffeine (1,3,7-trimethylxanthine), an ATM/ATR specific inhibitor,[29] and was impaired from the substitution of serine 88 with an alanine residue (Fig. 2b).

We then assayed the ability of ATM to phosphorylate the full-length HMGA1 recombinant protein, fused to a six-histidine tag. ATM kinase and its kinase-dead mutant were immunoprecipitated from transiently transfected 293T cells. HMGA1 was strongly phosphorylated by the FLAG-ATM-wt kinase and only to a lesser extent by the FLAG-ATM-kd mutant, in which the kinase activity is impaired. In both cases, the phosphorylation was strongly decreased by 5 mM caffeine and when serine 88 of HMGA1 was substituted by alanine (Fig. 2c, upper panel). The same amount of ATM and ATM kinase-dead proteins was used for the assays (Fig. 2c, lower panel). The above data indicate that HMGA1 phosphorylation by ATM is specific, as it is inhibited by both caffeine and a mutation impairing ATM kinase activity. Interestingly, some kinase activity was obtained when using an antibody cross-reacting with both ATM and ATR to immunoprecipitate extracts from lymphoblasts wild-type for ATM (GM2184) or ATM null (AT1526), respectively. In fact, a strong phosphorylation occurred to HMGA1 when the kinase was obtained from GM2184 cells (Fig. 2d, upper panel) but a fainter phosphorylation also occurred when the kinase was immunoprecipitated from AT1526 cells (Fig. 2d, middle panel). Western blot analysis using an antibody against ATR confirmed that the endogenous kinase was effectively immunoprecipitated from AT1526 cells (data not shown). Therefore, it is likely that also the ATR kinase, another member of the PIKKs family, has the ability to phosphorylate serine 88 of HMGA1. Phosphorylation was inhibited in the HMGA1 mutant in which serine 88 is mutated to alanine and in the HMGA1 mutant 1–79, that lacks the C-terminal of the protein containing serine 88. Phosphorylation was inhibited by 5 mM caffeine as well (Fig. 2d). The Coomassie staining indicates the amount of recombinant proteins used as substrates for the kinase assays (Fig. 2d, lower panel).

To verify that HMGA1 is effectively a substrate of ATM kinase activity in response to DNA damage *in vivo*, we treated HA-HMGA1-transfected 293 cells with a 10 Gy dose of IR to induce endogenous ATM activation. Cells were collected 5 min after treatment and extracted proteins immunoprecipitated with antibodies that recognise serine and threonine residues phosphorylated by ATM (Anti-P-Sub-ATM). Analysis of the immunoprecipitates through Western blot with an anti-HA antibody showed a band corresponding to the HA-HMGA1 protein, indicating that, following IR exposure, HMGA1 is phosphorylated *in vivo* by ATM (Fig. 2e). The specificity of HMGA1 phosphorylation by ATM was assessed by the absence of HMGA1 immunoprecipitation in the presence of 5 mM caffeine (Fig. 2e).

3.4. *Colocalisation of HMGA1b and ATMS1981p*

To support further the hypothesis that HMGA1b is a target of the ATM kinase we investigated whether the two proteins colocalise to the same regions of the nuclear compartment by double-immunofluorescence labelling. Mouse embryonic fibroblasts (MEFs), wild-type for both *ATM* and *Hmga1* genes, were either treated or not treated with a 2 Gy dose of IR. Following double staining with antibodies against HMGA1b (red channel) and against the activated, phosphorylated (serine 1981) form of ATM, ATMS1981p, (green channel), cells were analysed by confocal microscopy (Fig. 3a). As expected, ATM kinase was massively activated after irradiation and, intriguingly, it partially colocalises with the endogenous HMGA1b

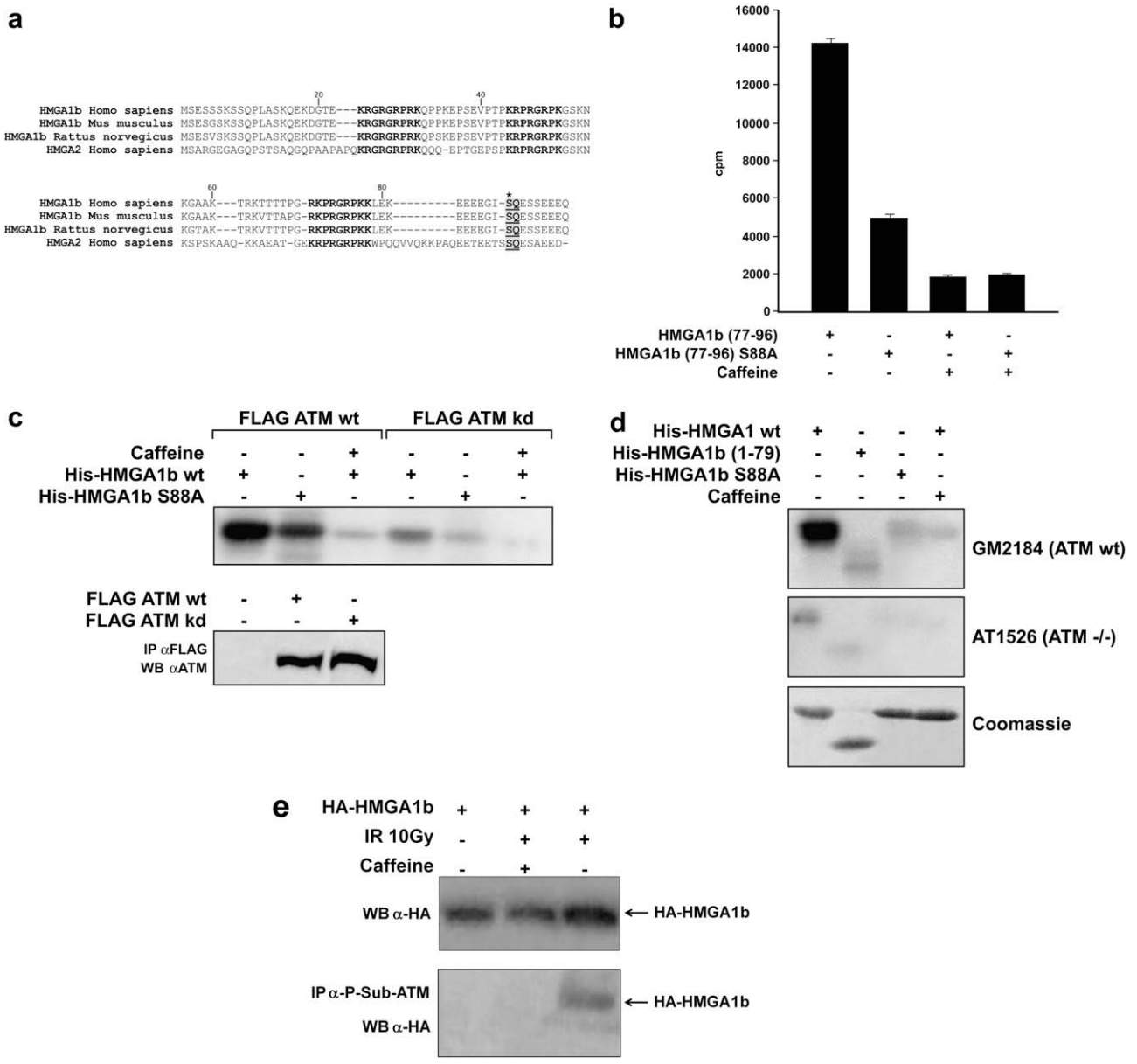

Fig. 2 – *HMGA1 phosphorylation by ATM kinase.* **(a) Amino acid sequence alignment of HMGA1b and HMGA2 from the indicated species (AT-hooks are shown in bold, ATM consensus site is underlined and serine 88 is marked with an asterisk). (b) *In vitro* kinase assay testing ATM kinase activity on the HMGA1 carboxy-terminal peptide (aa 77–96) wild-type or mutated (S88A). Phosphorylation was assessed with or without caffeine (5 mM). A representative experiment (out of three different ones, each performed in duplicate) is shown. (c) *In vitro* kinase assays using FLAG-ATM wild-type (wt) or its kinase-dead (kd) mutant on the histidine-tagged HMGA1b recombinant proteins both wild-type (with or without 5 mM caffeine) and mutated in the putative ATM consensus motif (S88A). Following the kinase reaction, proteins were resolved by SDS–PAGE and the autoradiography of the dried gel is shown (upper panel). FLAG-ATM wt and kd were immunoprecipitated from transiently transfected 293T cells with anti-FLAG antibody. One fifth of each immunoprecipitate was probed with anti-ATM antibody (lower panel). (d) *In vitro* kinase assays were performed using the endogenous ATM kinase immunoprecipitated from human GM2184 lymphoblasts or from AT1526 (ATM –/–) as negative control. Kinase activity was assayed on the histidine-tagged HMGA1b recombinant proteins either wild-type (with or without 5 mM caffeine), mutated in serine 88 or deleted of the carboxy-terminal tail containing serine 88. Following the kinase reaction, proteins were resolved by SDS–PAGE and the autoradiography of the dried gel is shown (upper and middle panels). Similar amounts of recombinant proteins were used for the assay as shown by Coomassie staining (lower panel). (e) 293T cells transfected with a vector expressing HMGA1b were untreated or treated with a 10 Gy dose of IR to induce activation of endogenous ATM. Total cell extracts were immunoprecipitated with an antibody able to recognise serine and threonine residues phosphorylated by activated ATM (Anti-P-Sub-ATM). Immunoprecipitates were analysed by SDS–PAGE followed by Western blot with anti-HA antibody. 293T cells were also treated with 5 mM caffeine as a control of the phosphorylation specificity.**

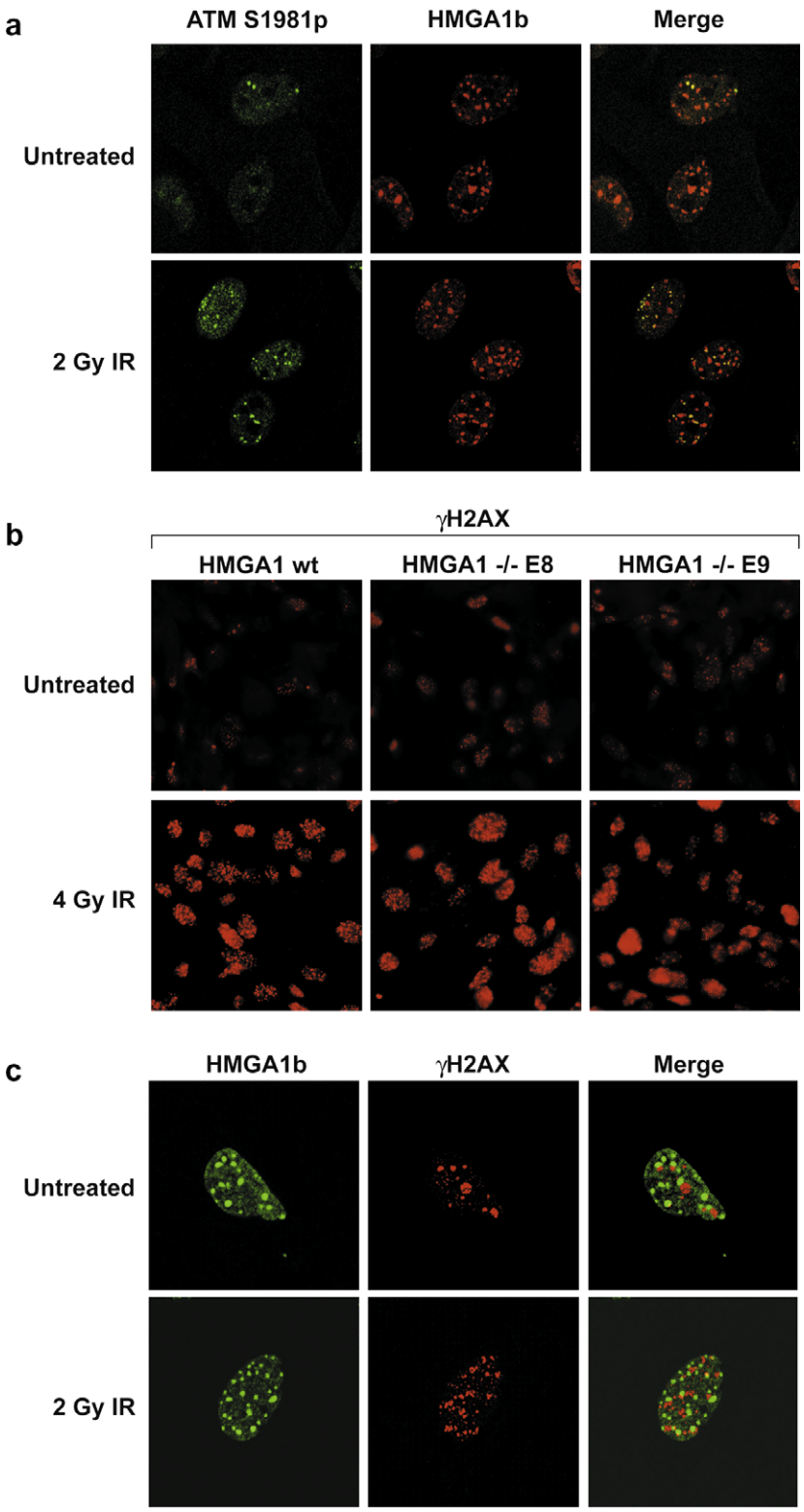

Fig. 3 – *Colocalisation of HMGA1, ATM and γH2AX foci.* (a) HMGA1 colocalises with the ATM active kinase. MEFs were untreated or treated with a 2 Gy dose of IR, and then analysed by confocal microscopy following double-immunofluorescence staining with antibodies against ATM S1981p (green channel) and HMGA1b (red channel). (b) γH2AX foci formation in *Hmga1* null MEFs. MEFs wt and –/– for *Hmga1* were untreated or treated with a 4 Gy dose of IR. Immunofluorescence staining is with an antibody against γH2AX (red channel). (c) HMGA1b does not colocalise with γH2AX foci. Wild-type MEFs were untreated or treated with a 2 Gy dose of IR, and then analysed by confocal microscopy following double-immunofluorescence staining with antibodies against HMGA1b (green channel) and γH2AX (red channel).

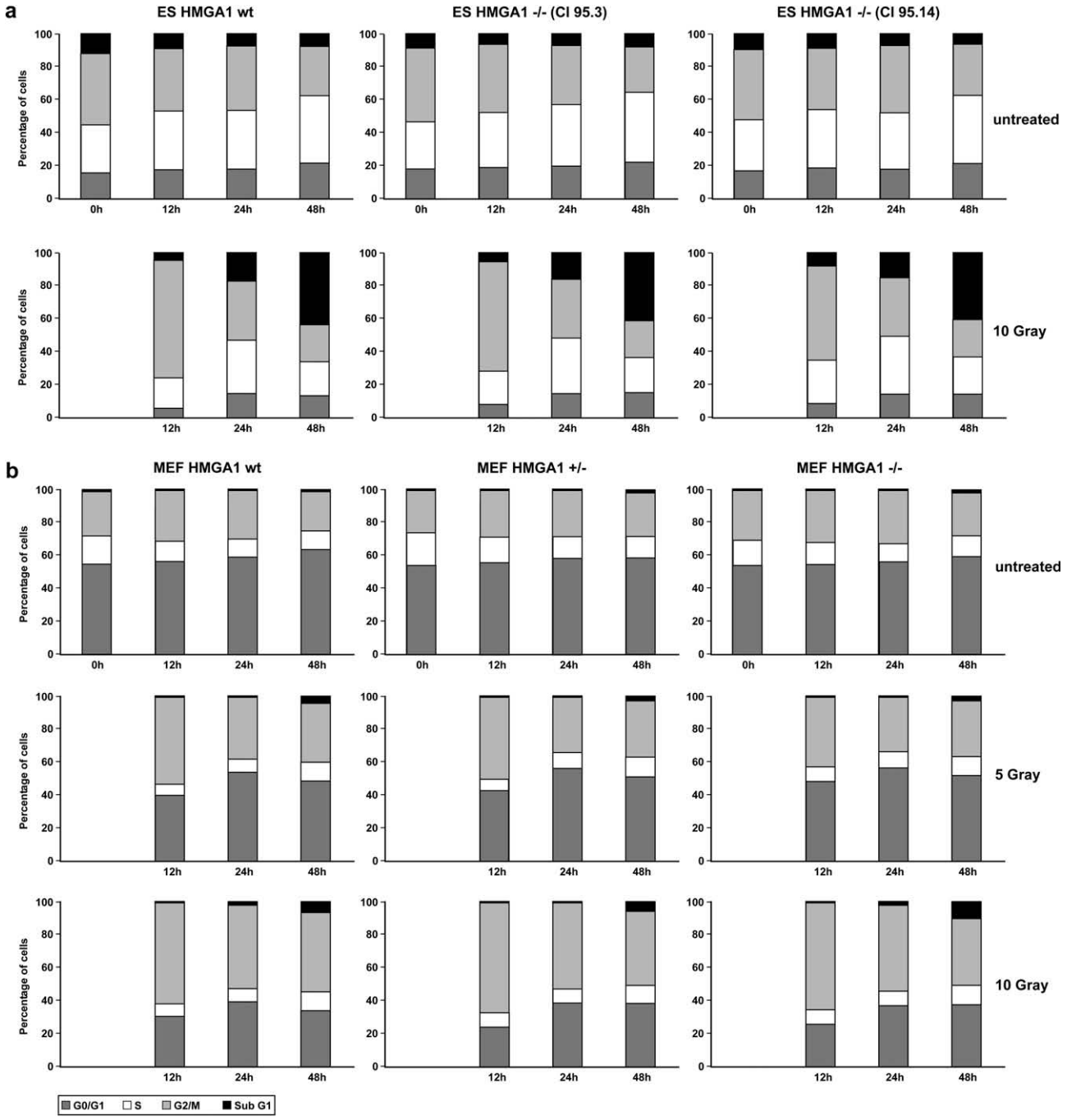

Fig. 4 – *Cell cycle checkpoints are not impaired in Hmga1 null cells following IR.* (a) ES *Hmga1* wt or *Hmga1* –/– (Clones 95.3 and 95.14) were either untreated or treated with a 10 Gy dose of IR. Cells were harvested at different timepoints following BrdU treatment and stained with a FITC-conjugated anti-BrdU antibody and 7-AAD. Cell cycle profiles were obtained by FACS analysis and the distribution of the cells in each different phase is reported from a representative experiment (out of three different ones, each performed in duplicate). (b) MEFs from *Hmga1* wild-type, +/– and –/– embryos were either untreated or treated with doses of 5 and 10 Gy IR. Cells were harvested at different timepoints following BrdU treatment and stained with a FITC-conjugated anti-BrdU antibody and 7-AAD. Cell cycle profiles were obtained by FACS analysis and the distribution of the cells in each different phase is reported from a representative experiment (out of two different ones, each performed in triplicate).

protein (Fig. 3a, merge), both when activated in untreated cells and when activated by γ-irradiation. This colocalisation provides additional evidence that HMGA1b may act *in vivo* as a substrate of the functional ATM kinase.

3.5. *HMGA1 does not localise with IR-induced γH2AX foci*

The phosphorylation of histone H2AX (γH2AX) is amongst the earliest responses to DNA damage, and it is considered the

earliest detectable marker for DSBs.[30] Since many proteins involved in DNA repair quickly relocalise to the γH2AX nuclear foci[31], we sought to investigate first whether γH2AX effectively forms foci in *Hmga1* null cells, then if HMGA1 relocalises to the γH2AX foci following DNA damage. Mouse embryonic fibroblasts (MEFs) wild-type or null for the *Hmga1* gene (*Hmga1* –/– E8 and E9) were either untreated or exposed to a 4 Gy dose of IR and after 3 h fixed and stained with an antibody against the phosphorylated form of histone H2AX. Immunofluorescence showed that, following IR treatment, γH2AX foci are effectively induced in *Hmga1* –/– as in wild-type cells (Fig. 3b, red channel).

To assess if HMGA1 is recruited to the same DSBs sites where γH2AX acts, we treated wild-type MEFs with a 2 Gy dose of IR. After three hours IR-induced DNA damage cells were fixed and double labelled with antibodies against HMGA1b (green channel) and γH2AX (red channel). Confocal microscopy revealed that in mouse embryonic fibroblasts HMGA1b does not localise with IR-induced γH2AX foci at least at the dose and timepoint used (Fig. 3c).

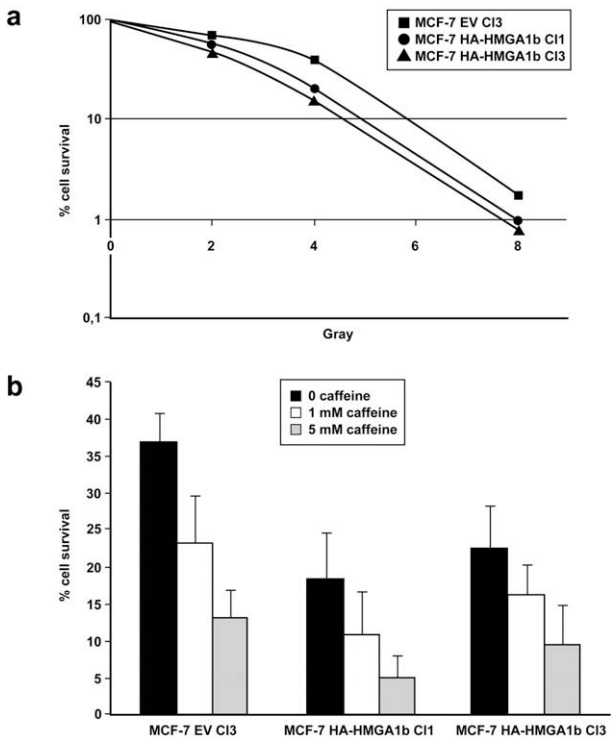

Fig. 5 – *Cell survival is decreased in HMGA1b expressing MCF-7 cells following IR*. (a) Clonogenic survival assay of the indicated MCF-7 clones exposed to 0, 2, 4, 8 Gy of IR. The percentage of survival is reported from a representative experiment (out of three independent ones, each performed in triplicate). (b) Clonogenic survival assay of MCF-7 clones exposed to a 4 Gy dose of IR and treated with the indicated amount of caffeine. The percentage of survival represents the mean of three different experiments (+s.d.), each performed in triplicate.

3.6. *Cell cycle checkpoints are not impaired in Hmga1 null cells following IR*

The ATM-mediated pathway is responsible for the activation of cell cycle checkpoints following DNA damage. The resulting process allows the proper assembly of the DNA repair machinery. To investigate whether HMGA1 might be involved in this pathway, we analysed the cell cycle profile of mouse embryonic stem (ES) cells or fibroblasts (MEFs) null for *Hmga1* in response to IR.

ES cells devoid of the feeder fibroblasts were exposed to a 10 Gy dose of IR and harvested at different timepoints (0, 12, 24 and 48 h) after 1 h of 5-bromo-2-deoxyuridine (BrdU) treatment (Fig. 4a). At 12 h, following IR treatment, both *Hmga1* –/– clones (95.3 and 95.14) and wild-type ES cells accumulate in G2/M. At 24 h cells restarted cycling or underwent apoptosis that was massive at 48 h. Anyway, no significant differences were observed between wild-type and *Hmga1* –/– cells at least at the IR dose tested.

We also analysed cell cycle profiles of MEFs obtained from *Hmga1* wild-type, +/– and –/– embryos at 14.5 dpc. MEFs at early passages were exposed to doses of 5 and 10 Gy IR, then treated with BrdU and analysed at 12, 24 and 48 h (Fig. 4b). At 12 h MEFs of all three genotypes arrested in G2/M in a dose-dependent manner. At 24 and 48 h, the block was slowly released and only a small percentage of cells underwent apoptosis (less than 10%). As for the ES cells we did not observe any statistically significant difference between wild-type or *Hmga1* null cells at the IR doses and timepoints analysed. However, even though it seems that lack of HMGA1 does not affect the ability of ES cells and MEFs to activate cell cycle checkpoints following IR, we cannot rule out the possibility that the other member of the HMGA family, HMGA2, might compensate for HMGA1 loss.

3.7. *Cell survival is decreased in HMGA1b expressing MCF-7 cells following IR*

Cells defective in genes involved in the response to DNA damage usually show an altered long-term survival following exposure to the damaging agent. Therefore, we sought to investigate whether HMGA1 was able to affect cell survival following IR treatment. To this aim we used a different cellular system such as the human breast cancer cell line MCF-7, in which neither *HMGA1* nor *HMGA2* genes are expressed. Moreover, HMGA1b expression has been previously shown to sensitise MCF-7 cells to damage-induced by UV and cis-platin treatment.[12] We compared two different clones of MCF-7 stably transfected with an HMGA1b expressing vector to the control cells, transfected with the empty vector (EV). Cells were exposed to doses of 2, 4 and 8 Gy of IR and after 2 weeks clonogenic survival was evaluated by colony counting. Both HMGA1b expressing clones (MCF-7 HA-HMGA1b Cl1 and Cl3) showed a decrease in the percentage of cell survival compared to the control MCF-7 EV Cl3 (Fig. 5a). Interestingly, this response was highly reproducible and described also in response to the radiomimetic antibiotic bleomycin.[12] To assess whether the enhanced radiosensitivity of HMGA1b expressing cells was correlated to the ATM/ATR pathway, cells were exposed to a 4 Gy IR dose, treated with two different

doses of caffeine (1 and 5 mM, respectively) and analysed after two weeks. Caffeine treatment effectively enhanced cell radiosensitivity in a dose-dependent manner, but no significant differences were observed between HMGA1b expressing MCF-7 clones and MCF-7 EV Cl3 control cells (Fig. 5b).

4. Discussion

Recently, several works correlated HMGA expression to enhanced cell sensitivity in response to different DNA-damaging agents.[5,16,17] Here, we report a novel interaction between the HMGA1 family member and the ATM protein kinase, the major key player in the activation of the cellular response aimed to safeguard genome integrity following DNA damage. We show that HMGA1b and ATM are able to co-immunoprecipitate in 293T cells and that at least two AT-hook domains of HMGA1 are necessary for this interaction. Since ATM phosphorylates its substrates on serine or threonine that precede a glutamine residue, we looked for the presence of these S/TQ motifs on the HMGA protein sequences. Interestingly, both the HMGA1 and the HMGA2 members of the HMGA family present such motifs in the carboxy-terminal region of the protein, and this SQ motif also appears to be highly conserved amongst different species making it tempting to speculate that it may be crucial to the protein function. Subsequently, we demonstrated that HMGA1 is indeed an ATM target *in vitro* using both the HMGA1 C-terminal peptide and the full-length protein. HMGA1 phosphorylation was strongly reduced when using caffeine or the ATM kinase-dead mutant. Moreover, we showed that HMGA1 phosphorylation was indeed site-specific since it was abolished when serine 88 was mutated to alanine. Intriguingly, we found trace HMGA1b phosphorylation when immunoprecipitating extracts from ATM –/– cells with an antibody cross-reacting with the ATR kinase. It is, therefore, likely that HMGA1 might be a target also of the ATR kinase that shares with ATM the same consensus sequence and several substrates,[18] and it has been recently shown to be activated by ATM following IR.[32]

Finally, using an antibody raised against a pool of ATM/ATR substrates to immunoprecipitate HMGA1b after IR exposure, we also demonstrated that ATM phosphorylates HMGA1b *in vivo*. Accordingly, this phosphorylation was inhibited by caffeine.

Following DNA damage, in fact, ATM is activated through autophosphorylation at serine 1981 resulting in the dissociation of inactive dimers.[21] The active ATM monomers in part are free to move throughout the nucleus and in part are recruited at the site of DNA damage.[18] The M/R/N complex appears to be responsible for the initial recruitment of ATM at DSBs sites,[33–35] then MDC1 has been recently shown to bind γH2AX and retain active ATM on the chromosome regions adjacent to the break sites,[36] leading to further expansion of H2AX phosphorylation. The phosphorylation of H2AX by ATM is amongst the earliest responses to DSBs and controls the accumulation of checkpoint/repair proteins to large chromatin regions surrounding DNA damage sites. γH2AX has been proposed to function as a docking protein for the retention of the DNA-damage response factors,[37] or it may modulate the chromatin structure to facilitate the accumulation of checkpoint proteins.[37] We observed efficient formation of γH2AX foci following IR in *Hmga1* –/– MEFs. Interestingly, as assessed by immunofluorescence and confocal microscopy there is no colocalisation between the HMGA1b and γH2AX proteins. Since HMGA and H2AX are both chromatinic proteins involved in chromatin remodelling it is tempting to speculate that HMGA1 phosphorylation might serve to displace HMGA and favour assembly of H2AX in the regions of DNA damage. This may be consistent with the recent finding that HMGA2 interferes with the basal H2AX phosphorylation mechanism,[17] but additional studies are needed to further address this issue.

In an attempt to gain insight into the physiological role of the HMGA1 and ATM interaction, we decided to investigate whether IR-induced cell cycle checkpoint activation was somehow impaired in cells lacking the *Hmga1* gene. Following the DNA damage, ATM triggers a complex regulatory pathway aimed to allow for DNA repair before proceeding through the cell cycle, and many proteins involved in this pathway show defects in IR-induced checkpoints, MDC1,[38] H2AX and 53BP1,[37] CHK1[39] and CHK2.[40,41] However, following IR treatment, both *Hmga1* –/– ES cells and MEFs did not show any defects in cell cycle checkpoint activation relative to wild-type cells under the conditions used in this study. One possible explanation may lie in that both ES cells and MEFs express the HMGA2 member of the HMGA family, which may compensate for HMGA1 loss. As a result, we are generating *Hmga1*/*Hmga2* double knock-out alleles in mice that will attempt to address this issue. As an alternative means to investigate this question, we used the human MCF-7 tumour-derived cell line that does not express either HMGA family members and analysed the effect of ectopic HMGA1b overexpression following IR-induced DNA damage. Interestingly, clonogenic survival following IR treatment was decreased in the HMGA1b expressing MCF-7 clones. Consistently, the same effect has been described in response to the radiomimetic antibiotic bleomycin,[12] suggesting that HMGA1 proteins play a role in the cellular response to DSBs-causing agents. It is not yet clear whether the ATM signalling pathway regulates HMGA1 in this context, since ATM inhibition by caffeine does not rescue survival of HMGA1b expressing cells.

In conclusion, we report a novel interaction between the HMGA1 and the ATM kinase and, whilst the physiological role of this interaction remains to be assessed, we propose that HMGA1 should be regarded as a potential ATM-downstream target. These findings are likely to contribute to our understanding of HMGA1 function in the mechanism of tumourigenesis and reveal new insights into potential therapeutic strategies. In fact, HMGA1 expression enhances sensitivity of breast cancer cells to ionising radiation (as reported here) or to other DNA-damaging agents such as bleomycin, cisplatin and UV irradiation.[12,16] Therefore, patients bearing HMGA1 expressing tumours might benefit from adjuvant therapy based on such DNA-damaging agents.

Conflict of interest statement

All the authors disclose any actual or potential conflict of interest including any financial, personal or other relation-

ships with other people or organisations that could inappropriately influence their work.

Acknowledgements

We are very grateful to Dr. M.B. Kastan for providing the FLAG-ATM wild-type and kinase-dead constructs. We thank Dr. G. Viglietto and Dr. F. Carlomagno for technical hints and valuable suggestions. This work was supported by grants from the Associazione Italiana Ricerca sul Cancro (AIRC), Progetto Strategico Oncologia, Consiglio Nazionale delle Ricerche, the Ministero dell'Università e della Ricerca Scientifica e Tecnologica (MIUR). This work was supported from NOGEC-Naples Oncogenomic Center. We thank the Associazione Partenopea per le Ricerche Oncologiche (APRO) for its support.

REFERENCES

1. Reeves R, Beckerbauer L. HMGI/Y proteins: flexible regulators of transcription and chromatin structure. *Biochim Biophys Acta* 2001;**1519**:13–29.
2. Martinez Hoyos J, Fedele M, Battista S, et al. Identification of the genes up- and down-regulated by the high mobility group A1 (HMGA1) proteins: tissue specificity of the HMGA1-dependent gene regulation. *Cancer Res* 2004;**64**:5728–35.
3. Chiappetta G, Avantaggiato V, Visconti R, et al. High level expression of the HMGI (Y) gene during embryonic development. *Oncogene* 1996;**13**:2439–46.
4. Chiappetta G, Tallini G, De Biasio MC, et al. Detection of high mobility group I HMGI(Y) protein in the diagnosis of thyroid tumors: HMGI(Y) expression represents a potential diagnostic indicator of carcinoma. *Cancer Res* 1998;**58**:4193–8.
5. Baldassarre G, Battista S, Belletti B, et al. Negative regulation of BRCA1 gene expression by HMGA1 proteins accounts for the reduced BRCA1 protein levels in sporadic breast carcinoma. *Mol Cell Biol* 2003;**23**:2225–38.
6. Masciullo V, Baldassarre G, Pentimalli F, et al. HMGA1 protein over-expression is a frequent feature of epithelial ovarian carcinomas. *Carcinogenesis* 2003;**24**:1191–8.
7. Tamimi Y, van der Poel HG, Denyn MM, et al. Increased expression of high mobility group protein I(Y) in high grade prostatic cancer determined by in situ hybridization. *Cancer Res* 1993;**53**:5512–6.
8. Berlingieri MT, Pierantoni GM, Giancotti V, Santoro M, Fusco A. Thyroid cell transformation requires the expression of the HMGA1 proteins. *Oncogene* 2002;**21**:2971–80.
9. Scala S, Portella G, Fedele M, Chiappetta G, Fusco A. Adenovirus-mediated suppression of HMGI(Y) protein synthesis as potential therapy of human malignant neoplasias. *Proc Natl Acad Sci USA* 2000;**97**:4256–61.
10. Wood LJ, Maher JF, Bunton TE, Resar LM. The oncogenic properties of the HMG-I gene family. *Cancer Res* 2000;**60**:4256–61.
11. Reeves R, Edberg DD, Li Y. Architectural transcription factor HMGI(Y) promotes tumor progression and mesenchymal transition of human epithelial cells. *Mol Cell Biol* 2001;**21**:575–94.
12. Baldassarre G, Belletti B, Battista S, et al. HMGA1 protein expression sensitizes cells to cisplatin-induced cell death. *Oncogene* 2005;**24**:6809–19.
13. Fedele M, Pentimalli F, Baldassarre G, et al. Transgenic mice overexpressing the wild-type form of the HMGA1 gene develop mixed growth hormone/prolactin cell pituitary adenomas and natural killer cell lymphomas. *Oncogene* 2005;**24**:3427–35.
14. Takaha N, Hawkins AL, Griffin CA, Isaacs WB, Coffey DS. High mobility group protein I(Y): a candidate architectural protein for chromosomal rearrangements in prostate cancer cells. *Cancer Res* 2002;**62**:647–51.
15. Scully R, Livingston DM. In search of the tumour-suppressor functions of BRCA1 and BRCA2. *Nature* 2000;**408**:429–32.
16. Adair JE, Kwon Y, Dement GA, Smerdon MJ, Reeves R. Inhibition of nucleotide excision repair by high mobility group protein HMGA1. *J Biol Chem* 2005;**280**:32184–92.
17. Boo LM, Lin HH, Chung V, et al. High mobility group A2 potentiates genotoxic stress in part through the modulation of basal and DNA damage-dependent phosphatidylinositol 3-kinase-related protein kinase activation. *Cancer Res* 2005;**65**:6622–30.
18. Shiloh Y. ATM and related protein kinases: safeguarding genome integrity. *Nat Rev Cancer* 2003;**3**:155–68.
19. Savitsky K, Bar-Shira A, Gilad S, et al. A single ataxia telangiectasia gene with a product similar to PI-3 kinase. *Science* 1995;**268**:1749–53.
20. McKinnon PJ. ATM and ataxia telangiectasia. *EMBO Rep* 2004;**5**:772–6.
21. Bakkenist CJ, Kastan MB. DNA damage activates ATM through intermolecular autophosphorylation and dimer dissociation. *Nature* 2003;**421**:499–506.
22. O'Neill T, Dwyer AJ, Ziv Y, et al. Utilization of oriented peptide libraries to identify substrate motifs selected by ATM. *J Biol Chem* 2000;**275**:22719–27.
23. Battista S, Pentimalli F, Baldassarre G, et al. Loss of Hmga1 gene function affects embryonic stem cell lympho-hematopoietic differentiation. *FASEB J* 2003;**11**:1496–8.
24. Pierantoni GM, Fedele M, Pentimalli F, et al. High mobility group I (Y) proteins bind HIPK2, a serine-threonine kinase protein which inhibits cell growth. *Oncogene* 2001;**43**:6132–41.
25. Canman CE, Lim DS, Cimprich KA, et al. Activation of the ATM kinase by ionizing radiation and phosphorylation of p53. *Science* 1998;**281**:1677–9.
26. Edberg DD, Bruce JE, Siems WF, Reeves R. In vivo posttranslational modifications of the high mobility group A1a proteins in breast cancer cells of differing metastatic potential. *Biochemistry* 2004;**43**:11500–15.
27. Sgarra R, Rustighi A, Tessari MA, et al. Nuclear phosphoproteins HMGA and their relationship with chromatin structure and cancer. *FEBS Lett* 2004;**574**:1–8.
28. Zou Y, Wang Y. Tandem mass spectrometry for the examination of the posttranslational modifications of high-mobility group A1 proteins: symmetric and asymmetric dimethylation of Arg25 in HMGA1a protein. *Biochemistry* 2005;**44**:6293–301.
29. Sarkaria JN, Busby EC, Tibbetts RS, et al. Inhibition of ATM and ATR kinase activities by the radiosensitizing agent, caffeine. *Cancer Res* 1999;**59**:4375–82.
30. Rogakou EP, Pilch DR, Orr AH, Ivanova VS, Bonner WM. DNA double-stranded breaks induce histone H2AX phosphorylation on serine 139. *J Biol Chem* 1998;**273**:5858–68.
31. Paull TT, Rogakou EP, Yamazaki V, Kirchgessner CU, Gellert M, Bonner WM. A critical role for histone H2AX in recruitment of repair factors to nuclear foci after DNA damage. *Curr Biol* 2000;**10**:886–95.
32. Jazayeri A, Falck J, Lukas C, et al. ATM- and cell cycle-dependent regulation of ATR in response to DNA double-strand breaks. *Nat Cell Biol* 2006;**8**:37–45.

33. Falck J, Coates J, Jackson SP. Conserved modes of recruitment of ATM, ATR and DNA-PKcs to sites of DNA damage. *Nature* 2005;**434**:605–11.
34. Lee JH, Paull TT. ATM activation by DNA double-strand breaks through the Mre11/Rad50/Nbs1 complex. *Science* 2005;**308**:551–4.
35. You Z, Chahwan C, Bailis J, Hunter T, Russell P. ATM activation and its recruitment to damaged DNA require binding to the C terminus of Nbs1. *Mol Cell Biol* 2005;**25**:5363–79.
36. Lou Z, Minter-Dykhouse K, Franco S, et al. MDC1 maintains genomic stability by participating in the amplification of ATM-dependent DNA damage signals. *Mol Cell* 2006;**21**:187–200.
37. Fernandez-Capetillo O, Chen HT, Celeste A, et al. DNA damage-induced G2-M checkpoint activation by histone H2Ax and 53BP1. *Nat Cell Biol* 2002;**4**:993–7.
38. Stewart GS, Wang B, Bignell CR, Taylor AM, Elledge SJ. MDC1 is a mediator of the mammalian DNA damage checkpoint. *Nature* 2003;**421**:961–6.
39. Gatei M, Sloper K, Sorensen C, et al. Ataxia-telangiectasia-mutated (ATM) and NBS1-dependent phosphorylation of Chk1 on Ser-317 in response to ionizing radiation. *J Biol Chem* 2003;**278**:14806–11.
40. Hirao A, Cheung A, Duncan G, et al. Chk2 is a tumor suppressor that regulates apoptosis in both an ataxia telangiectasia mutated (ATM)-dependent and an ATM-independent manner. *Mol Cell Biol* 2002;**22**:6521–32.
41. Takai H, Naka K, Okada Y, et al. Chk2-deficient mice exhibit radioresistance and defective p53-mediated transcription. *Embo J* 2002;**21**:5195–205.

Oncogene (2009) 28, 1432–1442

www.nature.com/onc

ORIGINAL ARTICLE

Regulation of microRNA expression by HMGA1 proteins

I De Martino[1,2,3], R Visone[1,3], M Fedele[1,2], F Petrocca[3], D Palmieri[1], JM Hoyos[1], F Forzati[1], CM Croce[3] and A Fusco[1,2]

[1]*Istituto di Endocrinologia ed Oncologia Sperimentale del CNR c/o Dipartimento di Biologia e Patologia Cellulare e Molecolare, Facoltà di Medicina e Chirurgia di Napoli, Università degli Studi di Napoli 'Federico II', Naples, Italy;* [2]*NOGEC (Naples Oncogenomic Center)-CEINGE, Biotecnologie Avanzate-Napoli and SEMM—European School of Molecular Medicine—Naples Site, Naples, Italy and* [3]*Department of Molecular Virology, Immunology, and Medical Genetics, Comprehensive Cancer Center, Ohio State University, Columbus, OH, USA*

The High Mobility Group proteins HMGA1 are nuclear architectural factors that play a critical role in a wide range of biological processes. Since recent studies have identified the microRNAs (miRNAs) as important regulators of gene expression, modulating critical cellular functions such as proliferation, apoptosis and differentiation, the aim of our work was to identify the miRNAs that are physiologically regulated by HMGA1 proteins. To this purpose, we have analysed the miRNA expression profile of mouse embryonic fibroblasts (MEFs) carrying two, one or no *Hmga1* functional alleles using a microarray (miRNA microarray). By this approach, we found a miRNA expression profile that differentiates *Hmga1*-null MEFs from the wild-type ones. In particular, a significant decrease in miR-196a-2, miR-101b, miR-331 and miR-29a was detected in homozygous *Hmga1*-knockout MEFs in comparison with wild-type cells. Consistently, these miRNAs are downregulated in most of the analysed tissues of *Hmga1*-null mice in comparison with the wild-type mice. ChIP assay shows that HMGA1 is able to bind regions upstream of these miRNAs. Moreover, we identified the HMGA2 gene product as a putative target of miR-196a-2, suggesting that HMGA1 proteins are able to downregulate the expression of the other member of the HMGA family through the regulation of the miR-196a-2 expression. Finally, ATXN1 and STC1 gene products have been identified as targets of miR-101b. Therefore, it is reasonable to hypothesize that HMGA1 proteins are involved in several functions by regulating miRNA expression.
Oncogene (2009) **28,** 1432–1442; doi:10.1038/onc.2008.495; published online 26 January 2009

Keywords: HMGA1; microRNA; MEF; ATXN1; STC1; HMGA2

Correspondence: Professor A Fusco, Istituto di Endocrinologia ed Oncologia Sperimentale del CNR 'Gaetano Salvatore', Università di Napoli Federico II, via Pansini 5, 80131 Napoli, Italy.
E-mail: afusco@napoli.com or alfusco@unina.it
Received 24 July 2008; revised 28 November 2008; accepted 17 December 2008; published online 26 January 2009

Introduction

The High Mobility Group A (HMGA) protein family includes HMGA1a and HMGA1b, which are encoded by the *HMGA1* gene through an alternative splicing (Johnson *et al*., 1989), and the closely related HMGA2 protein, which is encoded by a different gene (Manfioletti *et al*., 1991). These proteins bind the minor groove of AT-rich DNA sequences through three short basic repeats, called 'AT-hooks', located at the NH2-terminal region of the proteins. The mammalian HMGA proteins play key roles in chromatin architecture and gene control by serving as generalized chromatin effectors, either enhancing or suppressing the ability of most usual transcriptional activators and repressors to act within the confines of chromatinized DNA (Reeves and Nissen, 1990; Thanos and Maniatis, 1995).

Both *HMGA* genes are widely expressed during embryogenesis, whereas their expression is low or absent in most of the normal adult tissues (Zhou *et al*., 1995; Chiappetta *et al*., 1996). Conversely, their expression again becomes abundant in most human malignant neoplasias (Tallini and Dal Cin, 1999). Several studies indicate that HMGA gene overexpression plays a critical role in the process of carcinogenesis and their oncogenic activity has been demonstrated *in vitro* and *in vivo* (Fusco and Fedele, 2007). In fact, either HMGA1 or HMGA2 overexpression is able to transform mouse and rat fibroblasts (Fedele *et al*., 1998; Scala *et al*., 2000), and transgenic mice overexpressing either HMGA1 or HMGA2 develop natural killer-T lymphomas and pituitary adenomas (Baldassarre *et al*., 2001; Fedele *et al*., 2002, 2005). Interestingly, the *HMGA1* gene also seems to have a tumor suppressor role in oncogenesis since the *Hmga1*-null mice, even at the heterozygous state, develop B-cell lymphomas and myeloid malignancies, other than cardiac hypertrophy and type II diabetes (Foti *et al*., 2005; Fedele *et al*., 2006).

In a previous work, we searched for genes regulated by HMGA1 proteins, using microarray analysis in embryonic stem cells bearing one or two disrupted *Hmga1* alleles. We identified that 87 transcripts

increased and 163 transcripts decreased by at least four-fold in *Hmga1*$^{-/-}$ embryonic stem cells. For some of them, a *Hmga1*-dose dependency was observed. For a couple of analysed HMGA1-regulated genes, electrophoretic mobility shift assay and chromatin immunoprecipitation (ChIP) revealed a direct binding of HMGA1 proteins to their promoters, suggesting an HMGA1-direct regulation of their expression (Martinez Hoyos *et al*., 2004).

MicroRNAs (miRNAs) are a class of genes encoding short RNAs, which control gene expression by inhibiting translation or inducing cleavage of target mRNAs. miRNAs are aberrantly expressed in cancer tissues, and links between deregulated miRNAs and the molecular pathways involved in carcinogenesis have been established (Negrini *et al*., 2007). Several studies have shown that miRNAs play important roles in essential processes such as differentiation, cell growth and cell death (Miska, 2005; Zamore and Haley, 2005). Recent evidences indicate that miRNAs could contribute to oncogenesis, participating as tumor suppressors or as oncogenes (Kent and Mendell, 2006). In fact, miR-21 was shown to directly target the tumor suppressor PTEN (encoding a phosphatase that can inhibit growth and/or survival pathways) in cholangiocarcinoma cells (Meng *et al*., 2007). Moreover, the miR-221/222 cluster, upregulated in thyroid and prostate cancer, was shown to target the p27^{kip1} protein, a critical negative regulator of the cell cycle (Galardi *et al*., 2007; Visone *et al*., 2007). Therefore, it is reasonable to hypothesize that HMGA1 proteins are involved in several functions regulating the miRNA expression.

In the present work, we have carried out miRNA expression profiling of mouse embryonic fibroblasts (MEFs) isolated from *Hmga1*-knockout and wild-type mice to identify the miRNAs regulated by the HMGA1 proteins. Among the miRNAs differentially expressed in wild-type and *Hmga1*-null MEFs, we focused our attention on a subset of miRNAs, including the miR-196a-2 and miR-101b, downregulated in homozygous *Hmga1*-knockout MEFs with respect to the wild-type ones. Finally, we identified the *HMGA2* gene product as a target of miR-196a-2 and the *ATXN1* and *STC1* gene products as targets of miR-101b.

Results

miRNA expression profile of embryonic fibroblasts isolated from Hmga1-*knockout mice*

We used a miRNA microarray (Liu *et al*., 2004) to evaluate the miRNA expression profile of MEFs deriving from *Hmga1*-knockout mice. The wild-type MEFs were matched with those bearing one or two disrupted *Hmga1* alleles. Applying the analysis of variance, we obtained a list of differentially expressed miRNAs ($P<0.05$) between wild-type and homozygous mutants (Table 1). Six miRNAs (miR-196a-2, miR-101b, miR-331, miR-29a, miR-346 and miR-130b) were overexpressed with a fold-change equal or higher than two in the wild-type samples versus homozygous mutants. In contrast, none of the analysed miRNAs showed more than two-fold reduction in its expression in the wild-type compared to *Hmga1*$^{-/-}$

Table 1 miRNAs differentially expressed between MEFs obtained from wild-type (MEFs$^{+/+}$), heterozygous (MEFs$^{+/-}$) and homozygous (MEFs$^{-/-}$) mice for the *Hmga1*-null mutation

	miRNA name	*Fold-change (MEFs$^{+/+}$ vs MEFs$^{+/-}$)*	P-*value*	*Fold-change (MEFs$^{+/+}$ vs MEFs$^{-/-}$)*	P-*value*
1	mmu-mir-196a-2No2	1.89	0.00238	3.70	0.0471
2	mmu-mir-101bNo2	1.28	0.0491	2.43	0.0466
3	mmu-mir-331No2	1.19	0.00280	2.29	0.0364
4	mmu-mir-29aNo2	1.19	0.0471	2.28	0.0299
5	hsa-mir-346No1	1.07	0.0174	2.10	0.0275
6	mmu-mir-130bNo1	1.00	0.0167	2.00	0.0224
7	mmu-mir-199bNo2	0.97	0.0306	1.96	0.00879
8	hsa-mir-199b-precNo2	0.97	0.0178	1.96	0.0143
9	mmu-mir-194-2No2	0.95	0.0212	1.93	0.00535
10	mmu-mir-134-precNo2	0.93	0.0306	1.91	0.00435
11	mmu-mir-210No2	0.87	0.0158	1.82	0.00256
12	mmu-mir-130-prec	0.85	0.0197	1.80	0.00178
13	hsa-mir-016a-chr13	−0.99	0.0483	0.51	0.000595
14	hsa-mir-222-precNo2	−1.00	0.0479	0.50	0.00026
15	mmu-mir-321No2	−1.01	0.0578	0.50	0.000247
16	mmu-mir-28No2	−1.05	0.0986	0.48	0.00659
17	mmu-let-7bNo1	−1.08	0.0489	0.47	0.0336
18	mmu-mir-125b-precNo1	−1.10	0.0255	0.47	0.00745
19	mmu-mir-125b-1No1	−1.11	0.0339	0.46	0.00447
20	mmu-mir-030e-prec	−1.14	0.0787	0.45	0.00338
21	mmu-mir-218-2precNo1	−1.21	0.0396	0.43	0.00774
22	hsa-mir-30c-1No1	−1.21	0.0499	0.43	0.00554
23	mmu-mir-321No1	−1.22	0.0458	0.43	0.00121
24	mmu-mir-299No1	−1.30	0.0115	0.41	0.00114

Abbreviation: MEFs, mouse embryonic fibroblasts.

MEFs. Subsequently, we validated the results obtained by miRNA microarray analysis by real-time PCR on the miR-101b, miR-196a-2, miR-331 and miR-29a (Figure 1).

Interestingly, for miR-196a-2 and miR-101b, the differences in their expression between wild-type and *Hmga1*-null MEFs were even higher than those shown by the microarray analysis. Then, we decided to concentrate on the miR-101b and miR-196a-2, which showed the highest fold-change decrease in *Hmga1*-null MEFs (Table 1).

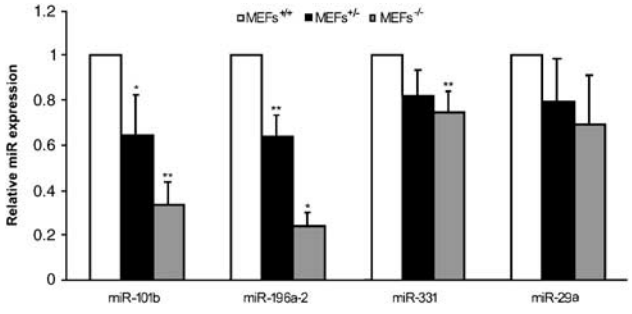

Figure 1 Validation of some miRNA microarray data by quantitative real-time reverse transcription-PCR (qRT–PCR). qRT–PCR analysis of miR-101b, miR-196a-2, miR-331 and miR-29a precursors was carried out on MEFs obtained from wild-type (MEFs$^{+/+}$), heterozygous (MEFs$^{+/-}$) and homozygous (MEFs$^{-/-}$) mice for the *Hmga1*-null mutation. The fold-change values indicate the relative change in the expression levels between homozygous and heterozygous samples and the wild-type sample, assuming that the value of the wild-type sample was equal to 1. Each bar represents the mean value ± s.e. from three independent experiments performed in triplicates $*P<0.05$, $**P<0.01$ vs MEFs$^{+/+}$.

Subsequently, we analysed miR-196a-2 and miR-101b expressions by real-time RT-PCR on different tissues from *Hmga1*$^{+/+}$, *Hmga1*$^{+/-}$ and *Hmga1*$^{-/-}$ mice. As shown in the Figure 2a, miR-101b was downregulated, as described for MEFs, in the spleen, heart, thymus and brain of heterozygous and homozygous *Hmga1*-null mice with respect to the wild-type tissues, whereas no differences in its expression were observed in the liver, and its expression was not detected in the lung. The expression trend of miR-196a-2 in the liver, heart, lung and brain was similar to that observed in *Hmga1*$^{+/+}$ with respect to *Hmga1*$^{-/-}$ MEFs, being significantly downregulated in heterozygous and homozygous *Hmga1*-null mice. Conversely, no differences in miR-196a-2 expression were observed in the spleen, and no expression at all was observed in the thymus (Figure 2b). In some cases, such as miR-196a-2 in the liver (Figure 2b) and miR-101b in the spleen (Figure 2a), the reduction of their expression was HMGA1-dose-dependent. These results are consistent with our previous ones showing that the gene expression regulation by the HMGA1 proteins is dependent on the cellular context (Martinez Hoyos *et al*., 2004).

HMGA1 proteins directly bind the miR-101b and miR-196a-2 upstream regions

To verify that HMGA1 proteins are able to bind to the miR-101b or miR-196a-2 upstream regions *in vivo*, we performed ChIP experiments in *Hmga1*$^{+/+}$, *Hmga1*$^{+/-}$ and *Hmga1*$^{-/-}$ MEFs. Chromatin prepared as described under Materials and methods was immunoprecipitated with anti-HMGA1 or rabbit IgG antibodies, used as internal control. In particular, we analysed a region of

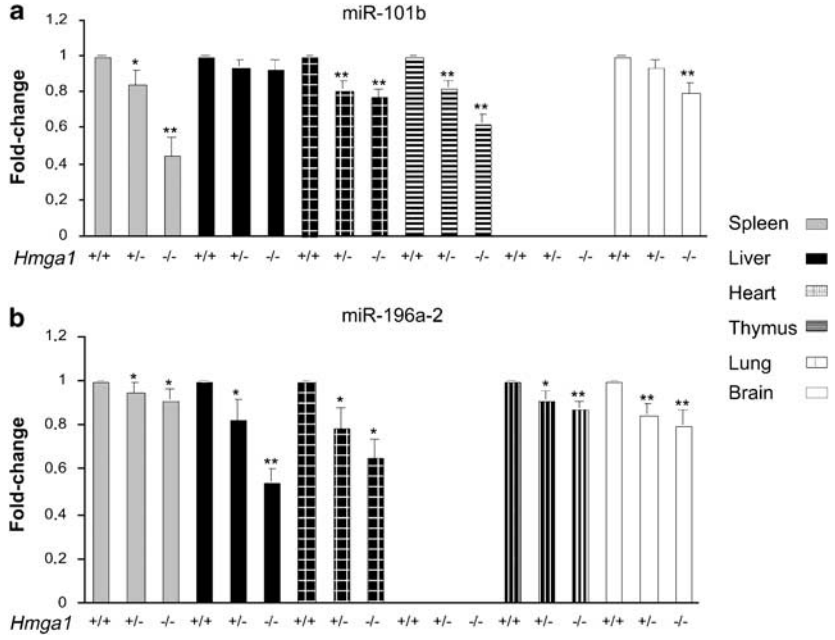

Figure 2 Expression of miR-196a-2 and miR-101b in *Hmga1*-knockout mouse tissues. qRT–PCR analysis of (**a**) miR-101b and (**b**) miR-196a-2 precursors was carried out on the spleen, liver, heart, thymus, lung and brain deriving from Hmga1$^{+/+}$, Hmga1$^{+/-}$ and Hmga1$^{-/-}$ mice. Each bar represents the mean value ± s.e. from three different mice. $*P<0.05$, $**P<0.01$ vs wild-type control.

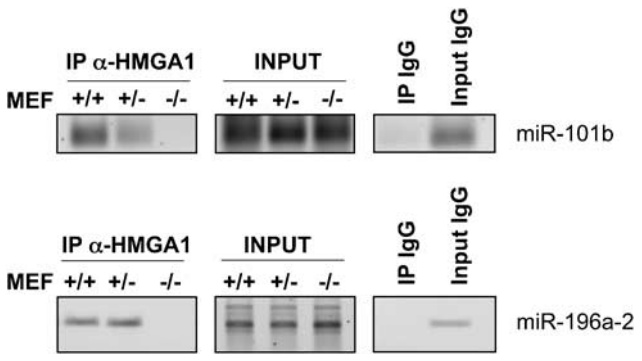

Figure 3 HMGA1 bind to the promoter of miR-101b and miR-196a-2. ChIP assay was carried out on wild-type and *Hmga1*-knockout MEFs. The recovered DNA was used as a template for PCR reactions with primers that amplify the upstream regions of miR-101b and miR-196a-2.

2,000 bp upstream of the precursor sequence of miR-101b and miR-196a-2 to search for AT-rich putative HMGA1-binding sites. The results shown in Figure 3 demonstrate that HMGA1 proteins bind to these sequences. In fact, the miR-101b and miR-196a-2 upstream regions were amplified from the DNA recovered with anti-HMGA1 antibody in wild-type and *Hmga1*$^{+/-}$, but not in *Hmga1*$^{-/-}$ MEFs. Moreover, no amplification was observed in samples immunoprecipitated with rabbit IgG.

ATXN1 *and* STC1 *are targets of miR-101b*

To search for potential mRNA targets of the HMGA1-regulated miRNAs, we used the miRGen program (http://www.diana.pcbi.upenn.edu/miRGen.html) as a bioinformatic tool. Among the several genes predicted as potential targets of the miR-101b, we selected *ATXN1* and *STC1* because of their biological function in development and cancer. The gene *ATXN1*, which is mutated to contain an expanded CAG trinucleotide repeat in spinocerebellar ataxia-1, encodes for the protein Ataxin 1. Ataxin 1 is detected in various brain regions and in non-neuronal tissues, such as the heart, skeletal muscle and liver (Servadio *et al*., 1995; Tsai *et al*., 2004). Stanniocalcin1, encoded by *STC1* gene, is a glycoprotein hormone and it has a role in many physiological processes, including bone development, reproduction, wound healing, angiogenesis and modulation of inflammatory response (Ishibashi and Imai, 2002; Chang *et al*., 2003). The *STC1* gene is expressed in a wide variety of tissues, including the kidney, prostate, thyroid, bone and ovary (Chang *et al*., 1995; Olsen *et al*., 1996; Varghese *et al*., 1998). Recently, *STC1* overexpression has been found in hepatocellular, colorectal, breast and medullary thyroid carcinomas (Fujiwara *et al*., 2000; Okabe *et al*., 2001; Watanabe *et al*., 2002; McCudden *et al*., 2004).

Three sites in the 3′-UTR of *ATXN1* gene and three in the 3′-UTR of *STC1* gene, that match the miR-101b 'seed sequence', were predicted (Figure 4a). To validate the influence of miR-101b on the selected candidate targets, we transfected the miR-101b or its inhibitor, 2′-O-Me-101b, into the NIH3T3 cells, and searched for changes in ATXN1 and STC1 protein levels by western blot analysis. Introduction of miR-101b decreased the protein levels significantly (Figures 4b and c). Conversely, the inhibitor, 2′-O-Me-101b, does not change STC1 and ATXN1 protein amounts significantly.

Interestingly, no significant changes in the ATXN1 or STC1 mRNA levels were observed in the cells transfected with the miR-101b or its inhibitor (Figure 4d). This result indicates a role of miR-101b in STC1 and ATXN1 post-transcriptional regulation, and excludes that miR-101b may affect ATXN1 or STC1 mRNA degradation.

Most miRNAs are thought to control gene expression by base pairing with the miRNA-recognizing elements (miR-RE) found in their messenger target. To demonstrate that the direct interaction between the miR-101b and STC1 or ATXN1 mRNA was responsible for decreased expression of these proteins, we inserted downstream of the luciferase ORF the 1310 bp (3390–4680) of the 3′-UTR of the ATXN1 mRNA, or the 988 bp (1029–1995) of the 3′-UTR of the STC1 mRNA, respectively. These reporter vectors were transfected into NIH3T3 cells with (a) the miR-101b oligonucleotide precursor, (b) the 2′-O-Me-101b and (c) a control not targeting scrambled oligonucleotide. The luciferase activity was markedly diminished after miR-101b transfection, as compared with the scrambled oligonucleotide ($P<0.05$). Conversely, an increase in the luciferase activity was observed after transfection with the miR-101b inhibitor ($P<0.01$ for STC1 and $P<0.05$ for ATXN1) (Figure 5a). These results indicate that this miR interferes with ATXN1 and STC1 translation through direct interaction with their respective 3′-UTRs. This conclusion is further supported by similar experiments in which we used as reporter construct the same vector of the previous experiments, but carrying target sites modified by introducing point deletion in one, two or three sites together (Figure 5b). For both target genes, only the reporter vector carrying deletion in all target sites was insensitive to the effect of miR-101b ($P<0.01$) (Figures 5c and d), proving that the modification in only one or two target sites of the 3′-UTR is not sufficient to block the inhibitory function of this miR.

miR-196a-2 downregulates HMGA2

Using the same bioinformatic tool, we also searched for potential mRNA targets of mouse miR-196a-2. This analysis identified several candidate genes, but we put our attention on *Hmga2* (Figure 6a), another member of HMGA family, which maps on chromosome 12q13-15 and is causally involved in a variety of benign and malignant tumors (Ashar *et al*., 1995; Schoenmakers *et al*., 1995; Fedele *et al*., 2001; Fusco and Fedele, 2007). To better investigate the influence of miR-196a-2 on *Hmga2* expression, we searched for changes in HMGA2 protein and mRNA levels in NIH3T3 cells transfected with the miR-196a-2 precursor (miR-196a-2) or its

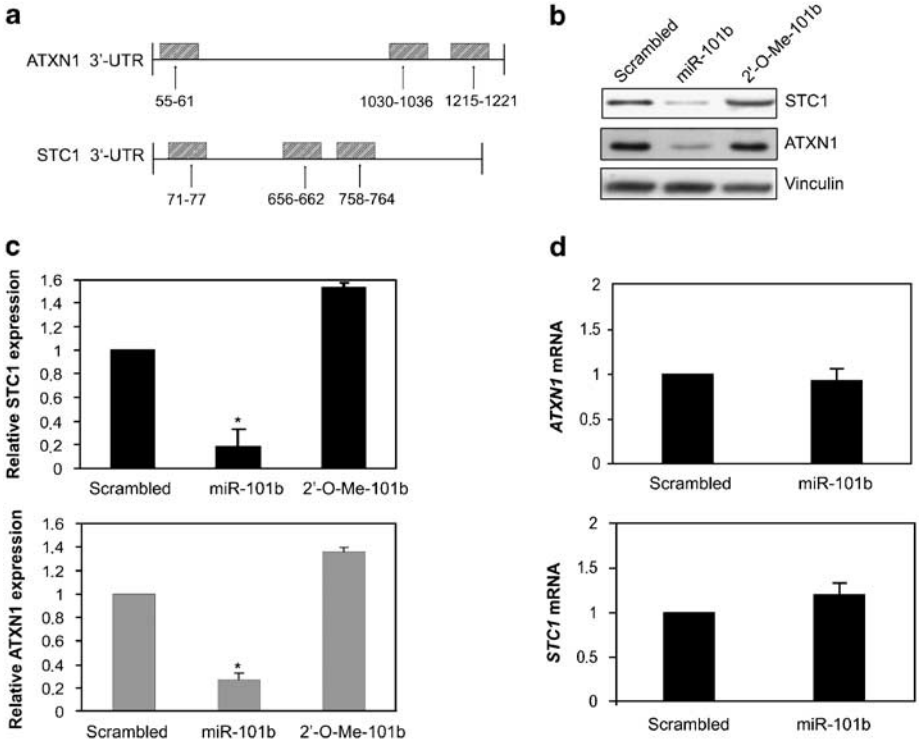

Figure 4 *ATXN1* and *STC1* are target genes of miR-101b. (**a**) Schematic representation of *STC1* and *ATXN1* genes 3′-UTR target sites for miR-101b. (**b**) Immunoblots for STC1 and ATXN1. Proteins were extracted from untransfected and miR-101b sense- or antisense-transfected NIH3T3 cells 48 h after transfection. Vinculin immunoblot was used as loading control. (**c**) Densitometric analysis of the western blots shown in panel b. Each bar represents the mean ratio ± s.e., between STC1 (or ATXN1) and vinculin, of three independent experiments. (**d**) qRT–PCR analysis of *ATXN1* and *STC1* mRNA in the same samples shown in panel b. Fold-change values indicate the relative change in STC1 and ATXN1 expression levels between miRNA-treated and scrambled oligonucleotide-treated cells, normalized with GAPDH. The error bars represent the mean ± s.e. ($n=3$). *$P<0.05$ vs scrambled control.

inhibitor (2′-O-Me-196a-2) in comparison with scrambled oligonucleotide-transfected cells. As shown in Figures 6b and c, the introduction of the miR-196a-2 precursor significantly decreased the HMGA2 protein levels, differently from the 2′-O-Me-196a-2, which does not significantly change the HMGA2 protein amounts compared to the cells transfected with a scrambled oligonucleotide.

No significant changes in the HMGA2 mRNA levels were observed in the cells transfected with the miR-196a-2 or its inhibitors (Figure 6d). The inverse pattern of expression of *Hmga2* and miR-196a-2 suggested an *in vivo* interaction that we further investigated by luciferase assays. In fact, to show a direct interaction between the 3′-UTR of *Hmga2* and miR-196a-2, we inserted the 3′-UTR region predicted to interact with this miR into a luciferase vector. Then, we tested the activity of the miR-196a-2 by cotransfecting the luciferase reporter vector bearing the 3′-UTR of *Hmga2* with (a) the miR-196a-2 oligonucleotide precursors, (b) the 2′-O-Me-196a-2 and (c) a control not targeting scrambled oligonucleotide. Consistent with the above data, indicating HMGA2 as a target of miR-196a-2, the relative luciferase activity was markedly diminished in cells transfected with miR-196a-2 compared to those transfected with the scrambled oligonucleotide ($P<0.05$). Conversely, a significant increase in the luciferase activity was observed after transfection with the miR-196a-2 inhibitor (Figure 7a).

To show that the effect of miR-196a-2 on the luciferase gene is dependent on the presence of the miR-196a-2-binding sites, we generated a panel of reporter constructs containing the HMGA2 3′-UTR, with the miR-196a-2-binding sites mutated individually or in combination (Figure 7b). Although the mutation of one site did not influence the inhibitory effect of miR-196a-2 on reporter gene expression, mutation of two sites together reduced the inhibitory effect to three-fold ($P<0.01$), suggesting that these two sites function cooperatively in mediating the inhibition of HMGA2 protein synthesis (Figure 7c).

Discussion

The aim of this study was to identify miRNAs that are physiologically regulated by the HMGA1 proteins. To this purpose, we analysed, using a miRNA microarray platform, the miRNA expression profile of the MEFs carrying two, one or no *Hmga1* functional alleles. We identified four miRNAs significantly downregulated in homozygous *Hmga1*-null MEFs with respect to the wild-type samples. Their expression, in particular that of miR-101b and miR-196a-2,

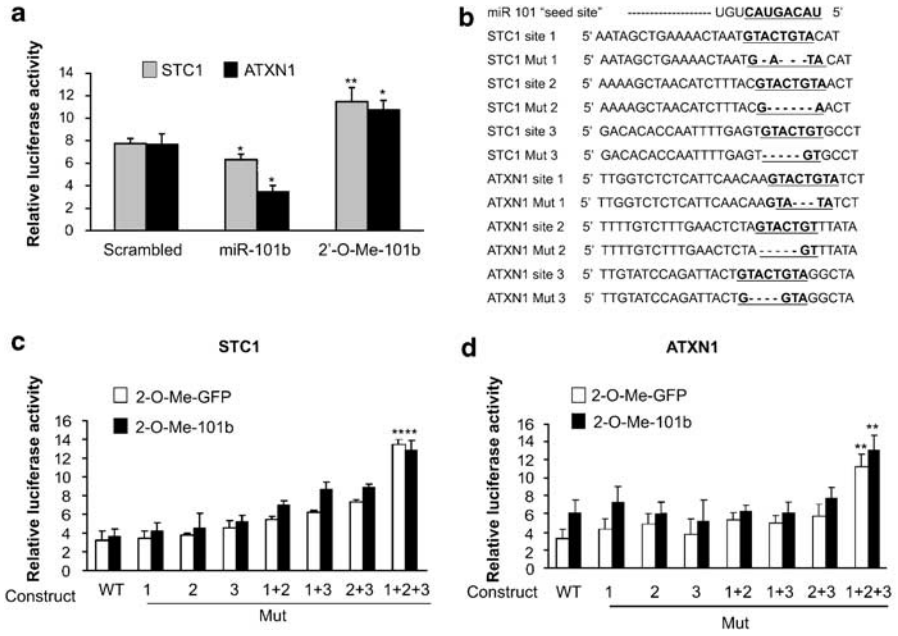

Figure 5 The 3′-UTR of *STC1* or of *ATXN1*, enables miR-101b regulation. (**a**) Relative luciferase activity in NIH3T3 cells transiently transfected with miR-101b oligonucleotide (sense and antisense) and control scrambled oligonucleotide. Relative activity of firefly luciferase expression was standardized to a transfection control, using *Renilla* luciferase. The scale bars represent the mean ± s.e. ($n=3$). $^{**}P<0.01$, $^{*}P<0.05$ compared with the scrambled oligonucleotide. (**b**) Schematic representation of the miR-101b site regions (bold and dashed) wild-type and mutated in the constructs used in the luciferase assays shown in c and d. (**c** and **d**) Relative luciferase activity in NIH3T3 cells transfected with different constructs shown in panel a. Results are reported as mean expression values of three independent experiments, with error bars indicating standard error. $^{**}P<0.01$.

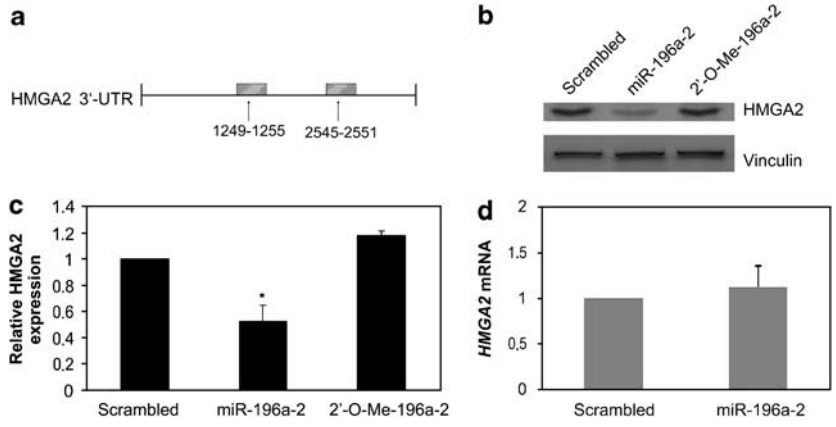

Figure 6 HMGA2 is target of miR-196a-2. (**a**) Schematic representation of *HMGA2* gene 3′-UTR target sites for miR-196a2. (**b**) Immunoblots for HMGA2 and vinculin protein as loading control. Proteins were extracted from untransfected and miR-196a-2 sense- or antisense-transfected NIH3T3 cell 48 h after transfection. (**c**) Densitometric analysis of the western blots shown in panel b. Each bar represents the mean ratio ± s.e., between HMGA2 and vinculin, of three independent experiments. (**d**) qRT–PCR analysis in HMGA2 mRNA in the same samples shown in panel b. Fold-change values indicate the relative change in HMGA2 expression levels between miR-treated and scrambled oligonucleotide-treated cells, normalized with GAPDH. The error bars represent the mean ± s.e. ($n=3$). $^{*}P<0.05$ vs scrambled control.

is regulated by HMGA1 in a dose-dependent manner, with an intermediate expression level in MEFs carrying only one *Hmga1* functional allele. Interestingly, none of the miRNAs analysed showed a significant increase in the MEFs null for *Hmga1*. This result would suggest that, at least in MEFs, the HMGA1 proteins positively regulate a limited number of miRNAs, whereas they do not seem to have a significant negative role in miRNA transcription.

We focused our studies on miR-101b and miR-196a-2, which showed the highest fold-change. This regulation by HMGA1 was also confirmed in other mouse tissues, but not in all those analysed, confirming that the regulation of gene expression by the HMGA1 proteins

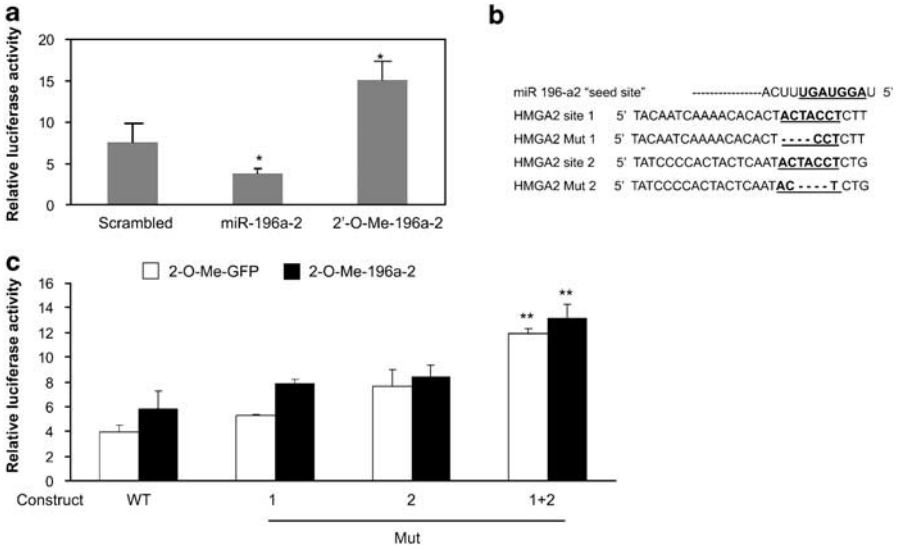

Figure 7 The 3′-UTR of HMGA2 gene enables miR-196a-2 regulation. (**a**) Relative luciferase activity in NIH3T3 cells transiently transfected with miR-196a-2 oligonucleotide (sense and antisense) and a control non-targeting scrambled oligonucleotide. Relative activity of firefly luciferase expression was standardized to a transfection control, using *Renilla* luciferase. The scale bars represent the mean ± s.e. ($n=3$).*$P<0.05$ compared with the scrambled oligonucleotide. (**b**) Schematic representation of the miR-196a-2 site regions (bold and dashed) wild-type and mutated in the constructs used in the luciferase assays shown in panel c. (**c**) Relative luciferase activity in NIH3T3 cells transfected with different constructs shown in panel a. Results are reported as mean expression values of three independent experiments, with error bars indicating standard error. **$P<0.01$.

is dependent on the cellular context. ChIP analysis confirmed that HMGA1 was able to bind to the upstream region of both these miRNAs, suggesting a direct control of the miR-101b and miR-196a-2 expressions by HMGA1.

We looked for possible targets of these miRNAs using appropriate bioinformatic programs. As far as the miR-101b is concerned, two potential targets were identified: the Ataxin1 (ATXN1) and Stanniocalcin1 (STC1) proteins. Overexpression of miR-101b in NIH3T3 cells leads to a reduction of both these proteins, and to a reduced luciferase activity of ATXN1, or STC1 gene 3′-UTR-based reporter constructs. ATXN1 is an RNA-binding protein thought to act as a transcriptional repressor (Yue *et al*, 2001; Irwin *et al*., 2005). The expression of pathogenic ATXN1 protein carrying expanded tracts of polyQ results in Spinocerebellar Ataxia type 1 (SCA1), a disease that decimates cerebellar Purkinje cells and brain stem neurons (Skinner *et al*., 1997). Therefore, it is likely that HMGA1 might have a certain role in the development of the cerebellum, even though *Hmga1*-null mice do not show a gross impairment of the cerebellar functions. Moreover, since HMGA1 is overexpressed in most neuroblastoma tumors (Giannini *et al*., 1999, 2000), it is reasonable to hypothesize that the HMGA1 protein might contribute to the growth of the neuron stem cells, and to their transformation by modulating the ATXN1 expression. Studies are in progress to evaluate ATXN1 protein levels in neuroblastomas. While this manuscript was under submission for publication, a paper showing that the ATXN1 is a target of miR-101b was being published. The authors show that the miR-101b, together with miR-19 and miR-130, cooperatively regulate ATXN1 levels and their inhibition enhanced the cytotoxicity of polyglutamine-expanded ATXN1 in human cells (Lee *et al*., 2008). They confirm that miRNA-mediated post-transcriptional regulation of ATXN1 modulates SCA1 neuropathology by affecting the amount of the protein expressed. These data seem completely consistent with the data reported in this paper.

Another target of the miR-101b is the *STC1* gene. It codes for a homodimeric glycoprotein hormone (Wagner *et al*., 1986). The modulation of its expression has been revealed in numerous developmental, physiological and pathological processes. Recently, STC1 has also been reported to be induced in a variety of tumors including the breast (McCudden *et al*., 2004), colon (Gerritsen *et al*., 2002), ovary (Ismail *et al*., 2000), lung cancer (Garber *et al*., 2001), thyroid medullary carcinoma (Watanabe *et al*., 2002), hepatocarcinoma (Okabe *et al*., 2001), pheochromocytoma (Eisenhofer *et al*., 2004), neuroblastoma (Wong *et al*., 2002), osteosarcoma and fibrosarcoma (Jellinek *et al*., 2000). The possible use of STC1 expression levels for the diagnosis of human breast, hepatocellular and colorectal cancer has also been proposed (Fujiwara *et al*., 2000; Wascher *et al*., 2003). Moreover, it has been shown that the inherited mutations of the *RET* gene, responsible for the MEN2A and MEN2B, are able to induce STC1 expression (Watanabe *et al*., 2002). Recently, a critical role of STC1 expression in the formation of tumor vasculature has been proposed. Indeed, it has been shown that STC1 expression is markedly increased in hypoxia, common phenomenon that occurs in region of most solid human tumor in the latter stage of carcinogenesis (Gerritsen

et al., 2002). STC1 expression would be induced by Hypoxia-inducible factor 1a (Yeung *et al*., 2005) and by vascular endothelial growth factor (Holmes and Zachary, 2008). Therefore, its increased level by miR-101b downregulation after HMGA1 induction might have an important role in the progression step of carcinogenesis in several human neoplasias all featured by HMGA1 overexpression. More recently STC1 has been proposed as a putative proapoptotic factor in the regulation of programmed cell death induced by p53 (Lai *et al*., 2007).

As far as the miR-196a-2 is concerned, we have identified as target the HMGA2 protein, the other member of the HMGA family.

This protein is implicated, through different mechanisms, in both benign and malignant neoplasias. Rearrangements of HMGA genes are a feature of most benign human mesenchymal tumors. Conversely, unrearranged HMGA overexpression is a feature of malignant tumors and is also causally related to neoplastic cell transformation. In fact, the block of the HMGA2 protein synthesis prevents thyroid cell transformation by acute murine retroviruses (Berlingieri *et al*., 1995). Very recently, it has been shown that HMGA2 promotes neural stem cell self-renewal in young mice reducing p16 and p19 (Nishino *et al*., 2008). Then, it is reasonable to hypothesize that the downregulation of miR-196a-2 leading to increased HMGA2 levels could represent a further mechanism by which HMGA1 overexpression can contribute to cell transformation. Also the *HMGA2* gene has been found overexpressed in a large variety of experimental and human malignant neoplasias (Fusco and Fedele, 2007). The identification of HMGA2 as a target of miR-196a-2 might also have some interesting implications in adipocytic cell growth and differentiation, in which HMGA1 and HMGA2 seem to have opposite functions (Battista *et al*., 1999; Melillo *et al*., 2001). Consistent with the results reported here, we have recently found that the HMGA2 expression is increased in the *Hmga1*-null MEFs (De Martino, unpublished data). Moreover, miR-196a-2 would represent the third miRNA able to target the HMGA2 mRNA. In fact, it has been previously shown that *let*-7 (Lee and Dutta, 2007) and miR-98 (Hebert *et al*., 2007) negatively regulate HMGA2 expression.

In conclusion, here we report that HMGA1 proteins are able to positively regulate the expression of miR-101b and miR-196a-2 that have *ATXN1* and *STC1*, and *HMGA2* as genes target, respectively. This could represent another mechanism by which HMGA1 proteins play a role in the processes of differentiation and carcinogenesis.

Materials and methods

Cell lines and transfections

MEFs have been established from wild-type, *Hmga1*$^{+/-}$ and *Hmga1*$^{-/-}$ embryos 12.5 days *post coitum* following standard procedures. Cells were grown in Dulbecco's modified Eagle's medium (DMEM) supplemented with 10% FCS (fetal calf serum), glutamine and non-essential amino acids (Life Technologies Inc., Rockville, MD, USA) in a 5% CO_2 atmosphere. NIH3T3 were cultured at 37 °C (5% CO_2) in DMEM containing 10% FBS (fetal bovine serum) supplemented with penicillin and streptomycin in a humidified atmosphere of 95% air and 5% CO_2.

For transfection assay, NIH3T3 cells were plated at a density of 2.5×10^5 cells/well, in six-well plates, with three replicate wells for each condition, and transfected with Lipofectamine 2000 (Invitrogen, Carlsbad, CA, USA) according to the manufacturer's instructions. 2′-O-Me-101b (CUUC AGCUAUCACAGUACUGUAL) and 2′-O-Me-196a-2 (CC AACAACAUGAAACUACCUAL) oligonucleotides were used in the antisense experiments. All 2′-O-methyl oligonucleotides were synthesized by Fidelity Systems, Inc. (Gaithersburg, MD, USA) as described previously (Meister *et al*., 2004) and were used at 200 nM concentration. RNA oligonucleotides corresponding to pre-miR negative control (no. AM17110, Ambion, Austin, TX, USA), pre-miR-101b (AM12364) and pre-miR-196a-2AM10068) were used at 100 nM final concentration in the sense experiments.

RNA extraction and quantitative reverse transcription-PCR

Total RNA isolation from mouse tissues and cells was carried out with Trizol (Invitrogen) according to the manufacturer's instructions. The integrity of the RNA was assessed by denaturing agarose gel electrophoresis (virtual presence of sharp 28S and 18S bands). Spectrophotometry qRT–PCRs analysis were carried out on the RNA isolated from tissues and MEFs of *Hmga1*-knockout mice and from transfected cells by using AmpliTaq DNA polymerase (Applied Biosystems, Foster City, CA, USA) and the *mir*Vana qRT–PCR miRNA Detection Kit (Ambion) following the manufacturer's instructions. Reactions contained *mir*Vana qRT–PCR Primer Sets (Ambion), specific for miR-101b, miR-196a-2 and GAPDH (used to normalize RNA levels). A qRT–PCR analysis for ATXN1, STC1 and HMGA2 mRNA was carried out by using TaqMan Gene Expression Assay (Ambion).

miRNA microarray

Microarray experimental procedures were performed as described earlier (Liu *et al*., 2004). Briefly, labeled targets from 5 μg of total RNA from each sample were biotin-labeled during reverse transcription using random hexamers. Hybridization was carried out on miRNA microarray (KCI version 1.0; (Liu *et al*., 2004)) containing 368 probes in triplicate, corresponding to 245 human and mouse miRNA genes. Hybridization signals were detected by biotin binding of a Streptavidin-Alexa 647 conjugate using a Perkin-Elmer ScanArray XL5K (Perkin-Elmer, Wellesley, MA, USA). Scanner images were quantified by the Quantarray software. Raw data were normalized and analysed in GENESPRING software, version 7.2 (Silicon Genetics, Redwood City, CA, USA). Expression data were median-centered by using the GENESPRING normalization option.

Quantitative RT-PCR for miRNA precursors

Quantitative real-time PCR was performed as described by (Schmittgen *et al*., 2004). Briefly, RNA was reverse transcribed to cDNA with gene-specific primers and Thermoscript (Invitrogen), and the relative amount of each miRNA was normalized to the GAPDH RNA using the equation $2^{-\Delta C_T}$, where $\Delta C_T = (C_{T\ \mathrm{miRNA}} - C_{T\ \mathrm{GAPDH\ RNA}})$. PCR reactions were carried out in triplicate using iCycler (Bio-Rad, Hercules, CA, USA) with SYBR Green PCR Master Mix (Applied Biosystems, Foster City, CA, USA) as follows: 95 °C for 10 min and

40 cycles (95 °C for 15 s and 60 °C for 1 min). A dissociation curve was run after each PCR reaction to verify amplification specificity. The miRNAs analysed included miR-196a-2 and miR-101b precursors. The primers used were described in Supplementary Table 1.

Plasmids and constructs

The 3′-UTR region of *STC1* and *ATXN1* genes including binding sites for miR-101b, and the 3′-UTR region of HMGA2 gene including binding sites for miR-196a-2, were amplified by PCR from genomic DNA by using the primers described in Supplementary Table 1.

The amplified fragments were cloned into pGL_3-Control firefly luciferase vector (Promega, Madison, WI, USA) at the XbaI site immediately downstream from the stop codon of luciferase.

Deletions into the miR-101b-binding sites of the *ATXN1* gene or *STC1* gene, 3′-UTR or into the miR-196a-2-binding sites of the *Hmga2* gene, 3′-UTR were introduced by using QuikChange Site-Directed Mutagenesis Kit (Stratagene, La Jolla, CA, USA) following the manufacturer's instructions. The primers used are listed in Supplementary Table 1.

Transfection efficiency was corrected by transfection of *Renilla* luciferase vector (pRL-CMV, Promega).

Luciferase target assays

NIH3T3 cells were co-transfected in 12-well plates with the modified firefly luciferase vector described above, the *Renilla* luciferase reporter plasmid and with the RNA oligonucleotides. Firefly and *Renilla* luciferase activities were measured 24 h after transfection with the Dual-Luciferase Reporter Assay System (Promega). Firefly activity was normalized to *Renilla* activity as control of the transfection efficiency.

Protein extraction, western blotting, and antibodies

Tissues and cells were lysed in lysis buffer containing 1% NP-40, 1 mM EDTA, 50 mM Tris-HCl (pH 7.5) and 150 mM NaCl, supplemented with complete protease inhibitors mixture (Roche Diagnostic Corp., Indianapolis, IN, USA). Total proteins were separated by SDS-polyacrylamide gel electrophoresis and transferred to nitrocellulose membranes (Bio-Rad). Membranes were blocked with 5% nonfat milk and incubated with antibodies against STC1 (sc-14346, Santa Cruz Biotechnology Inc., Santa Cruz, CA, USA), ATXN1 (sc-8766, Santa Cruz Biotechnology Inc.), HMGA2 (polyclonal rabbit antibody raised against a synthetic peptide located in the NH2-terminal region), vinculin (sc-7649, Santa Cruz Biotechnology Inc.). Bound antibody was detected by the appropriate secondary antibody and revealed with an enhanced chemiluminescence system (Amersham-Pharmacia Biotech, Piscataway, NJ, USA). The level of expression of different proteins was analysed by using the public domain software Image J (a Java image processing program inspired by National Institutes of Health (NIH) Image for Macintosh) by working in a linear range. It can calculate area and pixel value statistics of user-defined selections. Briefly, it was done as follows: X-ray films were scanned and saved as eight-bit grayscale JPEG files. The percentage of measurable pixels in the image was set (and highlighted in red) by using the adjust image threshold command. The number of square pixels in the section selected (the protein bands) was then counted by measuring the area in the binary or threshold image.

ChIP

Approximately 3×10^7 *Hmga1*$^{+/+}$, *Hmga1*$^{+/-}$ and *Hmga1*$^{-/-}$ MEFs were grown on 75 cm^2 dishes. ChIP was carried out with a ChIP assay kit (Upstate Biotechnology, Lake Placid, NY, USA) according to the manufacturer's instruction. PCR reactions were performed with AmpliTaq gold DNA polymerase (Perkin-Elmer). The recovered DNA was PCR-amplified with the primers described in Supplementary Table 1.

Statistical analysis

For the comparison between two groups of experiments, Student's *t*-test was used. The statistical significant difference was considered when *P*-value was less than 0.05. miRNA microarray data were compared with the GENESPRING ANOVA tool.

Acknowledgements

We thank Professor Stefano Volinia for miRNA microarray data analysis. This work was supported by grants from the Associazione Italiana Ricerca sul Cancro (AIRC), and the Ministero dell'Università e della Ricerca Scientifica e Tecnologica (MIUR). This work was supported from NOGEC-Naples Oncogenomic Center. We thank the Associazione Partenopea per le Ricerche Oncologiche (APRO) for its support.

References

Ashar HR, Fejzo MS, Tkachenko A, Zhou X, Fletcher JA, Weremowicz S *et al*. (1995). Disruption of the architectural factor HMGI-C: DNA-binding AT hook motifs fused in lipomas to distinct transcriptional regulatory domains. *Cell* **82**: 57–65.

Baldassarre G, Fedele M, Battista S, Vecchione A, Klein-Szanto AJ, Santoro M *et al*. (2001). Onset of natural killer cell lymphomas in transgenic mice carrying a truncated HMGI-C gene by the chronic stimulation of the IL-2 and IL-15 pathway. *Proc Natl Acad Sci USA* **98**: 7970–7975.

Battista S, Fidanza V, Fedele M, Klein-Szanto AJ, Outwater E, Brunner H *et al*. (1999). The expression of a truncated HMGI-C gene induces gigantism associated with lipomatosis. *Cancer Res* **59**: 4793–4797.

Berlingieri MT, Manfioletti G, Santoro M, Bandiera A, Visconti R, Giancotti V *et al*. (1995). Inhibition of HMGI-C protein synthesis suppresses retrovirally induced neoplastic transformation of rat thyroid cells. *Mol Cell Biol* **15**: 1545–1553.

Chang AC, Janosi J, Hulsbeek M, de Jong D, Jeffrey KJ, Noble JR *et al*. (1995). A novel human cDNA highly homologous to the fish hormone stanniocalcin. *Mol Cell Endocrinol* **112**: 241–247.

Chang AC, Jellinek DA, Reddel RR. (2003). Mammalian stanniocalcins and cancer. *Endocr Relat Cancer* **10**: 359–373.

Chiappetta G, Avantaggiato V, Visconti R, Fedele M, Battista S, Trapasso F *et al*. (1996). High level expression of the HMGI (Y) gene during embryonic development. *Oncogene* **13**: 2439–2446.

De Martino I, Visone R, Palmieri D, Cappabianca P, Chieffi P, Forzati F *et al*. (2007). The *Mia*/*Cd-rap* gene expression is downregulated by the HMGA proteins in mouse pituitary adenomas. *Endocr Relat Cancer* **14**: 875–886.

Eisenhofer G, Huynh TT, Pacak K, Brouwers FM, Walther MM, Linehan WM *et al*. (2004). Distinct gene expression profiles in norepinephrine- and epinephrine-producing hereditary and sporadic pheochromocytomas: activation of hypoxia-driven angiogenic

pathways in von Hippel-Lindau syndrome. *Endocr Relat Cancer* **11**: 897–911.

Fedele M, Berlingieri MT, Scala S, Chiariotti L, Viglietto G, Rippel V *et al*. (1998). Truncated and chimeric HMGI-C genes induce neoplastic transformation of NIH3T3 murine fibroblasts. *Oncogene* **17**: 413–418.

Fedele M, Battista S, Manfioletti G, Croce CM, Giancotti V, Fusco A. (2001). Role of the high mobility group A proteins in human lipomas. *Carcinogenesis* **22**: 1583–1591. Review.

Fedele M, Battista S, Kenyon L, Baldassarre G, Fidanza V, Klein-Szanto AJ *et al*. (2002). Overexpression of the HMGA2 gene in transgenic mice leads to the onset of pituitary adenomas. *Oncogene* **21**: 3190–3198.

Fedele M, Pentimalli F, Baldassarre G, Battista S, Klein-Szanto AJ, Kenyon L *et al*. (2005). Transgenic mice overexpressing the wild-type form of the HMGA1 gene develop mixed growth hormone/prolactin cell pituitary adenomas and natural killer cell lymphomas. *Oncogene* **24**: 3427–3435.

Fedele M, Fidanza V, Battista S, Pentimalli F, Klein-Szanto AJ, Visone R *et al*. (2006). Haploinsufficiency of the Hmga1 gene causes cardiac hypertrophy and myelo-lymphoproliferative disorders in mice. *Cancer Res* **66**: 2536–2543.

Foti D, Chiefari E, Fedele M, Iuliano R, Brunetti L, Paonessa F *et al*. (2005). Lack of the architectural factor HMGA1 causes insulin resistance and diabetes in humans and mice. *Nat Med* **7**: 765–773.

Fujiwara Y, Sugita Y, Nakamori S, Miyamoto A, Shiozaki K, Nagano H *et al*. (2000). Assessment of Stanniocalcin-1 mRNA as a molecular marker for micrometastases of various human cancers. *Int J Oncol* **16**: 799–804.

Fusco A, Fedele M. (2007). Roles of HMGA proteins in cancer. *Nat Rev Cancer* **12**: 899–910. Review.

Galardi S, Mercatelli N, Giorda E, Massalini S, Frajese GV, Ciafrè SA *et al*. (2007). miR-221 and miR-222 expression affects the proliferation potential of human prostate carcinoma cell lines by targeting p27Kip1. *J Biol Chem* **282**: 23716–23724.

Garber ME, Troyanskaya OG, Schluens K, Petersen S, Thaesler Z, Pacyna-Gengelbach M *et al*. (2001). Diversity of gene expression in adenocarcinoma of the lung. *Proc Natl Acad Sci USA* **98**: 13784–13789.

Gerritsen ME, Soriano R, Yang S, Ingle G, Zlot C, Toy K *et al*. (2002). In silico data filtering to identify new angiogenesis targets from a large *in vitro* gene profiling data set. *Physiol Genomics* **10**: 13–20.

Giannini G, Di Marcotullio L, Ristori E, Zani M, Crescenzi M, Scarpa S *et al*. (1999). HMGI(Y) and HMGI-C genes are expressed in neuroblastoma cell lines and tumors and affect retinoic acid responsiveness. *Cancer Res* **59**: 2484–2492.

Giannini G, Kim CJ, Di Marcotullio L, Manfioletti G, Cardinali B, Cerignoli F *et al*. (2000). Expression of the HMGI(Y) gene products in human neuroblastic tumours correlates with differentiation status. *Br J Cancer* **83**: 1503–1509.

Hebert C, Norris K, Scheper MA, Nikitakis N, Sauk JJ. (2007). High mobility group A2 is a target for miRNA-98 in head and neck squamous cell carcinoma. *Mol Cancer* **6**: 5.

Holmes DI, Zachary IC. (2008). Vascular endothelial growth factor regulates stanniocalcin-1 expression via neuropilin-1-dependent regulation of KDR and synergism with fibroblast growth factor-2. *Cell Signal* **20**: 569–579.

Irwin S, Vandelft M, Pinchev D, Howell JL, Graczyk J, Orr HT *et al*. (2005). RNA association and nucleocytoplasmic shuttling by ataxin-1. *J Cell Sci* **118**: 233–242.

Ishibashi K, Imai M. (2002). Prospect of a stanniocalcin endocrine/paracrine system in mammals. *Am J Physiol Renal Physiol* **282**: F367–F375.

Ismail RS, Baldwin RL, Fang J, Browning D, Karlan BY, Gasson JC *et al*. (2000). Differential gene expression between normal and tumor-derived ovarian epithelial cells. *Cancer Res* **60**: 6744–6749.

Jellinek DA, Chang AC, Larsen MR, Wang X, Robinson PJ, Reddel RR. (2000). Stanniocalcin 1 and 2 are secreted as phosphoproteins from human fibrosarcoma cells. *Biochem J* **350**: 453–461.

Johnson KR, Lehn DA, Reeves R. (1989). Alternative processing of mRNAs encoding mammalian chromosomal high-mobility-group proteins HMG-I and HMG-Y. *Mol Cell Biol* **9**: 2114–2123.

Kent OA, Mendell JT. (2006). A small piece in the cancer puzzle: microRNAs as tumor suppressors and oncogenes. *Oncogene* **25**: 6188–6196. Review.

Lai KP, Law AY, Yeung HY, Lee LS, Wagner GF, Wong CK. (2007). Induction of stanniocalcin-1 expression in apoptotic human nasopharyngeal cancer cells by p53. *Biochem Biophys Res Commun* **356**: 968–975.

Lee Y, Samaco RC, Gatchel JR, Thaller C, Orr HT, Zoghbi HY. (2008). miR-19, miR-101 and miR-130 co-regulate ATXN1 levels to potentially modulate SCA1 pathogenesis. *Nat Neurosci* **11**: 1137–1139.

Lee YS, Dutta A. (2007). The tumor suppressor microRNA let-7 represses the HMGA2 oncogene. *Genes Dev* **21**: 1025–1030.

Liu CG, Calin GA, Meloon B, Gamliel N, Sevignani C, Ferracin M *et al*. (2004). An oligonucleotide microchip for genome-wide microRNA profiling in human and mouse tissues. *Proc Natl Acad Sci USA* **101**: 9740–9744.

Manfioletti G, Giancotti V, Bandiera A, Buratti E, Sautiere P, Cary P *et al*. (1991). cDNA cloning of the HMGI-C phosphoprotein, a nuclear protein associated with neoplastic and undifferentiated phenotypes. *Nucleic Acids Res* **19**: 6793–6797.

Martinez Hoyos J, Fedele M, Battista S, Pentimalli F, Kruhoffer M, Arra C *et al*. (2004). Identification of the genes up- and down-regulated by the high mobility group A1 (HMGA1) proteins: tissue specificity of the HMGA1-dependent gene regulation. *Cancer Res* **64**: 5728–5735.

McCudden CR, Majewski A, Chakrabarti S, Wagner GF. (2004). Co-localization of stanniocalcin-1 ligand and receptor in human breast carcinomas. *Mol Cell Endocrinol* **213**: 167–172.

Meister G, Landthaler M, Dorsett Y, Tuschl T. (2004). Sequence-specific inhibition of microRNA- and siRNA-induced RNA silencing. *RNA* **10**: 544–550.

Melillo RM, Pierantoni GM, Scala S, Battista S, Fedele Mv, Stella A *et al*. (2001). Critical role of the HMGI(Y) proteins in adipocytic cell growth and differentiation. *Mol Cell Biol* **21**: 2485–2495.

Meng F, Henson R, Wehbe-Janek H, Ghoshal K, Jacob ST, Patel T. (2007). MicroRNA-21 regulates expression of the PTEN tumor suppressor gene in human hepatocellular cancer. *Gastroenterology* **133**: 647–658.

Miska EA. (2005). How microRNAs control cell division, differentiation, and death. *Curr Opin Genet Dev* **5**: 563–568.

Negrini M, Ferracin M, Sabbioni S, Croce CM. (2007). MicroRNAs in human cancer: from research to therapy. *J Cell Sci* **120**: 1833–1840.

Nishino J, Kim I, Chada K, Morrison SJ. (2008). Hmga2 promotes neural stem cell self-renewal in young but not old mice by reducing $p16^{Ink4a}$ and $p19^{Arf}$ expression. *Cell* **135**: 227–239.

Olsen HS, Cepeda MA, Zhang QQ, Rosen CA, Vozzolo BL. (1996). Human stanniocalcin: a possible hormonal regulator of mineral metabolism. *Proc Natl Acad Sci USA* **93**: 1792–1796.

Okabe H, Satoh S, Kato T, Kitahara O, Yanagawa R, Yamaoka Y *et al*. (2001). Genome-wide analysis of gene expression in human hepatocellular carcinomas using cDNA microarray: identification of genes involved in viral carcinogenesis and tumor progression. *Cancer Res* **61**: 2129–2137.

Reeves R, Nissen MS. (1990). The AT DNA binding domain of mammalian high mobility group I chromosomal protein. A novel peptide motif for recognizing DNA structure. *J Biol Chem* **265**: 8576–8582.

Scala S, Portella G, Fedele M, Chiappetta G, Fusco A. (2000). Adenovirus-mediated suppression of HMGI(Y) protein synthesis as potential therapy of human malignant neoplasias. *Proc Natl Acad Sci USA* **97**: 4256–4261.

Schmittgen TD, Jiang J, Liu Q, Yang L. (2004). A high-throughput method to monitor the expression of microRNA precursors. *Nucleic Acids Res* **32**: e43.

Schoenmakers EF, Wanschura S, Mols R, Bullerdiek J, Van den Berghe H, Van de Ven WJ. (1995). Recurrent rearrangements in the high mobility group protein gene, HMGI-C, in benign mesenchymal tumors. *Nat Genet* **10**: 436–444.

Servadio A, Koshy B, Armstrong D, Antalffy B, Orr HT, Zoghbi HY. (1995). Expression analysis of the ataxin-1 protein in tissues from normal and spinocerebellar ataxia type 1 individuals. *Nat Genet* **10**: 94–98.

Skinner PJ, Koshy BT, Cummings CJ, Klement IA, Helin K, Servadio A *et al*. (1997). Ataxin-1 with an expanded glutamine tract alters nuclear matrix-associated structures. *Nature* **389**: 971–974.

Tallini G, Dal Cin P. (1999). HMGI(Y) and HMGI-C dysregulation: a common occurrence in human tumors. *Adv Anat Pathol* **6**: 237–246.

Thanos D, Maniatis T. (1995). Virus induction of human IFN ß gene expression requires the assembly of an enhanceosome. *Cell* **83**: 1091–1100.

Tsai CC, Kao HY, Mitzutani A, Banayo E, Rajan H, McKeown M *et al*. (2004). Ataxin 1, a SCA1 neurodegenerative disorder protein, is functionally linked to the silencing mediator of retinoid and thyroid hormone receptors. *Proc Natl Acad Sci USA* **101**: 4047–4052.

Varghese R, Wong CK, Deol H, Wagner GF, DiMattia GE. (1998). Comparative analysis of mammalian stanniocalcin genes. *Endocrinology* **139**: 4714–4725.

Visone R, Russo L, Pallante P, De Martino I, Ferraro A, Leone V *et al*. (2007). MicroRNAs (miR)-221 and miR-222, both overexpressed in human thyroid papillary carcinomas, regulate p27Kip1 protein levels and cell cycle. *Endocr Relat Cancer* **14**: 791–798.

Wagner GF, Hampong M, Park CM, Copp DH. (1986). Purification, characterization, and bioassay of teleocalcin, a glycoprotein from salmon corpuscles of Stannius. *Gen Comp Endocrinol* **63**: 481–491.

Wascher RA, Huynh KT, Giuliano AE, Hansen NM, Singer FR, Elashoff D *et al*. (2003). Stanniocalcin-1: a novel molecular blood and bone marrow marker for human breast cancer. *Clin Cancer Res* **9**: 1427–1435.

Watanabe T, Ichihara M, Hashimoto M, Shimono K, Shimoyama Y, Nagasaka T *et al*. (2002). Characterization of gene expression induced by RET with MEN2A or MEN2B mutation. *Am Pathol* **161**: 249–256.

Wong CK, Yeung HY, Mak NK, DiMattia GE, Chan DK, Wagner GF. (2002). Effects of dibutyryl cAMP on stanniocalcin and stanniocalcin-related protein mRNA expression in neuroblastoma cells. *J Endocrinol* **173**: 199–209.

Yeung HY, Lai KP, Chan HY, Mak NK, Wagner GF, Wong CK. (2005). Hypoxia-inducible factor-1-mediated activation of stanniocalcin-1 in human cancer cells. *Endocrinology* **146**: 4951–4960.

Yue S, Serra HG, Zoghbi HY, Orr HT. (2001). The spinocerebellar ataxia type 1 protein, ataxin-1, has RNA-binding activity that is inversely affected by the length of its polyglutamine tract. *Hum Mol Genet* **10**: 25–30.

Zamore PD, Haley B. (2005). Ribo-gnome: the big world of small RNAs. *Science* **309**: 1519–1524.

Zhou X, Benson KF, Ashar HR, Chada K. (1995). Mutation responsible for the mouse pygmy phenotype in the developmentally regulated factor HMGI-C. *Nature* **376**: 771–774.

Supplementary Information accompanies the paper on the Oncogene website (http://www.nature.com/onc)

HMGA Proteins Up-regulate *CCNB2* Gene in Mouse and Human Pituitary Adenomas

Ivana De Martino,[1,5] Rosa Visone,[1,5] Anne Wierinckx,[6] Dario Palmieri,[1,5] Angelo Ferraro,[5] Paolo Cappabianca,[2] Gennaro Chiappetta,[4] Floriana Forzati,[1,5] Gaetano Lombardi,[3] Annamaria Colao,[3] Jacqueline Trouillas,[6] Monica Fedele,[1,5] and Alfredo Fusco[1,5]

[1]Istituto di Endocrinologia ed Oncologia Sperimentale del Consiglio Nazionale delle Ricerche c/o Dipartimento di Biologia e Patologia Cellulare e Molecolare, Facoltà di Medicina e Chirurgia di Napoli, [2]Dipartimento di Scienze Neurologiche, Divisione di Neurochirurgia, and [3]Dipartimento di Endocrinologia, Universita' degli Studi di Napoli Federico II, [4]Istituto Nazionale dei Tumori, Fondazione Pascale, and [5]Naples Oncogenomic Center-CEINGE, Biotecnologie Avanzate-Napoli and SEMM-European School of Molecular Medicine-Naples Site, Naples, Italy; and [6]Institut National de la Sante et de la Recherche Medicale, Lyon, France

Abstract

The high mobility group As (HMGAs) belong to a family of nonhistone nuclear proteins that orchestrate the assembly of nucleoprotein complexes. Through a complex network of protein-DNA and protein-protein interaction, they play important roles in gene transcription, recombination, and chromatin structure. This protein family is involved, through different mechanisms, in both benign and malignant neoplasias. We have recently reported that transgenic mice carrying the *Hmga1* or *Hmga2* genes under transcriptional control of the cytomegalovirus promoter develop pituitary adenomas secreting prolactin and growth hormone. We have shown that the mechanism of the HMGA2-induced pituitary adenoma is based on the increased E2F1 activity. The expression profile of mouse normal pituitary glands and adenomas induced in HMGA transgenic mice revealed an increased expression of the *ccnb2* gene, coding for the cyclin B2 protein, in the neoplastic tissues compared with the normal pituitary gland. Here, we show, by electrophoretic mobility shift assay and chromatin immunoprecipitation, a direct binding of HMGA proteins to the promoter of *ccnb2* gene, whereas luciferase assays showed that HMGAs are able to up-regulate *ccnb2* promoter activity. Finally, we report an increased *CCNB2* expression in human pituitary adenomas of different histotypes that is directly correlated with *HMGA1* and *HMGA2* expression. Because cyclin B2 is involved in the regulation of the cell cycle, these results taken together indicate that HMGA-induced cyclin B2 overexpression gives an important contribution to experimental and human pituitary tumorigenesis. [Cancer Res 2009;69(5):1844–50]

Introduction

The high mobility group A (HMGA) protein family includes HMGA1a and HMGA1b, which are encoded by the same gene through alternative splicing (1), as well as the closely related HMGA2 protein (2). These proteins are nonhistone architectural nuclear factors, which bind the minor groove of AT-rich DNA sequences through three short basic repeats, called "AT-hooks"", located at the NH_2- terminal region of the proteins. The involvement of HMGA proteins in embryogenesis, cell proliferation, differentiation, apoptosis and, above all, cancer development has been extensively shown (3). In particular, HMGA proteins seem to play their major physiologic role during embryonic development. In fact, their expression is very high during embryogenesis, whereas it is very low or negligible in normal adult tissues (4, 5). Conversely, HMGA protein expression has been found abundant in several malignant neoplasias, including pancreas, thyroid, colon, breast, lung, ovary, prostate carcinomas, squamous carcinomas of the oral cavity, and head and neck tumors (6).

Both *HMGA1* and *HMGA2* show oncogenic activity *in vitro* and *in vivo*: they are able to transform mouse and rat fibroblasts in culture (7, 8), and both the HMGA1 and HMGA2 transgenic mice develop GH/PRL-secreting pituitary adenomas and T/NK lymphomas (9–11). Recently, we have reported that HMGA2-mediated E2F1 activation is a crucial event in the onset of these tumors in transgenic mice (12), and likely also in human prolactinomas where *HMGA2* gene amplification and overexpression have been shown (13). To identify other genes involved in the process of pituitary tumorigenesis induced by the *HMGA* genes, we have analyzed the gene expression profile of two HMGA1- and three HMGA2-pituitary adenomas in comparison with a pool of 10 normal pituitary glands from control mice using the Affymetrix MG MU11K oligonucleotide array representing ~13,000 unique genes. Among these genes, we previously focused our attention on the *Mia/Cd-rap* gene, whose expression was essentially suppressed in all pituitary adenomas tested by cDNA microarray. We showed that the HMGA proteins directly bind to the promoter of the *Mia/Cd-rap* gene and are able to down-regulate its expression (14).

Here, we focus our attention on the *ccnb2* gene, coding for the cyclin B2 protein, which showed an 8-fold change increase in the pituitary adenomas in comparison with normal pituitary glands from control mice (14). Cyclin B2 is a member of the B-type cyclin family, including B1 and B2. The B-type cyclins associate with $p34^{cdc2}$ kinase and are essential components of the cell cycle regulatory machinery, being directly involved in the G_2-M transition (15). Consistent with this finding, *ccnb2*-knockout mice, although develop normally, are smaller than normal mice and have reduced litter sizes, which suggests that cyclin B2 expression gives some growth advantage (16). Moreover, several studies have reported the accumulation of Cyclins B1 and B2 in human malignant tumors, such as colorectal and lung cancer (17–20). Also, in human pituitary adenomas cyclins amplification and

Requests for reprints: Monica Fedele, Istituto di Endocrinologia ed Oncologia Sperimentale del Consiglio Nazionale delle Ricerche, via Pansini 5, 80131 Naples, Italy. Phone: 39-081-7463054; Fax: 39-081-7463749; E-mail: mfedele@unina.it or monica.fedele@cnr.it or Alfredo Fusco, Istituto di Endocrinologia ed Oncologia Sperimentale del Consiglio Nazionale delle Ricerche, via Pansini 5, 80131 Naples, Italy. Phone: 39-081-7463602; Fax: 39-081-2296674; E-mail: afusco@napoli.com or alfusco@unina.it.

doi:10.1158/0008-5472.CAN-08-4133

overexpression have been observed (21–23). More specifically, in human prolactinomas, an increase of *CCNB1* mRNA expression, related to aggressiveness, has been recently reported (24).

Here, we report that HMGA proteins are able to bind *in vitro* and *in vivo* the promoter of *cyclin B2* gene, and to up-regulate its activity. Furthermore, an increased expression of Cyclin B2, correlated with HMGA1 and HMGA2 expression, has been shown in human pituitary adenomas of different histotypes, suggesting its contribution to the process of human pituitary tumorigenesis where HMGA proteins are involved.

Materials and Methods

Cell cultures. NIH3T3 cells were grown in DMEM supplemented with 10% FCS. AtT20 and aT3-1 are murine pituitary adenoma cells secreting adrenocorticorticotropic hormone (ACTH) and gonadotroph hormones, respectively. RC-4B/C are rat pituitary adenoma cells secreting GH, follicle-stimulating hormone (FSH), luteinizing hormone, GnRH, ACTH, and TSHb, whereas GH1, GH3, and GH4c1 are rat pituitary adenoma cells secreting prolactin and growth hormone. All these cell lines, purchased from American Type Culture Collection, were cultured in DMEM containing 10% fetal bovine serum (HyClone) and 50 μg/mL gentamicin (Life Technologies, Inc.) in a humidified atmosphere of 95% air and 5% CO_2.

Cyclin B2 promoter construct, transient transfection, and luciferase assay. The wild-type cyclin B2-luciferase vector (B2-luci) was generously provided by Giulia Piaggio (25). Transfections for luciferase assays were carried out in NIH3T3 mouse fibroblasts and GH3 rat pituitary adenoma cells by using Lipofectamine 2000 method (Invitrogen) and microporator MP-100 (Digital Bio), respectively, according to the manufacturer's instructions. A total of 2×10^5 NIH3T3 cells and 4×10^6 GH3 cells were transiently transfected with 1 μg of B2-luci and with the indicate amounts of pCEFLHa-HMGA1 (26) and pCEFLHa-HMGA2 (12), together with 0.5 μg of Renilla and various amounts of the pCEFLHa plasmid to keep the total DNA concentration constant. Transfection efficiencies were normalized by using Renilla luciferase expression assayed with the dual luciferase system (Promega). All tranfection experiments were repeated at least thrice.

Protein extraction and Western blot. Tissues and cell culture were lysed in buffer 1% NP40, 1 mmol/L EDTA, 50 mmol/L Tris-HCl (pH 7.5), and 150 mmol/L NaCl, supplemented with complete protease inhibitors mixture (Roche Diagnostic Corp.). Total proteins were separated by SDS-PAGE and transferred to nitrocellulose membranes (Bio-Rad). Membranes were blocked with 5% nonfat milk and incubated with antibody against Cyclin B2 (N-20 Santa Cruz, sc-5235). Bound antibody was detected by the appropriate secondary antibody and revealed with an enhanced chemiluminescence system (Amersham-Pharmacia Biotech).

Tissue samples. The human samples were obtained from 45 patients as surgical excision biopsies from patients of "Federico II" University (Naples) and "Faculté de Médecine Lyon-RTH Laennec" (Lyon). One part of pituitary adenoma was saved for routine histopathology evaluation and the other one taken from each patient was immediately frozen at −80°C until the extraction of nucleic acids. All tissue samples were fixed immediately after surgical removal in a solution of 4% paraformaldehyde in PBS w/v. The criteria for inclusion in the study were that the routinely processed paraffin blocks were suitable for immunohistochemistry and adequate clinical information.

Immunohistochemical analysis. Paraffin sections (5–6 μm) were deparaffinized, placed in a solution of absolute methanol and 0.3% hydrogen peroxide v/v for 30 min, and then washed in PBS before immunoperoxidase staining. The slides were subsequently incubated with biotinylated goat anti-rabbit/anti-mouse IgG for 20 min (Dako LSAB2 System) and then with streptavidin horseradish peroxidase for 20 more min. For immunostaining, the slides were incubated in diaminobenzidine (DAB-DAKO) solution containing 0.06 mmol/L DAB and 2 mmol/L hydrogen peroxide in 0.05% PBS v/v (pH 7.6) for 5 min. After chromogen development, the slides were washed, dehydrated with alcohol and xylene, and mounted with coverslips using a permanent mounting medium (Permount). Micrographs were taken on Kodak Ektachrome film with a photo Zeiss system. For Cyclin B2 immunohistochemistry, antibodies (2 μg/mL) raised against the recombinant Cyclin B2 protein were used. The specificity of the reaction was validated by the absence of staining when carcinoma samples were stained with antibodies preincubated with the peptide against which the antibodies were raised. Similarly, no positivity was observed when tumor samples were stained with a preimmune serum.

RNA extraction, cDNA preparation, semiquantitative and quantitative reverse transcription-PCR. Total RNA isolation from human tissues was performed with Trizol (Invitrogen) according to the manufacturer's instructions. RNA was extracted from fresh specimens after pulverizing the

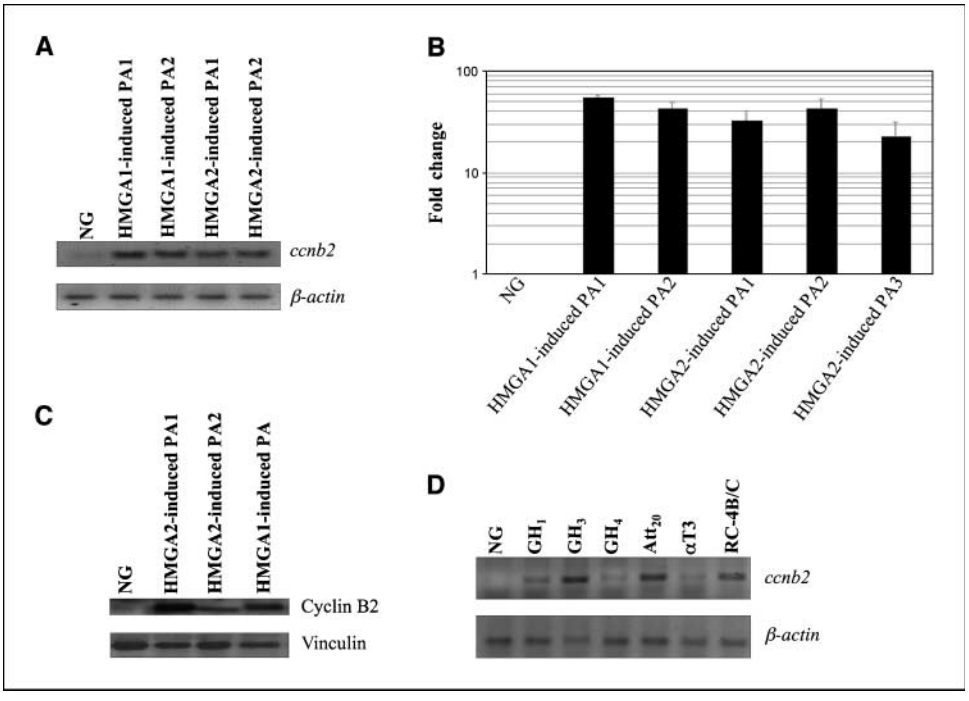

Figure 1. Cyclin B2 expression in pituitary adenomas developing in HMGA-transgenic mice and pituitary adenoma cell lines. The expression of *ccnb2* gene has been studied by semi–qRT-PCR (*A*) and qRT-PCR (*B*) on a panel of HMGA2- and HMGA1-induced pituitary adenomas as well as on a pool of wild-type pituitary glands (*NG*). *C,* cyclin B2 protein expression in pituitary adenomas and normal pituitary glands from HMGA- (both HMGA1 and HMGA2) transgenic and wild-type mice, respectively. *D, Ccnb2* gene expression was assayed by semi–qRT-PCR on a panel of seven cell lines originating from rat and mouse pituitary adenomas of different histotype in comparison with a pool of wild-type mouse and rat pituitary glands. Amplification of the β-*actin* gene as well as incubation with vinculin-specific antibodies have been performed as controls for the RNA and protein amounts used, respectively.

tumors with a stainless steel mortar and pestle that were chilled on dry ice. The integrity of the RNA was assessed by denaturing agarose gel electrophoresis. One microgram of total RNA of each sample was reverse-transcribed with the QuantiTect Reverse Transcription (QIAGEN group) using an optimized blend of oligo-dT and random primers according to the manufacturer's instructions. One microgram of total RNA of each sample was reverse-transcribed with the QuantiTect Reverse Transcription (QIAGEN group) using an optimized blend of oligo-dT and random primers according to the manufacturer's instructions. To ensure that RNA samples were not contaminated with DNA, negative controls were obtained by performing the PCR on samples that were not reverse transcribed but identically processed. For semiquantitative PCR, reactions were optimized for the number of cycles to ensure product intensity within the linear phase of amplification. The PCR products were separated on a 2% agarose gel, stained with ethidium bromide, and scanned using a Typhoon 9200 scanner. Digitized data were analyzed using Imagequant (Molecular Dynamics). The primer sequences for the amplification of the murine *cyclin B2* gene are as follows: 5′-CCTCAGAACACCAAAGTACC-3 (forward) and 5′-CTTCATGGA-GACATCCTCAG-3′ (reverse).

Quantitative PCR was performed with SYBR Green PCR Master Mix (Applied Biosystems) as follows: 95°C 10 min and 40 cycles (95°C 15 s and 60°C 1 min). A dissociation curve was run after each PCR to verify amplification specificity. Each reaction was performed in duplicate. To calculate the relative expression levels, we used the $2^{-\Delta\Delta CT}$ method (27).

The primer sequences for the amplification of the human genes are:

Cyclin B2 forward: 5′-TGGAAAAGTTGGCTCCAAAG-3′,
Cyclin B2 reverse 5′-TCAGAAAAAGCTTGGCAGAGA-3′,
HMGA2 forward: 5′-GCGCCTCAGAAGAGAGGAC-3′,
HMGA2 reverse 5′-GGTCTCTTAGGAGAGGGCTCA-3′
HMGA1 forward 5′-AAAAGGACGGCACTGAGAAG-3′,
HMGA1 reverse 5′-CTCTTAGGTGTTGGCACTTCG-3′,
G6PDH forward: 5′-ACAGAGTGAGCCCTTCTTCAA-3′,
G6PDH reverse 5′-GGAGGCTGCATCATCGTACT-3′.

Electrophoretic mobility-shift assay. Protein/DNA-binding was determined by electrophoretic mobility shift assay (EMSA), as previously described (28). Briefly, 5 to 20 ng of recombinant protein were incubated in the presence of radiolabeled oligonucleotide (specific activity, 8,000–20,000 cpm/fmol). A 200-fold excess of specific unlabeled competitor oligonucleotide was added. The double-strand oligonucleotides used was a region spanning from base −1189 to −69 of the mouse *cyclin B2* promoter (5′-AGCAAATTGACAAGCAAATACAAGCCAGCCAATCAACGTG-3′). For antibody competition, analyses samples were preincubated, on ice for at least 30 min, with 0.5 μg of previously described anti-HMGA1 (26) or anti-HMGA2 antibodies (12). The DNA-protein complexes were resolved on 6% nondenaturing acrylamide gels and visualized by exposure to autoradiographic films.

Chromatin immunoprecipitation. Chromatin immunoprecipitation (ChIP) was carried out with an acetyl-histone H3 imunoprecipitation assay kit (Upstate Biotechnology) according to the manufacturer's instruction. Approximately 3×10^7 cells of the NIH3T3 cell line or ~1 mg of chopped HMGA-transgenic pituitary adenomas were cross-linked by the addition of formaldehyde (1% final concentration). Cross-linking was allowed to proceed at room temperature for 5 min and was terminated with glycine (final concentration, 0.125 mol/L). Cells and tissues were lysed in buffer containing 5 mmol/L PIPES (pH 8.0), 85 mmol/L KCl, 0.5% NP40, and protease inhibitors (1 mmol/L phenylmethylsulfonyl fluoride, 10 μg/mL aprotinin, 10 μg/mL leupeptin), on ice for 10 min. Nuclei were pelleted by centrifugation at 5,000 rpm for 5 min at 4°C and resuspended in buffer containing 50 mmol/L Tris-Cl (pH 8.1), 10 mmol/L EDTA, 1% SDS, the same protease inhibitors, and incubated on ice for 10 min. Chromatin was sonicated on ice to an average length of ~400 bp with a Branson sonicator model 250. Samples were centrifuged at 14,000 rpm for 10 min at 4°C. Chromatin was precleared with protein A-Sepharose (blocked previously with 1 mg/mL bovine serum albumin) at 4°C for 2 h. Precleared chromatin

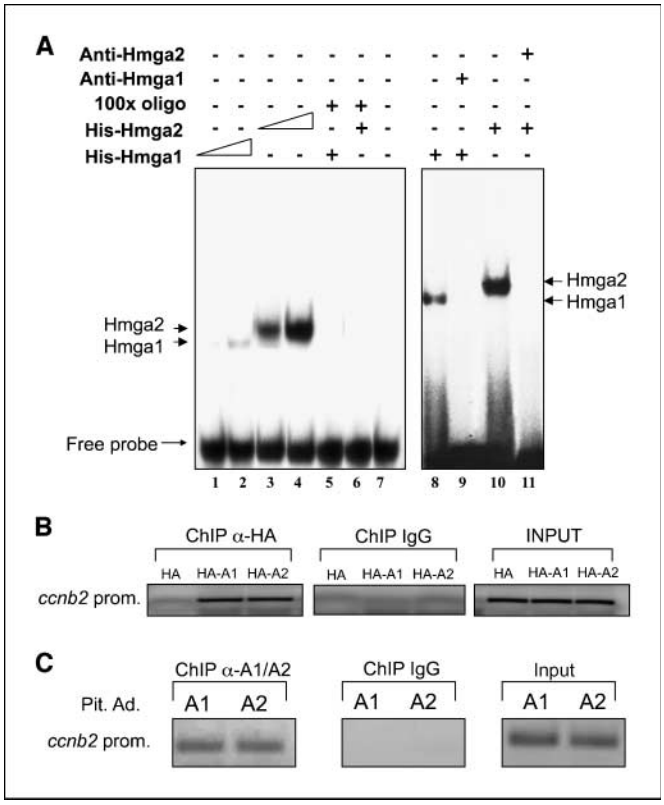

Figure 2. HMGA proteins bind the *ccnb2* promoter. *A,* EMSA performed with a radiolabeled oligonucleotide spanning from base −1189 to −69 of the mouse *ccnb2* promoter region, and incubated with 5 ng (*lane 1*) and 20 ng (*lanes 2, 5, 8*, and *9*) of the recombinant HMGA1-His protein or with 5 ng (*lanes 3, 6, 10*, and *11*) and 20 ng (*lane 4*) of the recombinant HMGA2-His protein. To assess the specificity of the binding, a 100× excess of unlabeled oligonucleotides (*lanes 5* and *6*) or anti-HMGA1 (*lane 9*) and anti-HMGA2 (*lane 11*) antibodies were incubated as specific competitors. *B,* ChIP assay performed on NIH3T3 cells transfected with pCEFLHA (*HA*), pCEFLHA-HMGA1 (*HA-A1*), or pCEFLHA-HMGA2 (*HA-A2*). *C,* ChIP performed on pituitary adenomas from HMGA1- and HMGA2-transgenic mice to detect the endogenous *in vivo* binding of HMGA proteins to *ccnb2* promoter gene. *Input,* PCR products with chromosomal DNA without immunoprecipitation. As an immunoprecipitation control, IgG was used.

of each sample was incubated at 4°C overnight with 2 μg of antibody anti-HA (sc-7392; Santa Cruz Biotechnology), for transfected cells, anti-HMGA1 (26), for HMGA1-transgenic pituitary adenomas, and anti-HMGA2 (12), for HMGA2-transgenic pituitary adenomas. An aliquot of wild-type samples was incubated also with anti-IgG antibody. Next, 60 μL of a 50% slurry of blocked protein G Sepharose were added, and immune complexes were recovered. The supernatants were saved as "input." Immunoprecipitates were washed twice with 2 mmol/L EDTA, 50 mmol/L Tris-Cl (pH 8.0) buffer, and 4 times with 100 mmol/L Tris-Cl (pH 8.0), 500 mmol/L LiCl, 1% NP40, and 1% deoxycholic acid buffer. The antibody-bound chromatin was eluted from the beads with 200 μL of elution buffer (50 mmol/L NaHCO3, 1% SDS). Samples were incubated at 67°C for 5 h in the presence of 10 μg RNase and NaCl to a final concentration of 0.3 mol/L to reverse formaldehyde cross-links. Samples were then precipitated with ethanol at −20°C overnight. Pellets were resuspended in 10 mmol/L Tris (pH 8)-1 mmol/L EDTA and treated with proteinase K to a final concentration of 0.5 mg/mL at 45°C for 1 h. DNA was extracted with phenol/chloroform/isoamyl alcohol, ethanol-precipitated, and resuspended in water. Input DNA and immunoprecipitated DNAs were analyzed by PCR for the presence of *cyclin B2* promoter sequence. PCR reactions were performed with AmpliTaq gold DNA polymerase (Perkin-Elmer). The primers used to amplify the sequence of the *ccnb2* promoter were 5′-TAAGGATGATGGACCAAGAG-3′ (forward) and 5′-CCCTCGACCTAAATTACACA-3′ (reverse). PCR products were

resolved on a 2% agarose gel, stained with ethidium bromide, and scanned using a Typhoon 9200 scanner.

Statistical analysis. For the comparison between two groups of experiments, Student's *t* test was used. The statistical significant difference was considered when *P* value was <0.05. The Pearson correlation was performed to determine the association of *CCNB2* with *HMGA1* or *HMGA2* expression levels in human pituitary adenomas. A correlation coefficient (r) close to 1 was considerate indicative of a significant direct correlation.

Results

Cyclin B2 is overexpressed in pituitary adenoma developing in HMGA-transgenic mice. The analysis of mRNA expression profile of HMGA1- and HMGA2-induced pituitary adenomas showed an 8-fold change increase expression of the *ccnb2* gene in the neoplastic tissues in comparison with the normal pituitary from control mice (14). This result has been validated by semiquantitative (Fig. 1*A*) and quantitative reverse transcription-PCR (qRT-PCR; Fig. 1*B*) in two HMGA1- and three HMGA2 pituitary adenomas. In fact, the quantitative PCR showed a higher than 20-fold increase in specific *ccnb2* mRNA expression. Western blot analysis showed the accumulation of cyclin B2 protein in pituitary adenomas of the HMGA1 and HMGA2 transgenic mice but not its presence in normal pituitary gland (Fig. 1*C*). However, in the case of the pituitary adenoma sample PA2, no correlation has been found between RNA and protein level. This could be due to the possible action of some still unidentified microRNA/s in this adenoma. Subsequently, we analyzed by RT-PCR the expression of the *ccnb2* gene also in murine and rat cell lines derived from pituitary adenomas of different histotype. As shown in Fig. 1*D*, the expression of *ccnb2* is undetectable in normal pituitary (*NG*) gland, both from mouse and rat, whereas it is expressed in all analyzed cell lines. These results suggest cyclin B2 as a direct target of HMGA proteins in pituitary tumorigenesis.

HMGA proteins bind to the *ccnb2* promoter and positively regulate its activity. To investigate whether the HMGA proteins are directly involved in *ccnb2* transcriptional regulation, we evaluated the HMGA ability to bind the *ccnb2*-promoter *in vitro* using oligonucleotides spanning from base −1189 to −69 of the mouse *ccnb2* promoter region (29) including AT-rich putative HMGA-binding sites. As shown in Fig. 2*A* (*lanes 1–2*) increasing amounts (5 and 20 ng) of the recombinant HMGA1 protein were capable of binding the ^{32}P-end–labeled double-strand oligonucleotide in EMSA. The binding specificity was shown by competition experiments showing loss of binding with the addition of 100-fold molar excess of the specific unlabeled oligonucleotide (*lane 5*). In addition, competition experiments with specific anti-HMGA1 and anti-HMGA2 antibodies further confirmed the specificity of the HMGA/DNA complexes (Fig. 2*A, lanes 8–9*). Analogous results were obtained when the same experiments were performed using the recombinant HMGA2 protein (Fig. 2*A, lanes 3–4, 6*, and *10–11*).

To verify that HMGA proteins are able to bind to *ccnb2* promoter also *in vivo*, we performed experiments of ChIP in the NIH3T3 cell line transiently transfected with either the HA-HMGA1 or HA-HMGA2 expression plasmids. Chromatin prepared as described under Materials and Methods was immunoprecipitated with anti-HA or rabbit IgG antibodies, used as internal control. The results, shown in Fig. 2*B*, confirmed that both HMGA1 and HMGA2 proteins bind to the promoter of the *ccnb2* gene. In fact, the *ccnb2* promoter region was amplified from the DNA recovered with anti-HA antibody in HA-HMGA1– and HA-HMGA2–transfected cells but not in the cells transfected with the backbone vector. Moreover, no amplification was observed in the same samples immunoprecipitated with rabbit IgG. To confirm this result in our *in vivo* model system of pituitary adenoma, the ChIP of both HMGA1 and HMGA2 was also analyzed in pituitary adenomas coming from HMGA1 and HMGA2 transgenic mice, respectively. As shown in

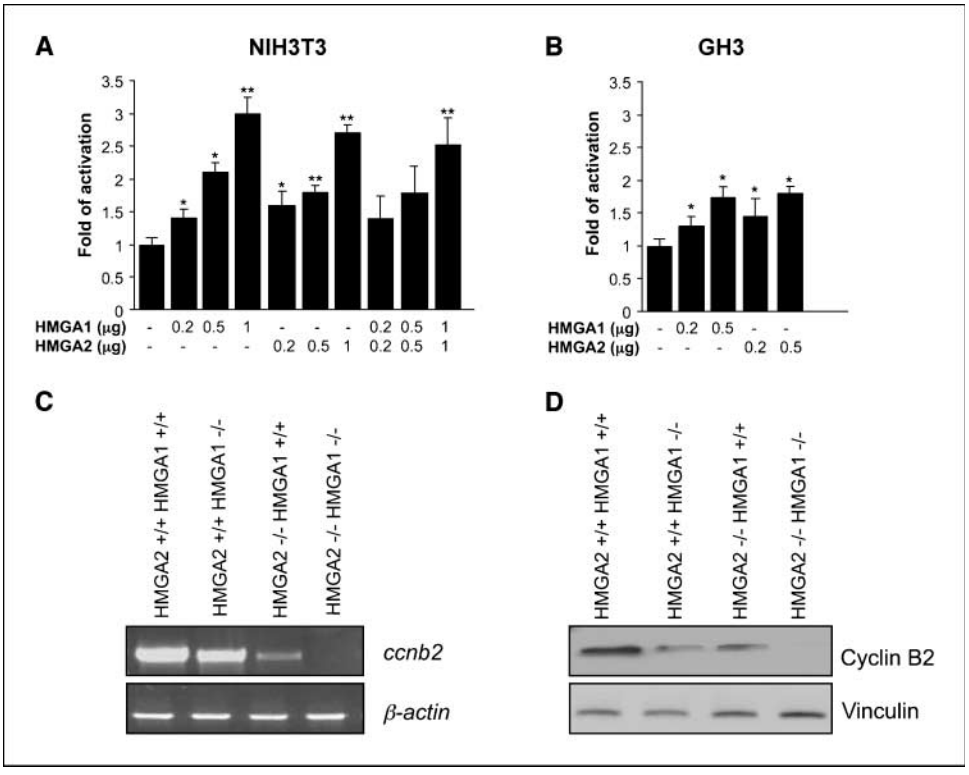

Figure 3. HMGA proteins up-regulate the *ccnb2* gene. *A* to *B,* luciferase activity (*fold of activation*) of the *ccnb2* promoter in the NIH3T3 (*A*) and GH3 (*B*) cell lines. As indicated, growing amounts of either HMGA1 or HMGA2, or both, expression vectors were cotransfected with the B2-luci plasmid. *Columns,* mean expression values of three independent experiments; *bars,* SD. $P < 0.05$ (*), $P < 0.01$ (**), versus control (*C*) *ccnb2* mRNA expression in MEFs derived from knockout mice for *Hmga1, Hmga2*, or both the genes. As a control for equal mRNA loading, *β-actin* was amplified on the same samples. *D,* Cyclin B2 protein expression in extracts from MEFs derived from knockout mice for *Hmga1, Hmga2*, or both the genes. As a control for equal protein loading, the blotted proteins were incubated with a vinculin-specific antibody.

Fig. 2*C*, both the HMGA proteins do bind the *ccnb2* promoter in pituitary adenoma tissues.

To investigate the functional effect of the binding of HMGA proteins to the *ccnb2* promoter, we transiently transfected the NIH3T3 cell line, which expresses low levels of HMGA proteins, with a construct expressing the luciferase gene under the control of the mouse *ccnb2* promoter region (B2-luci). As shown in Fig. 3*A*, cotransfection with the HMGA1, or HMGA2 expression vectors, led to a significant increase of the luciferase activity in a dose-dependent manner. Neither synergistic nor additive effect on the activity of the *ccnb2* promoter was observed when both the HMGA1 and HMGA2 expression vectors were transfected together. To confirm these results in a pituitary cell context, we also performed analogous luciferase assays in the GH3 cell line. The results, shown in Fig. 3*B*, are quite similar to those observed in the NIH3T3 cells.

To further validate that cyclin B2 expression is dependent on HMGA proteins, we analyzed cyclin B2 mRNA and protein levels in murine embryonic fibroblasts (MEF) derived from knockout mice for *Hmga1, Hmga2*, or both genes. As shown in Fig. 3*C*, the cyclin B2 transcript is significantly lower in *Hmga1* and *Hmga2* minus MEFs compared with the wild-type ones, and almost undetectable in the MEFs where both members of the HMGA family have been disrupted. Analogous results were obtained for the protein levels (Fig. 3*D*).

Cyclin B2 is overexpressed in human pituitary adenomas. The high expression of cyclin B2 in HMGA-induced mouse pituitary adenomas and in murine and rat cell lines derived from pituitary adenomas prompted us to verify whether cyclin B2 overexpression could be a feature also of human pituitary adenomas. Therefore, we analyzed the expression of *CCNB2* in a panel of 45 human pituitary adenomas (including 15 nonfunctioning adenomas, 6 somatotrophic adenomas GH-secreting, 16 prolactinomas, 2 mixed GH/PRL-cell adenomas, 6 gonadotrophic adenomas FSH-secreting) by qRT-PCR. As shown in Fig. 4*A*, *CCNB2* was expressed in all the adenomas analyzed at a much higher level in comparison with the normal pituitary gland. Interestingly, *HMGA1* and *HMGA2* expression was increased in all the tumors analyzed when compared with normal tissue and a direct correlation between *HMGA1, HMGA2*, and *CCNB2* mRNA levels was observed. In fact, as shown in Fig. 4*B* and *C*, the correlation coefficients for the fold changes between adenomas and normal gland, calculated in both *CCNB2* and *HMGA1*, as well as *CCNB2* and *HMGA2* expression levels, were r = 0.80 ($P < 0.001$) and r = 0,90 ($P < 0.001$), respectively.

To verify whether the increase in Cyclin B2–specific mRNA levels corresponded to an increase also in protein levels, we evaluated Cyclin B2 protein expression in pituitary adenomas by Western blot and immunohistochemistry. As shown in Fig. 5*A*, a band of 51 kDa

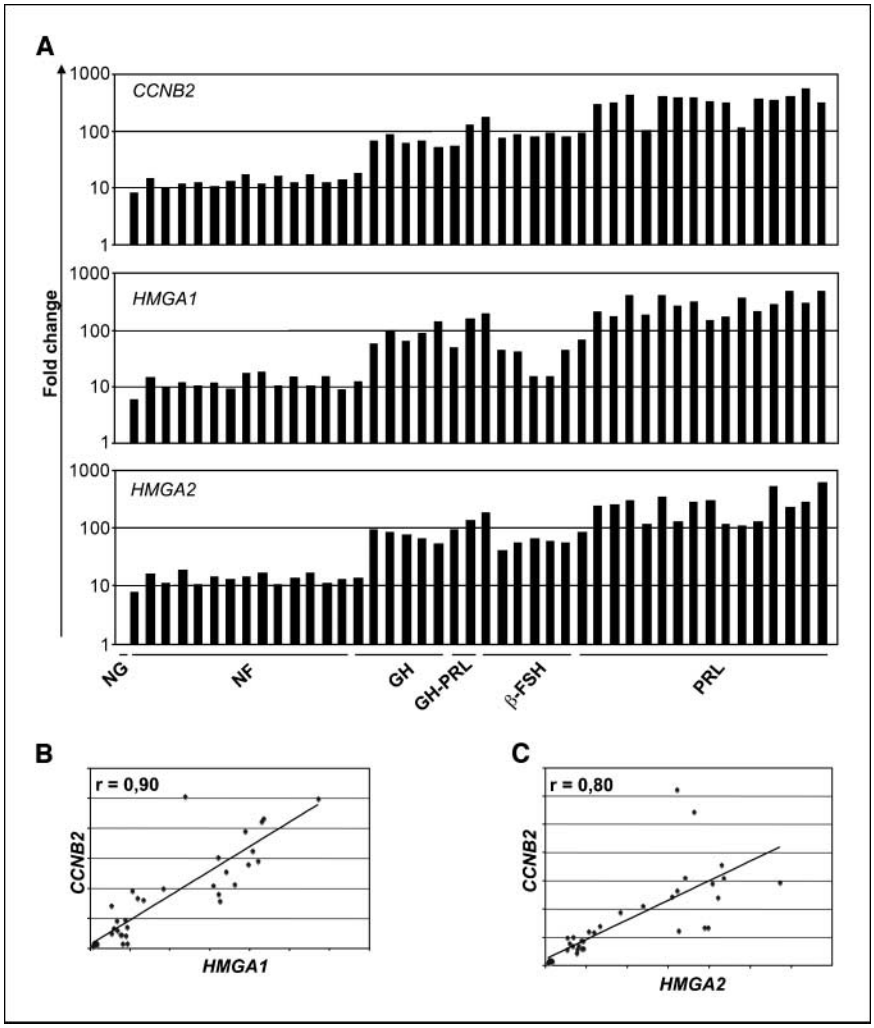

Figure 4. qRT-PCR analysis of *CCNB2, HMGA1* and *HMGA2* expression in human pituitary adenomas. *A,* qRT-PCR analysis of *CCNB2* (*top*), *HMGA1* (*middle*), and *HMGA2* (*bottom*) was performed on a panel of nonfunctioning (*NF*), somatotrophic (*GH*), prolactinoma (*PRL*), mixed GH/PRL-cell (*GH-PRL*), and gonadotrophic (*β-FSH*) pituitary adenoma samples of human origin. The fold change values indicate the relative change in expression levels between tumor samples and a pool of normal pituitary tissues assuming that the value of these normal samples was equal to 1. *B* to *C,* statistical analysis of the correlation between *CCNB2* and *HMGA1* (*B*) or *HMGA2* (*C*) relative expression in pituitary adenomas versus normal gland. *r,* Pearson correlation coefficient.

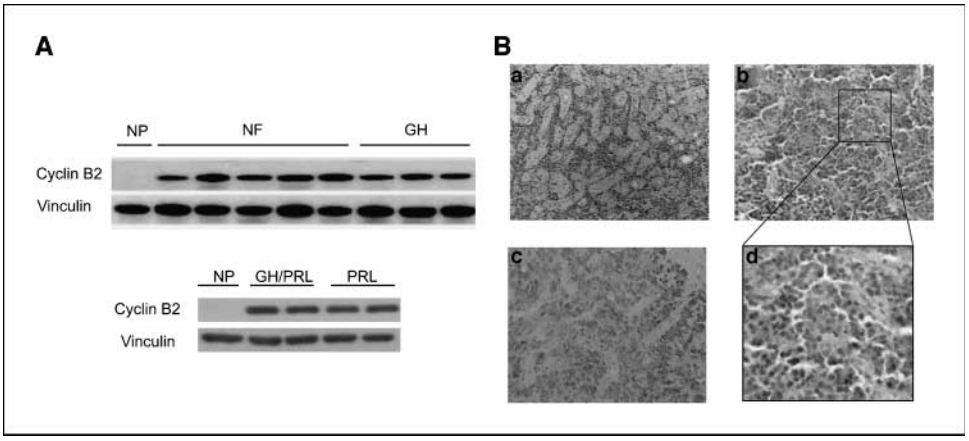

Figure 5. Analysis of Cyclin B2 protein expression in human pituitary adenomas. *A,* cyclin B2 protein expression in extracts coming from pituitary adenomas of different histotypes and normal pituitary gland. Blot against vinculin has been performed as control for equal protein loading. *B,* paraffin sections from a representative prolactinoma and normal pituitary tissue were analyzed by immunohistochemistry using antibodies raised against Cyclin B2. *a,* immunostaining of a normal hypophysis: no immunoreactivity was observed (×200); *b,* immunostaining of a representative prolactinoma (×200) showing a cytoplasmic positivity; *c,* immunostaining of the same samples as in *b*, in the absence of the primary antibody: no immunoreactivity was observed; *d,* immunostaining of the same prolactinoma as in *b* at a higher magnification (×400). *NP,* normal pituitary gland; *NF,* nonfunctioning adenoma; *GH,* GH-secreting adenoma; *GH/PRL,* GH/prolactin-secreting adenoma; *PRL,* prolactin-secreting adenoma.

corresponding to the cyclin B2 protein was found in all 12 pituitary tumors analyzed, independently from the hystotype, whereas it was not detected in normal pituitary gland. Then, immunohistochemical analysis was performed using antibodies raised versus the NH_2-terminal region of the Cyclin B2 protein. In Fig. 5*B*, we show a representative case: no staining was detected in the normal gland (*a*). Conversely, a specific cytoplasmic staining was found in all the pituitary prolactinomas analyzed (*b, c, d*; data not shown).

Discussion

A previous analysis of mRNA expression profiles showed an 8-fold increase in cyclin B2 gene (*ccnb2*) expression in pituitary adenomas developing in Hmga1- and Hmga2-transgenic mice in comparison with a pool of normal pituitary glands from control mice (14). The B-type are the primary mitotic cyclins, although several yeast B-type cyclins have been reported to function earlier in the cell cycle, particularly in the S phase (30, 31). There are two mammalian B-type cyclins, B1 and B2, which differ in their NH_2 termini but have 57% similarity (32, 33). Both B-type cyclins, in association with cdc2, play a critical role in regulating the G_2-M phase transition of the cell cycle (15). Consistent with a general role in cell growth, several studies have reported the accumulation of cyclins B in human tumors, including pituitary adenomas (17–21, 24). However, cyclin B2 involvement in pituitary tumorigenesis has not emerged yet, and the molecular mechanisms underlying its deregulation in cancer have not been definitively elucidated. Indeed, it is known that *CCNB2* promoter is activated by NF-Y (25), but very little is known about its regulation in tumors (20).

Our above reported and previously published data suggested that the increase in cyclin B2 expression might have a role in the generation of pituitary adenomas in Hmga1- and Hmga2-transgenic mice. Therefore, we considered interesting to evaluate whether the induction of cyclin B2 was a direct or indirect effect of HMGA overexpression, and if this was restricted to the experimental pituitary adenomas, or was a general event occurring in human pituitary adenomas as well. EMSA and ChIP revealed a direct binding of HMGA proteins to the promoter of *ccnb2*. Moreover, luciferase assays showed that both the HMGA proteins were able to up-regulate *ccnb2* promoter activity. Finally, we showed an increased expression of cyclin B2 in human pituitary adenomas of different histotypes that is associated to HMGA1 and HMGA2 expression.

A clear validation of the induction of the *ccnb2* gene expression comes from our analysis of *ccnb2* mRNA levels in Hmga1- or Hmga2-null MEFs. In fact, *ccnb2* expression was reduced in MEFs carrying a disrupted *Hmga1* or *Hmga2* gene, and was almost undetectable in MEFs where neither *Hmga* gene was expressed.

It is reasonable to retain that the decreased cyclin B2 expression in Hmga2-null and Hmga1/Hmga2-double-null mice may also account for the pygmy phenotype of the mice knockout for Hmga2 and the very small size (less than half of that of the pygmy mice) of the mice double-knockout for Hmga1 and Hmga2.[7]

We have previously shown that a critical mechanism in the induction of pituitary adenomas by HMGA2 is the ability of HMGA2 to interact with pRB and induce E2F1 activity in mouse pituitary adenomas by displacing HDAC1 from the pRB/E2F1 complex—a process that results in E2F1 acetylation. Subsequently, we showed that *Mia/Cd-rap* gene expression was suppressed in HMGA-induced pituitary adenomas. Therefore, the induction of cyclin B2 by HMGA2 could represent a further mechanism by which HMGA2 would contribute to the development of pituitary adenoma in mice and humans because HMGA2 gene amplification and overexpression have been reported by our group in human prolactinomas (13). It is reasonable to hypothesize that cyclin B2 induction by HMGA proteins may contribute to high-rate cell proliferation of the malignant neoplasias where HMGA proteins are abundantly expressed.

In conclusion, our data show that HMGA proteins positively regulate cyclin B2 expression, indicating a new possible mechanism by which they may be correlated to mouse and human pituitary tumorigenesis.

[7] I. De Martino et al., manuscript in preparation.

Disclosure of Potential Conflicts of Interest

No potential conflicts of interest were disclosed.

Acknowledgments

Received 10/28/2008; revised 12/16/2008; accepted 12/23/2008; published OnlineFirst 02/17/2009.

Grant support: Associazione Italiana Ricerca sul Cancro and the Ministero dell'Università e della Ricerca Scientifica e Tecnologica. This work was also supported from NOGEC-Naples Oncogenomic Center.

The costs of publication of this article were defrayed in part by the payment of page charges. This article must therefore be hereby marked *advertisement* in accordance with 18 U.S.C. Section 1734 solely to indicate this fact.

We thank Giulia Piaggio for kindly providing the *ccnb2*-promoter construct, and the Associazione Partenopea per le Ricerche Oncologiche for its support.

References

1. Johnson KR, Lehn DA, Reeves R. Alternative processing of mRNA's coding for human HMG I, HMG Y. proteins. Mol Cell Biol 1989;9:2114–23.
2. Manfioletti G, Giancotti V, Bandiera A, et al. cDNA cloning of the HMGI-C phosphoprotein, a nuclear protein associated with neoplastic and undifferentiated phenotypes. Nucleic Acids Res 1991;19:6793–7.
3. Reeves R. Molecular biology of HMGA proteins: hubs of nuclear function. Gene 2001;277:63–81.
4. Chiappetta G, Avantaggiato V, Visconti R, et al. High level expression of the HMGI (Y) gene during embryonic development. Oncogene 1996;13:2439–46.
5. Zhou X, Benson KF, Ashar HR, Chada K. Mutation responsible for the mouse pygmy phenotype in the developmentally regulated factor HMGI-C. Nature 1995; 376:771–4.
6. Fusco A, Fedele M. Roles of HMGA proteins in cancer [review]. Nat Rev Cancer 2007;12:899–910.
7. Fedele M, Berlingieri MT, Scala S, et al. Truncated and chimeric HMGI-C genes induce neoplastic transformation of NIH3T3 murine fibroblasts. Oncogene 1998;17: 413–8.
8. Wood LJ, Maher JF, Bunton TE, Resar LM. The oncogenic properties of the HMG-I gene family. Cancer Res 2000;60:4256–61.
9. Baldassarre G, Fedele M, Battista S, et al. Onset of natural killer cell lymphomas in transgenic mice carrying a truncated HMGI-C gene by the chronic stimulation of the IL-2 and IL-15 pathway. Proc Natl Acad Sci U S A 2001;98:7970–5.
10. Fedele M, Battista S, Kenyon L, et al. Overexpression of the HMGA2 gene in transgenic mice leads to the onset of pituitary adenomas. Oncogene 2002;21:3190–8.
11. Fedele M, Pentimalli F, Baldassarre G, et al. Transgenic mice overexpressing the wild-type form of the HMGA1 gene develop mixed growth hormone/ prolactin cell pituitary adenomas and natural killer cell lymphomas. Oncogene 2005;24:3427–35.
12. Fedele M, Visone R, De Martino I, et al. HMGA2 induces pituitary tumorigenesis by enhancing E2F1 activity. Cancer Cell 2006;9:459–71.
13. Finelli P, Pierantoni GM, Giardino D, et al. The High Mobility Group A2 gene is amplified and overexpressed in human prolactinomas. Cancer Res 2002; 62:2398–405.
14. De Martino I, Visone R, Palmieri D, et al. The *Mia/Cd-rap* gene expression is downregulated by the HMGA proteins in mouse pituitary adenomas. Endocr Relat Cancer 2007;14:875–86.
15. Minshull J, Blow JJ, Hunt T. Translation of cyclin mRNA is necessary for extracts of activated xenopus eggs to enter mitosis. Cell 1989;56:947–56.
16. Brandeis M, Rosewell I, Carrington M, et al. Cyclin B2-null mice develop normally and are fertile whereas cyclin B1-null mice die *in utero*. Proc Natl Acad Sci U S A 1998;95:4344–9.
17. Wang A, Yoshimi N, Ino N, Tanaka T, Mori H. Overexpression of cyclin B1 in human colorectal cancers. J Cancer Res Clin Oncol 1997;123:124–7.
18. Soria JC, Jang SJ, Khuri FR, et al. Overexpression of cyclin B1 in early-stage non-small cell lung cancer and its clinical implication. Cancer Res 2000;60:4000–4.
19. Sarafan-Vasseur N, Lamy A, Bourguignon J, et al. Overexpression of B-type cyclins alters chromosomal segregation. Oncogene 2002;21:2051–7.
20. Park SH, Yu GR, Kim WH, Moon WS, Kim JH, Kim DG. NF-Y-dependent cyclin B2 expression in colorectal adenocarcinoma. Clin Cancer Res 2007;13: 858–67.
21. Turner HE, Nagy Z, Sullivan N, Esiri MM, Wass JA. Expression analysis of cyclins in pituitary adenomas and the normal pituitary gland. Clin Endocrinol (Oxf) 2000; 53:337–44.
22. Hibberts NA, Simpson DJ, Bicknell JE, et al. Analysis of Cyclin D1 (*CCND1*) allelic imbalance and overexpression in sporadic human pituitary tumors. Clin Cancer Res 1999;5:2133–9.
23. Simpson DJ, Fryer AA, Grossman AB, et al. Cyclin D1 (*CCND1*) genotype is associated with tumour grade in sporadic pituitary adenomas. Carcinogenesis 2001;22: 1801–7.
24. Wierinckx A, Auger C, Devauchelle P, et al. A diagnostic marker set for invasion, proliferation, and aggressiveness of prolactin pituitary tumors. Endocr Relat Cancer 2007;14:887–900.
25. Bolognese F, Wasner M, Lange-zu Dohna C, et al. The cyclin B2 promoter depends on NF-Y, a trimer whose CCAAT-binding activity is cell-cycle regulated. Oncogene 1999;18:1845–53.
26. Melillo RM, Pierantoni GM, Scala S, et al. Critical role of the HMGI(Y) proteins in adipocytic cell growth and differentiation. Mol Cell Biol 2001;21:2485–95.
27. Livak KJ, Schmittgen TD. Analysis of relative gene expression data using real-time quantitative PCR and the 2(-ΔΔ C(T)) Method. Methods 2001;25:402–8.
28. Battista S, Fedele M, Martinez Hoyos J, et al. High Mobility Group A1 proteins downregulate RAG2 gene expression. Biochem J 2005;389:91–7.
29. Lange-zu Dohna C, Brandeis M, Berr F, Mössner J, Engeland K. A CDE/CHR tandem element regulates cell cycle-dependent repression of cyclin B2 transcription. FEBS Lett 2000;484:77–81.
30. Epstein CB, Cross FR. CLB5: a novel B cyclin from budding yeast with a role in S phase. Genes 1992;6: 1695–706.
31. Fitch I, Dahmann C, Surana U, et al. Characterization of four B-type cyclin genes of the budding yeast Saccharomyces cerevisiae. Mol Biol Cell 1992;3: 805–18.
32. Chapman DL, Wolgemuth DJ. Isolation of the murine cyclin B2 cDNA and characterization of the lineage and temporal specificity of expression of the B1 and B2 cyclins during oogenesis, spermatogenesis and early embryogenesis. Development 1993;118:229–40.
33. Jackman M, Firth M, Pines J. Human cyclins B1and B2 are localized to strikingly different structures: B1to microtubules, B2 primarily to the Golgi apparatus. EMBO J 1995;14:1646–54.

BMC Biology

Research article

The cAMP-HMGA1-RBP4 system: a novel biochemical pathway for modulating glucose homeostasis

Eusebio Chiefari[†1], Francesco Paonessa[†1], Stefania Iiritano[1], Ilaria Le Pera[1], Dario Palmieri[3], Giuseppe Brunetti[4], Angelo Lupo[5,6], Vittorio Colantuoni[5,6], Daniela Foti[1], Elio Gulletta[1], Giovambattista De Sarro[1], Alfredo Fusco[3] and Antonio Brunetti*[1,2]

Address: [1]Dipartimento di Medicina Sperimentale e Clinica 'G. Salvatore', 88100 Catanzaro, Italy, [2]Cattedra di Endocrinologia, Università 'Magna Græcia' di Catanzaro, 88100 Catanzaro, Italy, [3]Dipartimento di Biologia e Patologia Cellulare e Molecolare c/o Istituto di Endocrinologia ed Oncologia Sperimentale del CNR, Università di Napoli 'Federico II', 80131 Napoli, Italy, [4]Dipartimento di Scienze Biomolecolari e Biotecnologie, Università di Milano, 20133 Milan, Italy, [5]Dipartimento di Scienze Biologiche ed Ambientali, Facoltà di Scienze MM.FF.NN., Università del Sannio, 82100 Benevento, Italy and [6]Dipartimento di Biochimica e Biotecnologie Mediche, Università di Napoli 'Federico II', 80131 Napoli, Italy

Email: Eusebio Chiefari - echiefari@libero.it; Francesco Paonessa - fpao@hotmail.it; Stefania Iiritano - iiritanostefania@yahoo.it; Ilaria Le Pera - lepera@unicz.it; Dario Palmieri - dario.palmieri@unina.it; Giuseppe Brunetti - giuseppe.brunetti@unimi.it; Angelo Lupo - lupo@unisannio.it; Vittorio Colantuoni - colantuoni@unisannio.it; Daniela Foti - foti@unicz.it; Elio Gulletta - gulletta@unicz.it; Giovambattista De Sarro - desarro@unicz.it; Alfredo Fusco - afusco@napoli.com; Antonio Brunetti* - brunetti@unicz.it

* Corresponding author †Equal contributors

Published: 21 May 2009

BMC Biology 2009, **7**:24 doi:10.1186/1741-7007-7-24

Received: 8 December 2008
Accepted: 21 May 2009

This article is available from: http://www.biomedcentral.com/1741-7007/7/24

Abstract

Background: We previously showed that mice lacking the high mobility group A1 gene (*Hmga1*-knockout mice) developed a type 2-like diabetic phenotype, in which cell-surface insulin receptors were dramatically reduced (below 10% of those in the controls) in the major targets of insulin action, and glucose intolerance was associated with increased peripheral insulin sensitivity. This particular phenotype supports the existence of compensatory mechanisms of insulin resistance that promote glucose uptake and disposal in peripheral tissues by either insulin-dependent or insulin-independent mechanisms. We explored the role of these mechanisms in the regulation of glucose homeostasis by studying the *Hmga1*-knockout mouse model. Also, the hypothesis that increased insulin sensitivity in *Hmga1*-deficient mice could be related to the deficit of an insulin resistance factor is discussed.

Results: We first show that HMGA1 is needed for basal and cAMP-induced retinol-binding protein 4 (*RBP4*) gene and protein expression in living cells of both human and mouse origin. Then, by employing the *Hmga1*-knockout mouse model, we provide evidence for the identification of a novel biochemical pathway involving HMGA1 and the RBP4, whose activation by the cAMP-signaling pathway may play an essential role for maintaining glucose metabolism homeostasis *in vivo*, in certain adverse metabolic conditions in which insulin action is precluded. In comparative studies of normal and mutant mice, glucagon administration caused a considerable upregulation of HMGA1 and RBP4 expression both at the mRNA and protein level in wild-type animals. Conversely, in *Hmga1*-knockout mice, basal and glucagon-mediated expression of RBP4 was severely attenuated and correlated inversely with increased *Glut4* mRNA and protein abundance in skeletal muscle and fat, in which the activation state of the protein kinase Akt, an important downstream mediator of

the metabolic effects of insulin on Glut4 translocation and carbohydrate metabolism, was simultaneously increased.

Conclusion: These results indicate that HMGA1 is an important modulator of *RBP4* gene expression *in vivo*. Further, they provide evidence for the identification of a novel biochemical pathway involving the cAMP-HMGA1-RBP4 system, whose activation may play a role in glucose homeostasis in both rodents and humans. Elucidating these mechanisms has importance for both fundamental biology and therapeutic implications.

Background

Insulin resistance is a metabolic condition found relatively frequently among humans with chronic hyperinsulinemia and in experimental animal models with defective insulin signaling [1-3]. Recently, a link has been established between peripheral insulin sensitivity and the retinol (vitamin A) metabolism, and insulin resistance in rodents and humans has been linked to abnormalities of the vitamin A signaling pathway [4-6]. According to these studies, impaired glucose uptake in adipose tissue results in secondary systemic insulin resistance through release of the adipose-derived serum RBP4 [4,5]. However, it is unknown whether RBP4 effects on insulin sensitivity are vitamin A-dependent or vitamin A-independent. RBP4 (also called RBP) is mainly produced by the liver but also by adipocytes [7]. In plasma, retinol-RBP4 is found in an equimolar complex with transthyretin (TTR), which is a thyroid hormone transport protein that is synthesized in and secreted from the liver. This ternary complex prevents retinol-RBP4 excretion by the kidney [8]. By impairing insulin signaling in muscle, RBP4 inhibits glucose uptake and interferes with insulin-mediated suppression of glucose production in the liver, causing blood glucose levels to rise [4]. Conversely, mice lacking the *RBP4* gene show increased insulin sensitivity, and normalizing increased RBP4 serum levels improves insulin resistance and glucose intolerance [4].

HMGA1 is a small basic protein that binds to adenine-thymine (A-T) rich regions of DNA and functions mainly as a specific cofactor for gene activation [9]. HMGA1 by itself has no intrinsic transcriptional activity; rather, it can transactivate promoters through mechanisms that facilitate the assembly and stability of a multicomponent enhancer complex, the so-called enhanceosome, that drives gene transcription [9,10].

As part of an investigation into the molecular basis regulating the human insulin receptor gene, we previously showed that HMGA1 is required for proper insulin receptor gene transcription [11,12]. More recently, we showed that loss of HMGA1 expression, induced in mice by disrupting the *HMGA1* gene, caused a type 2-like diabetic phenotype, in which, however, impaired glucose tolerance and overt diabetes coexisted with a condition of peripheral insulin hypersensitivity [13]. Concomitant insulin resistance and insulin hypersensitivity in peripheral tissues may paradoxically coexist as observed in livers of lipodystrophic and *ob*/*ob* mice [14], as well as in *Cdk4* knockout mice with defective pancreatic beta cell development and blunted insulin secretion [15]. The hypothesis that the paradoxical insulin hypersensitivity of *Hmga1*-deficient mice could be due to a deficit, in these animals, of RBP4 is supported by our data. Herein, by employing the *Hmga1*-knockout mouse model, we provide compelling evidence for the identification of a novel biochemical pathway involving HMGA1 and RBP4, whose activation by the cAMP pathway may play an important role in maintaining glucose metabolism homeostasis *in vivo*, in both rodents and humans. The importance of HMGA1 in *RBP4* gene transcription was substantiated in *Hmga1*-deficient mice, in which loss of HMGA1 expression considerably decreased *RBP4* mRNA abundance and RBP4 protein production.

Results

RBP4 gene transcription is induced by HMGA1 and cAMP

We first performed experiments to see whether HMGA1 had a role in activating the mouse *RBP4* gene promoter at the transcriptional level. To test this possibility, HepG2 human hepatoma cells and mouse Hepa1 hepatoma cells were cotransfected transiently with mouse *RBP4*-Luc reporter plasmid plus increasing amounts of the HMGA1 expression vector. As shown in Figure 1, overexpression of HMGA1 considerably increased *RBP4*-Luc activity in both cell types and this effect occurred in a dose-dependent manner. Consistent with these results, *RBP4* mRNA abundance was increased in cells overexpressing HMGA1 and was reduced in cells pretreated with siRNA targeting HMGA1 (Figure 1), indicating that activation of the *RBP4* gene requires HMGA1. These data were substantiated by chromatin immunoprecipitation (ChIP) assay, showing that binding of HMGA1 to the endogenous *RBP4* locus was increased in whole, intact HepG2 and Hepa1 cells naturally expressing HMGA1, and was decreased in cells exposed to siRNA against HMGA1 (Figure 1). Based on these results, in addition to previous observations indicating that cAMP, or agents which elevate intracellular cAMP, increase *RBP* transcript levels [16], we were interested to see whether a functional link could be established

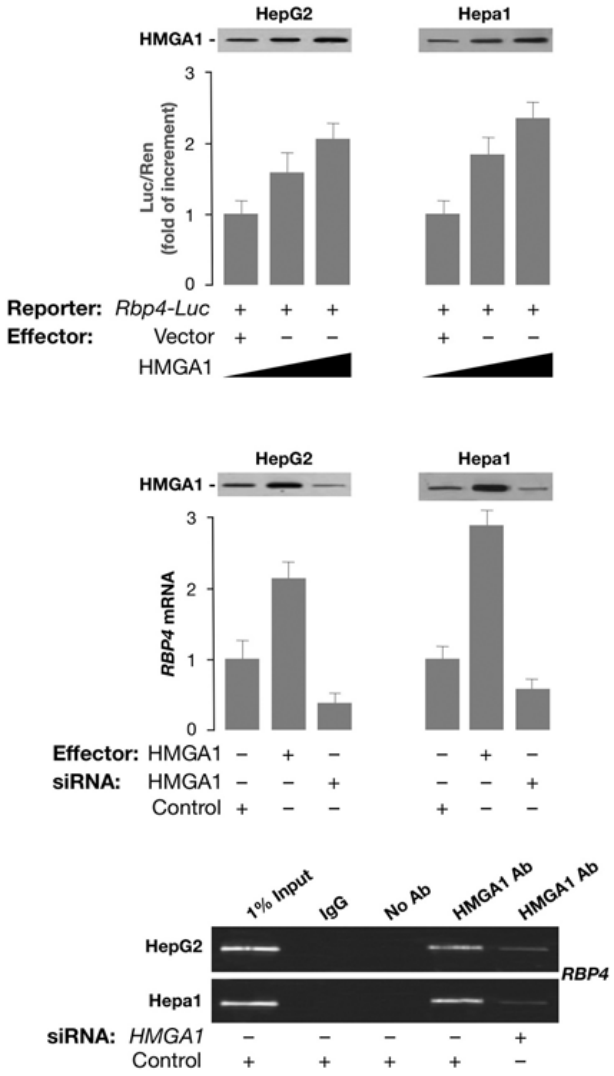

Figure 1

***RBP4* gene expression is induced by HMGA1**. **(Top)** Mouse *RBP4*-Luc reporter vector (2 μg) was transfected into HepG2 and Hepa1 cells plus increasing amounts (0, 0.5, or 1 μg) of *HMGA1* expression plasmid. Data represent the means ± standard errors for three separate experiments; values are expressed as factors by which induced activity increased above the level of Luc activity obtained in transfections with *RBP4*-Luc reporter vector plus the empty expression vector, which is assigned an arbitrary value of 1. **(Middle)** *HMGA1* expression plasmid was transfected into HepG2 and Hepa1cells. After 6 h of transfection, the cells were treated with anti-*HMGA1* (100 pmol), siRNA, or a non-targeting control siRNA, and endogenous *RBP4* mRNA expression was measured 48 to 96 h later. Western blots of HMGA1 in each condition are shown in the autoradiograms. **(Bottom)** ChIP of the *RBP4* promoter gene in HepG2 and Hepa1 cells, either untreated or pretreated with *HMGA1* siRNA. ChIP was done using an anti-HMGA1 specific antibody (Ab).

between cAMP, HMGA1, and RBP4. To this end, we first confirmed and extended the observation made by Jessen and Satre [16] that *RBP* is induced by cAMP in Hepa1 cells. As measured by Northern blot analysis of total RNA (Figure 2), *RBP4* mRNA increased ≈ 5-fold over the basal level in Hepa1 cells treated with 0.5 mM 8-bromo cAMP (Br-cAMP), a standard concentration for c-AMP induction experiments [16]. As shown in Figure 2, *RBP4* mRNA levels increased starting at 3 h, peaking at 24 h and then declining, suggesting a transient transcriptional stimulation. To establish whether HMGA1 was required for basal and cAMP-dependent *RBP4* transcription, we transfected the HMGA1 expression vector in Hepa1 cells treated or not with Br-cAMP and RBP4 protein levels were analyzed 48 h later by Western blot. As shown in Figure 2, RBP4 protein expression was enhanced in cells overexpressing HMGA1 and even further in cells treated with cAMP, in which an increase in HMGA1 protein expression was simultaneously observed, suggesting that induction of RBP4 by cAMP may occur, at least in part, through activation of endogenous HMGA1 expression. This hypothesis was supported by the fact that RBP4 was reduced in cAMP treated cells in which endogenous levels of HMGA1 were specifically lowered by transfecting cells with HMGA1 antisense expression plasmid (Figure 2). However, further experiments are needed to fully explain the role of cAMP on HMGA1 expression. The functional significance of HMGA1 in *RBP4* gene expression was confirmed in transient transcription assays in Hepa1 (and differentiated 3T3-L1, data not shown) cells, in which overexpression of HMGA1 caused an increase in both basal and cAMP-induced Luc activity from the mouse *RBP*-Luc reporter plasmid (Figure 3). This effect was substantiated in HEK-293 cAMP-responsive cells, a cell line ideally suited for studying the effects of HMGA1 on transcription since it does not express appreciable levels of this protein. As shown in Figure 3, in support of the role that HMGA1 plays in the context of *RBP4* gene, the direct effect of cAMP was less effective in promoting *RBP4* transcription in HEK-293 cells expressing low levels of HMGA1, becoming considerably higher in cells with forced expression of HMGA1.

Thus, these data together demonstrate that HMGA1 is of major importance for transcriptional regulation of the RBP4 gene, and indicate that a functional link exists between cAMP, HMGA1, and RBP4.

Hmga1-deficient mice have reduced expression of RBP4 in liver and fat tissue and reduced serum RBP4 levels

In the light of the above experimental results, indicating that HMGA1 plays a positive role in *RBP4* gene transcription in living cultured cells, it was interesting to analyze the functional consequences of genetic ablation of HMGA1 on RBP4 *in vivo*, in *Hmga1*-knockout mice. To

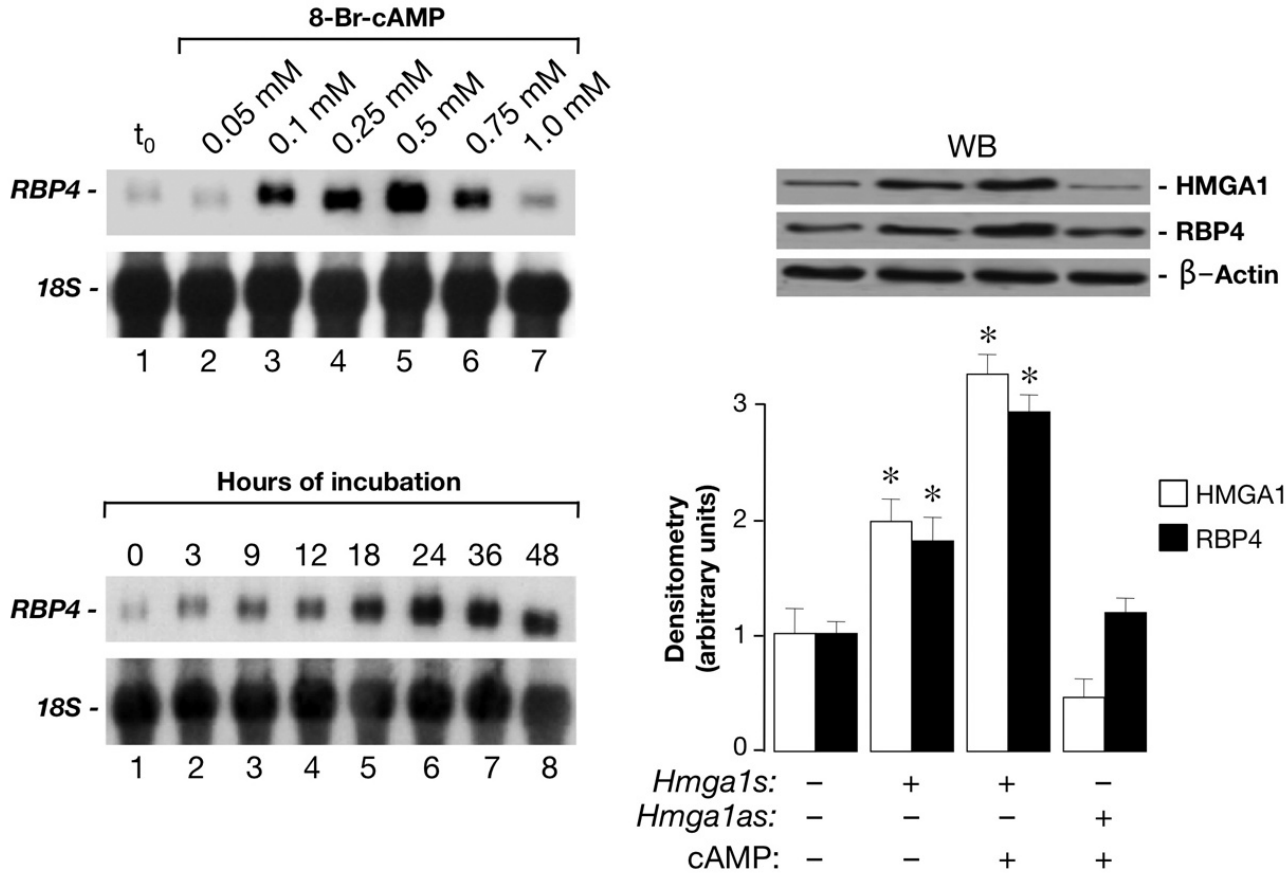

Figure 2

Stimulation of *RBP4* mRNA and protein expression by cAMP and HMGA1. **(Upper left)** 20 μg of total RNA from Hepa1 cells treated with the indicated concentrations of Br-cAMP for 24 h (lanes 1–7) were analysed by Northern blot. Hybridization was carried out with an *RBP4* cDNA or an *18S* RNA probe as a control of the RNA loaded on each lane. **(Lower left)** 20 μg of total RNA from Hepa1 cells treated with 0.5 mM Br-cAMP for the indicated times were loaded on each lane (lanes 1–8) and analysed as above. **(Right)** Hepa1 cells, in the absence or presence of an expression plasmid (1 μg) containing the *HMGA1* cDNA in either the sense (*s*) or antisense (*as*) orientation, were left untreated or treated with Br-cAMP (0.5 mM), total protein extracts were prepared 48 h later and HMGA1 and RBP4 protein expression levels were detected by Western blot (WB) with anti-HMGA1 and anti-RBP4 antibodies, respectively. β-actin, control of cellular protein loading. Densitometric analyses of three to five independent blots are shown.

this end, we performed studies aimed at investigating the expression of *RBP4* mRNA and protein in *Hmga1*-deficient mice and wild-type controls. As shown in Figure 4, *RBP4* mRNA was severely attenuated in both liver and fat from *Hmga1*-null mice, and reduced by 50% in *Hmga1* heterozygous mutants, as assessed by real-time quantitative polymerase chain reaction (qRT-PCR). Reduced *RBP4* mRNA levels in liver and adipose tissue paralleled the decrease in RBP4 serum levels as detected by Western blot analysis of serum samples from age- and body weight-matched mice with diverse genotypes (Figure 4), thereby showing the requirement of HMGA1 for full RBP4 expression in whole animals.

HMGA1 and RBP4 expression increase in liver and fat of normal mice after intraperitoneal glucagon injection

Based on our observations in intact cultured cells, indicating a role for the cAMP signaling pathway in *HMGA1* and *RBP4* gene expression, cAMP-inducible transcriptional activation of the *Hmga1* and *RBP4* genes was investigated *in vivo*, in whole animals, by systemic administration of the intracellular cAMP-elevating hormone glucagon. Under these conditions, glucagon-stimulated cAMP responses in terms of both *Hmga1* and *RBP4* mRNA expression were first analyzed in wild-type control mice. Consistent with our data in Hepa1 cells, *Hmga1* and *RBP4* mRNA levels significantly increased in liver and fat of nor-

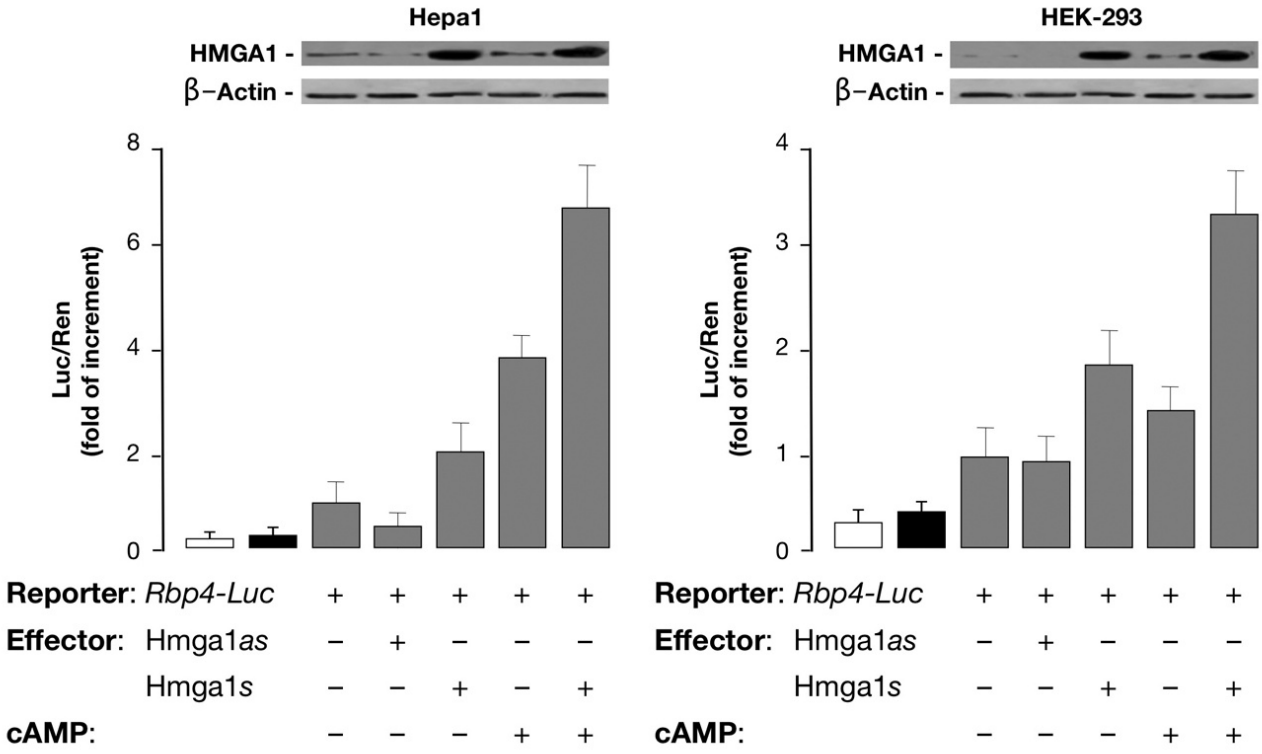

Figure 3

Role of HMGA1 in basal and cAMP-induced RBP4 expression. *Rbp4*-Luc reporter vector and *HMGA1* expression plasmid (sense or antisense) were cotransfected into Hepa1 and HEK-293 cells, either untreated or treated with Br-cAMP. Data represent the means ± standard errors for three separate experiments. Transcriptional activity of the *RBP4* gene promoter is shown as the ratio of luciferase activity to *Renilla* activity (Luc/Ren) as described in the experimental procedures. Values are expressed as the factors by which induced activity increased above the level of Luc activity obtained in transfections with the reporter vector alone, which is assigned an arbitrary value of 1. Open bar, mock (no DNA); black bar, pGL3-basic (vector without an insert). Western blots of HMGA1 and β-actin in each condition are shown in the autoradiograms.

mal mice after intraperitoneal injection of glucagon (Figure 5). Time course analyses revealed that the induction and accumulation of *Hmga1* mRNA preceded the expression of *RBP4* mRNA in both tissues. In liver, *RBP4* mRNA appeared after that for *Hmga1*, peaked after 6 h following glucagon injection, and then remained at a plateau (Figure 5). In fat, *RBP4* mRNA appeared at 1 h after *Hmga1* mRNA, peaked after 6 h of glucagon stimulation, and decreased smoothly thereafter (Figure 5). Increased levels of *Hmga1* and *RBP4* mRNAs were paralleled by the increase of Hmga1 and RBP4 protein expression, as measured by Western blot analysis of proteins from liver and fat of glucagon-injected animals (Figure 5). Interestingly, when similar experiments were carried out in glucagon injected *Hmga1*-deficient mice, tissue expression of *RBP4* mRNA was severely attenuated in liver and fat from heterozygous (*Hmga1*$^{+/-}$) and *Hmga1*-null (*Hmga1*$^{-/-}$) animals (Figure 6), thereby indicating that HMGA1 is indeed required for maximal induction of the *RBP4* gene *in vivo*, in the whole organism, and that the glucagon/adenylate cyclase system regulates both *HMGA1* and *RBP4* gene and protein expression. Consistent with this conclusion, liver *RBP4* mRNA and protein expression levels were lower in fed wild-type mice, becoming higher during fasting, when circulating glucagon increases (Figure 6).

As a measure of the glucagon efficacy in glucagon-injected mice, a liver biopsy was taken before and after glucagon injection, and cAMP levels in liver were determined for both control and *Hmga1*-deficient mice (Figure 6, inset). No substantial difference was found in basal levels of cAMP (0.45 and 0.50 in *Hmga1*$^{-/-}$ and *Hmga1*$^{+/-}$, respectively, versus 0.52 μmol/g tissue in controls). After glucagon injection, hepatic levels of cAMP increased to 1.50 μmol/g tissue in control mice, compared with 1.48 and 1.52 in *Hmga1*$^{-/-}$ and *Hmga1*$^{+/-}$ mice, respectively. Results

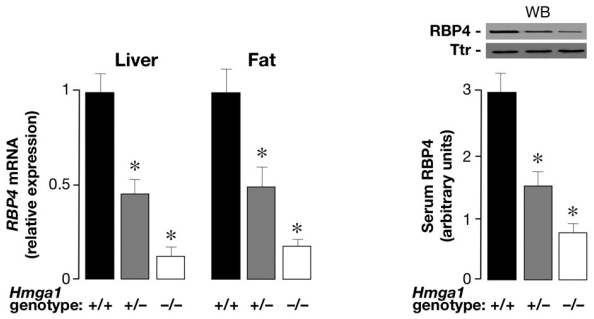

Figure 4
RBP4 expression in wild-type and *Hmga1*-deficient mice. RBP4 mRNA in liver and fat from control and *Hmga1*-deficient mice, as measured by qRT-PCR (left), and densitometric quantification of RBP4 serum levels as detected by Western blot (WB) of serum samples (2 μl) from mice with diverse genotypes (right). In WB analysis, an anti-transthyretin (TTR) antibody was used to confirm similar amounts of protein on each lane. Results are from 4–6 mice in each group. **P* < 0.01 versus control mice.

similar to those shown in the inset of Figure 6 were also obtained in epididymal and subcutaneous fat pads from control and mutant animals (data not shown), thus indicating that the glucagon-stimulated cAMP synthesis did not differ among mice with diverse genotypes.

Hmga1-deficient mice have increased Glut4 expression and insulin signaling activity in skeletal muscle and fat

Systemic insulin resistance has been associated with elevation of serum RBP4, whereas genetic and pharmacological interventions aimed at decreasing serum RBP4 levels enhance insulin action and improve insulin sensitivity [4]. Increased peripheral insulin sensitivity during insulin-tolerance test was previously observed by us in *Hmga1*-knockout mice [13]. To verify whether a functional link indeed existed between HMGA1 and RBP4, and whether insulin hypersensitivity in *Hmga1*-deficient mice could be mediated by the HMGA1-RBP4 system, we carried out quantitative measurements of *Glut4* mRNA transcript abundance. Examination by qRT-PCR showed a significant increase of *Glut4* transcripts in both skeletal muscle and adipose tissues from *Hmga1*-deficient mice compared with controls (Figure 7). Accordingly, immunoblotting of muscle and fat tissue showed a 2- to 3-fold increase of Glut4 in the insulin hypersensitive *Hmga1*-knockout mice compared with controls (Figure 7), clearly indicating that an inverse correlation between RBP4 and Glut4 indeed exists *in vivo*, in this animal model of diabetes, in which reduced RBP4 may contribute to the maintenance of glucose homeostasis by increasing insulin signaling and peripheral insulin sensitivity. In agreement with this interpretation, the activation state of the protein kinase Akt, an important downstream target of PI 3-kinase regulating insulin serum effects on Glut4 translocation and carbohydrate metabolism [17], was increased in mutant animals. As shown in Figure 7, basal phospho-Akt immunoreactivity was higher in skeletal muscle and adipose tissues from *Hmga1*-deficient mice compared with wild-type controls, and this increase paralleled closely the increase of Glut4 protein in adipose and muscle plasma membranes from heterozygous and homozygous *Hmga1* mutants. In line with previous observations on transcriptional repression of the mouse *Glut4* gene by cAMP [18], endocrine upregulation of Glut4 in *Hmga1*-deficient mice was substantiated further by *in vitro* experiments (not shown), indicating that in isolated adipocytes treated with Br-cAMP, *Glut4* mRNA was decreased in all three genotypes. A positive correlation of RBP4 levels with markers of lipid metabolism adversely affecting insulin sensitivity has been reported recently in both clinical and experimental studies [19,20]. *Hmga1*-knockout mice had lower levels of serum free fatty acids (0.45 ± 0.13 and 0.34 ± 0.07 in $Hmga1^{+/+}$ and $Hmga1^{-/-}$, respectively; $P < 0.05$), which might contribute to their improved insulin sensitivity.

Recombinant RBP4 injection reduces Glut4 and insulin signaling activity in muscle and fat tissue of Hmga1-deficient mice, and attenuates insulin hypersensitivity of these animals

To demonstrate that increased insulin sensitivity in mutant mice was directly due to HMGA1 regulation of RBP4, we determined the effect of recombinant RBP4 administration on Akt phosphorylation and Glut4 protein expression in skeletal muscle from *Hmga1*-deficient mice. As shown in Figure 8, Akt phosphorylation was reduced in muscle from RBP4-injected mutant animals compared with saline-injected *Hmga1* mutants. The reduction in Akt phosphorylation in these genotypes correlated inversely with RBP4 serum levels in the same animals (Figure 8) and paralleled the reduction of Glut4 in skeletal muscle and adipose (not shown) plasma membranes (Figure 8), indicating that, in these conditions, activation of the Akt-Glut4 pathway is regulated, at least in part, by circulating RBP4. Plasma insulin levels were slightly higher in RBP4-injected mice, but no significant difference was found (1.6 ± 0.2 and 1.2 ± 0.2 in RBP4-injected $Hmga1^{+/-}$ and $Hmga1^{-/-}$ respectively, versus 1.4 ± 0.1 and 0.9 ± 0.1 ng/ml in saline-injected $Hmga1^{+/-}$ and $Hmga1^{-/-}$ mice).

Consistent with the condition of insulin hypersensitivity, we previously reported that the glucose-lowering effect of exogenous insulin was enhanced in *Hmga1*-deficient mice during insulin-tolerance test (ITT) [13]. To support further the role of RBP4 in insulin hypersensitivity in *Hmga1* mutants, we have determined the effect of RBP4 adminis-

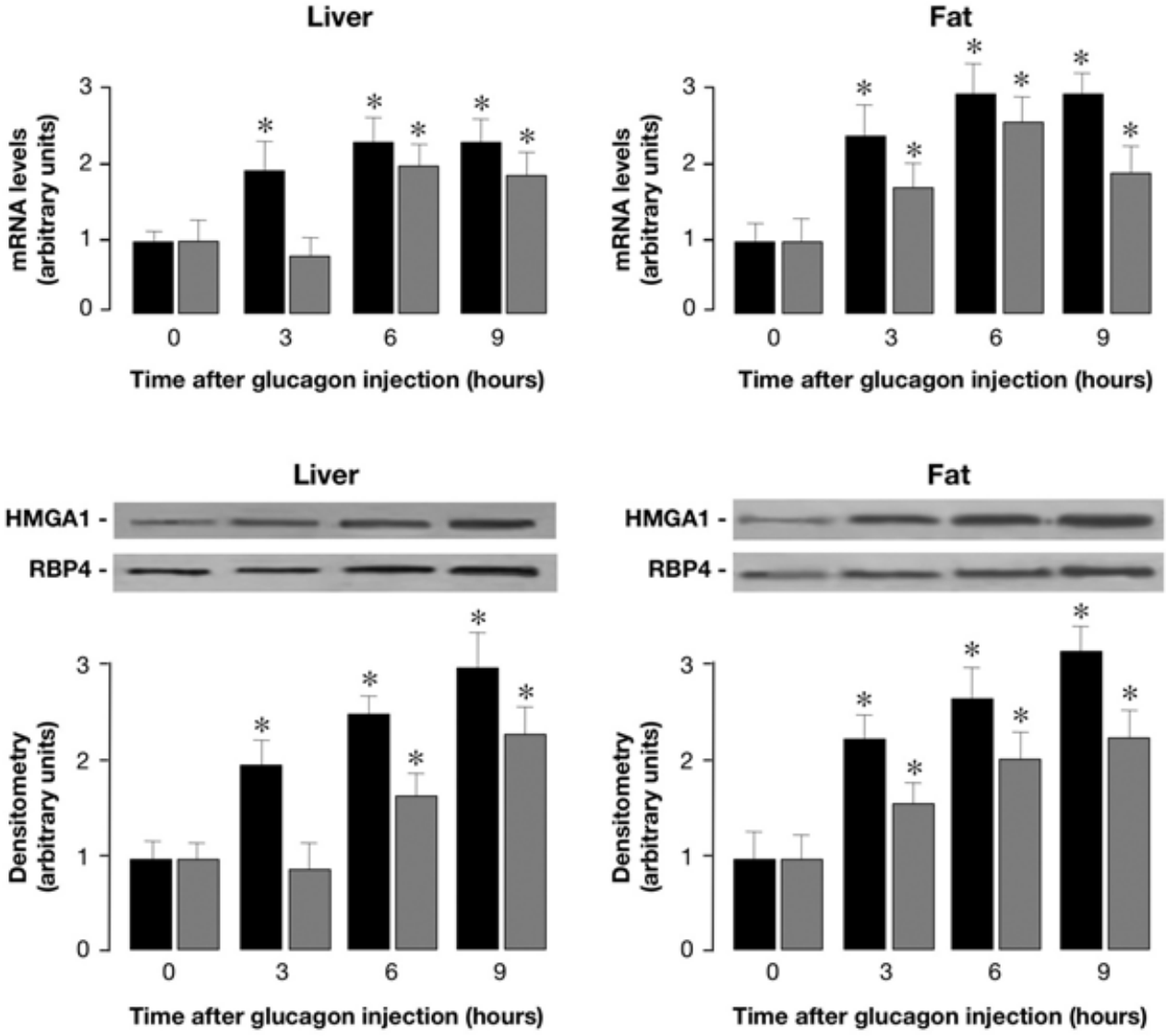

Figure 5

***Hmga1* and *RBP4* mRNA and protein expression *in vivo*, in glucagon-injected wild-type mice**. Total RNA was isolated from liver (upper left) and fat (upper right) of 3-h-fasted mice, before and after intraperitoneal injection of glucagon. Levels of *Hmga1* and *RBP4* mRNA were measured at the indicated time intervals by qRT-PCR and normalized to *RPS9* mRNA abundance, as described in *Methods*. Results are the mean values ± s.e.m. from 4–6 animals per group. Black bars, *Hmga1* mRNA; gray bars, *RBP4* mRNA. Representative Western blots from liver (lower left) and fat (lower right) of mice before and after glucagon injection are shown. Densitometric analyses of immunoblots are shown in bar graphs as the mean ± s.e.m. of data from 3–5 mice per each time point. Black bars, HMGA1; gray bars, RBP4.*$P < 0.05$ versus control mice (time 0).

tration on the glucose fall induced by insulin in these genotypes during ITT. As shown in Figure 9, injection of human RBP4 in heterozygous and homozygous *Hmga1* mutants caused a less dramatic fall in blood glucose levels, lessening the hypoglycemic response to intraperitoneal insulin observed in the saline-injected animals. Thus, taken together, our findings consistently support the role of HMGA1 as a key element in the transcriptional regulation of genes involved in glucose metabolism and add new insights into the compensatory mechanisms that may contribute to counteract insulin resistance *in vivo*. By directly regulating *RBP4* gene transcription, HMGA1 enhances peripheral insulin sensitivity, ensuring glucose uptake in skeletal muscle. This, if on one hand might rep-

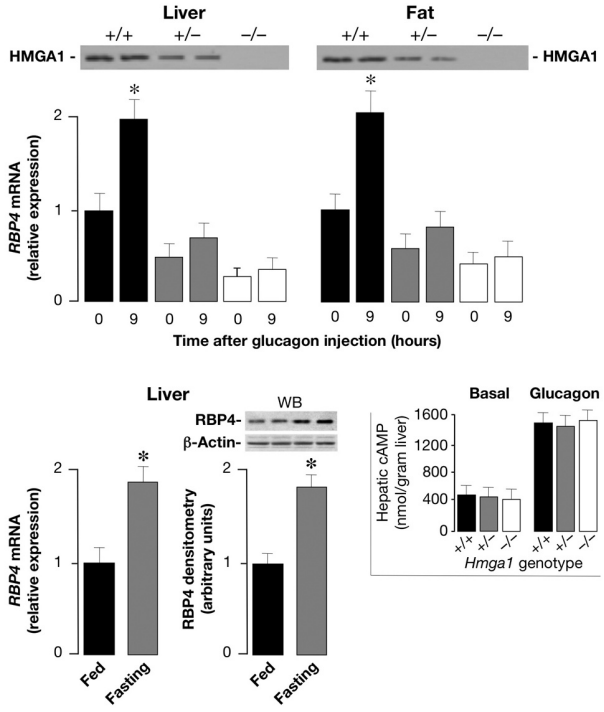

Figure 6
Comparison of *RBP4* mRNA levels in glucagon-injected wild-type and *Hmga1*-deficient mice, and liver RBP4 expression in wild-type mice during fasting and fed. Total RNA was isolated from liver and fat of 3-h-fasted mice, before (time 0) and after 9 h of intraperitoneal injection of glucagon, and *RBP4* mRNA was measured by qRT-PCR and normalized to *RPS9* mRNA abundance. Results are the mean values ± s.e.m. from 6–8 animals per group. Black bars, *Hmga1*$^{+/+}$, *n* = 8; gray bars, *Hmga1*$^{+/-}$, *n* = 6; white bars, *Hmga1*$^{-/-}$, *n* = 6. **P* < 0.05 versus each control (time 0). Western blots for HMGA1 protein expression are shown in liver and fat from all three genotypes (top). The levels of *RBP4* mRNA and protein (shown at the bottom of the figure) were measured in liver of fed and 6-h-fasted wild-type mice (6 animals per group), using qRT-PCR and Western blot (WB), respectively. **P* < 0.05 versus fed mice. Inset, cAMP was measured in liver from control and *Hmga1*-deficient mice, in both basal conditions and 3 h after the intraperitoneal injection of glucagon (1 mg/kg body weight), as described in the *Methods* section. The data are mean ± s.e.m. for 4–6 animals per group.

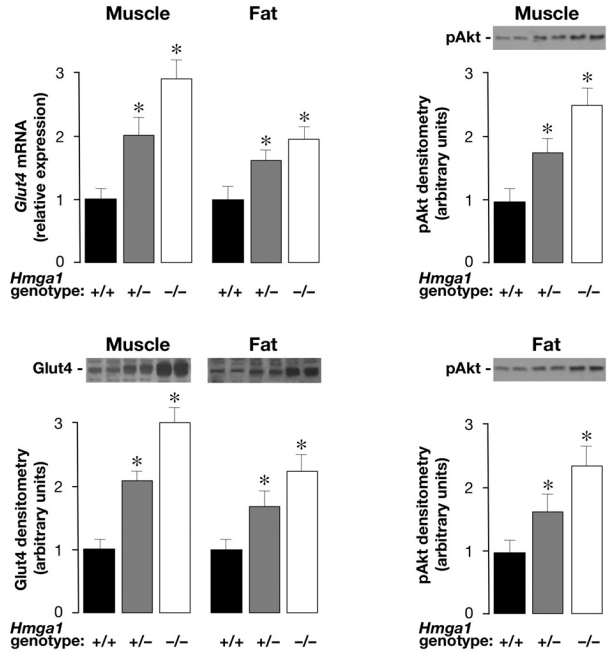

Figure 7
Glut4 and pAkt expression in wild-type and *Hmga1*-deficient mice. *Glut4* mRNA (upper left) and protein content (lower left) in muscle and fat parallel pAkt protein abundance in skeletal muscle (upper right) and adipose tissue (lower right) from control and *Hmga1*-deficient mice. Representative Western blots of Glut4 and pAkt proteins are shown, together with the densitometric analyses of six to eight independent blots. Black bars, *Hmga1*$^{+/+}$, *n* = 8; gray bars, *Hmga1*$^{+/-}$, *n* = 6; white bars, *Hmga1*$^{-/-}$, *n* = 6. **P* < 0.05 versus *Hmga1*$^{+/+}$.

resent an adaptive mechanism to ameliorate insulin resistance in animals with a disadvantageous metabolic risk profile, on the other might indicate that the cAMP/HMGA1-mediated RBP4 expression during fasting (when glucagon peaks) may act physiologically to reduce insulin sensitivity in peripheral tissues, thereby contributing to the maintenance of euglycemia under this condition. This was supported by the observation that after an overnight fasting period (12–16 h) plasma glucose concentration in wild-type mice was higher than that of *Hmga1*-deficient mice (89 ± 5 in *Hmga1*$^{+/+}$ mice, versus 72 ± 6 and 62 ± 5 mg/dl in *Hmga1*$^{+/-}$ and *Hmga1*$^{-/-}$ mice, respectively; $P < 0.05$).

Discussion

We have previously shown that loss of HMGA1 protein expression, induced in mice by disrupting the *HMGA1* gene, severely decreased insulin receptor expression (below 10% of control animals) and phosphorylation in the major targets of insulin action, largely impaired insulin signaling, and reduced insulin secretion, producing a type 2-like diabetic phenotype in which defects in both peripheral insulin sensitivity and pancreatic beta-cell insulin secretion were coexpressed simultaneously [13]. However, despite the severe decrease in insulin receptor signaling and insulin receptor production, the glucose-lowering effect of exogenous insulin was enhanced in *Hmga1*-deficient mice during ITT, and the glucose infusion rate necessary to maintain euglycemia was higher in

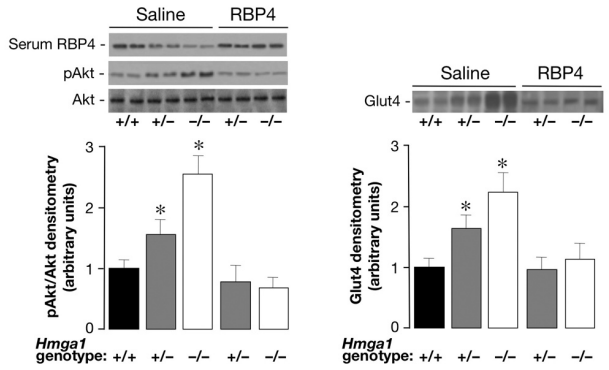

Figure 8
Effects of recombinant RBP4 administration on Akt phosphorylation and Glut4 protein expression in *Hmga1*-deficient mice. Basal (saline) levels of pAkt (left) and Glut4 (right) were increased in skeletal muscle of saline-injected *Hmga1*-deficient mice compared with controls, and were reduced following RBP4-injection ($n = 6$ per genotype). Densitometric quantifications of three independent experiments from 3 animals per genotype are shown, together with representative Western blots of pAkt, Glut4, and serum RBP4 of saline and RBP4-injected mice. *$P < 0.05$ versus *Hmga1*$^{+/+}$.

mutant mice during hyperinsulinemic-euglycemic clamp [13], supporting the existence of alternative pathways of insulin signaling promoting glucose uptake and disposal in certain adverse metabolic conditions such as those found in the *Hmga1*-knockout mouse. The existence of signaling pathways promoting glucose uptake and utilization in peripheral tissues through mechanisms that are independent of insulin has been postulated before, on the basis of experimental observations supporting the existence of molecular circuits/pathways that can compensate for the decrease in insulin-stimulated glucose uptake *in vivo*, in both animal models and human patients with type 2 diabetes [21-23]. However, how these compensatory mechanisms are activated has remained hitherto largely undefined. As previously shown, consistent with the ubiquitous distribution of HMGA1, insulin receptor expression was also reduced in pancreatic tissue from *Hmga1*-deficient mice [13]. Loss of insulin secretion in response to glucose has been reported in IRβ knockout mice with tissue-specific knockout of the insulin receptor in pancreatic beta cells [24]. As in the IRβ knockout mice, plasma insulin after glucose challenge was considerably reduced in *Hmga1*-mutant animals, in which the acute first-phase insulin secretory response was severely blunted [13], indicating a glucose-induced insulin secretory defect. In addition, substantial abnormalities in pancreatic islet morphology and size have been described in *Hmga1*-knockout mice [13], indicating that decreased insulin secretion in this genotype may also depend on reduced beta-cell mass. Thus, defects in both pancreatic beta-cell insulin secretion and peripheral insulin action coexist simultaneously in this knockout mouse model of diabetes, in which activation of compensatory mechanisms to efficiently overcome these metabolic abnormalities may be of vital importance.

Downregulation of Glut4 in adipose tissue is a typical feature of insulin-resistant states, such as obesity and type 2 diabetes [25]. It has been found that the decrease in Glut4 expression that occurs in the fatty tissue of obese animals and humans is accompanied by increased expression and secretion of the adipocyte-derived RBP4 fraction [4,5], suggesting that RBP4 production is tightly regulated by adipose tissue glucose uptake. RBP4 has been recently implicated in systemic insulin sensitivity in rodents and humans, in which elevated serum RBP4 levels were associated with reduced expression of Glut4 in adipocytes, and correlated inversely with peripheral insulin sensitivity. However, based on current data, the role of RBP4 in insulin sensitivity in humans is still controversial and might be restricted to rodent models only. Interspecies differences are known to exist and discrepancies between humans and mice might emphasize the role of non-genetic environmental factors and genetic modifiers in determining the phenotypic variations in RBP4 and insulin sensitivity between humans and animal models. Our results in the present study clearly indicate that in *Hmga1*-knockout mice RBP4 levels are considerably decreased in serum and in whole liver and adipose tissue extracts, strictly linking HMGA1 and RBP4 expression. We propose that HMGA1 deficiency adversely affects RBP4 expression and this, in animals with a disadvantageous metabolic risk profile like that observed in the *Hmga1*-knockout mouse model, might reflect an adaptive mechanism to increase glucose uptake and glucose disposal. Consistent with the results obtained in *Hmga1*-deficient mice, RBP4 was considerably reduced in cells of both human (HepG2) and mouse (Hepa1) origin readily expressing RBP4, following perturbation of endogenous HMGA1 protein expression in cells treated with siRNA against HMGA1. Conversely, an increase in *RBP4* mRNA abundance was observed in both cell lines following forced expression of HMGA1, consistently supporting a role for HMGA1 in the transcriptional activation of the *RBP4* gene. These findings were substantiated further by ChIP analysis, showing that HMGA1 indeed binds to the *RBP4* locus in intact living cells.

Signal transduction pathways which raise intracellular cAMP have been reported to have a potential role in the regulation of *RBP4* gene expression [16]. Although the molecular mechanisms underlying this effect remain poorly understood, evidence exists supporting the notion that the regulation of *RBP4* gene transcription via the

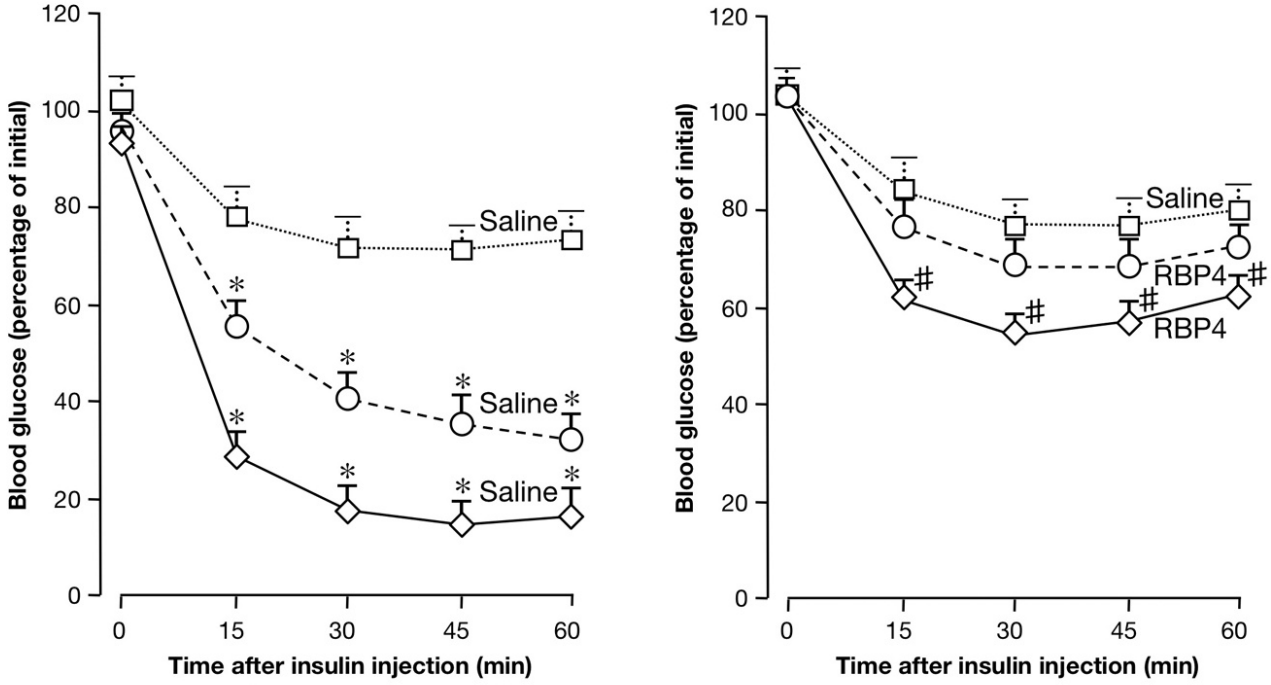

Figure 9

Effects of RBP4 on insulin sensitivity. Insulin-tolerance test (ITT) was assessed in *Hmga1*-deficient mice injected with saline alone (left), and in *Hmga1* mutants injected chronically with purified RBP4 (right) (n = 6–8 per genotype in each condition). ITT was performed by measuring blood glucose levels in 12-h-fasted conscious mice injected intraperitoneally with human insulin (Human Actrapid, Novo Nordisk), 1 U/kg body weight. Open squares, *Hmga1*$^{+/+}$; open circles, *Hmga1*$^{+/-}$; open diamonds, *Hmga1*$^{-/-}$. The degree of statistical significance was less in RBP4-injected *Hmga1*-deficient mice compared with the significance for saline-injected *Hmga1* mutants. *P < 0.0001, saline-injected *Hmga1*-deficient mice versus *Hmga1*$^{+/+}$; # P < 0.05, RBP4-injected *Hmga1*$^{-/-}$ mice versus *Hmga1*$^{+/+}$.

cAMP signaling pathway may be physiologically relevant. One important physiological condition in which intracellular cAMP increases is in response to low glucose availability. In this metabolic setting, a concomitant predominance of circulating counter-regulatory hormones, in particular pancreatic glucagon acting via the cAMP pathway, induces glycogenolysis and gluconeogenesis in the liver, which produce and release hepatic glucose in the blood. In this regard, the cAMP-element-binding protein (CREB) has been identified as a critical transcriptional checkpoint which, in response to cAMP, promotes hepatic glucose output through the synergistic activation of distinct transcriptional effector pathways, which include the PPAR gamma coactivator 1 (PGC1) and the NR4A orphan nuclear receptors [26].

In this paper, we report that systemic injection of glucagon to wild-type control mice caused an increase in *RBP4* mRNA and protein expression, along with an increase of both intracellular cAMP and HMGA1 levels. Glucagon effects were attenuated in *Hmga1*-deficient mice, supporting a distinct role for HMGA1 in the regulation of *RBP4* gene expression and functionally linking this two genes. As a consequence of the functional link between HMGA1 and RBP4, a significant increase in *Glut4* mRNA and protein was observed in both skeletal muscle and adipose tissues from *Hmga1*-deficient mice compared with controls. An inverse relationship between RBP4 and Glut4 has been described previously, in the adipose-*Glut4*$^{-/-}$ mouse, in which the decrease in Glut4 expression that occurs in the fatty tissue of this mutant genotype is accompanied by increased expression and secretion of the fat-derived RBP4 [4]. In our model, instead, *RBP4* expression is genetically impaired due to the lack of HMGA1 and Glut4 is increased in both muscle and fat, suggesting that abnormalities in RBP4 and/or metabolites of the vitamin A metabolism may directly affect whole-body insulin action and peripheral insulin sensitivity. In support of this possibility, identification of regulatory single nucleotide polymorphisms in the *RBP4* gene associated with type 2 diabetes has been recently reported [27,28], while correlations of RBP4 with insulin resistance have been confirmed

in experimental clinical approaches in humans [7]. Although conflicting results have been reported, raising doubt about the postulated relationship of RBP4 with insulin sensitivity in humans, our results in *Hmga1*-deficient mice confirm that an inverse correlation indeed exists between RBP4 and insulin sensitivity *in vivo*, in this animal model of diabetes, lending support to previous hypotheses that lowering RBP4 levels would be helpful in ameliorating insulin resistance, at least in mice.

Overall, our findings provide mechanistic insight into the regulation of glucose uptake and disposal in peripheral tissues, and support further the role of HMGA1 as a molecule that is likely to be an important emerging factor in the transcriptional activity of genes implicated in the maintenance of glucose homeostasis and metabolic control, such as the insulin receptor gene [11-13], the leptin gene [29], and, as shown here, the *RBP4* gene. Apart from the intrinsic biological interest in elucidating the mechanisms leading to improvement in insulin sensitivity, a clear understanding of the molecular process involved is of potential importance in the development of new therapeutic strategies for patients with metabolic disorders such as obesity, diabetes, and other insulin resistant states.

Conclusion

We propose that HMGA1 can serve as a modulator of both *RBP4* gene expression and protein function and represents an important novel mediator of glucose homeostasis *in vivo*.

Methods

Plasmids, transfections, and ChIP

The *RBP4*-Luc reporter plasmid was obtained by cloning the *NheI*/*XhoI* 1427-bp sequence of the mouse *RBP4* promoter (-1417 to +10) into pGL3 (Promega). This fragment was amplified from genomic DNA using the following modified primers: 5'-TTGCTAGCATGGCTAAGGTGCTTGTTGAAA-3', 5'-TTCTCGAGCACACCCACTCCATCTCACC-3' and the integrity of this construct was checked by DNA sequencing. *RBP4*-Luc reporter plasmid, together with either the control vector plasmid or expression plasmid encoding HMGA1 [11], was transiently transfected into cultured cells using LipofectAMINE 2000 reagent (Invitrogen), and Luc activity was assayed 48 h later, as previously described [30]. Renilla control vector served as an internal control of transfection efficiency, together with measurements of protein expression levels. For antisense HMGA1 experiments, *RBP4*-containing vector was cotransfected into Hepa1 cells with the expression plasmid pcDNA1 containing the *HMGA1* cDNA in the antisense orientation [12]. Small interfering RNA (siRNA) targeted to *HMGA1* [30] was transfected into cells at 50% to 60% confluency and cells were analyzed 48 to 96 h later. ChIP assay was performed in HepG2 and Hepa1 cells, either untreated or pretreated with *HMGA1* siRNA as described previously [31]. Formaldehyde-fixed DNA-protein complex was immunoprecipitated with anti-HMGA1 antibody. Primers for the *RBP4* sequence were used for PCR amplification of immunoprecipitated DNA (30 cycles), using PCR ready-to-go beads (Amersham Pharmacia Biotech). PCR products were electrophoretically resolved on 1.5% agarose gel and visualized by ethidium bromide staining.

Animals

Male *Hmga1*-deficient and wild-type mice aged 6–9 months were studied. The generation of these animals and many of the physiological characteristics of the mice have been described in detail [13]. All animal work was carried out at the Animal Facility at the 'Istituto dei Tumori di Napoli', and at the Faculty of Pharmacy, Roccelletta di Borgia, Catanzaro, using approved animal protocols and in accordance with institutional guidelines. Serum free fatty acid levels were measured in wild-type and *Hmga1*-knockout mice (n = 12–16 per genotype) using the NEFA C kit (Wako).

Real-time PCR and Western blot

For qRT-PCR, total cellular RNA was extracted from tissues using the RNAqueous-4PCR kit and subjected to DNase treatment (Ambion). RNA levels were normalized against 18S ribosomal RNA in each sample, and cDNAs were synthesized from 2 μg of total RNA using the RETROscript first strand synthesis kit (Ambion). Primers for mouse *HMGA1* (NM_016660.2) (5'-GCAGGAAAAGGATGGGACTG-3'; 5'-AGCAGGGCTTCCAGTCCCAG-3'), *RBP4* (NM_011255.2) (5'-AGGAGAACTTCGACAAGGCT-3'; 5'-TTCCCAGTTGCTCAGAAGAC-3'), *Glut4* (NM_009204) (5'-TCATTGTCGGCATGGGTTT-3'; 5'-CGGCAAATAGAAGGAAGACGTA-3'), and *RPS9* (NM_ 029767.2) (5'-CTGGACGAGGGCAAGATGAAGC-3'; 5'-TGACGTTGGCGGATGAGCACA-3') were designed according to sequences from the GenBank database. A real-time thermocycler (Eppendorf Mastercycler ep realplex ES) was used to perform quantitative PCR. In a 20-μl final volume, 0.5 μl of the cDNA solution was mixed with SYBR Green RealMasterMix (Eppendorf), and 0.3 μM each of sense and antisense primers. The mixture was used as a template for the amplification by the following protocol: a denaturing step at 95°C for 2 min, then an amplification and quantification program repeated for 45 cycles of 95°C for 15 s, 55°C for 25 s, and 68°C for 25 s, followed by the melting curve step. SYBR Green fluorescence was measured, and relative quantification was made against the *RPS9* cDNA used as an internal standard. All PCR reactions were done in triplicate.

Western blot analysis was performed to analyze HMGA1 and RBP4 protein expression in whole-cell liver and fat extracts from normal and mutant mice, using polyclonal

specific antibodies raised against HMGA1 [11] and RBP4 (AdipoGen, Inc.). For the measurement of serum RBP4, blood was collected from the retro-orbital sinus, plasma protein extracts were resolved on 12% SDS-PAGE, blotted onto nitrocellulose membranes and RBP4 was detected using rabbit polyclonal antisera at 1:2000 dilution, as suggested by the manufacturer. TTR was detected using a goat anti-TTR polyclonal antibody (Santa Cruz Biotechnology). Rabbit anti-Glut4 polyclonal antibody was used as previously described [13].

In vivo studies with the peptide hormone glucagon

For systemic administration of exogenous glucagon, mice were injected in the peritoneal cavity with human glucagon (1 mg/kg body weight) or saline after 3 h of fasting. At this dose, the peak increase of plasma glucagon in all genotypes was ~96% ± 10% above pre-injection levels, reflecting similar previous observations in rodents [32]. At different times after the injection the mice were killed by cervical dislocation, the liver and fat were rapidly removed, frozen into liquid nitrogen and stored at -80°C until processed. For cAMP determination, frozen samples were first homogenized in ice-cold trichloroacetic acid (TCA) (6% wt/vol), and cAMP was determined using the cAMP enzyme immunoassay kit (Amersham Pharmacia Biotech), according to the instructions specified by the manufacturer.

RBP4 purification and injection

Human *RBP4* cDNA cloned into a pET3a expression vector was a kind gift from JW Kelly (The Scripps Research Institute). Based on previously published methodology [33], *RBP4* protein expression vector was transformed into the BL21 strain of *Escherichia coli* (Stratagene), expanded in suspension culture and induced for 6 h with 1 mM isopropyl-D-thiogalactopyranoside to stimulate protein expression. Bacteria were pelleted and lysed by osmotic shock [34]. From this point on, all steps, including denaturation, refolding, and RBP4 purification, were performed essentially as described elsewhere [35]. Protein fractions were examined by sodium dodecyl sulfate polyacrylamide gel electrophoresis (SDS-PAGE) and immunoblotting, and desired fractions were pooled together, concentrated with an Amicon Centriprep-10 concentrator (Millipore), and stored at -80°C.

To determine whether elevation of RBP4 affected insulin hypersensitivity *in vivo*, in *Hmga1*-deficient mice, heterozygous and homozygous *Hmga1* mutants, were intraperitoneally injected twice daily (at 12-h intervals) with 200 μg of purified human RBP4 (13 μg/g body weight per mouse) for 7 days. This resulted in a daily average serum level of human RBP4 similar to that of control mice (see Figure 8), which received physiological saline solution according to the same schedule above.

Statistical analysis

The ANOVA test was used to evaluate the differences between the groups of mice. For all analyses, $P < 0.05$ was considered significant.

Abbreviations

Akt: protein kinase B; Br-cAMP: 8-bromo cAMP; cAMP: cyclic adenosine monophosphate; CREB: cAMP-element-binding protein; Glut4: glucose transporter-4; HEK-293: human embryonic kidney-293; Hepa1: mouse hepatoma; HMGA1: high mobility group A1; ITT: insulin-tolerance test; PGC1: PPAR gamma coactivator 1; qRT-PCR: quantitative Real-Time PCR; RBP4: retinol-binding protein 4; siRNA: small interfering RNA; TCA: trichloroacetic acid; TTR: transthyretin.

Authors' contributions

EC and FP performed qRT-PCR studies as well as transient transfections with reporter and expression vectors, and participated in the design of the study. SI was involved in Western blotting studies and assisted FP in performing transfections with siRNA. ILP participated in Western blotting and performed cloning studies. DP, EG, GDS and AF participated in the analysis and discussion of the *in vivo* data from normal and mutant mice. GB, AL, and VC performed certain aspects of the assays detailed in Figures 1, 2 and 3 and contributed with Northern blotting studies. DF provided helpful discussion on this manuscript and participated in ChIP analysis. AB conceived, coordinated, and supervised the project, analyzed data, and wrote the manuscript. All authors read and approved the final manuscript.

Acknowledgements

We remain extraordinarily indebted to Drs R Citraro and N Costa and the entire staff of the animal facilities for animal care. We are most grateful to Dr JW Kelly for his generous gift of RBP4 expression vector, pET3a. We would also like to thank Mrs A Malta and Dr G Ceravolo for secretarial help. This work was supported by Telethon-Italy, grant GGP04245, and MIUR, protocol 2004062059-002 Italy (AB).

References

1. Kahn CR: **Insulin action, diabetogenes, and the cause of type II diabetes (Banting Lecture).** *Diabetes* 1994, **43:**1066-1084.
2. Polonsky KS, Sturis J, Bell GI: **Non-insulin-dependent diabetes mellitus – a genetically programmed failure of the beta cell to compensate for insulin resistance.** *New Engl J Med* 1996, **334:**777-783.
3. Taylor S: **Insulin resistance or insulin deficiency: which is the primary cause of NIDDM?** *Diabetes* 1994, **43:**735-740.
4. Yang Q, Grahm TE, Mody N, Preitner F, Peroni OD, Zabolotny JM, Kotani K, Quadro L, Kahn BB: **Serum retinol binding protein 4 contributes to insulin resistance in obesity and type 2 diabetes.** *Nature* 2005, **436:**356-362.
5. Graham TE, Yang Q, Blüher M, Hammarstedt A, Ciaraldi TP, Henry RR, Wason CJ, Oberbach A, Jansson P-A, Smith U, Kahn BB: **Retinol-binding protein 4 and insulin resistance in lean, obese, and diabetic subjects.** *New Engl J Med* 2006, **354:**2552-2563.
6. Ziouzenkova O, Orasanu G, Sharlach M, Akiyama TE, Berger JP, Viereck J, Hamilton JA, Tang G, Dolnikowski GG, Vogel S, Duester G,

Plutzky J: **Retinaldehyde represses adipogenesis and diet-induced obesity.** *Nat Med* 2007, **13:**695-702.
7. von Eynatten M, Humpert PM: **Retinol-binding protein-4 in experimental and clinical metabolic disease.** *Expert Rev Mol Diagn* 2008, **8:**289-299.
8. Monaco HL, Rizzi M, Coda A: **Structure of a complex of two plasma proteins: transthyretin and retinol binding protein.** *Science* 1995, **268:**1039-1041.
9. Bustin M, Reeves R: **High-mobility group proteins: architectural components that facilitate chromatin function.** *Prog Nucleic Acid Res Mol Biol* 1996, **54:**35-100.
10. Thanos D, Maniatis T: **Virus induction of human IFN beta gene expression requires the assembly of an enhanceosome.** *Cell* 1995, **83:**1091-1100.
11. Brunetti A, Manfioletti G, Chiefari E, Goldfine ID, Foti D: **Transcriptional regulation of human insulin receptor gene by the high-mobility group protein HMGI(Y).** *FASEB J* 2001, **15:**492-500.
12. Foti D, Iuliano R, Chiefari E, Brunetti A: **A nucleoprotein complex containing Sp1, C/EBP beta, and HMGI-Y controls human insulin receptor gene transcription.** *Mol Cell Biol* 2003, **23:**2720-2732.
13. Foti D, Chiefari E, Fedele M, Iuliano R, Brunetti L, Paonessa F, Barbetti F, Croce CM, Fusco A, Brunetti A: **Lack of the architectural factor HMGA1 causes insulin resistance and diabetes in humans and mice.** *Nat Med* 2005, **11:**765-773.
14. Shimomura I, Matsuda M, Hammer RE, Bashmakov Y, Brown MS, Goldstein JL: **Decreased IRS-2 and increased SREBP-1c lead to mixed insulin resistance and sensitivity in livers of lipodystrophic and ob/ob mice.** *Mol Cell* 2000, **6(1):**77-86.
15. Rane SG, Dubus P, Mettus RV, Galbreath EJ, Boden G, Reddy EP, Barbacid M: **Loss of Cdk4 expression causes insulin-deficient diabetes and Cdk4 activation results in β-islet cell hyperplasia.** *Nat Genet* 1999, **22:**44-52.
16. Jessen KA, Satre MA: **Induction of mouse retinol binding protein gene expression by cyclic AMP in Hepa 1–6 cells.** *Arch Biochem Biophys* 1998, **357:**126-130.
17. Cho H, Mu J, Kim JK, Thorvaldsen JL, Chu Q, Crenshaw EB 3rd, Kaestner KH, Bartolomei MS, Shulman GI, Birnbaum MJ: **Insulin resistance and a diabetes mellitus-like syndrome in mice lacking the protein kinase Akt2 (PKB beta).** *Science* 2001, **292:**1728-1731.
18. Kaestner KH, Flores-Riveros JR, McLenithan JC, Janicot M, Lane MD: **Transcriptional repression of the mouse insulin-responsive glucose transporter (GLUT4) gene by cAMP.** *Proc Natl Acad Sci USA* 1991, **88:**1933-1937.
19. von Eynatten M, Lepper PM, Liu D, Lang K, Baumann M, Nawroth PP, Bierhaus A, Dugi KA, Heemann U, Allolio B, Humpert PM: **Retinol-binding protein 4 is associated with components of the metabolic syndrome, but not with insulin resistance, in men with type 2 diabetes or coronary artery disease.** *Diabetologia* 2007, **50:**1930-1937.
20. Stefan N, Hennige AM, Staiger H, Machann J, Schick F, Schleicher E, Fritsche A, Haring HU: **High circulating retinol-binding protein 4 is associated with elevated liver fat but not with total, subcutaneous, visceral, or intramyocellular fat in humans.** *Diabetes Care* 2007, **30:**1173-1178.
21. Saltiel AR, Pessin JE: **Insulin signaling pathways in time and space.** *Trends Cell Biol* 2002, **12:**65-71.
22. Kitamura T, Kahn CR, Accili D: **Insulin receptor knockout mice.** *Annu Rev Physiol* 2003, **65:**313-332.
23. Bouché C, Serdy S, Kahn CR, Goldfine AB: **The cellular fate of glucose and its relevance in type 2 diabetes.** *Endocr Rev* 2004, **25(5):**807-30.
24. Kulkarni RN, Bruning JC, Winnay JN, Postic C, Magnuson MA, Kahn CR: **Tissue-specific knockout of the insulin receptor in pancreatic β cells creates an insulin secretory defect similar to that in type 2 diabetes.** *Cell* 1999, **96:**329-339.
25. Shepherd PR, Kahn BB: **Glucose transporters and insulin action-implications for insulin resistance and diabetes mellitus.** *New Engl J Med* 1999, **341:**248-257.
26. Desvergne B, Michalik L, Wahli W: **Transcriptional regulation of metabolism.** *Physiol Rev* 2006, **86:**465-514.
27. Munkhtulga L, Nakayama K, Utsumi N, Yanagisawa Y, Gotoh T, Omi T, Kumada M, Erdenebulgan B, Zolzaya K, Lkhagvasuren T, Iwamoto S: **Identification of a regulatory SNP in the retinol binding protein 4 gene associated with type 2 diabetes in Mongolia.** *Hum Genet* 2007, **120:**879-888.
28. Craig RL, Chu WS, Elbein SC: **Retinol binding protein 4 as a candidate gene for type 2 diabetes and prediabetic intermediate traits.** *Mol Genet Metab* 2007, **90:**338-344.
29. Melillo RM, Pierantoni GM, Scala S, Battista B, Fedele M, Stella A, De Biasio MC, Chiappetta G, Fidanza V, Condorelli G, Santoro M, Croce CM, Viglietto G, Fusco A: **Critical role of the HMGI(Y) proteins in adipocytic cell growth and differentiation.** *Mol Cell Biol* 2001, **21:**2485-2495.
30. Paonessa F, Foti D, Costa V, Chiefari E, Brunetti G, Leone F, Luciano F, Wu F, Lee AS, Gulletta E, Fusco A, Brunetti A: **Activator protein-2 overexpression accounts for increased insulin receptor expression in human breast cancer.** *Cancer Res* 2006, **66:**5085-5093.
31. Costa V, Paonessa F, Chiefari E, Palaia L, Brunetti G, Gulletta E, Fusco A, Brunetti A: **The insulin receptor: a new anticancer target for peroxisome proliferator-activated receptor-g (PPARg) and thiazolidinedione-PPARg agonists.** *Endocr Relat Cancer* 2008, **15:**325-335.
32. Velliquette RA, Koletsky RJ, Ernsberger P: **Plasma glucagon and free fatty acid responses to a glucose load in the obese spontaneous hypertensive rat (SHROB) model of matabolic syndrome X.** *Exp Biol Med (Maywood)* 2002, **227:**164-170.
33. Xie Y, Lashuel HA, Miroy GJ, Dikler S, Kelly JW: **Recombinant human retinol-binding protein refolding, native disulfide formation, and characterization.** *Protein Expr Purif* 1998, **14:**31-37.
34. Burger A, Berendes R, Voges D, Huber R, Demange P: **A rapid and efficient purification method for recombinant annexin V for biophysical studies.** *FEBS Lett* 1993, **329:**25-28.
35. Isken A, Golczak M, Oberhauser V, Hunzelmann S, Driever W, Imanishi Y, Palczewski K, von Lintig J: **RBP4 disrupts vitamin A uptake homeostasis in a STRA6-deficient animal model for Matthew-Wood syndrome.** *Cell Metab* 2008, **7:**258-268.